

UC Riverside

UC Riverside Electronic Theses and Dissertations

Title

Ylides: Stabilization of Novel, Low Valent Carbon-Based Ligands with Applications in Catalysis

Permalink

<https://escholarship.org/uc/item/233309ff>

Author

Asay, Matt

Publication Date

2009

Peer reviewed|Thesis/dissertation

UNIVERSITY OF CALIFORNIA
RIVERSIDE

Ylides: Stabilization of Novel, Low Valent Carbon-Based Ligands
with Applications in Catalysis

A Dissertation submitted in partial satisfaction
of the requirements for the degree of

Doctor of Philosophy

in

Chemistry

by

Matt J. Asay

March 2009

Dissertation Committee:

Dr. Guy Bertrand, Chairperson
Dr. Christopher Reed
Dr. Catharine Larsen

Copyright by
Matt J. Asay
2009

The Dissertation of Matt J. Asay is approved:

Committee Chairperson

University of California, Riverside

Acknowledgments

First and foremost I would like to thank Professor Guy Bertrand for allowing me to work in his group and giving me the opportunity to do the chemistry presented in this dissertation. I feel very lucky to have been able to work with him and learn from him. I also would like to thank my boss in France, Professor Antoine Baceiredo for the opportunity to work with him for a year at Paul Sabatier. Both of them are great mentors and did a great job helping me get to France for a truly great year. Prof. Schoeller for the nice calculations. Prof. Mueller and his student Arun for some last minute solid state NMR. There are also some excellent co-workers from whom I learned so much. The list is long but I would like to specifically thank Michele for all of her assistance at the beginning of my PhD but more importantly for keeping me well stocked with Spheres! Herr Dr. Carsten for showing me some of the intricacies of boron chemistry. He always was there with his pen and a napkin to discuss chemistry at any time and his technique is unmatched (see you in Berlin!). J.B. for starting with me but finishing way before me and always being ready for a song. Vince for his sometimes controversial ideas and his willingness to share them often while taking every ones money at the poker table (he had to feed his family). Alan for introducing me to San Diego sports and the good times associated with watching them try and fail (kind of like

the chemistry). Yutes for being just about the nicest guy you can imagine, always willing to help with anything and of course always willing to go play a round of golf. Rian “the Kiwi” for being the third in our prodigious Sunday morning golf game. We had some good times... Ah the golf gang getting ‘rubied’ and naming the holes at the Fairmount golf course... good times. Maoying “Ping” for being there to hassle sometimes. Joan “Jean-Den” for all the help when I got to France... a great New Years in Paris and a special thanks to his mom for making the best meal I have ever had! Kato-san for not only being my boss but being my friend, showing me some of his crystallization technique and always telling me when I was wrong (though I rarely listened). Heinz for the help with crystals. Olivier “Totti” for the intense soccer work outs and gun work outs and party work outs. The Guido for the many great phrases he would coin at the drop of a hat (“NOOO!!! I am not in SHAPE!!!”). Glenn, Adam “glovebox destroyer”, ZENG! (for comic relief), Guera, Mo, Bruno (Paul-Marc). A conditional thanks to David if he can make some of this stuff I’m leaving behind work! And all the other peeps in Riverside and Toulouse.

The text, tables, schemes, and figures of the following chapters, in part or in their entirety, are reproduced from the following published and accepted manuscripts.

- Chapter 1: **Synthesis of a Mixed Phosphonium-Sulfonium Bisylide $R_3P=C=SR_2$**
S. Pascual, M. Asay, O. Illa, T. Kato, G. Bertrand, N. Saffon-Merceron, V. Branchadell, A. Baceiredo, *Angewandte Chimie International Edition*, **2007**, *46*, 9078-9080.
- Chapter 2: **Cyclic (Amino)[bis(ylide)]carbene as an Anionic Bidentate Ligand for Transition-Metal Complexes**
M. Asay, B. Donnadieu, A. Baceiredo, M. Soleilhavoup, G. Bertrand, *Inorganic Chemistry*, **2008**, *47*, 3949-3951.
- Chapter 3: **Synthesis and Ligand Properties of a Stable Five-Membered-Ring Vinylideneephosphorane**
M. Asay, T. Kato, N. Saffon-Merceron, F. P. Cossío, A. Baceiredo, G. Bertrand, *Angewandte Chimie International Edition*, **2008**, *47*, 7530-7533.

ABSTRACT OF THE DISSERTATION

Ylides: Stabilization of Novel, Low Valent Carbon-Based Ligands with Applications in Catalysis

by

Matt J. Asay

Doctor of Philosophy, Graduate Program in Chemistry
University of California, Riverside, March 2009
Dr. Guy Bertrand, Chairperson

The ylide has found practical applications in synthesis for many years, especially in the creation of carbon-carbon double bonds by way of the Wittig reaction. However, this work is concerned with new applications of ylides, especially the unique stabilization powers of phosphorus and nitrogen ylides. While the species reported in this dissertation are fundamentally interesting they are also directed toward synthetically useful applications. The first such species reported herein is the first phosphorus-sulfur bis-ylide, an analog of the well known carbodiposphorane, and has coordination behavior that is similar. This type of species could be a valuable reagent to do tandem olefination and epoxidation reactions on aldehydes or ketones.

A major part of this work is directed at using ylides to create stable carbon based ligands for homogeneous catalysis. A stable cyclic(amino)[(bis)ylide] carbene is the first example. The carbenic stabilized by one anionic carbon of a phosphorus bis-ylide. The other anionic carbon remains free to coordinate transition metals creating very stable bidentate complexes.

The largest portion of this dissertation is focused on the synthesis and ligand behavior of the first stable, fully characterized cyclic vinylidenephosphorane. Once again the special properties of ylides, specifically phosphorus ylides are on display as only one phosphorus stabilizes the low valent carbon center. This new species is a very strong donor for late transition metals, stronger than phosphines and carbenes. As such it is an ideal ligand for numerous catalytic reactions. Two new catalysts using this ligand are made and successfully used in olefin metathesis and hydroamination reactions, respectively.

The final portion focuses on the use of N-Heterocyclic Carbenes (NHCs) to stabilize a propadienylidene, a valence isomer of cyclopropenylidene. While the free species alluded synthesis several adducts are stable including a silver complex that can be used in transmetallation reaction.

Table of Contents

	pages
Acknowledgments	iv-vi
Abstract	vii-viii
Table of Contents	ix-x
List of Schemes	xi-xii
List of Figures	xiii-xvii
List of Tables	xviii

Introduction

Ylides: Synthetically Useful, Fundamentally Fascinating	1-9
A New Era: Carbene Chemistry	9-19

Chapter 1 20-33

Synthesis of a Mixed Phosphonium–Sulfonium Bisylide $R_3P=C=SR_2$	
---	--

Chapter 2 34-52

Cyclic (Amino)[bis(ylide)]carbene as an Anionic Bidentate Ligand for Transition Metal Complexes	
---	--

Chapter 3 53-72

Synthesis and Ligand Properties of a Stable Five-Membered-Ring Vinylideneephosphorane	
---	--

Chapter 4	73-96
Catalytic Properties of a Vinylidenephosphorane in Ruthenium Metathesis Chemistry and Gold(I) Hydroamination Chemistry	
Chapter 5	97-119
Towards a Free Stable Allenylidene	
Concluding Remarks	120-121
Appendix	122-217

List of Schemes

0.1	Synthesis of the first ylide 3 with the initial miss assigned structure 2 and the first reported ylide 4 .	2
0.2	Reactivity of carbodiphosphorane E .	8
0.3	Stable cyclic carbodiphosphorane 8 and rhodium complex 9 .	8
1.1	Synthesis of sulfonium phosphaylide 2 .	21
1.2	Synthesis and reactivity of bisylide 3 .	22
1.3	Schematic representation of the modes of stabilization of carbodiphosphoranes A and P,S bisylides B .	27
2.1	Synthesis of Phosphonium salt 3 .	36
2.2	Mechanism of formation of phosphine 4 from phosphonium 3 .	37
2.3	Attempted preparation of carbene 7 and synthesis of the lithium adduct 8 .	39
2.4	Preparation of palladium complex 9 and Rhodium complexes 10 and 11 .	39
2.5	Possible mechanism of the formation of lithium adduct 5 .	43
3.1	Synthesis of cyclic phosphaallene 5 .	55
3.2	Synthesis of palladium complex 6 and rhodium complexes 7 and 8 .	60
4.1	Attempted synthesis of ruthenium complex 10 and synthesis of complex 11 .	78
4.2	Efficient synthesis of complex 11 .	79

4.3	RCM test reaction of diallyl malonates D to cyclopentenes E .	81
4.4	Gold catalyzed hydroamination of 3-hexyne.	86
4.5	Synthesis of gold chloride complex 15 .	87
5.1	Synthesis of 2-ethynyl-imidazolium salt 6 .	100
5.2	Reactivity of salt 6 to form lithium 7 and borane 8 adducts as well as silver complex 9 .	102
5.3	Synthesis of palladium complex 10 and ruthenium complex 11 .	107

List of Figures

0.1	General bonding and resonance structure of an ylide.	1
0.2	The Wittig Reaction.	4
0.3	Vitamin A with the crucial Wittig formed double bond circled.	5
0.4	Phosphonium ylide anions C and D .	6
0.5	The resonance structures of carbodiphosphorane E .	7
0.6	Schematic representation of the electronic configuration of triplet 9 carbenes F and singlet carbenes G .	9
0.7	The first isolable stable carbene showing the carbenic 10 resonance form H ¹ , ylidic form H ² and phosphaalkyne form H ³ .	10
0.8	General structure of N-Heterocyclic Carbenes (NHCs) I with 11 their resonance structures and P-Heterocyclic Carbene (PHC) J .	11
0.9	The second generation Grubbs catalyst with an ancillary NHC 12 ligand K and the phosphine based first generation catalyst L .	12
0.10	Cyclic Alkyl Amino Carbenes (CAACs) M .	13
0.11	Bent allene (carbodicarbene) N with resonance structures.	15
0.12	Cyclic bent allene O .	16
1.1	Molecular structure of bisylides A , B and C .	20
1.2	X-ray crystal structures of 2 . Hydrogen atoms and triflate counterion omitted for clarity. Thermal ellipsoids are drawn at the 50% level. Selected bond lengths [Å] and angles [°]. P1–C1 1.721(5), S1–C1 1.690(4), P1–C2 1.796(4), S1–C3 1.810(5), P1–C1–S1 118.0(3).	23
1.3	X-ray crystal structures of 2 . Hydrogen atoms and triflate counterion omitted for clarity. Thermal ellipsoids are drawn at the 50% level. Selected bond lengths [Å] and angles [°]. P1–C1	24

- 1.721(5), S1–C1 1.690(4), P1–C2 1.796(4), S1–C3 1.810(5),
P1–C1–S1 118.0(3).
- 1.4 X-ray crystal structure **5**. Hydrogen atoms omitted for clarity. 24
Thermal ellipsoids are drawn at the 50% level. Selected bond
lengths [Å] and angles [°]. P1–C1 1.709(5), S1–C1 1.677(5),
P1–C2 1.804(5), C1–Cu1 1.903(4), N1–Cu1 1.874(4),
P1–C1–S1 115.3(2), C1–Cu1–N1 176.97(18), S1–C1–Cu
1125.7(3), P1–C1–Cu1 118.7(2).
- 1.5 Structures of **6** (a) and **7** (b) optimized at the B3LYP/6-31 + 25
G(d,p) level of calculation. Interatomic distances are in Å and
bond angles in degrees. Hydrogen atoms and the triflate anion
(for **7**) are omitted for clarity.
- 1.6 Highest occupied molecular orbitals of **6** : HOMO (left) and 26
HOMO-1 (right).
- 2.1 Carbenes **A–D**, (amino)[bis(ylide)carbene] **E** and the NHC-ylide 35
carbene **F**.
- 2.2 Molecular structure of phosphine **4**. Hydrogen atoms omitted for 37
clarity. Thermal ellipsoids at 50% probability.
- 2.3 Molecular structure of palladium complex **9**. Hydrogen atoms 41
omitted for clarity. Thermal ellipsoids at 50% probability.
Selected bond lengths [Å] and angles [°]: C1–N1 1.3778(17),
C1–C2 1.4013(18), C1–Pd1 2.0302(13), C5–Pd1 2.1268(15),
C2–P1 1.7472(14), C5–P1 1.7523(15); N1–C1–C2 104.61(11).
- 2.4 Molecular structure of rhodium complex **10**. Hydrogen atoms 41
omitted for clarity. Thermal ellipsoids at 50% probability.
Selected bond lengths [Å] and angles [°]: C1–N1 1.3842(16),
C1–C2 1.4045(19), C1–Rh1 2.0698(13), C5–Rh1 2.1250(14),
C2–P1 1.7359(13), C5–P1 1.7482(15); N1–C1–C2 103.73(11).
- 3.1 Similarities and differences between NHCs **A**, 54
carbodiphosphoranes **B**, push-push allenes **C**,
vinylidenephosphoranes **D**, push-pull allenes **E**, and push-pull

	carbenes F .	
3.2	X-ray crystal structure of phosphonium salt 4 . Hydrogen atoms and triflate anion are omitted for clarity. Thermal ellipsoids are at 50 % probability. Selected bond lengths (Å) and angles (°): P1–C1 1.782(3), C1–C4 1.329(4), P1–C2 1.791(2), C2–C3 1.342(3), C3–C4 1.497(4); P1–C1–C4 107.99(19), P1–C2–C3 107.17(19), C1–P1–C2 94.65(12).	56
3.3	X-ray crystal structure of phosphaallene ylide 5 . Hydrogen atoms are omitted for clarity. Thermal ellipsoids are at 50 % probability. Selected bond lengths (Å) and angles (°): P1–C1 1.783(15), C1–C4 1.358(2), P1–C2 1.789(16), C2–C3 1.342(2), C3–C4 1.510(2); P1–C1–C4 99.94(11), P1–C2–C3 101.97(12), C1–P1–C2 102.04(8).	57
3.4	Calculated HOMO and LUMO of phosphaallene 5 .	59
3.5	X-ray crystal structure of 6 . Hydrogen atoms are omitted for clarity. Selected bond lengths (Å) and angles (°): P1–C1 1.799(3), C1–C4 1.349(4), P1–C2 1.794(3), C2–C3 1.336(4), C3–C4 1.495(3), C1–Pd1 2.053(3); P1–C1–C4 102.58(18), P1–C2–C3 104.93(19), C1–P1–C2 98.20(13).	61
3.6	X-ray crystal structure of 7 .	62
4.1	General structure of NHCs A and vinylidenephosphoranes B (with resonance structures).	74
4.2	Grubbs first generation ruthenium metathesis catalyst 1 , second generation 2 , and Hoveyda-Grubbs first 3 and second 4 generation catalysts.	75
4.3	Vinylidenephosphorane ligand 5 and rhodium CO complex C .	75
4.4	Six-membered NHC ligand 6 , four-membered NHC ligand 7 and CAAC ligand 8 .	76
4.5	X-ray crystal structure of Hoveyda-Grubbs vinylidenephosphorane catalyst 11 . Hydrogen atoms are omitted for clarity. Thermal ellipsoids are drawn at 50% probability.	80

Selected bond lengths (Å) and angles (°): P1–C11 1.836 (9), C11–C12 1.370(11), C11–Ru1 1.996(8), C1–Ru1 1.803(8), O1–Ru1 2.333(6), Cl1–Ru1 2.338(2), Cl2–Ru1 2.319(3); P1–C11–C12 102.3(6), C1–Ru1–C11 90.8(4), O1–Ru1–C11 168.9(3) Cl1–Ru1–Cl2 148.12(8).

4.6	Conversion to disubstituted metathesis product E ($R = R' = H$) with catalyst 1 (■), 2 (x), 3 (▲), 4 (+) and 11 (◆).	82
4.7	Natural log plot of the starting material versus time showing linear, pseudo first order reaction kinetics and thus no catalyst decomposition.	83
4.8	A quantitative conversion versus time plot of the RCM reaction of 11 after a second equivalent of diethyldiallyl malonate.	84
5.1	Parent cyclopropenylidene A , NHC B , parent propadienylidene C as well as the stabilized cyclopropenylidene 1 and propadienylidene 2 .	98
5.2	Computationally optimized structure of 2 .	98
5.3	X-ray crystal structure of 2-ethynl-imidazolium salt 6 . Hydrogen atoms and iodide anions are omitted for clarity. Thermal ellipsoids are at 50 % probability. Selected bond lengths (Å) and angles (°): C1–C2 1.420(19), C2–C3 1.18(2), N1–C1 1.339(11), C1–C2–C3 180.000(9), N1–C1–N1a 109.1(11).	100
5.4	Structures and resonance forms for phosphonium allenylidene borane complex D , carbodiphosphorane E and carbodicarbene (bent-allene) F .	103
5.5	X-ray crystal structure of silver salt 9 . Hydrogen atoms, the anion and the solvents of crystallization are omitted for clarity. Thermal ellipsoids are at 50 % probability. Selected bond lengths (Å) and angles (°): Ag1–C2 2.026(10), C1–C2 1.235(15), C1–C8 1.408(15), C8–N3 1.351(12); N3–C8–N4 106.7(8), Ag1–C2–C1 178.8(10), C2–C1–C8 176.8(10), C2–Ag1–C2a 179.0(4).	105
5.6	X-ray crystal structure of palladium complex 10 . Hydrogen	108

atoms, counterions and solvent molecules are omitted for clarity. Thermal ellipsoids are at 50 % probability. Selected bond lengths (Å) and angles (°): Pd1–C1 1.986(2), C1–C2 1.199(3), C2–C3 1.408(3), Pd1–P1 2.3206(5); Pd1–C1–C2 178.39(19), C1–C2–C3 171.6(2), N1–C3–N2 126.05(17), C1–Pd1–P1 92.61(6), C1–Pd1–C1a 180.00(12).

- 5.7 X-ray crystal structure of phosphaallene ylide **5**. Hydrogen 110 atoms, counterions and solvent molecules are omitted for clarity. Thermal ellipsoids are at 50 % probability. Selected bond lengths (Å) and angles (°): Ru1–C6 2.027(4), C6–C7 1.226(7), C7–C8 1.395(6), Ru1–P1 2.3488(11); Ru1–C6–C7 177.1(4), C6–C7–C8 172.0(5), N3–C8–N4 107.5(4), C6–Ru1–P1 91.60(12), C6–Ru1–C6a 180.0(2).
- 5.8 Optimized structures of silver complex **9** and palladium complex **10** (hydrogens and counterions omitted for clarity). 112

List of Tables

1.1	Natural population analysis ^[a] of 6 and 7 (R = NMe ₂)	27
5.1	Computational data for compound 2 .	98
5.2	Computational data for Complex 9 and 10 .	112

Introduction

Ylides: Synthetically Useful, Fundamentally Fascinating

Ylides are molecules which have a carbanion directly attached to a heteroatom that carries a substantial degree of positive charge. The prototypical heteroatom is phosphorus but nitrogen, sulfur, silicon, arsenic and antimony are also well known. In addition, the heteroatom is not necessarily a main group element but can also be a transition metal such as titanium.¹

Since ylides are in effect 1,2 hetero-zwitterions (**A**), a charge-free resonance structure would generally be preferred (**B**). However, the zwitterionic structure is commonly used because it better reflects the reactivity of this unique species (Figure 0.1).

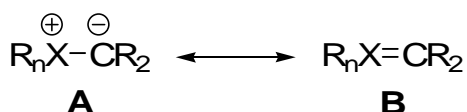
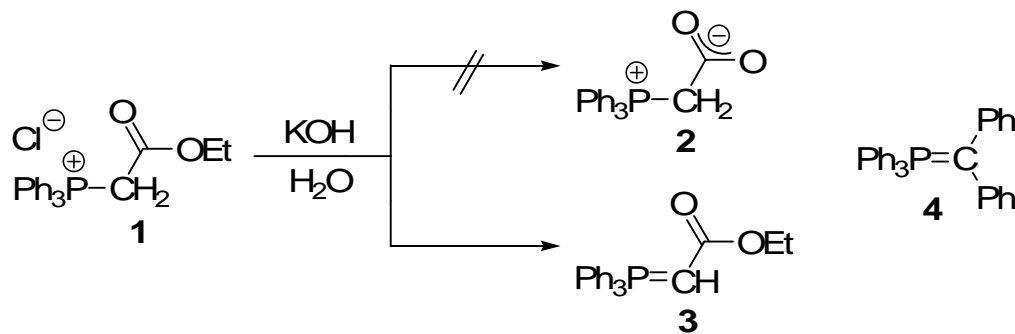


Figure 0.1. General bonding and resonance structure of an ylide.

The first ylide was synthesized by Michaelis and Gimborn in 1894,² by mixing the phosphonium chloride **1** with aqueous potassium hydroxide (Scheme 0.1). At the time the structure was miss assigned as the inner salt **2**. Michaelis and Gimborn can hardly be blamed for miss assigning the structure because carbanions had always been thought of as highly reactive species and, at the

time, to propose such a species to be stable would have been somewhat outlandish. However, by the time it was correctly identified as the ylide **3** by Aksnes, some 50 years later,³ Staudinger had already reported what was considered at the time the “first” ylide **4**.⁴ In fact in 1919 when Staudinger synthesized and correctly identified the first ylide, an arsenic ylide has also been synthesized, which was not correctly identified until many years later.⁵



Scheme 0.1. Synthesis of the first ylide **3** with the initial miss assigned structure **2** and the first reported ylide **4**.

In the years after 1919 there were also reports of the first sulfur⁶ and nitrogen⁷ ylides but the impetus of all this work was only fundamental chemical research. It was a serendipitous discovery by Wittig and co-workers in 1953 that really began intense research into ylides.⁸ While attempting to synthesize penta-alkyl phosphorus compounds they discovered the generality of what would become known as the Wittig reaction, a reaction that was already done by Staudinger 30 years before.⁴

It was only after the advent of the Wittig reaction that the nature of the ylidic bond was intensely investigated and a large effort was put forth to understand the bonding and relative stability of ylides.

It was quickly noted that nitrogen and phosphorus ylides had very different stabilities and reactivities. This fact was initially attributed to the availability of low lying d-orbitals in phosphorus. Hybridization using s, p and d orbitals had been used to explain the ability of phosphorus to form hypervalent σ^5 , λ^5 and σ^6 , λ^6 compounds and was therefore invoked in the case of phosphorus ylides, which, according to structure **B**, can be considered σ^4 , λ^5 species.⁹ However, with the growth of computational chemistry it has been shown that, while d-orbitals are necessary for accurate quantum chemical calculations,¹⁰ the contribution is such that the hybridization involving these d-orbitals is not reasonable; they do contribute but strictly as π -accepting orbitals. Another orbital argument for the stability of phosphorus ylides is the presence of low lying σ^* orbitals on phosphorus, which accept electron density from the carbanionic center in what has been termed negative hyperconjugation.¹¹ Again calculations have shown such interactions to exist but that the effect is quite small.

As mentioned previously the zwitterionic form **A** of ylides is oft used because it gives information about the reactivity of the molecule. Both calculations¹² and experimental results^{1, 13} confirm that in the case of phosphorus ylides the P-C bond is shorter than typical P-C bonds. However, while there are some orbital interactions (negative hyperconjugation, $\pi \rightarrow$ d-orbital), the carbon has a

significant negative charge, is not planar and there is free rotation about the P-C bond, which is in variance with the assignment of a double bond.¹⁴ Additionally the carbanion undergoes typical substitution and addition reactions of a nucleophile.

It is not the rather mundane substitution reactions that have led to the abundance of research but rather the special reactivity afforded by the heteroatom. This reactivity is best demonstrated by the first and best known ylide reaction: The Wittig Reaction (Figure 0.2). In this reaction a phosphorus ylide is reacted stoichiometrically with an aldehyde ($R^3 = H$) or ketone ($R^3 = \text{alkyl, aryl}$) to give an olefin and triphenylphosphine oxide.

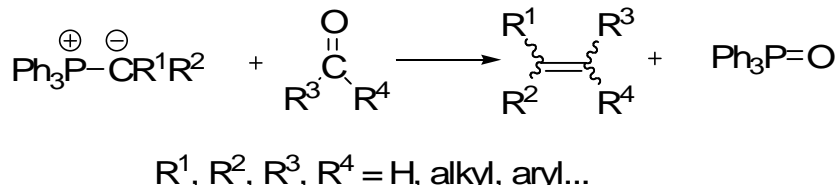


Figure 0.2. The Wittig Reaction.

Wittig received the 1979 Nobel Prize for chemistry in large part due to his research into the reaction that bears his name. In the years that followed the initial discovery the true importance of this new protocol became evident. The Wittig reaction is very tolerant to many functional groups allowing for the construction of olefins in complex molecules. It gives almost exclusively the Z-isomer and contrary to elimination reactions is completely regioselective

(because Zaitsev's rule does not apply). The power and regiospecificity is demonstrated by the facile preparation of anti-Bredt olefins.¹⁵ A more striking demonstration of the utility of this reaction is in the first total synthesis of vitamin A (Figure 0.3).¹⁶

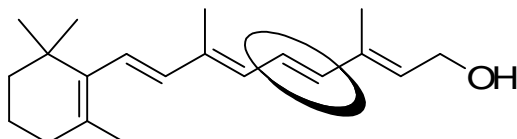


Figure 0.3. Vitamin A with the crucial Wittig formed double bond circled.

The phosphorus ylide started the research into the utility of ylides in synthesis but many others followed shortly thereafter. Similar reactions can be done with titanium ylides (Tebbe's olefination)¹⁷ and sulfonium ylides (Corey-Chaykovsky epoxidation reaction).¹⁸ There are also many other reactions directly related to the Wittig reaction such as the Horner-Wadsworth-Emmons olefination that uses carbanions stabilized by phosphonates,¹⁹ Julia Coupling that uses sulfone stabilized carbanions,²⁰ and the Peterson Olefination that uses a silyl stabilized carbanion, just to name a few.²¹

While practical uses of the ylide were very fruitful there was also interest in the fundamental aspects. As previously mentioned the unique stabilization imparted by the phosphorus was the subject of considerable debate but this stabilization was nonetheless used to synthesize novel species.

The number of novel and fundamentally interesting species containing ylide or ylide like moieties is nearly as vast as their uses in synthetic transformations. Only species of relative interest will be highlighted.

Phosphonium ylide anions (Figure 0.4) can be generated by two deprotonations of a phosphonium precursor. This type of species was proposed by Wittig and Reiber²² and subsequently synthesized and characterized. The first case involved deprotonation and two separate methyl groups creating a bidentate anion which coordinated lithium (**C**).^{22, 23} Later attempts to twice deprotonate the same methyl group arrived at somewhat controversial results.²⁴ Corey and co-workers²⁵ claimed to have twice deprotonated triphenylmethylphosphonium salts to give **D**¹ while Schaub and co-workers claimed that they were unable to recreate the results. In the end it was found that ortho metalation of one phenyl group occurred **D**² but that the anion reported by Corey was also present and perhaps in equilibrium with the ortho metalated product.²⁶

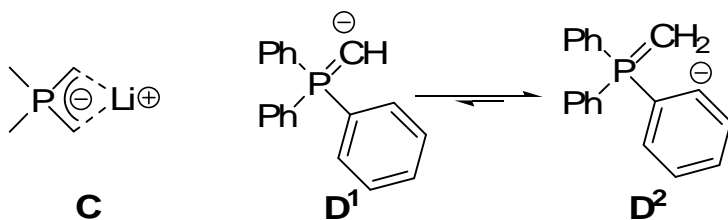


Figure 0.4. Phosphonium ylide anions **C** and **D**.

A similar species is the carbodiphosphorane, which was first reported by Ramirez and co-workers.²⁷ In this case a carbon is twice deprotonated, however the carbon is located between two phosphonium groups and, therefore, is neutral. The unique nature of the ylide bond is highlighted by the two resonance structures **E**¹ and **E**². Once again the classical allene form **E**¹ is not representative because the structure is bent, which can easily be explained by resonance structure **E**² (Figure 0.5). In fact, the extreme form that has a C⁰ stabilized by two phosphines (**E**³) has been discussed in the literature.²⁸

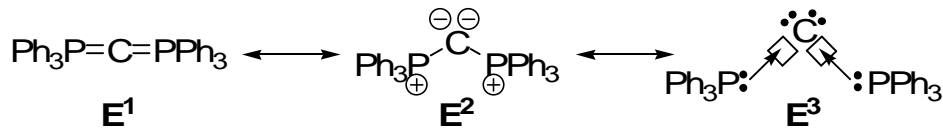
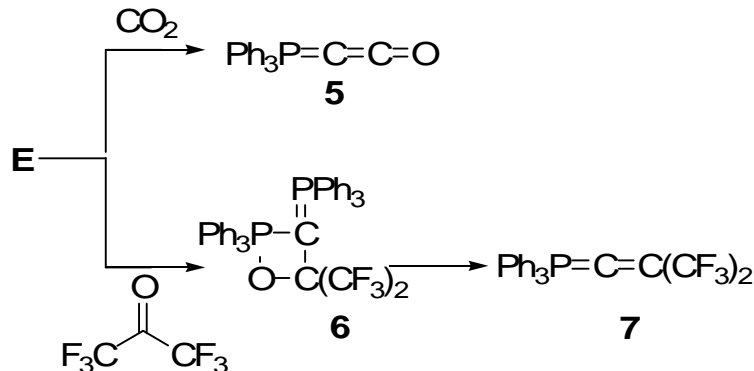


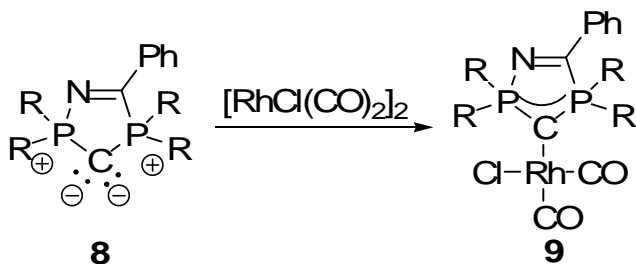
Figure 0.5. The resonance structures of carbodiphosphorane **E**.

The reactivity of carbodiphosphoranes has also been investigated leading to some interesting results. While they exhibit only limited Wittig like reactivity but the few examples are of particular interest. Hexaphenylcarbodiphosphorane **E** reacts with carbon dioxide in Wittig fashion to give a phosphacumulene **5** (Scheme 0.2).²⁹ Also the reaction with hexafluoroacetone led to the isolation of the first oxaphosphentane **6**, which is an important intermediate in the proposed mechanism of the Wittig reaction. Upon heating this species gave the Wittig product **7** which gives further credence to the proposed mechanism.³⁰



Scheme 0.2. Reactivity of carborodiphosphorane E.

Carbodiphosphoranes also can act as ligands to transition metals. Formally they could act as four electron donors. In practice however, the acyclic versions form fragile complexes most likely due to the rather large P-C-P bond angle (130.1° for **E**).³¹ There are several reports of cyclic carbodiphosphoranes but only two have been isolated and fully characterized.³² Of these two, only **8** (Scheme 0.3) has been coordinated to metals and it was found that the cyclic carbodiphosphorane acted as one of the strongest σ-donor ligands yet reported according to the CO stretching frequencies of the **8**RhCl(CO)₂ complex **9**.^{32a}



Scheme 0.3. Stable cyclic carbodiphosphorane **8** and rhodium complex **9**.

The ability of phosphorus to stabilize carbanions also plays an important role in the development a closely related field: Carbene chemistry.

A New Era: Carbene Chemistry

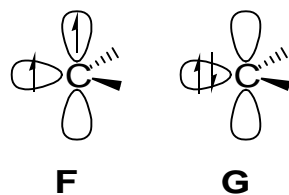


Figure 0.6. Schematic representation of the electronic configuration of triplet carbene **F** and singlet carbene **G**.

Carbenes are neutral divalent carbon molecules. They can exist in one of two electronic states (Figure 0.6). The triplet state (**F**) has two unpaired electrons one in the sp^2 hybridized orbital and the other in the $p\pi$ orbital. At ambient temperature they have lifetimes too short to be characterized therefore they are typically generated and studied in low temperature matrices. Singlet carbenes (**G**) on the other hand have a pair of electrons in the sp^2 hybridized orbital and a formally vacant $p\pi$ orbital. The ground state of the parent carbene :CH₂ is a triplet because the energy required to pair the two electrons is higher than the energy of one electron in the $p\pi$ orbital. However, by changing the relative energies of the two orbitals, the singlet state can be stabilized until it becomes the ground state. This is achieved by changing the electronic properties of the substituents. This, in

concert with adequate steric protection has made the isolation of singlet carbenes possible.

Carbene chemistry is nearly contemporary to ylide chemistry predating it by only nine years when Buchner and Curtis first published their research about transient carbenes.³³ However, the development has been somewhat slower. Transient carbenes and carbene transition metal chemistry has been extensively researched but stable, isolable, free carbene chemistry only began in 1988 with the isolation of the first example; the phosphino-silyl carbene **H**.³⁴ It is interesting to point out that aside from the carbenic resonance form **H**¹, that there is also a phosphorus ylide resonance (or more precisely a phosphorus vinyl ylide) structure **H**² as well as the phosphaalkyne form **H**³. The first example was a liquid and therefore could not be crystallized, but by changing the R groups a crystalline species could be synthesized upon which X-ray diffraction studies were done. The crystal structure shows the species to be bent as expected for resonance forms **H**¹ and **H**².³⁵ Extensive calculations were done that demonstrated the ylidic form **H**² to be dominant. Despite this, **H** demonstrates reactive behavior expected for all three resonance forms.

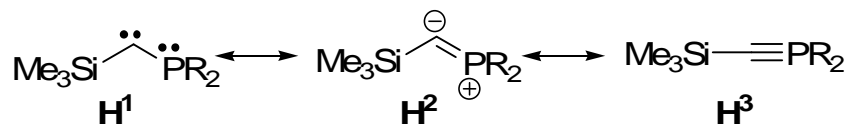


Figure 0.7. The first isolable stable carbene showing the carbenic resonance form **H**¹, ylidic form **H**² and phosphaalkyne form **H**³.

An ylidic resonance structure in stable carbenes is nearly always present. For example, N-Heterocyclic Carbenes (NHCs) **I** first isolated in 1991³⁶ are stabilized by two nitrogen ylide resonance forms as shown in Figure 0.8. Many examples are crystalline solids that are indefinitely stable thermally if kept out of the presence of oxygen and water. Because of their remarkable stability, the advent of the NHC began a new era of intense carbene research.³⁷

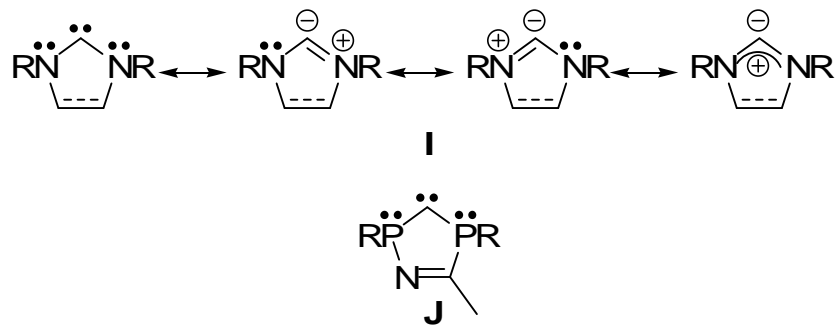


Figure 0.8. General structure of N-Heterocyclic Carbenes (NHCs) **I** with their resonance structures and P-Heterocyclic Carbene (PHC) **J**.

The mechanism of stabilization of nitrogen ylides, and by extension NHCs, is much different than phosphorus. There are no d-orbitals available to act as electron acceptors and negative hyperconjugation is not a factor because the σ^* orbitals are too high in energy. The largest stabilizing contribution of nitrogen is the lone pair of electrons that are efficient donors into the $p\pi$ orbital of the carbene. This contrasts the stabilization mode of carbene **H**, where negative hyperconjugation to both phosphorus and silicon supplement the donation of the phosphorus lone pair, which is significantly weaker than nitrogen. The $p\pi$

donation difference can be drastically demonstrated by calculating the energy difference between the singlet and triplet states (ΔE_{s-t}). In the case of NHCs, ΔE_{s-t} has been calculated to be 84.5 kcal/mol, while P-Heterocyclic carbene of type **J** (Figure 0.8) have a calculated value of 21.0 kcal/mol.³⁸ While phosphorus maintains a special place of stability and utility in ylide chemistry, nitrogen and NHCs hold a similar place in carbene chemistry.

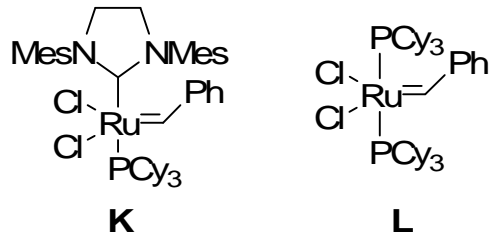


Figure 0.9. The second generation Grubbs catalyst with an ancillary NHC ligand **K** and the phosphine based first generation catalyst **L**.

While NHCs of type **I** have garnered the most attention there is a large array of substitution patterns that have led to carbenes of varying stability a full list of which is beyond the scope of the current discussion. Some general consideration should, however, be noted. Carbene transition metal complexes have been known since the 1960's³⁹ but their use as ancillary ligands for homogeneous catalysts has become increasingly important since the advent of NHCs which are relatively easy to handle and the free species can be used to make many complexes. Also they are similar to phosphines in that they are strong σ -donors and weak π -acceptors: Two qualities that create electron rich metal centers which are

desirable for many catalytic transformations. The clearest example of this is the second generation Grubb's metathesis catalyst **K** wherein one phosphine of the first generation catalyst **L** is replaced by an NHC (Figure 0.9).⁴⁰ Catalyst **K** displays increased activity yet remains as robust or even more so than **L**. While this is a telling case it is not alone and NHCs have been used to replace phosphine ligands in many catalysts to great effect. In contrast, carbene **H** does not even coordinate transition metals. The reason for this is many fold but calculations have been done that demonstrate a general trend of poor ligand behavior from acyclic carbenes (either lack of coordination or labile coordination). The calculations show that the angle at the carbene center plays an important role in the coordination behavior because as the angle decreases the s character of the occupied carbene orbital increases, this in turn improves the strength of the coordination. There is also steric concerns that stem from larger carbene bond angles.⁴¹

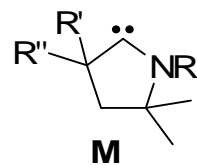


Figure 0.10. Cyclic Alkyl Amino Carbenes (CAACs) **M**.

For this reason the many acyclic carbenes are fundamentally interesting but have found few practical uses and therefore cyclic carbenes have been the focal point of recent research. While NHCs are demonstrably better ligands than

phosphines in many cases, there are continued efforts to further increase the donating ability of carbene ligands. To do this one nitrogen substituent could be replaced by a sp^3 carbon, which acts as a spectator group (a group that does not electronically contribute to the stabilization of the carbene), within the cyclic skeleton to give Cyclic Alkyl Amino Carbenes (CAACs) of type **M** (Figure 0.10).⁴²

The CAACs were proved to be stronger transition metal ligands than NHCs and have shown several remarkable catalytic results.⁴² The reason for the increased coordination ability is obviously the lack of one nitrogen. While nitrogen has proved to be the perfect π donor substituent it falls short of the ideal substituent because it is by far more electronegative than carbon and thus acts as a σ withdrawing group. The effect is a decrease in the electron density at the carbene center and a corresponding loss in coordination strength. Because only one electron donating group is necessary the array of carbenes possible increases greatly.

Carbenes have been utilized in another fashion relative to this work and once again as phosphine analogs to create what has been termed by Frenking as a carbodicarbene (**N** Figure 0.11).⁴³ The concept is similar to carbodiphosphoranes **E**,²⁸ and can be drawn in the same way (**N**¹) but of course in this case the stabilization is not technically ylidic in nature because the 1,2 zwitterion does not contain a heteroatom but rather two carbon atoms and the cationic charge is delocalized to the vicinal nitrogens. Once again an allenic form **N**² would seem to be the more logical form except for the fact that the bond angle is significantly

bent (134.8°) leading to the appellation bent allen e.⁴⁴ A structure where a C⁰ is stabilized by two coordinating carbenes (N³) has even been suggested but calculations and the short carbon-carbon bonds would tend to minimize the importance of this structure.



Figure 0.11. Bent allene (carbodicarbene) **N** with resonance structures.

The idea behind the development of bent allenes is not just fundamental. The goal was also to create transition metal ligands that are stronger donors than carbenes. With a formal dianionic carbon-donor, metal to ligand π back-bonding would be essentially eliminated, making bent allenes complexes incredibly electron rich and potentially ideal ligands for catalysis. The arguments against acyclic carbenes should also hold true and while acyclic bent allene **N** does bind to metals the complexes are not robust (Figure 0.12). Therefore, cyclic bent allenes **O** have been synthesized and their use as homogeneous catalyst ligands is currently actively being researched.⁴⁵

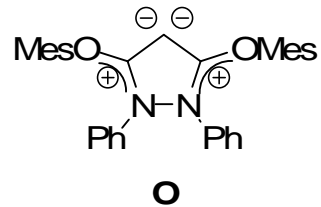


Figure 0.12. Cyclic bent allene **O**.

This work is related to all of these subjects. The goal of which was to use the unique properties of ylides and carbenes to develop new species that are either fundamentally interesting for their unique structures and properties, useful ligands with novel properties for use in transition metal catalysis, or both.

References

1. Ylides and Imines of Phosphorus (ed. A. W. Johnson) Wiley-Interscience, New York, NY, **1993**.
2. A. Michaelis, H. V. Gimborn, *Cher. Ber.* **1894**, 27, 272.
3. G. Aksnes, *Acta Chem. Scand.* **1961**, 15, 438.
4. H. Staudinger, J. Meyer, *Helv. Chim. Acta.* **1919**, 2, 635.
5. a) A. Michaelis, *Liebigs Ann. Chem.* **1902**, 321, 174, b) F. Krohnke, *Chem. Ber.* **1950**, 83, 291.
6. C. K. Ingold, J. A. Jessop, *J. Chem. Soc.* **1930**, 713.
7. F. Krohnke, *Chem. Ber.* **1935**, 68, 1177.
8. G. Wittig, G. Geissler, *Liebigs Ann. Chem.* **1953**, 580, 44.
9. Ylide Chemistry (ed. A. T. Blomquist) Academic Press, New York, NY, **1966**.
10. A. Streitweiser, A. Rajca, R. S. McDowell, R. Glaser, *J. Am. Chem. Soc.* **1987**, 109, 4184.
11. A. E. Reed, G. Weinhold, L. A. Curtiss, *Chem. Revs.* **1988**, 88, 899.
12. S. M. Bachrauch, *J. Org. Chem.* **1992**, 57, 4367
13. J. C. J. Bart, *J. Chem. Soc. (B)*, **1969**, 350
14. a) D. A. Dixon, T. H. Dunning, R. A. Eades, P. G. Gassman, *J. Am. Chem. Soc.* **1983**, 105, 7011, b) R. A. Eades, P. G. Gassman, D. A. Dixon, *J. Am. Chem. Soc.* **1981**, 103, 1066.
15. W. G. Daubin, J. D. Robbins, *Tetrahedron Lett.* **1975**, 2, 151.
16. G. Wittig, H. Pommer, Ger. Patent 32741 IVB/120, **1954**.
17. F. N. Tebbe, G. W. Parshall, G. S. Reddy, *J. Am. Chem. Soc.* **1978**, 100, 3611.
18. E. J. Corey, M. Chaykovsky, *J. Am. Chem. Soc.* **1962**, 84, 867.

-
19. a) L. Horner, H. Hoffmann, H. G. Wippel, G. Klahre, *Chem. Ber.* **1959**, 92, 2499, b) W. S. Wadsworth, W. D. Emmons, *J. Am. Chem. Soc.* **1961**, 62, 1733.
 20. M. Julia, J. M. Paris, *Tetrahedron Lett.* **1973**, 4833.
 21. D. J. Peterson, *J. Org. Chem.* **1968**, 33, 780.
 22. G. Wittig, M. Reiber, *Liebigs Ann. Chem.* **1949**, 562, 177.
 23. H. Schmidbaur, W. Tronich, *Chem. Ber.* **1968**, 101, 3556.
 24. M. Schlosser, T. Kadibelbon, G. Steinhoff, *Angew. Chem.* **1966**, 5, 968.
 25. E. J. Corey, J. Kang, K. Kyler, *Tetrahedron Lett.* **1985**, 26, 555.
 26. a) B. Schaub, T. Jenny, M. Schlosser, *Tetrahedron Lett.* **1984**, 4097, b) B. Schaub, M. Schlosser, *Tetrahedron Lett.* **1985**, 1623.
 27. F. Ramirez, N. B. Desai, B. Hansen, N. McKelvie, *J. Am. Chem. Soc.* **1961**, 83, 3539.
 28. R. Tonner, F. Öxler, B. Neumüller, W. Petz, G. Frenking, *Angew. Chem. Int. Ed.* **2006**, 45, 8038.
 29. C. N. Matthews, G. H. Birum, *Acc. Chem. Res.* **1969**, 2, 373.
 30. G. H. Birum, C. N. Matthews, *J. Org. Chem.* **1967**, 32, 3554.
 31. a) G. Ege, K. Gilbert, *Tetrahedron Lett.* **1979**, 1567; b) G. Ege, K. Gilbert, *J. Heterocycl. Chem.* **1981**, 18, 675; c) G. Markl, *Naturforsch.* **1962**, 17B, 782.
 32. a) H. Schmidbaur, T. Costa, B. Milewski-Mahrila, U. Schubert, *Angew. Chem.* **1980**, 92, 557, b) S. Marrot, T. Kato, H. Gornitzka, A. Baceiredo, *Angew. Chem. Int. Ed.* **2006**, 45, 2598.
 33. E. Buchner and T. Curtius, *Ber. Dtsch. Chem. Ges.* **1885**, 8, 2377.
 34. A. Igau, H. Grützmacher, A. Baceiredo, G. Bertrand, *J. Am. Chem. Soc.* **1988**, 110, 6463.
 35. T. Kato, H. Gornitzka, A. Baceiredo, A. Savin, G. Bertrand, *J. Am. Chem. Soc.* **2000**, 122, 998.

-
36. A. J. Arduengo III, R. L. Harlow, M. Kline, *J. Am. Chem. Soc.* **1991**, *113*, 361.
 37. a) F. E. Hahn, M. C. Jahnke, *Angew. Chem., Int. Ed.* **2008**, *47*, 3122; b) N-Heterocyclic Carbenes in Synthesis; (ed. S. P. Nolan), Wiley-VCH: New York, **2006**; c) F. Glorius, N-Heterocyclic Carbenes in Transition Metal Catalysis (Topics in Organometallic Chemistry); Springer-Verlag: New York, **2006**; d) F. E. Hahn, *Angew. Chem., Int. Ed.* **2006**, *45*, 1348;; e) N. Kuhn, A. Al-Sheikh, *Coord. Chem. Rev.* **2005**, *249*, 829; f) E. Peris, R. H. Crabtree, *Coord. Chem. Rev.* **2004**, *248*, 2239; g) C. M. Crudden, D. P. Allen, *Coord. Chem. Rev.* **2004**, *248*, 2247; h) V. Cesar; S. Bellemín-Lapönnaz, L. H. Gade, *Chem. Soc. Rev.* **2004**, *33*, 619, i) N. M. Scott, S. P. Nolan, *Eur. J. Inorg. Chem.* **2005**, 1815; j) M. C. Perry, K. Burgess, *Tetrahedron: Asymmetry* **2003**, *14*, 951, k) W. A. Herrmann, *Angew. Chem., Int. Ed.* **2002**, *41*, 1290; l) D. Bourissou, O. Guerret, F. P. Gabbai, G. Bertrand, *Chem. Rev.* **2000**, *100*, 39.
 38. D. Martin, A. Baceiredo, H. Gornitzka, W. W. Schoeller, G. Bertrand, *Angew. Chem., Int. Ed.* **2005**, *44*, 1700.
 39. E. O. Fischer, A. Maasböl, *Angew. Chem. Int. Ed. Engl.* **1964**, *3*, 580.
 40. Handbook of Metathesis (ed. R. H. Grubbs) Wiley, Weinheim, Germany, **2003**.
 41. a) W. W. Schoeller, D. Eisner, S. Grigoleit, A. B. Rozhenko, A. Alijah, *J. Am. Chem. Soc.* **2000**, *122*, 10115; b) W. W. Schoeller, A. B. Rozhenko, A. Alijah, *J. Organomet. Chem.* **2001**, *617*, 435, c) W. W. Schoeller, *Eur. J. Inorg. Chem.* **2000**, 369.
 42. V. Lavallo, Y. Canac, C. Präsang, B. Donnadieu, G. Bertrand, *Angew. Chem. Int. Ed.* **2005**, *44*, 5705.
 43. R. Tonner, G. Frenking, *Angew. Chem. Int. Ed.* **2007**, *46*, 8697.
 44. a) A. Dyker, V. Lavallo, B. Donnadieu, G. Bertrand, *Angew. Chem. Int. Ed.* **2008**, *47*, 3206; b) A. Fürstner, M. Alcarazo, R. Goddard, C. W. Lehmann, *Angew. Chem. Int. Ed.* **2008**, *47*, 3210.
 45. V. Lavallo, A. Dyker, B. Donnadieu, G. Bertrand, *Angew. Chem. Int. Ed.* **2008**, *47*, 5411.

Chapter 1

Synthesis of a Mixed Phosphonium–Sulfonium Bisylide $R_3P=C=SR_2$

Phosphonium and sulfonium ylides are highly nucleophilic species, which feature a totally different reactivity. Whereas the former have been used extensively for olefination reactions,¹ the latter have mostly been involved in epoxidation reactions.² Carbodiphosphoranes (**A**) (Figure 1.1) contain two cumulated phosphorus ylide functions, and formally possess a carbon atom with two negative charges, which are stabilized by two phosphonium groups. Since their discovery in 1961 by Ramirez et al.,³ their unique bonding system and reactivity have attracted considerable interest.^{1a, 4, 5} In contrast, only one example of a sulfur-containing bisylide (**B**) has been reported.⁶ Interestingly the crystal structure of sulfur bisylide **B** does indicate it can be best described with two ylidic bonds as is common with carbodiphosphoranes **A**.

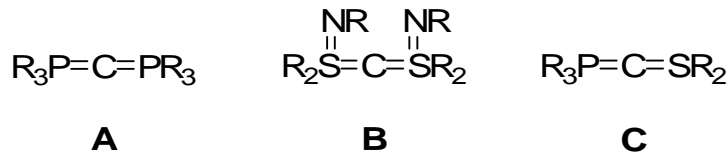
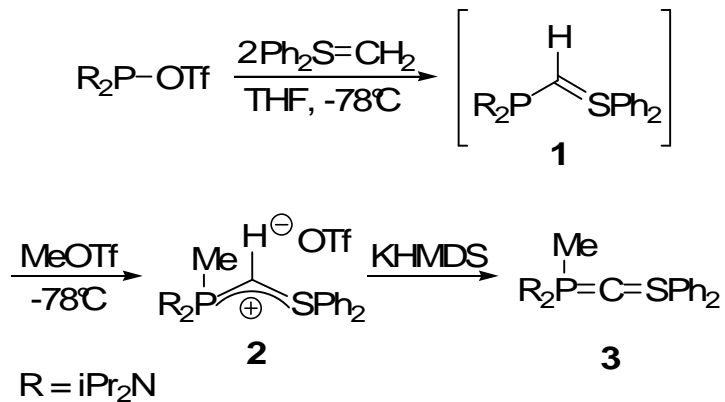


Figure 1.1. Molecular structure of bisylides **A**, **B** and **C**.

Here we report the synthesis and characterization of the first persistent mixed phosphorus–sulfur bisylide (**C**). Such compounds have never been isolated or even observed by spectroscopic methods

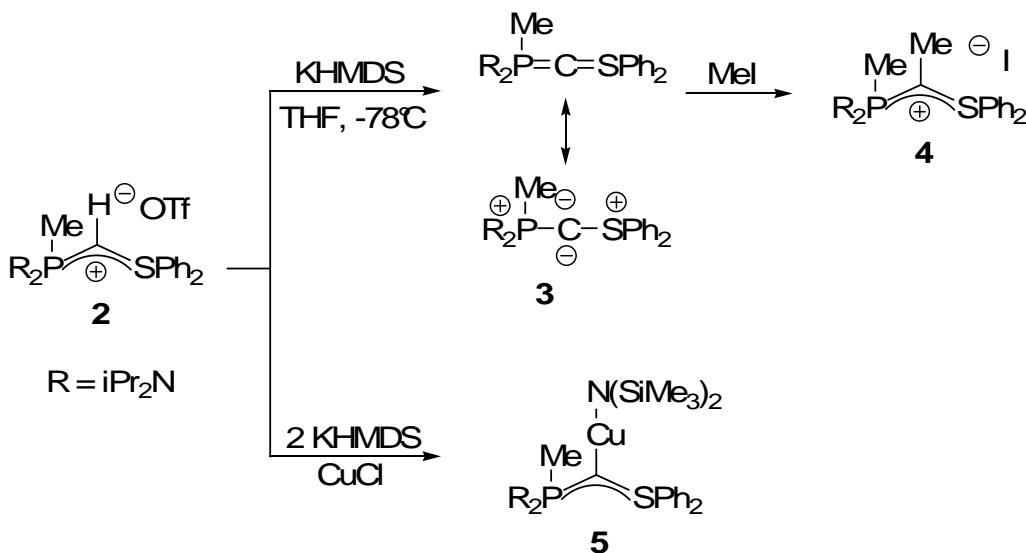
Abstraction of a proton from the corresponding conjugated acid is the classical method for preparing ylides; thus, phosphonium salt **2**, (Scheme 1.1) which already features the phosphorus-carbon-sulfur (PCS) skeleton, appeared to be a potential precursor for the desired cumulene **C**. Treatment of bis(diisopropylamino)phosphonium triflate⁷ with two equivalents of diphenylsulfonium ylide in THF solution at -78°C gave C-phosphonium sulfonium ylide **1** in quantitative yield, which could be characterized in solution (³¹P NMR: $\delta = 53.0$ ppm). However, ylide **1** appeared to be thermally labile, and therefore was treated in situ with one equivalent of MeOTf at -78°C. The P-methyl derivative **2** was isolated as a white powder in 91% yield, and X-ray quality single crystals were grown from a CH₂Cl₂/ether solution at -30°C (Scheme 1.1, Figure 1.2).⁸



Scheme 1.1. Synthesis of sulfonium phosphaylide **2**. Ph = Phenyl, Tf = Triflate

The cumulene **3** was cleanly generated at -78°C by deprotonation of the corresponding salt **2** with either potassium or sodium hexamethyldisilazane

(Scheme 1.2). The neutral structure of **3** was indicated by its very high solubility in non polar solvents such as pentane. Derivative **3** displays a singlet signal at $\delta = 44.0$ ppm in the $^{31}\text{P}\{1\text{H}\}$ NMR spectrum, while the central carbon atom appears as a doublet at $\delta = 36$ ppm ($J_{PC} = 86.4$ Hz) in the ^{13}C NMR spectrum. Although **3** is stable for days at temperatures lower than -20°C , it decomposes ($t_{1/2} = 10$ h, in C_6D_6) at room temperature to give a complex mixture.



Scheme 1.2. Synthesis and reactivity of bisylide **3**.

All attempts to grow X-ray quality single crystals for diffraction analysis failed because of the high reactivity of **3**. However, the formation of **3** was clearly demonstrated by its chemical reactivity. Addition of MeI to a solution of **3** in THF cleanly and quantitatively gave the C-methylated salt **4**, which was fully characterized, including by X-ray diffraction analysis (Figure 1.3).⁸ Furthermore, we also successfully synthesized the Cu(I) complex **5** by the reaction of **2** with

copper chloride in the presence of an excess of potassium hexamethyldisilazane (KHMDS). X-ray quality crystals of **5** were grown from a toluene solution, and its structure⁸ (Figure 1.4) showed a similar geometry to that of a carbodiphosphorane–CuI complex.⁹ The P1–C1–S1 angle is rather acute (115.38°) and the P–C1 (1.709 Å) and S–C1 bond lengths (1.677 Å) are slightly shorter than those of the corresponding protonated cation **2**.

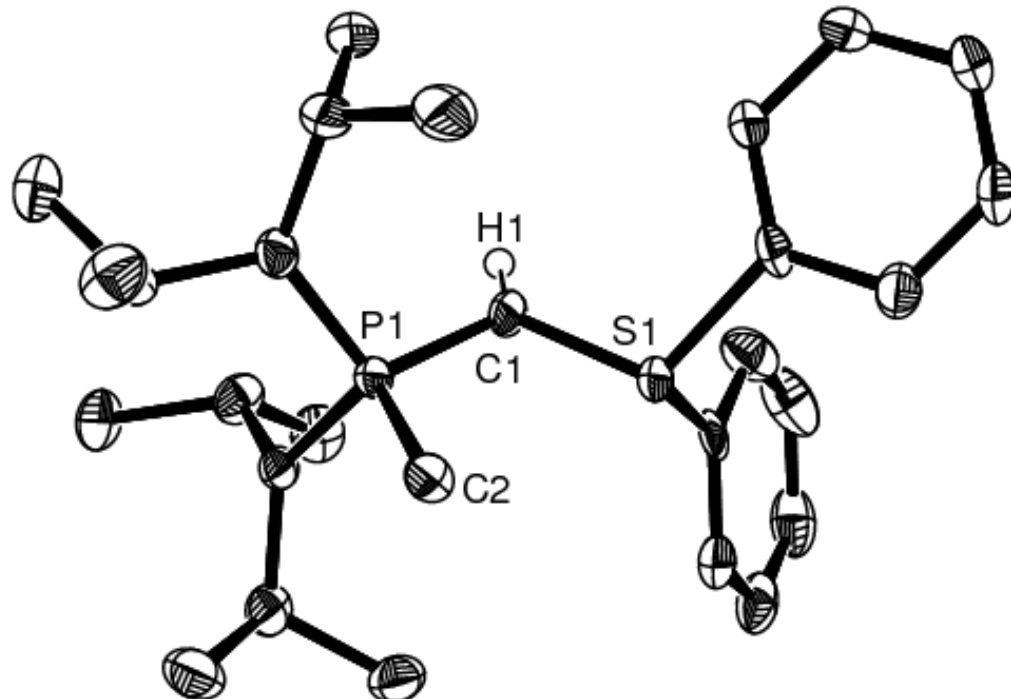


Figure 1.2. X-ray crystal structures of **2**. Hydrogen atoms and triflate counterion omitted for clarity. Thermal ellipsoids are drawn at the 50% level. Selected bond lengths [Å] and angles [°]. P1–C1 1.721(5), S1–C1 1.690(4), P1–C2 1.796(4), S1–C3 1.810(5), P1–C1–S1 118.0(3).

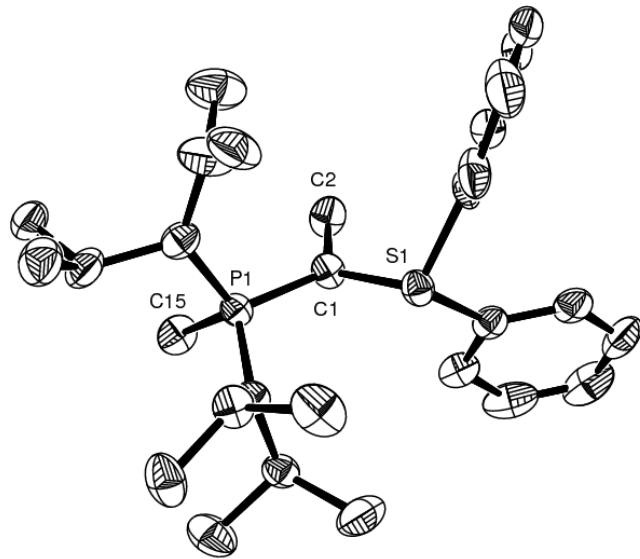


Figure 1.3. X-ray crystal structure of **4**. Hydrogen atoms and iodide counterion omitted for clarity. Thermal ellipsoids are drawn at the 50% level. Selected bond lengths [\AA] and angles [$^\circ$]. P1–C1 1.726(5), S1–C1 1.677(4), P1–C15 1.805(4), C1–C2 1.515(5), P1–C1–S1 117.7(2).

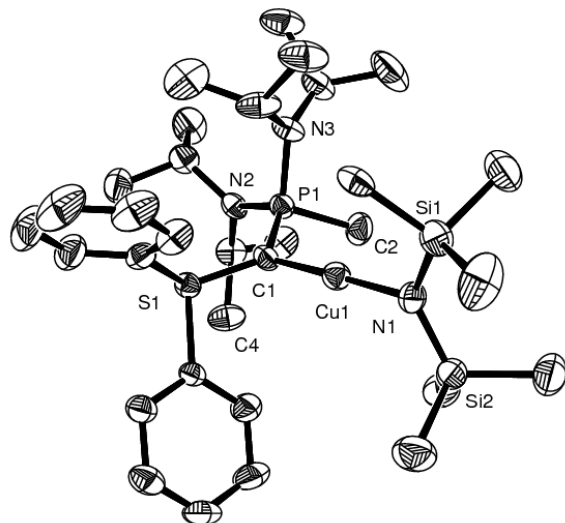


Figure 1.4. X-ray crystal structure **5**. Hydrogen atoms omitted for clarity. Thermal ellipsoids are drawn at the 50% level. Selected bond lengths [\AA] and angles [$^\circ$]. P1–C1 1.709(5), S1–C1 1.677(5), P1–C2 1.804(5), C1–Cu1 1.903(4), N1–Cu1 1.874(4), P1–C1–S1 115.3(2), C1–Cu1–N1 176.97(18), S1–C1–Cu 1125.7(3), P1–C1–Cu1 118.7(2).

To gain insight into the electronic structure of **3**, calculations by geometry optimization, natural population analysis (NPA), and natural bond orbital (NBO) analysis were performed on the model compound **6** [$R = N(Me)_2$] and its protonated triflate salt **7**. The geometries of **6** and **7** are shown in Figure 1.5.

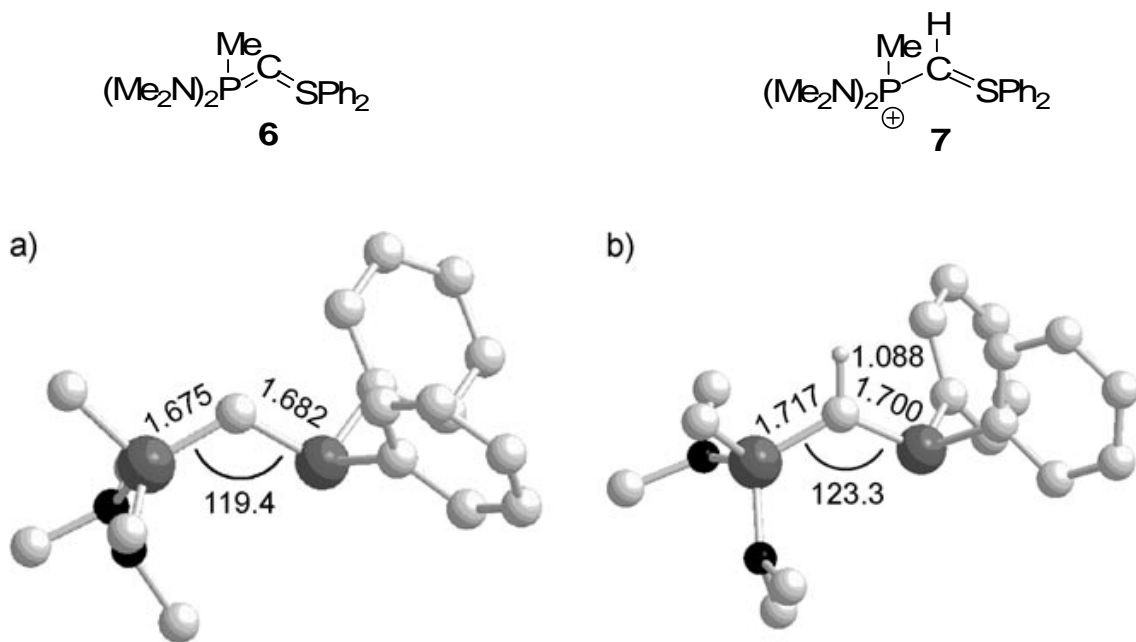


Figure 1.5. Structures of **6** (a) and **7** (b) optimized at the B3LYP/6-31 + G(d,p) level of calculation. Interatomic distances are in Å and bond angles in degrees. Hydrogen atoms and the triflate anion (for **7**) are omitted for clarity.

The optimized geometry of **7** agrees reasonably well with the experimentally obtained structure of **2**. Each molecule shows a strongly bent P–C–S arrangement. The deprotonation essentially affects only the P–C bond, as can be seen by the larger variation in bond lengths ($\Delta_{P-C} = 0.042 \text{ \AA}$; $\Delta_{S-C} = 0.018 \text{ \AA}$), and in the Wiberg bond indexes ($\Delta_{P-C} : 0.320$; $\Delta_{C-S} : 0.134$).

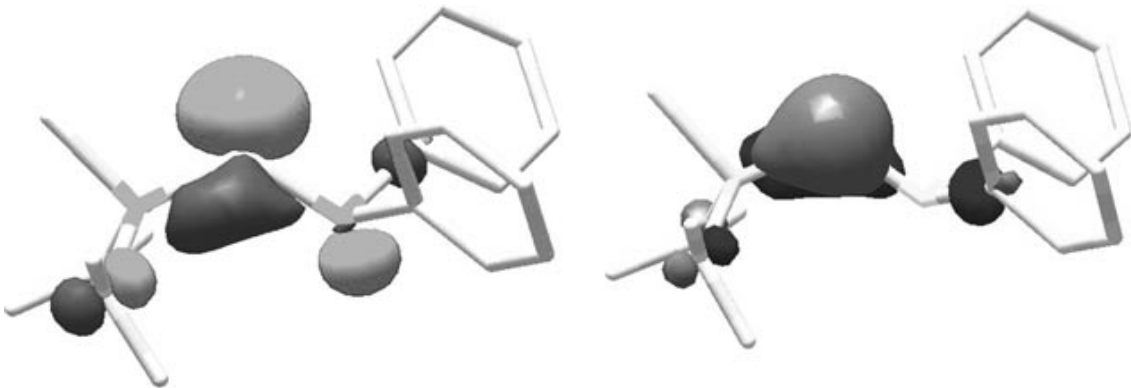


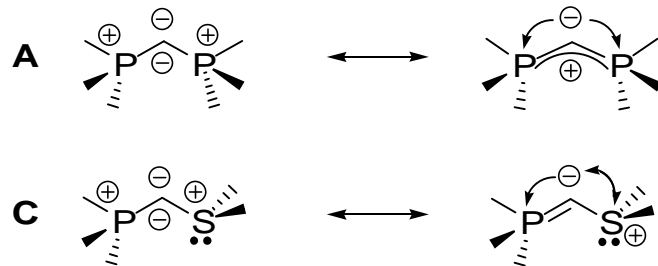
Figure 1.6. Highest occupied molecular orbitals of **6** : HOMO (left) and HOMO-1 (right).

Figure 1.6 shows the two highest occupied molecular orbitals (HOMOs) of **6**. The HOMO is an orbital of σ symmetry which corresponds mainly to the in-plane lone pair of electrons on the C atom, while HOMO-1 is the $\pi(P\text{-}C)$ bonding orbital, which is strongly polarized towards the C atom.

In the P–C–S moiety of **6**, the NBO procedure identified a P=C bond and a C–S bond, along with lone pair electrons on C and S atoms. The $\pi(P\text{-}C)$ orbital has a low occupancy (1.663) and it is strongly polarized toward the C atom (88% of contribution), which could also be viewed as a second lone pair of electrons on the C atom. The occupancy of the corresponding antibonding orbital (with an 88% contribution from the P atom) is 0.171.

Contrary to the carbodiphosphorane case where the n_{σ} orbital is stabilized by favorable interactions with $\sigma^*_{P\text{-}R}$ orbitals (negative hyperconjugation),¹⁰ the antiperiplanar relationship between the $n_{\sigma C}$ and n_S orbitals in P,S bisylides is

destabilizing.¹¹ This finding explains the small variation of the S–C bond length compared to that of the P–C bond after the deprotonation of **7** (Scheme 1.3).



Scheme 1.3. Schematic representation of the modes of stabilization of carboradiphosphoranes **A** and P,S bisylides **B**.

The NPA shows (Table 1.1) that the central carbon atom of **6** bears a strong negative charge (-1.357 a.u.), which is compensated by the positive charges of the SPh_2 and $\text{P}(\text{Me})(\text{NMe}_2)_2$ fragments. Upon protonation, the negative charge of the central carbon atom slightly decreases and most of the positive charge (0.320 a.u.) goes to the $\text{P}(\text{Me})(\text{NMe}_2)_2$ fragment.

Table 1.1: Natural population analysis^[a] of **6** and **7** ($\text{R} = \text{NMe}_2$)

Molecule	$\text{C}^{[b]}$	H	S	SPh_2	P	PMer_2
6	-1.357		0.874	0.585	1.947	0.771
7	-1.235	0.315	0.926	0.797	2.055	1.049

[a] In arbitrary units (a.u.). [b] Central carbon atom.

As expected, because of the high negative charge density on the central carbon atom, the gas-phase proton affinity of **6** (290.3 kcal mol⁻¹) is larger than that of carbodiphosphoranes (270–280 kcal mol⁻¹).¹²

The preparation of such derivatives should be of major significance because of the synthetic impact of both types of ylides (P and S). Additionally this species opens the way for a reagent that could be used for tandem Wittig olefination, Corey-Chaykovsky epoxidation. Such a reagent could also be used to compare and contrast the reactivities of phosphorus and sulfur ylides. This work as well as isolation of an indefinitely stable phosphorus-sulfur bisylide is ongoing.

Experimental

All manipulations were performed under an inert atmosphere of argon and by using standard Schlenk techniques. Dry, oxygen-free solvents were employed.

^1H , ^{13}C , ^{31}P NMR spectra were recorded on a Bruker WM 250 and Bruker Avance 300 spectrometers. ^1H and ^{13}C NMR chemical shift were reported in ppm relative to Me_4Si as an external standard. ^{31}P NMR downfield chemical shifts are expressed with a positive sign, in ppm, relative to the standard of 85% H_3PO_4 .

Diphenylsulfonium phosphaylide **2**: A solution of nBuLi (1.6m in hexanes, 2.0 mmol) was added dropwise to a solution of diphenylmethylsulfonium triflate (0.70 g, 2.0 mmol) in THF (10 mL) at -78°C affording the diphenylmethylsulfonium ylide. After 15 min at -78°C , a solution of bis(diisopropylamino)phosphonium triflate (0.38 g, 1.0 mmol) in THF (20 mL) was added, and the mixture was then stirred at the same temperature for 2 h. Then, methyl triflate (0.16 g, 1.0 mmol) was added and the reaction mixture was slowly warmed to room temperature over 12 h. After removal of all volatiles under vacuum, the product was extracted with CH_2Cl_2 . Derivative **2** was obtained in the solid state after crystallization from $\text{CH}_2\text{Cl}_2/\text{Et}_2\text{O}$ at -30°C (0.54 g, 91%). m.p. 102–103°C; $^{31}\text{P}\{\text{H}\}$ NMR (CDCl_3 , 25°C, 121 MHz): δ = 53.0 ppm; ^1H NMR (CDCl_3 , 25°C, 300 MHz): δ = 1.17 (d, $^4J_{\text{HH}} = 7$ Hz, 24H, CH_3), 2.02 (d, $^2J_{\text{PH}} = 12.9$ Hz, 3H, PCH_3), 2.42 (d, $^2J_{\text{PH}} = 13.9$ Hz, 1H, CH), 3.52–3.74 (m, 4H, CH), 7.43–7.52 ppm (m, 10H, CH_{arom}); ^{13}C NMR (CDCl_3 , 25°C, 75 MHz): δ = 15.9 (d, $^1J_{\text{CP}} = 109.0$ Hz, CH_3), 18.4 (d, $^1J_{\text{CP}} = 41.6$

Hz, PCH), 23.4 (s, CH₃), 46.9 (d, ²J_{CP} = 5.5 Hz, NCH), 121.6 (q, ¹J_{CF} = 319 Hz, CF₃), 127.1, 130.5, 131.7 (s, CH_{arom}), 137.5 ppm (s, C_{ipso}).

Phosphorus-sulfur bisylide 3: C₆D₆ (1 mL) was added to a mixture of KHMDS (0.12 g, 0.6 mmol) and phosphoniosulfonium ylide **2** (0.28 g, 0.5 mmol) at 0°C, and the mixture was then warmed to room temperature. The product **3** was characterized without any purification. ³¹P{¹H} NMR (CDCl₃, 25°C, 121 MHz): δ = 44.6 ppm; ¹H NMR (CDCl₃, 25°C, 300 MHz): δ = 1.17 (d, ⁴J_{HH} = 6.0 Hz, 12H, CH₃), 1.36 (d, ⁴J_{HH} = 6.0 Hz, 12H, CH₃), 1.79 (d, ²J_{PH} = 12.0 Hz, 3H, PCH₃), 3.44 (d-sept, ³J_{PH} = 15.0 Hz, ³J_{HH} = 6.0 Hz, 4H, CH), 7.01 (t, ³J_{HH} = 9.0 Hz, 2H, CH_{arom}), 7.19 (m, 4H, CH_{arom}), 8.00 ppm (d, ³J_{HH} = 6.0 Hz, 4H, CH_{arom}); ¹³C NMR (CDCl₃, 25°C, 75 MHz): δ = 21.5 (d, ¹J_{CP} = 75.7 Hz, PCH₃), 23.4 (d, ²J_{CP} < 1 Hz, CH₃), 24.0 (s, CH₃), 35.9 (d, ¹J_{CP} = 86.6 Hz, PCS), 45.5 (s, NCH), 123.0, 128.3, 128.6 (s, CH_{arom}), 151.2 ppm (d, ³J_{CP} = 23.7 Hz, C_{ipso}).

Compound 4: Methyl iodide (0.14 g, 1.0 mmol) was added to the solution of **2** in THF (2 mL), generated from **3** (0.59 g, 1.0 mmol) in the presence of KHMDS (0.24 g, 1.2 mmol) at -78°C. After warming the solution to room temperature, all volatiles were removed under vacuum. The product was extracted with CH₂Cl₂ and the pure product **4** was obtained after drying under vacuum. X-ray quality crystals were grown from CH₂Cl₂/Et₂O solution at -30°C (0.35 g, 57%); ³¹P{¹H} NMR (CDCl₃, 25°C, 121 MHz): δ = 66.1 ppm; ¹H NMR (CDCl₃, 25°C, 300 MHz): δ = 1.19 (d, ³J_{HH} = 7 Hz, 12H, CH₃), 1.23 (d, ³J_{HH} = 7 Hz, 12H, CH₃), 1.54 (d, ³J_{PH} =

11.9 Hz, 3H, PCH₃), 2.10 (d, ³J_{PH} = 13.5 Hz, 3H, CCH₃), 3.44 (d-sept, ³J_{PH} = 12.4 Hz, ³J_{HH} = 6.7 Hz, 4H, CH), 7.34–7.53 ppm (m, 10H, CH_{arom}); ¹³C NMR (CDCl₃, 25°C, 75 MHz): δ = 11.3 (d, ²J_{CP} = 11.1 Hz, CH₃), 17.9 (d, ¹J_{CP} = 96.1 Hz, PCH₃), 24.3 (d, ³J_{CP} = 2.8 Hz, CH₃), 24.7 (d, ³J_{CP} = 2.8 Hz, CH₃), 48.0 (d, ²J_{CP} = 6.5 Hz, NCH), 48.9 (d, ²J_{CP} = 6 Hz, NCH), 121.6 (q, ¹J_{CF} = 319 Hz, CF₃), 128.5, 130.5, 131.9 (s, CH_{arom}), 132.2 ppm (s, C_{ipso}).

Compound 5: A mixture of phosphonium salt **2** (0.20 g, 3.31 mmol), excess KHMDS (0.20 g, 9.94 mmol), and anhydrous copper(I) chloride (0.033 g, 3.31 mmol) were cooled to –78°C and then THF (4 mL) was added. The mixture was stirred and warmed to room temperature over 12 h. All volatiles were removed under vacuum and the product was extracted with toluene (3 mL). Pale yellow crystals were grown from a concentrated toluene solution (139 mg, 63%). m.p. 78–79°C; ³¹P{₁H} NMR (CDCl₃, 25°C, 121 MHz): δ = 66.5 ppm; ¹H NMR (C₆D₆, 25°C, 300 MHz): δ = 0.63 (s, 18H, SiCH₃), 1.07 (d, ³J_{HH} = 6.7 Hz, 12H, CH₃), 1.25 (d, ³J_{HH} = 6.7 Hz, 12H, CH₃), 2.04 (d, ³J_{PH} = 12.4 Hz, 3H, PCH₃), 7.07–7.24 (m, 6H, CH_{arom}), 8.07–8.10 ppm (m, 4H, CH_{arom}); ¹³C NMR (CDCl₃, 25°C, 75 MHz): δ = 11.3 (d, ²J_{CP} = 11.1 Hz, CH₃), 17.9 (d, ¹J_{CP} = 96.1 Hz, PCH₃), 24.3 (d, ³J_{CP} = 2.8 Hz, CH₃), 24.7 (d, ³J_{CP} = 2.8 Hz, CH₃), 48.0 (d, ²J_{CP} = 6.5 Hz, NCH), 48.9 (d, ²J_{CP} = 6 Hz, NCH), 121.6 (q, ¹J_{CF} = 319 Hz, CF₃), 128.5, 130.5, 131.9 (s, CH_{arom}), 132.2 ppm (s, C_{ipso}).

References

1. a) O. I. Kolodiaznyi in *Phosphorus Ylides: Chemistry and Application in Organic Synthesis*, Wiley-VCH, Weinheim, **1999**; b) A. D. Abell, M. K. Edmonds in *Organophosphorus Reagents* (Ed.: P. J. Murphy), Oxford University Press, Oxford, **2004**, pp. 99 – 127; c) M. Edmonds, A. Abell in *Modern Carbonyl Olefination* (Ed.: T. Takeda), Wiley-VCH, Weinheim, **2004**, pp. 1 – 17; d) K. C. Nicolaou, M.W. HKrter, J. L. Gunzner, A. Nadin, *Liebigs Ann.* **1997**, 1283; e) H. Pommer, *Angew. Chem. Int. Ed. Engl.* **1977**, *16*, 423.
2. For reviews on sulfonium ylides, see a) V. K. Aggarwal, C. L. Winn, *Acc. Chem. Res.* **2004**, *37*, 611; b) Nitrogen, Oxygen, and Sulfur Ylide Chemistry (Ed.: S. J. Clark), Oxford University Press, Oxford, **2002**; c) Y. G. Gololobov, A. N. Nesmeyanov, V. P. Lysenko, I. E. Boldeskul, *Tetrahedron* **1987**, *43*, 2609, and references therein.
3. F. Ramirez, N. B. Desai, B. Hansen, N. McKelvie, *J. Am. Chem. Soc.* **1961**, *83*, 3539.
4. For reviews on ylides and carbodiphosphoranes chemistry, see a) O. I. Kolodiaznyi, *Tetrahedron* **1996**, *52*, 1855; b) *Ylides and Imines of Phosphorus* (Ed.: A.W. Johnson), Wiley, New York, **1993**; c) H. Schmidbaur, *Angew. Chem. Int. Ed. Engl.* **1983**, *22*, 907.
5. Particularly, carbodiphosphoranes are electron-rich carboncentered ligands: a) S. Marrot, T. Kato, H. Gornitzka, A. Baceiredo, *Angew. Chem. Int. Ed.* **2006**, *45*, 2598; b) K. Kubo, N. D. Jones, M. J. Ferguson, R. McDonald, R. G. Cavell, *J. Am. Chem. Soc.* **2005**, *127*, 5314; c) W. Petz, C. Kutschera, B. Neumüller, *Organometallics* **2005**, *24*, 5038; d) W. Petz, C. Kutschera, M. Heitbaum, G. Frenking, R. Tonner, B. Neumüller, *Inorg. Chem.* **2005**, *44*, 1263.
6. T. Fujii, T. Ikeda, T. Mikami, T. Suzuki, T. Yoshimura *Angew. Chem.* **2002**, *114*, 2688–2690; *Angew. Chem. Int. Ed.* **2002**, *41*, 2576.
7. A. H. Cowley, R. Kemp, *Chem. Rev.* **1985**, *85*, 367.
8. CCDC 659272 (**2**), 659273 (**4**), and 659994 (**5**) contain the supplementary crystallographic data for this chapter. These data can be obtained free of charge from The Cambridge Crystallographic Data Centre via www.ccdc.cam.ac.uk/data_request/cif. Full data is also found in the appendix.

-
9. H. Schmidbaur, C. E. Zybill, G. Müller, C. Krüger, *Angew. Chem. Int. Ed. Engl.* **1983**, *22*, 729.
 10. D. G. Gilheany, *Chem. Rev.* **1994**, *94*, 1339.
 11. S. Wolfe, A. Stolow, L. A. LaJohn, *Tetrahedron Lett.* **1983**, *24*, 4071.
 12. R. Tonner, F. Öxler, B. Neumüller, W. Petz, G. Frenking, *Angew. Chem. Int. Ed.* **2006**, *45*, 8038.

Chapter 2

Cyclic (Amino)[bis(ylide)]carbene as an Anionic Bidentate Ligand for Transition Metal Complexes

N-Heterocyclic carbenes (NHCs) have been extensively studied both as free species¹ and as ligands for metal centers.² Replacement of one of the electronegative amino groups of NHCs **A** by an alkyl group results in cyclic (alkyl)(amino)carbenes (CAACs) **B**,^{3a-c} which feature a smaller HOMO-LUMO gap but importantly a HOMO that is higher in energy (stronger σ -donor character) (Figure 2.1). The unique ligand properties of CAACs have been demonstrated by the isolation of otherwise unstable low coordinate transition metal species,^{3d} and by the excellent catalytic properties of their palladium,^{3a} gold^{3e} and ruthenium complexes.^{3f,g} It seemed likely that the replacement of the σ -donor alkyl group of **B** by a carbon based π -donor, such as a phosphorus ylide, as shown in **C**, would further enhance the nucleophilic character of the carbene center. In fact, metal complexes featuring the benzo-fused version **D** as ligands have been isolated.^{4, 5} They were first synthesized from isocyanide complexes⁴ rather than free carbenes, which limited the choice of the substituents as well as of the metals that can be used. However, recently, Kawashima et al.⁵ reported the transient formation of carbene **D**, and the isolation of the ensuing Rh and Pd complexes. Based on the CO stretching frequency of the Rh(carbene)(CO)₂Cl

complex, they concluded that carbene **D** was indeed a stronger σ -donor than NHCs **A** and CAACs **B**.

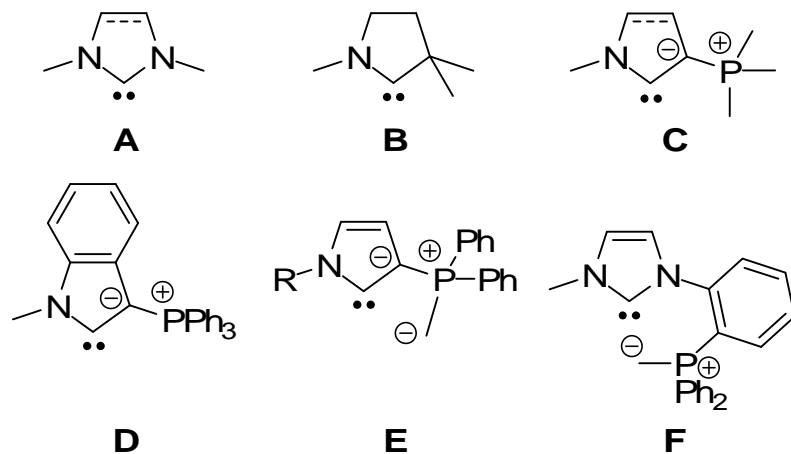
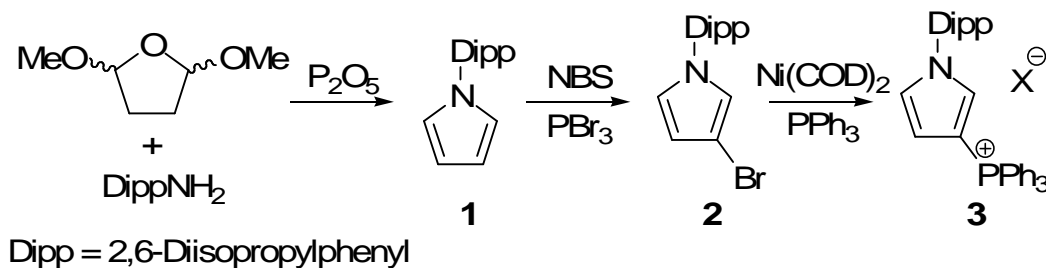


Figure 2.1. Carbenes **A-D**, (amino)[bis(ylide)carbene] **E** and the NHC-ylide carbene **F**.

Here we report that our search for preparing carbenes of type **C** has serendipitously led to the discovery of the first stable lithium adduct of a cyclic (amino)[bis(ylide)]carbene **E**.⁶ This compound undergoes transmetallation reactions, which allow for the synthesis of a variety of transition metal complexes in which **E** acts as an LX bidentate ligand. Note that the first complex featuring an NHC/ylide bidentate ligand **F** was recently reported, and shown to be an effective catalyst in the Tsuji-Trost allylation reaction.⁷

Phosphonium salt **3** was readily prepared in 48% over all yield by slightly modified reported procedures.⁸ Addition of 2,5-dimethoxytetrahydrofuran to 2,6-diisopropylaniline gives the N-substituted pyrrole **1**.^{8a} Selective bromination

leads to compound **2**,^{8b} which is converted into the desired phosphonium salt **3** by a nickel-catalyzed coupling with triphenylphosphine.^{8c} Simple anion exchange, using sodium tetraphenyl borate, was done in order to increase the solubility and to facilitate purification of the salt (Scheme 2.1).



Scheme 2.1. Synthesis of Phosphonium salt **3**.

Attempts to deprotonate phosphonium salt **3** with a variety of bases (LDA, TMPLi, KHMDS, tBuLi) led to complex mixtures. A mixture of phenyl lithium and **3** in THF led one major product by ^{31}P NMR at -31.1 ppm. However, there was no indication of a carbenic peak in the ^{13}C NMR. Additional NMR studies (^1H and ^{13}C) as well as single crystal X-ray diffraction analysis¹⁰ (Figure 2.2) proved that the product is actually phosphine **4**. The formation of **4** can be explained by the ortho-metallation of one of the phenyl rings of the starting material to form **5**, which subsequently attacks an adjacent phenyl ring to give **6** followed by re-aromatization through elimination of benzene and formation of **4** (Scheme 2.2).

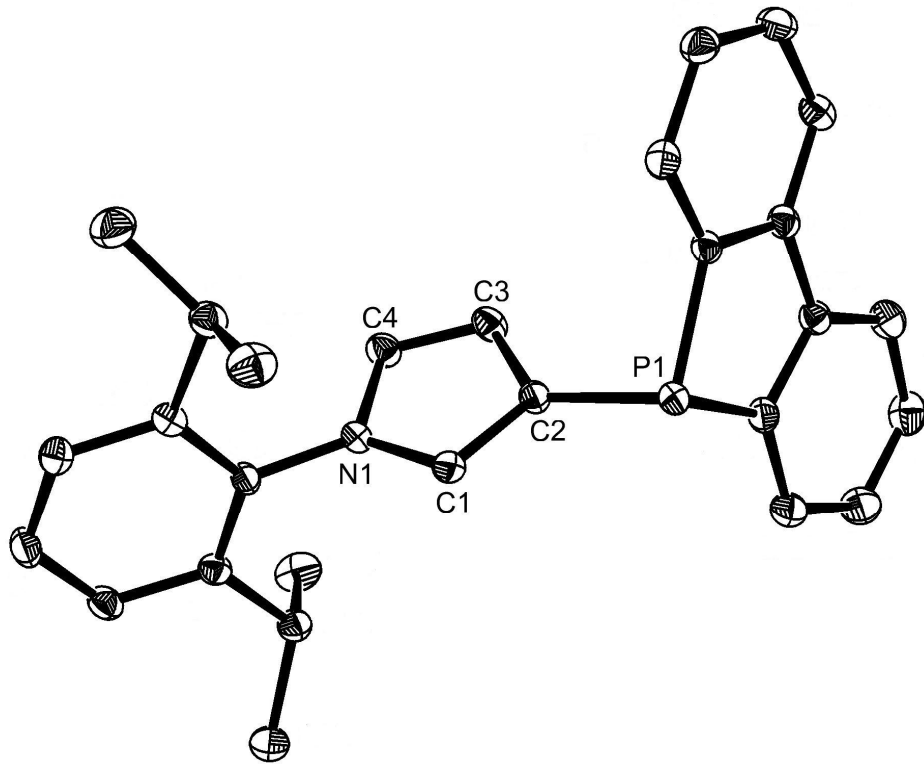
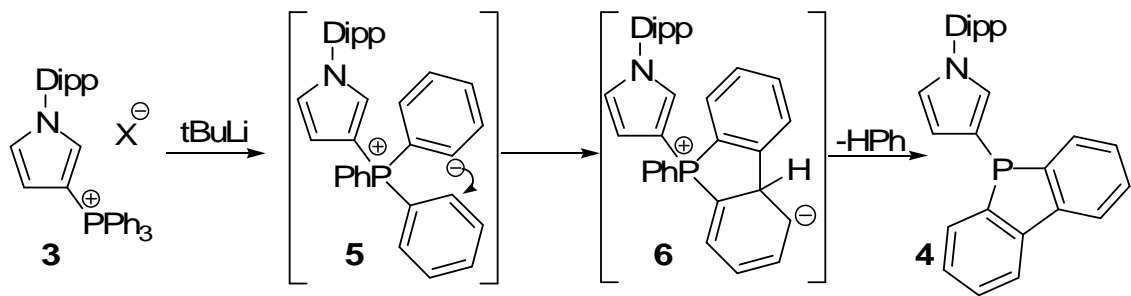


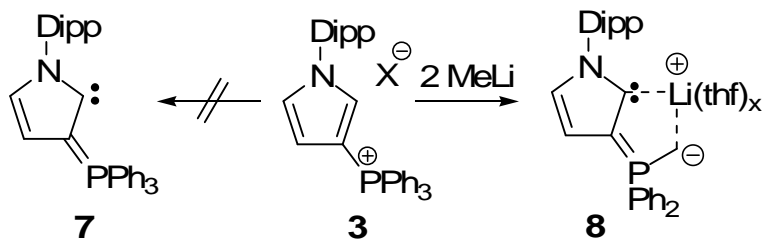
Figure 2.2. Molecular structure of phosphine **4**. Hydrogen atoms omitted for clarity. Thermal ellipsoids at 50% probability.



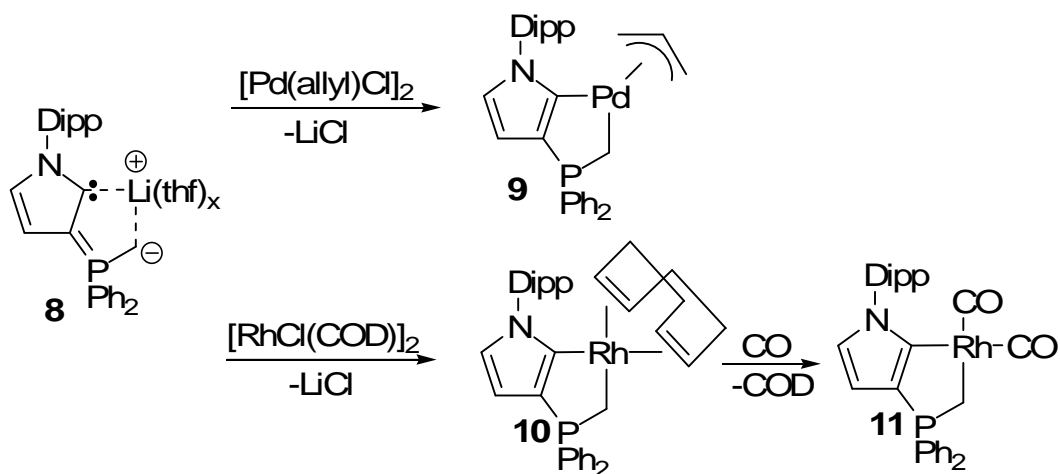
Scheme 2.2. Mechanism of formation of phosphine **4** from phosphonium **3**.

The reactivity of phenyllithium led us to use the smaller methylolithium, which gave a clean reaction, when using two equivalents, as evidenced by the

presence of a single signal in the ^{31}P NMR spectrum (+20 ppm). The ^{13}C NMR spectrum showed a doublet at 204 ppm ($^2\text{J}_{\text{CP}} = 54$ Hz), in the range expected for a carbene carbon;¹ however, there was a doublet at very high field (-4.4 ppm, $^1\text{J}_{\text{CP}} = 49$ Hz), which could not be attributed to **7** (Scheme 2.3). Interestingly, in the ^1H NMR spectrum, a doublet ($^2\text{J}_{\text{HP}} = 6.7$ Hz; phosphorus coupling was confirmed by decoupling experiments) also appeared at very high field (-0.07 ppm), and integrated for two protons. These data suggested the presence of an ylidic PCH_2 moiety. The ^1H NMR showed the presence of only 13 aromatic protons in the molecule indicating the loss of one phenyl group from the phosphorus, which is also evidenced by the formation of free benzene in the crude reaction mixture. These results as a whole were in favor of a compound featuring both a carbene center and a PCH_2 phosphorus ylide fragment, which cannot be rationalized by any reasonable neutral structure. Despite the high solubility of this compound in non polar solvents, including hexanes, it was clear that a salt has been formed. Indeed, ^6Li and ^7Li NMR demonstrated the presence of Li^+ but no Li-C coupling to either the carbenic carbon or the ylidic carbon could be detected, and no correlation was seen in 2D experiments. Lastly, the presence of coordinated THF was apparent from ^1H and ^{13}C NMR spectroscopy. At that point, it was concluded that the isolated compound was the lithium salt **8**,⁹ which is also in agreement with the stoichiometry of the reaction (2 eqs. of MeLi are necessary to go to completion).



Scheme 2.3. Attempted preparation of carbene **7** and synthesis of the lithium adduct **8**.



Scheme 2.4. Preparation of palladium complex **9** and Rhodium complexes **10** and **11**.

Although **8** is stable under an inert atmosphere, both in the solid state and in solution for several weeks, all attempts to grow single crystals suitable for an X-ray diffraction study failed. Therefore, in order to confirm the structure of **8**, we performed transmetallation reactions (Scheme 2.4). The addition of freshly prepared **8** to both $[\text{Pd}(\text{allyl})\text{Cl}]_2$ and $[\text{RhCl}(\text{COD})]_2$ cleanly led to complexes **9** and **10**, respectively, which were isolated as air stable crystalline solids in 47 and

56% yield (based on the starting phosphonium **3**), respectively. The formation of complexes **9** and **10** was clearly evidenced by ^{13}C NMR spectroscopy, the carbene signal shifting from 204 to 180 and 182 ppm, respectively, as is typical for transition metal carbene complexes.² The bonding of the ylidic carbon to the metal was also suggested by the downfield shift from -4.4 to -1.4 and 13.8 ppm, respectively. In the case of the Rh complex, both the carbenic and ylidic carbon appear as doublet of doublets ($\text{C}_{\text{carbene}} J_{\text{CP}} = 48 \text{ Hz}$ $J_{\text{CRh}} = 48 \text{ Hz}$, $\text{C}_{\text{ylide}} J_{\text{CP}} = 40 \text{ Hz}$ $J_{\text{CRh}} = 25 \text{ Hz}$) further demonstrating the bidentate behavior of **8**. Single crystals of complex **9** were grown from a concentrated acetonitrile solution, whereas those of complex **10** were obtained from a toluene solution. The crystals of **10** were also treated with carbon monoxide to give the dicarbonyl complex **11**. The infra red ν_{CO} stretching frequency were found to be 2040 and 1970 cm^{-1} . While these values can not be directly compared to other monodentate ligands the values were measure in the event future comparisons are necessary.

The molecular structure of complexes **9** and **10** determined by X-ray crystallography are shown in Figures 2.3 and 2.4.¹⁰ A closer look at the geometric parameters of complex **9** shows that the Pd-carbene (2.0302 Å) and Pd-CH₂ (2.1268 Å) bond lengths are very similar to those observed for the Pd(Allyl) complex bearing the neutral NHC-ylide bidentate ligand **F** (2.022-2.014 and 2.148-2.099 Å, respectively).⁷ In addition, the Rh-carbene bond length (2.0698 Å) in **10** is comparable to that found for other carbene complexes.²

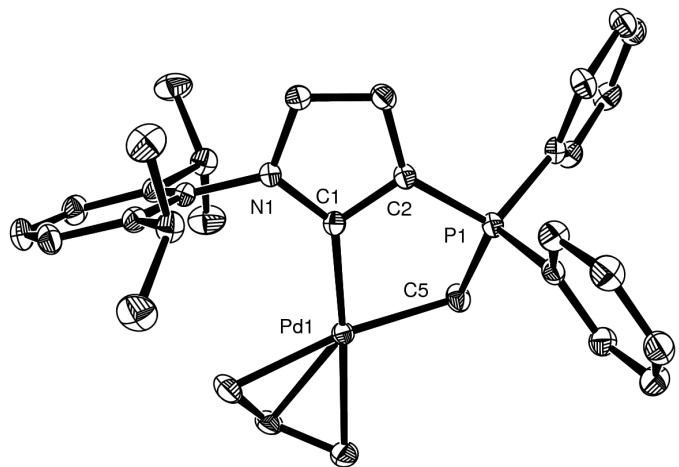


Figure 2.3. Molecular structure of palladium complex **9**. Hydrogen atoms omitted for clarity. Thermal ellipsoids at 50% probability. Selected bond lengths [\AA] and angles [$^\circ$]: C1-N1 1.3778(17), C1-C2 1.4013(18), C1-Pd1 2.0302(13), C5-Pd1 2.1268(15), C2-P1 1.7472(14), C5-P1 1.7523(15); N1-C1-C2 104.61(11).

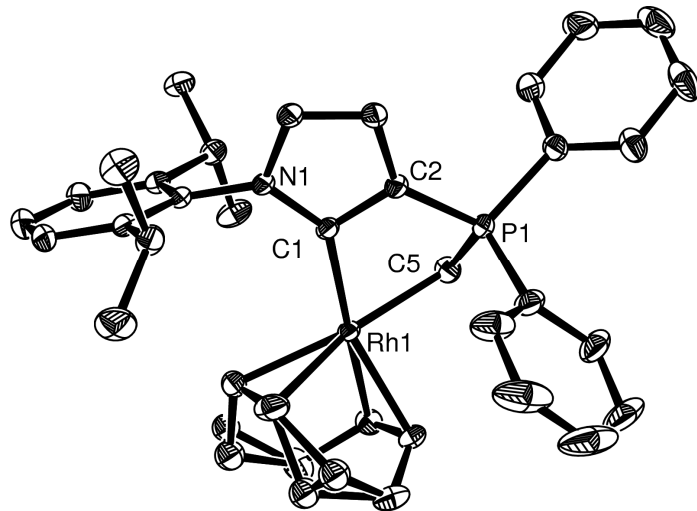
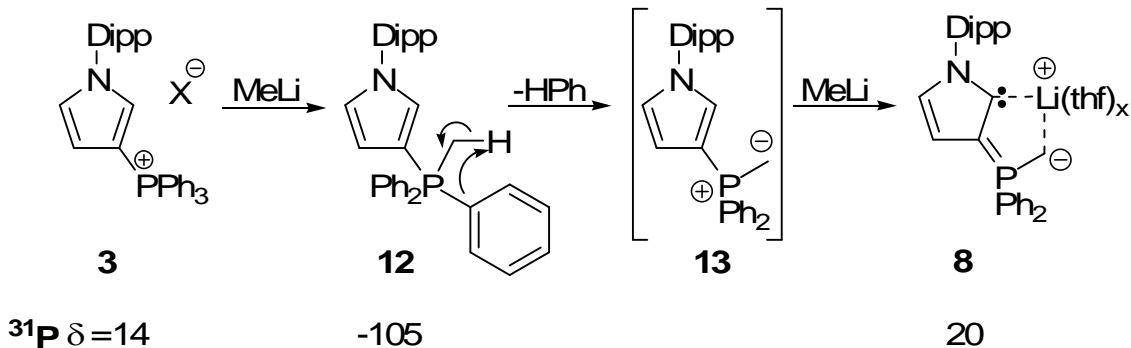


Figure 2.4. Molecular structure of rhodium complex **10**. Hydrogen atoms omitted for clarity. Thermal ellipsoids at 50% probability. Selected bond lengths [\AA] and angles [$^\circ$]: C1-N1 1.3842(16), C1-C2 1.4045(19), C1-Rh1 2.0698(13), C5-Rh1 2.1250(14), C2-P1 1.7359(13), C5-P1 1.7482(15); N1-C1-C2 103.73(11).

The formation of **8** by addition of two equivalents of MeLi to phosphonium **3** being unexpected, we turned our attention to the mechanism of the reaction. Addition of only one equivalent of MeLi to **3** leads to a mixture of unreacted starting material **3** and lithium salt **8**. However, when this reaction was monitored by variable temperature multinuclear NMR spectroscopy, signals corresponding to the intermediate **12** were observed (Scheme 2.5). Indeed, at -78 °C a new peak at -105.1 ppm appeared in the ^{31}P NMR spectrum, which is in the typical range for a penta-coordinate phosphorus compound.¹¹ In addition, the ^1H NMR spectrum shows the presence of a methyl group directly bonded to phosphorus (2.06 ppm, d, $^2J_{\text{HP}} = 7.56$ Hz); this was confirmed by ^{13}C NMR spectroscopy and HSQC experiments. These protons correlate with a methyl carbon at 34.8 ppm with the expected large $^1J_{\text{CP}}$ coupling constant (65.2 Hz). The formation of penta-coordinate phosphorus compounds by alkylation of phosphonium salts with alkyl lithiums have already been observed.¹² Then, upon warming to room temperature, no other intermediate could be detected. Based on literature precedents,¹³ it is reasonable to postulate, that the next step is the elimination of benzene with concomitant formation of ylide **13**. Then, the second equivalent of MeLi can deprotonate the heterocycle affording the observed lithium complex **8**.



Scheme 2.5. Possible mechanism of the formation of lithium adduct **8**.

In conclusion, a lithium adduct of a new type of bidentate anionic LX ligand in which L is a cyclic (amino)[bis(ylide)]carbene and X is the exocyclic part of the bis(ylide) has been synthesized. This adduct readily undergoes transmetallation reactions, which allows for the synthesis of divers transition metal complexes. The catalytic activity of the latter is currently under investigation as well as continuing efforts to synthesize a stable cyclic amino ylide carbene of type **C**.

Experimental

All manipulations were performed under an atmosphere of argon using standard schlenk techniques. All solvents were dried and distilled prior to use (THF, hexane, and toluene were dried and distilled over potassium, ether over sodium wire and dichloromethane and chloroform were dried and distilled over calcium hydride). ^1H , ^{13}C and ^{31}P NMR spectra were recorded on Varian Inova 500, Bruker Advace 300 and Bruker Advace 600 spectrometers. ^1H and ^{13}C NMR chemical shifts are reported in ppm relative to TMS as an external standard. ^{31}P NMR chemical shifts are reported in ppm relative to 85% H_3PO_4 as an external standard. Melting points are uncorrected.

Pyrrole **1** was synthesized similar to a previously described procedure. To a toluene (350 ml) solution of 2,5-dimethoxytetrahydrofuran (11.2 ml, 88 mmol) and 2,6-diisopropylaniline (15.1 ml, 80 mmol) was added phosphorus pentoxide (11.4g, 80mmol). The solution was heated to 120 °C for 45min. After evaporation under vacuum the crude reaction product was purified on a short silica column eluted with pentane/ethyl acetate (4:1) to give the pyrrole (16.4g, 90%) as yellow brown crystals (directly from the pentane/ethyl acetate solution) m.p. = 57-58 °C. ^1H NMR (CDCl_3 , 25 °C, 300 MHz) δ 1.36 (d, J = 7 Hz, 12H, CH_3), 2.69 (sept, J = 7 Hz, 2H, CH i-Pr), 6.52 (t, J = 2 Hz, 2H, $\text{CH}_{\text{pyrrole}}$), 6.56 (t, J = 2 Hz 2H, $\text{CH}_{\text{pyrrole}}$), 7.42-7.62 (m, 3H, CH_{aryl}); ^{13}C NMR (CDCl_3 , 25 °C, 75 MHz)

δ 25.0 (CH₃), 28.6 (CH i-Pr), 109.6 (CH_{pyrrole}), 123.5 (CH_{meta-aryl}), 124.0 (CH_{pyrrole}), 129.6 (CH_{para-aryl}), 138.0 (C_{ipso-aryl}), 147.6 (C_{ortho-aryl}).

Bromopyrrole 2. Regiospecific 3-bromination of Pyrrole **1** was done according to a published procedure. Pyrrole **1** (16.4 g, 72mmol) was dissolved in THF (300ml) and cooled to -78 °C phosphorus tribromide (1.4 g, 5mmol) was then added to the solution. NBS (12.8 g, 72mmol) was added slowly and the mixture was then brought to 0 °C and stirred for 12 hrs. The 3-bromopyrrole **2** was purified by column chromatography on alumina using hexanes as the eluant. After evaporation of solvents, 17.6 g (80%) of the slightly yellow oil **2** was obtained. ¹H NMR (CDCl₃, 25 °C, 300 MHz) δ 1.59 (dd, J = 6.9, 4.8 Hz, 12H, CH₃), 2.48 (sept, J = 6.9 Hz, 6.9H, CH i-Pr), 6.34 (t, J = 1.8 Hz, 1H, CH_{pyrrole}), 6.55 (t, J = 2.4 Hz 1H, CH_{pyrrole}), 6.61 (dd, J = 3.9, 2.1 Hz 1H, CH_{pyrrole}) 7.23-7.45 (m, 3H, CH_{aryl}); ¹³C NMR (CDCl₃, 25 °C, 75 MHz) δ 24.6 (CH₃), 24.8 (CH₃), 28.1 (CH i-Pr), 96.2 (CBr), 110.8 (CH_{pyrrole}), 111.4 (CH_{pyrrole}), 122.5 (CH_{pyrrole}) 123.7 (CH_{meta-aryl}), 129.5 (CH_{para-aryl}), 136.4 (C_{ipso-aryl}), 147.0 (C_{ortho-aryl}).

Phosphonium salt **3** was prepared by a catalytic coupling reaction. Excess triphenylphosphine (17 g 65 mmol) and nickel (COD)₂ (0.86 g, 3.1 mmol) were mixed in absolute ethanol (600ml) until a gold colored solution was obtained. Then the 3-bromo pyrrole **2** (19.1 g, 62 mmol) was added and the mixture was heated to reflux for 12 hours. The ethanol was removed under vacuum and the solid was washed with hexanes. The anion exchange was done in

dichloromethane (150 ml) using excess sodium tetraphenylborate (30 g, 88 mmol). After stirring for 12 hours the solvent was evaporated under vacuum and the pure salt was extracted in THF. The resultant white solid was recrystallized from a concentrated solution of dichloromethane and ether to give white crystals of **3** (33.1 g, 66%). m.p. : 102-103 °C; $^{31}\text{P}\{\text{H}\}$ NMR (CDCl_3 , 25 °C, 80 MHz) : δ 14.2; ^1H NMR (CDCl_3 , 25 °C, 300 MHz) δ 1.14 [d(broad), J = 26.8, 12H, CH_3], 2.25 [d(broad), J = 42.8 Hz, 2H CH i-Pr], 6.77 [s(broad), 1H, $\text{CH}_{\text{pyrrole}}$], 6.92 [s(broad), 1H, $\text{CH}_{\text{pyrrole}}$], 7.11 [s(broad), 1H, $\text{CH}_{\text{pyrrole}}$], 7.27-7.89 (m, 18H, CH aryl); ^{13}C NMR (CDCl_3 , 25 °C, 75 MHz) δ 24.1 (CH_3), 24.6 (CH_3), 28.5 (CH i-Pr), 98.2 (d, $^1\text{J}_{\text{CP}} = 115.1$ Hz, CP), 114.3 (d, $^2\text{J}_{\text{CP}} = 10.1$ Hz, $\text{CH}_{\text{pyrrole}}$), 119.3 (d, $^1\text{J}_{\text{CP}} = 92.9$ Hz, CP Ph), 124.1 ($\text{CH}_{\text{pyrrole}}$) 128.8 (d, $^2\text{J}_{\text{CP}} = 12.5$ Hz, $\text{CH}_{\text{pyrrole}}$), 130.3 ($\text{CH}_{\text{meta-aryl}}$), 130.6 (d, $^2\text{J}_{\text{CP}} = 13.2$ Hz, $\text{CH}_{\text{ortho-aryl}}$), 133.1 ($\text{CH}_{\text{para-aryl}}$) 133.5 (d, $^3\text{J}_{\text{CP}} = 10.7$ Hz, $\text{CH}_{\text{meta-ph}}$), 134.4 ($\text{C}_{\text{ortho-aryl}}$), 135.6 ($\text{CH}_{\text{para-ph}}$), 145.6 ($\text{C}_{\text{ipso-aryl}}$).

Phosphine 4: To a THF (1 ml) solution of salt **3** (107 mg, 0.13 mmol) was added phenyl lithium (2.0 M, 0.13 mmol, 0.66 ml) at -78 °C. The solution was allowed to warm to room temperature and the solvent was removed under vacuum. Phosphine **4** was extracted in hexanes. X-ray quality crystals were grown from a concentrated hexanes solution at -30 °C. (17 mg, 32%). $^{31}\text{P}\{\text{H}\}$ NMR (C_6D_6 , 25 °C, 242 MHz) : δ -31.1; ^1H NMR (C_6D_6 , 25 °C, 600 MHz) δ 0.92 (d, J = 8.4, 6H, CH_3), 0.98 (d, J = 8.4, 6H, CH_3), 2.44 (sept, J = 8.4 Hz, 2H CH i-Pr], 6.06 (m, 1H, $\text{CH}_{\text{pyrrole}}$), 6.32 (m, 1H, $\text{CH}_{\text{pyrrole}}$), 6.88 (m, 1H, $\text{CH}_{\text{pyrrole}}$), 7.05-7.75 (m, 11H,

CH aryl); ^{13}C NMR (C_6D_6 , 25 °C, 151 MHz) δ 24.1 (CH₃), 24.4 (CH₃), 28.1 (CH i-Pr), 112.4 (d, $J_{\text{CP}} = 5.9$ Hz, CH_{pyrrole}), 115.0 (d, $^1J_{\text{CP}} = 12.1$ Hz, C_{pyrrole}), 120.8 (d, $J_{\text{CP}} = 10.1$ Hz, CH_{pyrrole}), 121.3 (CH_{aryl}), 123.5 (CH_{aryl}), 123.6 (CH_{aryl}), 124.8 (d, $J_{\text{CP}} = 4.4$ Hz, CH_{pyrrole}), 125.4 (d, $J_{\text{CP}} = 4.5$ Hz, C_{aryl}), 127.3 (d, $J_{\text{CP}} = 7.6$ Hz, CH_{aryl}), 129.2 (CH_{aryl}), 129.8 (d, $J_{\text{CP}} = 39.0$ Hz, CH_{aryl}), 130.1 (d, $J_{\text{CP}} = 21.7$ Hz, CH_{aryl}), 137.3 (C_{aryl}), 144.2 (d, $J_{\text{CP}} = 4.6$ Hz, C_{aryl}) 145.7 (C_{aryl}) 147.2 (C_{aryl}).

Lithium salt **8** was prepared by dissolving the phosphonium salt **3** (0.243 g, 0.3mmol) in THF (4 ml) and cooling the solution to -78 °C at which point methyllithium (0.375 ml of 1.6 M solution in ether, 0.6 mmol) was added drop wise. The solution was immediately allowed to warm to room temperature. All volatiles were removed under vacuum and the product was extracted in hexanes. $^{31}\text{P}\{\text{H}\}$ NMR (THF-d₈, 25 °C, 242 MHz) : δ 20.4; ^1H NMR (THF-d₈, 25 °C, 600 MHz) δ -0.07 (d, $J_{\text{HP}} = 6.7$, 2H, ylide CH₂), 1.08 (d, $J = 6.9$ Hz, 6H CH₃ i-Pr), 1.15 (d, $J = 6.9$ Hz, 6H, CH₃ i-Pr), 3.00 (sept, $J = 6.9$ Hz, 2H, CH i-Pr), 6.06 (t, $J = 2.0$ Hz, 1H, CH_{pyrrole}), 6.89 (t, $J = 2.6$ Hz, 1H, CH_{pyrrole}), 7.12-7.64 (m, 13H, CH_{aryl}); ^{13}C NMR (THF-d₈, 25 °C, 151 MHz) δ -4.42 (d, $^1J_{\text{CP}} = 48.5$ Hz, ylide CH₂), 24.3 (CH₃), 28.6 (CH i-Pr), 112.4 (d, $^2J_{\text{CP}} = 20.0$ Hz, CH_{pyrrole}), 116.7 (d, $^1J_{\text{CP}} = 139.8$ Hz, C_{ipso-pyrrole}), 123.2 (CH_{meta-aryl}), 127.3 (CH_{para-aryl}) 127.4 (d, $^3J_{\text{CP}} = 10.3$ Hz, CH_{pyrrole}), 128.3 (d, $^2J_{\text{CP}} = 10.8$ Hz, CH_{ortho-ph}), 129.9 (d, $^4J_{\text{CP}} = 2.0$ Hz, CH_{para-ph}), 132.4 (d, $^3J_{\text{CP}} = 9.7$ Hz, CH_{meta-ph}) 140.9 (d, $^1J_{\text{CP}} = 71.0$ Hz, C_{ipso-ph}), 145.9 (C_{ipso-aryl}), 147.0 (C_{ortho-ph}), 204.2 (d, $^2J_{\text{CP}} = 54.2$ Hz, C_{carbene}).

Palladium complex **9** was formed by adding a solution of lithium salt **8** (0.55 mmol formed in situ according to the above procedure) to a solution of Palladium allyl chloride dimer (0.101 g, 0.27 mmol) in THF (2 ml). The solution was allowed to warm to room temperature and stir for 2 hrs. All volatiles were removed under vacuum and the complex was extracted into toluene. Yellow crystals formed in a concentrated solution of acetonitrile at -30 °C (0.148 g, 47%).
m.p. : 152-153 °C; $^{31}\text{P}\{\text{H}\}$ NMR (THF-d₈, 25 °C, 121 MHz) : δ 31.8; ^1H NMR (THF-d₈, 25 °C, 500 MHz) δ 1.08 (dd, J = 6.9, 2.7 Hz, 6H, CH₃ i-Pr), 1.14 (dd, J = 6.9, 23.3 Hz, 6H CH₃ i-Pr), 1.64 (dd, J = 8.3, 11.6 Hz, 1H, allyl), 1.69 (d, J = 12.8 Hz, 1H, ylide), 1.85 (dd, J = 9.1, 11.6 Hz, 1H, allyl), 2.04 (d, J = 13.0 Hz, 1H, ylide), 2.09 (d, J = 7.1 Hz, 1H, allyl), 2.58 (sept, J = 7.0 Hz, 1H, CH i-Pr), 2.82 (d, J = 6.9 Hz, 1H, CH i-Pr), 3.16 (dd, J = 2.2, 7.2 Hz, 1H, allyl), 4.49 (m, 1H allyl), 6.45 (d, J = 2.7 Hz, 1H, CH_{pyrrole}), 6.45 (t, J = 3.2 Hz, 1H, CH_{pyrrole}), 7.20 (d, J = 7.7 Hz, 2H, CH_{ortho-aryl}), 7.33-7.46 (m, 8H, CH_{aryl/ph}) 7.75 (ddd, J = 7.1, 11.7, 18.9 Hz, 4H, CH_{meta-ph}); ^{13}C NMR (THF-d₈, 25 °C, 125 MHz) δ -1.4 (d, $^1\text{J}_{\text{CP}}$ = 45.7 Hz, ylide CH₂), 24.2, 24.5, 25.1, and 25.6 (CH₃ i-Pr), 29.0 and 29.2 (CH i-Pr), 52.9 (CH₂ allyl), 53.6 (CH₂ allyl), 110.1 (d, $^2\text{J}_{\text{CP}}$ = 16.6 Hz, CH_{pyrrole}), 113.7 (CH allyl), 117.8 (d, $^1\text{J}_{\text{CP}}$ = 145.1 Hz, C_{ipso-pyrrole}), 123.7 (CH_{meta-aryl}), 128.1 (d, $^3\text{J}_{\text{CP}}$ = 10.3 Hz, CH_{pyrrole}), 129.0 (CH_{para-aryl}), 129.4 and 129.6 (d, $^2\text{J}_{\text{CP}}$ = 10.3 and 12.3 Hz, CH_{ortho-ph}), 132.0 and 132.1 (CH_{para-ph}), 132.7 and 132.8 (d, $^3\text{J}_{\text{CP}}$ = 8.3 and 8.3 Hz, CH_{meta-ph}), 134.0 and 134.1 (d, $^1\text{J}_{\text{CP}}$ = 74.7 and 72.6 Hz, C_{ipso-ph}), 144.0 (C_{ipso-aryl}), 147.3 and 147.5 (C_{ortho-aryl}), 180.1 (d, $^2\text{J}_{\text{CP}}$ = 49.8 Hz, C_{carbene}).

Rhodium complex **10** was formed by adding a solution of lithium salt **8** (0.84mmol formed in situ according to the above procedure) to a solution of [RhCl(COD)]₂ (0.216 g, 0.42mmol) in THF (2ml) at -78 °C. The solution was allowed to warm to room temperature and stir for 2 hrs. All volatiles were removed under vacuum and the complex was extracted with toluene. The solution was concentrated and orange crystals formed at -30 °C (0.302 g, 56%). m.p. : 179-181 °C; ³¹P{¹H} NMR (CDCl₃, 25 °C, 121 MHz) : δ 21.9; ¹H NMR (CDCl₃, 25 °C, 300 MHz) δ 1.22 (d, J = 6.6 Hz, 6H CH₃ i-Pr), 1.38 (dd, J_{HP} = 9.9, J_{HRh} = 2.3, 2H, ylide CH₂), 1.65 (d, 6H, J = 6.9 Hz, CH₃ i-Pr), 1.97 (dd, J = 7.7, 15.3 Hz, 4H COD), 2.2-2.3 (m, 4H COD), 3.12 (sept, J = 6.9 Hz, 2H, CH i-Pr), 4.13 (s, 2H COD), 4.34 (s, 2H COD), 6.60 (d, J = 2.7 Hz, 1H, CH_{pyrrole}), 6.99 (dd, J = 3.6, 2.7 Hz, 1H, CH_{pyrrole}), 7.10-7.94 (m, 13H, CH_{aryl}); ¹³C NMR (THF-d₈, 25 °C, 125 MHz) δ 13.8 (dd, ¹J_{CP} = 39.5 ¹J_{CRh} = 25.0 Hz, ylide CH₂), 24.3 (CH₃), 29.1 (CH i-Pr), 31.5 (CH₂ COD), 32.5 (CH₂ COD), 76.1 (d, ¹J_{CRh} = 10.4 Hz, CH COD), 82.5 (d, ¹J_{CRh} = 8.3 Hz, CH COD), 109.7 (d, ²J_{CP} = 18.7 Hz, CH_{pyrrole}), 118.4 (d, ¹J_{CP} = 143.1 Hz, C_{ipso-pyrrole}), 124.0 (CH_{meta-aryl}), 128.7 (d, ³J_{CP} = 10.3 Hz, CH_{pyrrole}), 129.0 (CH_{para-aryl}) 129.0 (CH_{para-aryl}), 129.2 (d, ²J_{CP} = 12.5 Hz, CH_{ortho-ph}), 131.8 (CH_{para-ph}), 132.9 (d, ³J_{CP} = 8.3 Hz, CH_{meta-ph}) 134.6 (d, ¹J_{CP} = 76.7 Hz, C_{ipso-ph}), 141.6 (C_{ipso-aryl}), 147.4 (C_{ortho-ph}), 182.0 (dd, ²J_{CP} = 47.7 Hz, ²J_{CRh} = 47.7 Hz, C_{carbene}).

Rhodium CO complex **11** was synthesized by bubbling CO gas through a dichloromethane (2 ml) solution of rhodium complex **10** (0.302 g, 0.45 mmol) for 15 min. The solvent and displaced cyclooctadiene were then removed under vacuum to give analytically pure **11** (0.277 g, 99%). m.p. : 154-156 °C; $^{31}\text{P}\{\text{H}\}$ NMR (CDCl_3 , 25 °C, 121 MHz) : δ 21.6; ^1H NMR (CDCl_3 , 25 °C, 500 MHz) δ 1.18 (d, $J = 7.0$ Hz, 6H CH_3 i-Pr), 1.34 (d, 6H, $J = 7.0$ Hz, CH_3 i-Pr), 1.65 (d, $J_{\text{HP}} = 10.5$, 2H, ylide CH_2), 2.66 (sept, $J = 7.1$ Hz, 2H, CH i-Pr), 6.50 (s, 1H, $\text{CH}_{\text{pyrrole}}$), 7.05 (d, $J = 3.1$ Hz, 1H, $\text{CH}_{\text{pyrrole}}$), 7.29 (d, $J = 7.5$, 2H, $\text{CH}_{\text{meta-dipp}}$), 7.46 (t, $J = 7.5$, 1H, $\text{CH}_{\text{para-dipp}}$), 7.39 (d, $J = 7.5$, 2H, $\text{CH}_{\text{meta-dipp}}$) 7.50-7.79 (m, 10H, CH_{PPh}); ^{13}C NMR (CDCl_3 , 25 °C, 125 MHz) δ 5.02 (dd, $^1\text{J}_{\text{CP}} = 22.6$ $^1\text{J}_{\text{CRh}} = 20.6$ Hz, ylide CH_2), 24.5 (CH_3), 25.6 (CH_3), 29.3 (CH i-Pr), 109.4 (d, $^2\text{J}_{\text{CP}} = 13.2$ Hz, $\text{CH}_{\text{pyrrole}}$), 119.1 (d, $^1\text{J}_{\text{CP}} = 133.1$ Hz, $\text{C}_{\text{ipso-pyrrole}}$), 123.8 ($\text{CH}_{\text{meta-aryl}}$), 127.9 (d, $^3\text{J}_{\text{CP}} = 9.5$ Hz, $\text{CH}_{\text{pyrrole}}$), 128.0 (d, $^2\text{J}_{\text{CP}} = 12.5$ Hz, $\text{CH}_{\text{ortho-ph}}$), 131.1 ($\text{CH}_{\text{para-aryl}}$), 129.2 ($\text{CH}_{\text{para-aryl}}$), 131.8 ($\text{CH}_{\text{para-ph}}$), 132.1 (d, $^3\text{J}_{\text{CP}} = 7.9$ Hz, $\text{CH}_{\text{meta-ph}}$) 132.6 (d, $^1\text{J}_{\text{CP}} = 76.7$ Hz, $\text{C}_{\text{ipso-ph}}$), 140.9 ($\text{C}_{\text{ipso-aryl}}$), 147.1 ($\text{C}_{\text{ortho-ph}}$), 181.7 (dd, $^2\text{J}_{\text{CP}} = 53.6$ Hz, $^2\text{J}_{\text{CRh}} = 41.3$ Hz, $\text{C}_{\text{carbene}}$), 188.0 (d, $^1\text{J}_{\text{CRh}} = 61.9$ Hz, $\text{C}_{\text{CO-trans}}$), 193.5 (dd, $^1\text{J}_{\text{CRh}} = 93.4$ Hz, $^3\text{J}_{\text{CP}} = 11.5$ Hz, $\text{C}_{\text{CO-cis}}$). IR CO stretching frequency = 1970, 2040 cm^{-1} .

References

1. For reviews on metal free NHCs, see: a) D. Enders, O. Niemeier, O. A. Henseler, *Chem. Rev.* **2007**, *107*, 5606-5655; b) N. Marion, S. Diez-Gonzalez, S. P. Nolan, *Angew. Chem., Int. Ed.* **2007**, *46*, 2988; c) Y. Canac, M. Soleilhavoup, S. Conejero, G. Bertrand, *J. Organomet. Chem.* **2004**, *689*, 3857; d) D. Bourissou, O. Guerret, F. P. Gabbaï, G. Bertrand, *Chem. Rev.* **2000**, *100*, 39; e) A. J. Arduengo III, *Acc. Chem. Res.* **1999**, *32*, 913.
2. For recent reviews on carbenes as ligands, see: a) E. Kantchev, C. O'Brien, M. Organ, *Angew. Chem. Int. Ed.* **2007**, *46*, 2768; b) H. M. Lee, C. C. Lee, P. Y. Cheng, *Curr. Org. Chem.* **2007**, *11*, 1491; c) S. T. Liddle, I. S. Edworthy, P. L. Arnold, *Chem. Soc. Rev.* **2007**, *36*, 1732; d) S. Diez-Gonzalez, S. P. Nolan, *Synlett* **2007**, 2158; e) D. Pugh, A. A. Danopoulos, *Coord. Chem. Rev.* **2007**, *251*, 610; f) I. J. F. Lin, C. S. Vasam, *Coord. Chem. Rev.* **2007**, *251*, 642; g) R. E. Douthwaite, *Coord. Chem. Rev.* **2007**, *251*, 702; h) L. H. Gade, S. Bellemín-Lapönnaz, *Coord. Chem. Rev.* **2007**, *251*, 718; i) E. Colacino, J. Martinez, F. Lamaty, *Coord. Chem. Rev.* **2007**, *251*, 726; j) V. Dragutan, I. Dragutan, L. Delaude, *Coord. Chem. Rev.* **2007**, *251*, 765; k) W. J. Sommer, M. Weck, *Coord. Chem. Rev.* **2007**, *251*, 860; l) S. Diez-Gonzalez, S. P. Nolan, *Coord. Chem. Rev.* **2007**, *251*, 874; m) F. E. Hahn, *Angew. Chem. Int. Ed.* **2006**, *45*, 1348; n) S. P. Nolan, *N-Heterocyclic Carbenes in Synthesis*; Wiley-VCH, **2006**; o) F. Glorius, *N-Heterocyclic Carbenes in Transition Metal Catalysis (Topics in Organometallic Chemistry)*; Springer Verlag, **2006**.
3. a) V. Lavallo, Y. Canac, C. Prasang, B. Donnadieu, G. Bertrand, *Angew. Chem. Int. Ed.* **2005**, *44*, 5705; b) R. Jazzar, R. D. Dewhurst, J. -B. Bourg, B. Donnadieu, Y. Canac, G. Bertrand, G. *Angew. Chem. Int. Ed.* **2007**, *46*, 2899; (c) R. Jazzar, J. -B. Bourg, R. D. Dewhurst, B. Donnadieu, Y. Canac, G. Bertrand, G. *J. Org. Chem.* **2007**, *72*, 3492; d) V. Lavallo, Y. Canac, A. DeHope, B. Donnadieu, G. Bertrand, *Angew. Chem., Int. Ed.* **2005**, *44*, 7236; e) V. Lavallo, G. D. Frey, S. Kousar, B. Donnadieu, G. Bertrand, *Proc. Natl. Acad. Sci. USA*, **2007**, *104*, 13569; f) D. R. Anderson, V. Lavallo, D. J. O'Leary, G. Bertrand, R. H. Grubbs, R. H. *Angew. Chem. Int. Ed.* **2007**, *46*, 7262; g) D. R. Anderson, R. Ung, G. Mkrtumyan, G. Bertrand, R. H. Grubbs, Y. Schrödi, *Organometallics* **2008**, *27*, 56.
4. a) G. Facchin, R. Campostrini, R. A. Michelin, *J. Organomet. Chem.* **1985**, *294*, C21; b) R. A. Michelin, G. Facchin, D. Braga, P. Sabatino, *Organometallics* **1986**, *5*, 2265; c) R. A. Michelin, M. Mozzon, G. Facchin,

-
- D. Braga, P. Sabatino, *J. Chem. Soc. Dalton Trans.* **1988**, 1803; d) G. Facchin, M. Mozzon, R. A. Michelin, M. T. A. Robeiro, A. J. L. Pombeiro, *J. Chem. Soc. Dalton Trans.* **1992**, 2827; e) M. Tamm, F. E. Hahn, F. E. *Coord. Chem. Rev.* **1999**, 182, 175; f) A. J. L. Pombeiro, *J. Organomet. Chem.* **2005**, 690, 6021.
5. S. Nakafuji, J. Kobayashi, T. Kawashima, *Angew. Chem. Int. Ed.* **2008**, 47, 1141.
 6. For a review on phosphorus diylides [R₂P+(CH₂-)2]: M. Taillefer, H. J. Cristau, *Top. Curr. Chem.* **2003**, 229, 41-73.
 7. Y. Canac, C. Duhayon, R. Chauvin, *Angew. Chem. Int. Ed.* **2007**, 46, 6313.
 8. a) Y. Fang, D. Leysen, H. C. J. Ottenheijm, *Syn. Comm.* **1995**, 25, 1857; b) E. Dvornikova, K. Kamienska-Trela, *Synlett.* **2002**, 1152; c) K. Manabe, *Tet. Lett.* **1998**, 5807.
 9. Several examples of carbene-Li⁺ adducts have already been reported: a) R. W. Alder, M. E. Blake, C. Bortolotti, S. Bufali, C. P. Butts, E. Linehan, J. M. Oliva, A. G. Orpen, M.J. Quayle, *Chem. Commun.*, **1999**, 241; b) A. J. Arduengo III, M. Tamm, J. C. Calabrese, F. Davidson, W. Marshall, *J. Chem. Lett.* **1999**, 10, 1021.
 10. Structural data have been deposited in the Cambridge Crystallographic Data Center under CCDC 676576 (**6**), and 676577 (**7**) and can be obtained free of charge at www.ccdc.cam.ac.uk/conts/retrieving.html. All the X-ray data (including compounds **4** and **9**) are also found in the appendix.
 11. a) L. W. Dennis, V. J. Bartuska, G. E. Maciel, *J. Am. Chem. Soc.* **1982**, 104, 230; a) V. H. Schmidbaur, P. Holl, *P. Z. Anorg. Allg. Chem.* **1979**, 458, 249.
 12. a) U. Monkowius, N. W. Mitzel, A. Schier, H. Schmidbaur, *J. Am. Chem. Soc.* **2002**, 124, 6126; b) D. Hellwinkel, *Top Curr Chem.* **1983**, 109 1; b) D. Hellwinkel, W. Lindner, *Chem. Ber.* **1976**, 109, 1497; c) D. Hellwinkel, W. Lindner, H. -J. Wilfinger, *Chem. Ber.* **1974**, 107, 1428; d) E. W. Turnblom, T. J. Katz, *J. Am. Chem. Soc.* **1973**, 95, 4292; e) E. M. Richards, J. C. Tebby, *J. Chem. Soc. C*, **1970**, 1425.
 13. a) D. Seyferth, W. B. Hughes, J. K. Heeren, *J. Am. Chem. Soc.* **1965**, 87, 2847; b) D. Seyferth, W. B. Hughes, J. K. Heeren, *J. Am. Chem. Soc.* **1965**, 87, 3467.

Chapter 3

Synthesis and Ligand Properties of a Stable Five-Membered-Ring

Vinylideneephosphorane

Over the years the success of homogeneous catalysis can be attributed largely to the development of a diverse range of ligand frameworks that have been used to tune the behavior of the various systems. Recently, the so-called N-heterocyclic carbenes (NHCs) **A** (Figure 3.1) have emerged as powerful ligands, largely because of their strong donor properties, which are due to the presence of a lone pair and a partially filled vacant orbital.¹ In our search for even stronger donor ligands, we became interested in carbodiphosphoranes,² and especially their cyclic versions **B**³ since we have learned from carbene chemistry that the latter lead to more robust transition metal complexes.⁴ We have demonstrated using the $\nu_{av}(\text{CO})$ infra-red frequency of $(\text{L})\text{Rh}(\text{CO})_2\text{Cl}$ complexes³ that these species, which feature a carbon bearing formally two lone pairs,⁵ were indeed stronger donors than NHCs **A**. Along this line, we have also reported the synthesis of acyclic and cyclic push-push bent-allenes (carbodicarbenes) **C**,⁶ which are electronically similar to carbodiphosphoranes.^{7,8} These results led us to consider a mixed system **D** with a phosphorus-carbon ylidic bond and a carbon-carbon double bond. Interestingly, such heteroallenes have a resonance form **D**³ directly related to the previously reported push-pull allenes **E**,⁹ and push-pull carbenes **F**,¹⁰ as

shown by their resonance forms. In contrast to the numerous examples of acyclic derivatives,² only one cyclic vinylidenephosphorane, stable at low temperature for a short period of time, has been described, and no crystallographic data or coordination behavior has been reported.¹¹

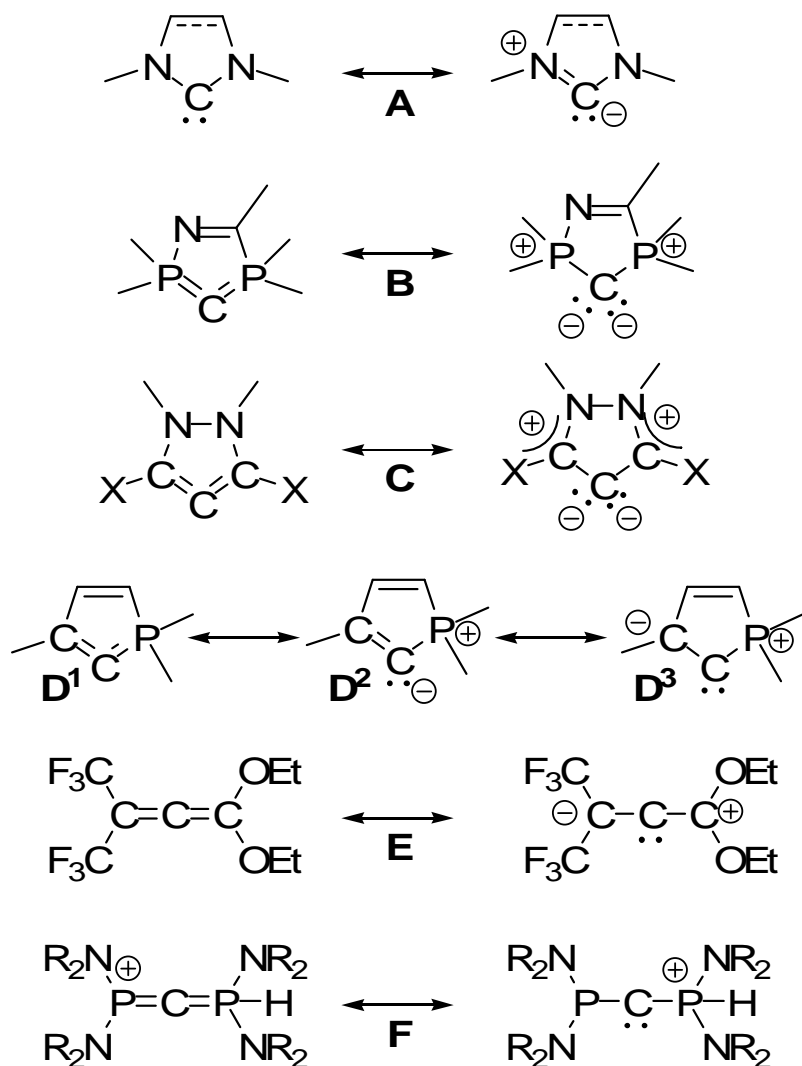
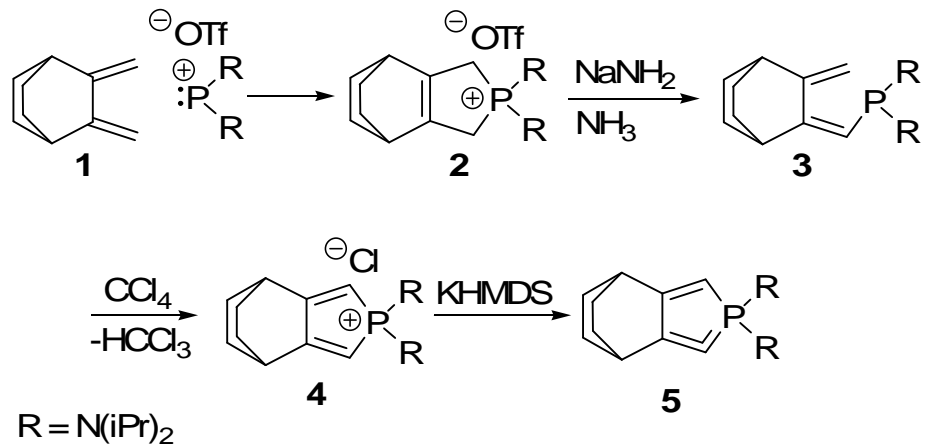


Figure 3.1. Similarities and differences between NHCs **A**, carbodiphosphoranes **B**, push-push allenes **C**, vinylidene phosphoranes **D**, push-pull allenes **E**, and push-pull carbenes **F**.

Herein we present the synthesis, single crystal X-ray diffraction study, and ligand properties of a cyclic vinylideneephosphorane **5** that is stable at room temperature both in solution and in the solid state.



Scheme 3.1. Synthesis of cyclic phosphaallene **5**.

The cyclic phosphonium salt **4**, without undesired acidic protons, was chosen as precursor for the target vinylideneephosphorane **5**. Starting from the readily available diene **1**,¹² a formal [4+1] cycloaddition with bis(diisopropyl)aminophosphonium triflate gives rise to the phospholenium salt **2** (Scheme 3.1).¹³ Deprotonation of **2** with NaNH₂ in liquid ammonia affords the ring-opened phosphine **3** (Z or E).¹⁴ Subsequent treatment with one equivalent of CCl₄ at room temperature leads directly to the desired phosphonium chloride **4** in a 65% yield.¹⁵ The structure of **4** was unambiguously established by NMR spectroscopy and X-ray crystallography¹⁶ (Figure 3.2). Heterocycle **4** has a planar five-membered ring with significant C=C-C=C diene character.

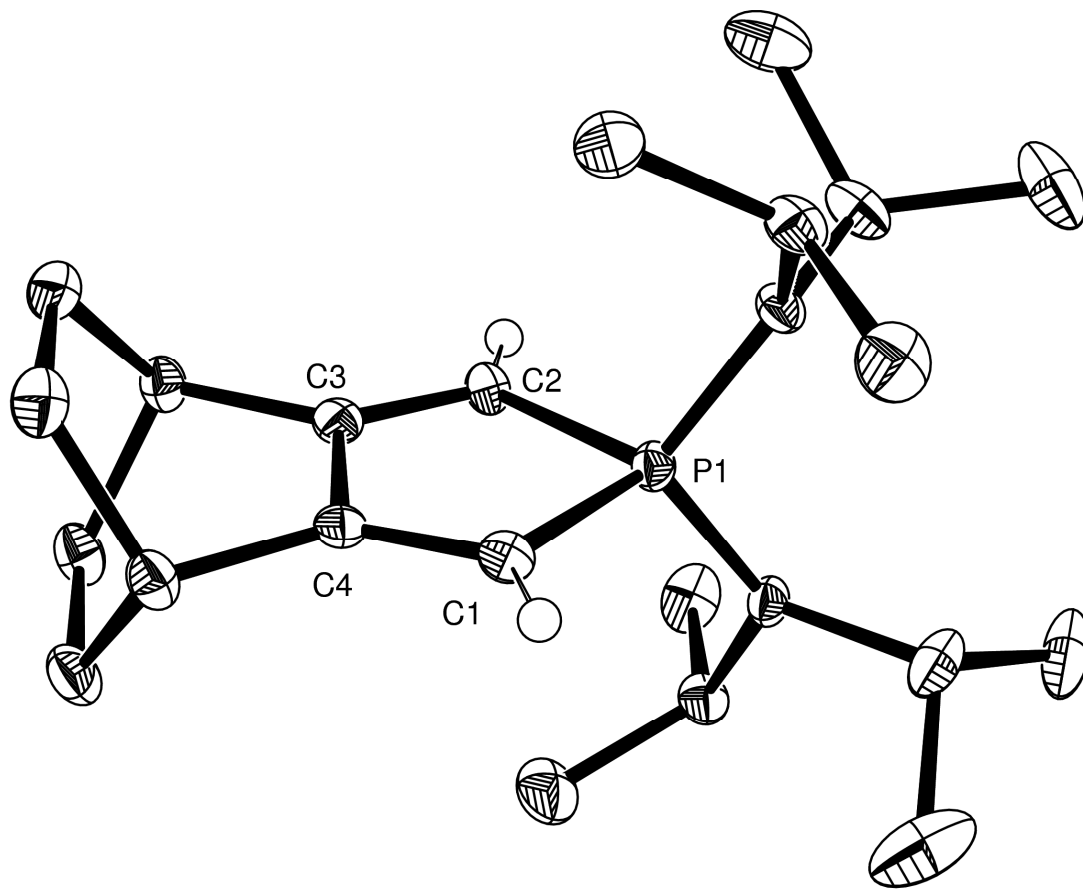


Figure 3.2. X-ray crystal structure of phosphonium salt **4**. Hydrogen atoms and triflate anion are omitted for clarity. Thermal ellipsoids are at 50 % probability. Selected bond lengths (\AA) and angles ($^\circ$): P1–C1 1.782(3), C1–C4 1.329(4), P1–C2 1.791(2), C2–C3 1.342(3), C3–C4 1.497(4); P1–C1–C4 107.99(19), P1–C2–C3 107.17(19), C1–P1–C2 94.65(12).

Deprotonation of salt **4** in THF using KHMDS leads to the desired vinylidenephosphorane **5** as the major product as indicated by ^{31}P NMR spectroscopy (+86 ppm). Compound **5** is indefinitely stable in solution and in the solid state. As expected, the ^1H and ^{13}C spectra show that the product is no longer symmetrical. The ^{13}C NMR signal of the central carbon atom was

observed at $\delta = 184.2$ ppm, which is significantly low-field shifted relative to the starting material (108.7 ppm). Interestingly, a similar low-field signal was observed for the push-pull allene **E** (199 ppm),⁹ which highlights, at least to some extent, the similarities between **D** and **E**. Compound **5** was isolated in crystalline form from a concentrated ether solution at -30 °C (32 % isolated yield, m.p. = 81-82 °C) and subjected to a single crystal X-ray analysis (Figure 3.3).¹⁶

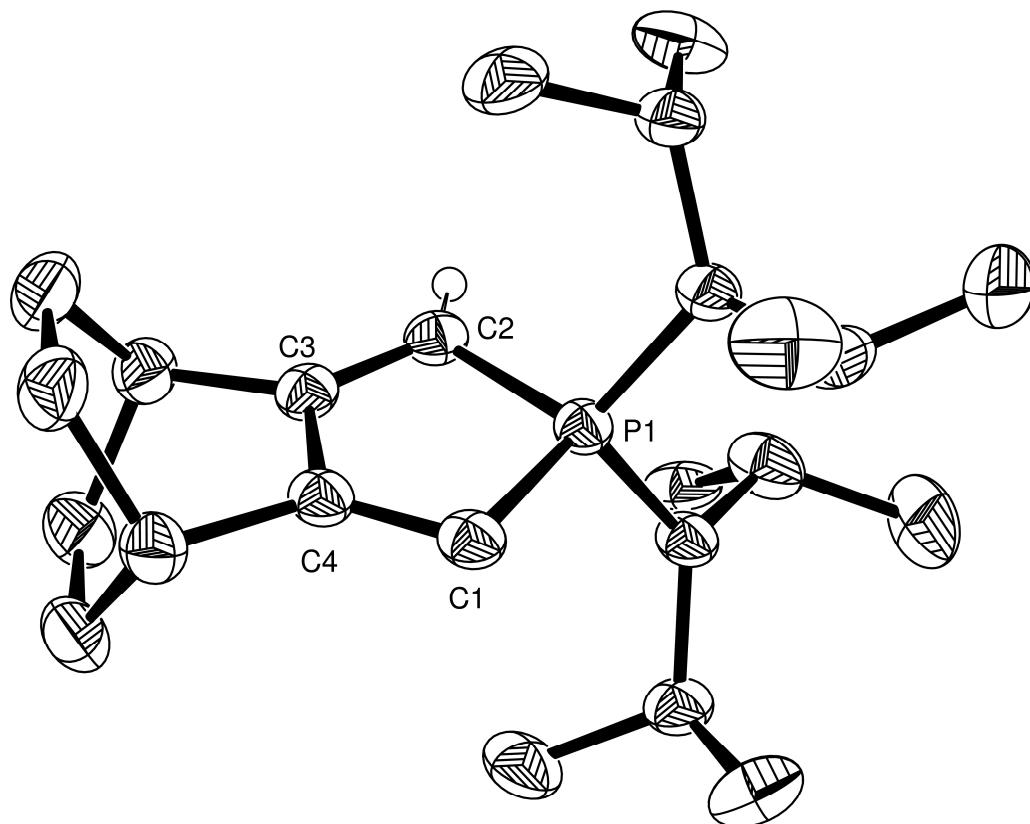


Figure 3.3. X-ray crystal structure of phosphaallene ylide **5**. Hydrogen atoms are omitted for clarity. Thermal ellipsoids are at 50 % probability. Selected bond lengths (Å) and angles (°): P1–C1 1.783(15), C1–C4 1.358(2), P1–C2 1.789(16), C2–C3 1.342(2), C3–C4 1.510(2); P1–C1–C4 99.94(11), P1–C2–C3 101.97(12), C1–P1–C2 102.04(8).

The most striking feature of **5** is the P1-C1 bond distance of 1.783 Å, which is essentially the same as that of the phosphonium precursor **4** (1.786 Å). This bond is exceptionally long compared to those observed for a non-stabilized phosphorus ylide (1.66 Å),^{17a} the previously reported five-membered cyclic carbodiphosphorane of type **B** (1.64-1.66 Å)³ and, even more strikingly, than that of an acyclic vinylidene phosphorane (1.68 Å).^{17b} The only significant change in geometry between **4** and **5** is the P1-C1-C4 bond angle, which decreased significantly from 107° to 100°. Interestingly, the same phenomenon is always observed for carbenes and bent-allenes when compared with their conjugate acid precursors.^{1, 6}

In order to better understand the electronic properties of **5**, DFT calculations were performed at the B3LYP/6-31G* level of theory.¹⁸ The calculated geometric parameters show an excellent agreement with those obtained experimentally (P1-C1 = 1.789 Å).¹⁹ As expected, the HOMO is localized primarily on C1 in the molecular plane. However, the LUMO is not the anti-bonding (σ^*) orbital of the phosphonio moiety, which is generally observed in other ylides,²⁰ but corresponds mainly to the π system, which demonstrates that the phosphorane acts as a π -acceptor (Fig. 3.4).

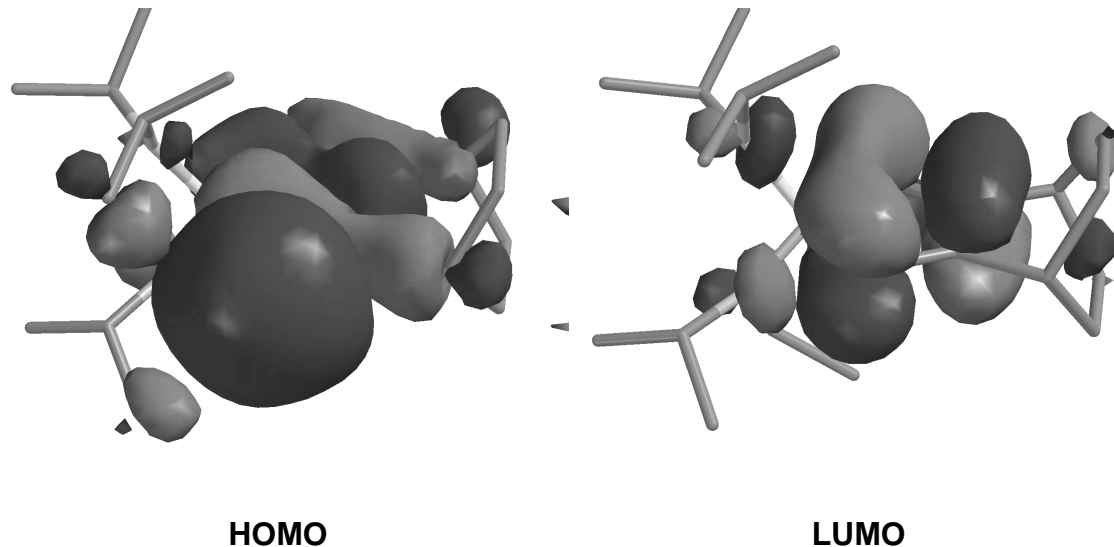


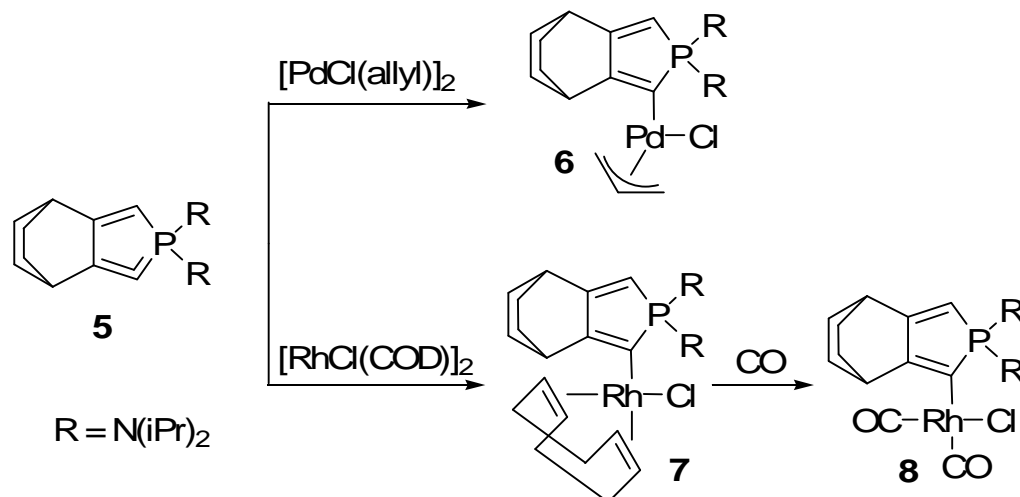
Figure 3.4. Calculated HOMO and LUMO of phosphaallene **5**.

The Wiberg bond orders²¹ were also calculated, and it was found that the organic part of the heterocycle has significant diene character ($C_1-C_4 = 1.817$, $C_4-C_3 = 1.018$, $C_3-C_2 = 1.769$). The C-P bond orders ($C_1-P_1 = 1.027$, $C_2-P_1 = 0.848$) indicate a weak interaction of the phosphonio group with the conjugated π -electrons and C_1 lone pair, which is in agreement with the observed long P-C bonds. These calculations along with the X-ray crystallographic data indicate that the predominant resonance form of **5** is D^2 .

The singlet-triplet energy gap of **5** was calculated to be 32.4 kcal/mol, which is smaller than NHCs (68.1-84.8 kcal/mol),¹ but in the range of those calculated for alkylaminocarbenes (23-46 kcal/mol).²² This, in addition to the acute $P_1-C_1-C_4$ bond angle, indicates that **5** is an excellent candidate to be a strong

electron-donating ligand, which should lead to robust transition metal complexes.

To investigate the ligand behavior freshly generated **5** was added to a solution of $[\text{PdCl}(\text{allyl})]_2$ which led to the desired complex **6** (Scheme 3.2). This was ascertained by the ^{13}C NMR spectra wherein the central carbon moved upfield (as is typical for metal complexes of NHCs **A**, carbodiphosphoranes **B**, and bent-allenes **C**) to 140.6 ppm (as a broad peak due to the dynamic behavior on the NMR timescale, similar broad peaks are observed for they allyl group) from 184.5. X-ray diffraction studies confirmed conclusively the structure of **6** (Figure 3.5).¹⁶



Scheme 3.2. Synthesis of palladium complex **6** and rhodium complexes **7** and **8**.

After successful complexation to palladium further investigation into the ligand properties of **5** were undertaken with rhodium. Similar to the palladium case,

freshly generated **5** was added to $[\text{RhCl}(\text{COD})]_2$ to form the corresponding complex **7**, which was isolated as a thermally very stable orange solid (m.p. 197–198 °C). The formation of **7** can clearly be ascertained by ^{13}C NMR where, once again, the central carbon peak moves upfield to 148.0 ppm (dd , $^1J_{\text{CP}} = 41.5$ Hz, $^1J_{\text{CRh}} = 13.7$ Hz). As expected, the X-ray crystal structure¹⁶ confirmed the η^1 -ligation although a disorder precludes discussion of structural details (Figure 3.6).

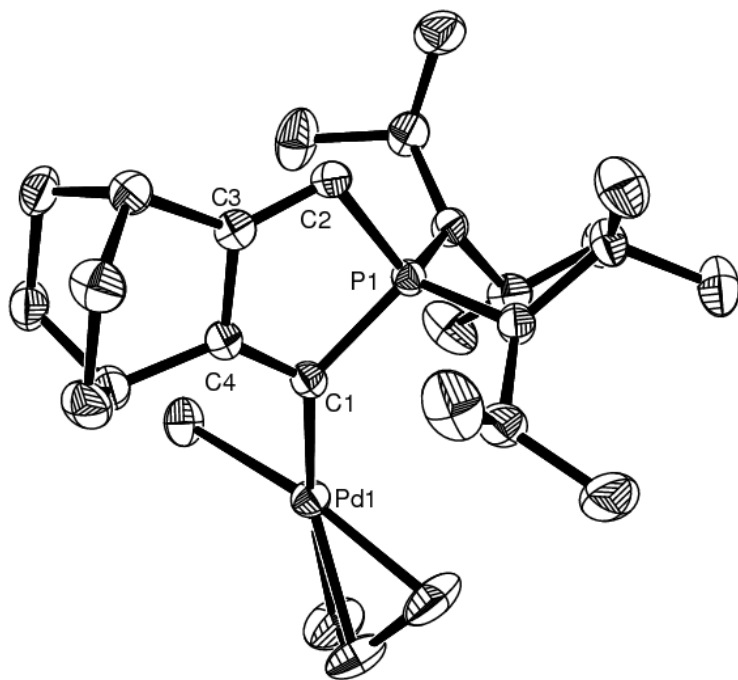


Figure 3.5. X-ray crystal structure of **6**. Hydrogen atoms are omitted for clarity. Selected bond lengths (Å) and angles (°): P1–C1 1.799(3), C1–C4 1.349(4), P1–C2 1.794(3), C2–C3 1.336(4), C3–C4 1.495(3), C1–Pd1 2.053(3); P1–C1–C4 102.58(18), P1–C2–C3 104.93(19), C1–P1–C2 98.20(13).

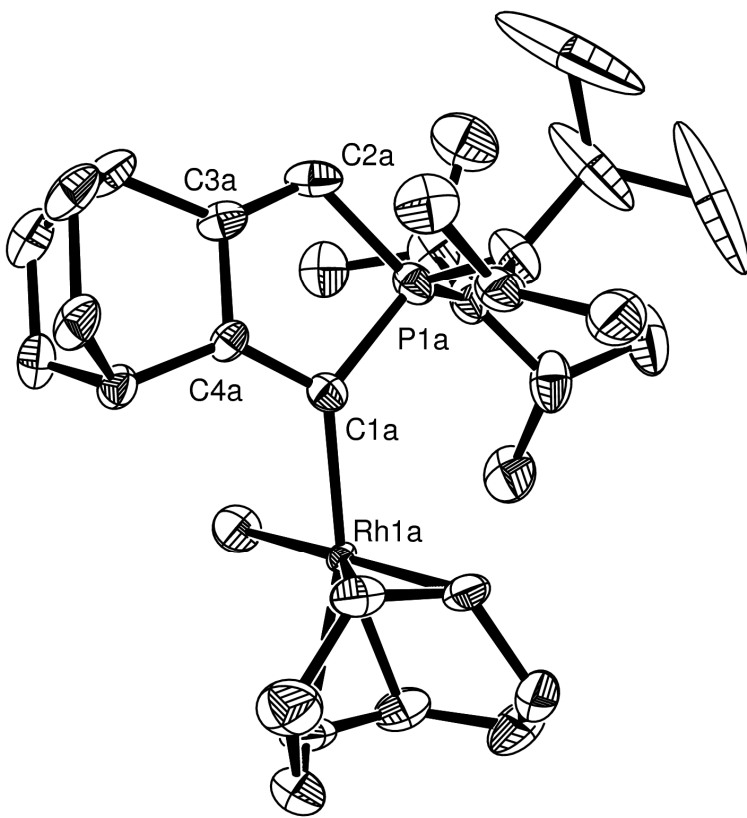


Figure 3.6 X-ray crystal structure of **7**.

The corresponding dicarbonyl complex **8** can easily be synthesized by bubbling carbon monoxide through a dichloromethane solution of **7**. The infrared spectrum shows the characteristic CO stretching frequencies with an average value of 2017 cm^{-1} . This value clearly shows that the cyclic vinylidenephosphorane **5** is a much stronger donor than five-membered NHCs **A** ($2036\text{-}2060\text{ cm}^{-1}$),²³ comparable to bent-allenes **C** (2018 cm^{-1}),⁶ but weaker than carbodiphosphoranes **B** (2001 cm^{-1}).³ However, it is important to note that complexes **7** and **8** appear to be much more robust than the corresponding carbodiphosphorane complexes.

In conclusion, a room temperature stable cyclic vinylidenephosphorane has been synthesized. It features a very long phosphorus carbon bond, much longer than in the acyclic version, leaving the carbon lone pair fully available for coordination to metals. Accordingly, this species behaves as a strong electron-donating ligand for transition metals and coordinates both rhodium and palladium. This opens the way for use of this new ligand as an ancillary ligand in homogeneous catalysis.

Experimental

All manipulations were performed under an atmosphere of argon using standard schlenk techniques. All solvents were dried and distilled prior to use (THF, hexane, and toluene were dried and distilled over potassium, ether over sodium wire and dichloromethane and chloroform were dried and distilled over calcium hydride). ^1H , ^{13}C and ^{31}P NMR spectra were recorded on Bruker Advance 300 and 600 spectrometers. ^1H and ^{13}C NMR chemical shifts are reported in ppm relative to TMS as an external standard. ^{31}P NMR chemical shifts are reported in ppm relative to 85% H_3PO_4 as an external standard. Melting points are uncorrected.

Bicyclic diene **1** was synthesized similar to a published procedure.¹²

Phospholenium salt **2**: It was synthesized similar to a published procedure.¹³ Excess diene **1** (3.1 g, 23 mmol) in dichloromethane (10 ml) was added to a solution of bis(diisopropylamino) phosphonium triflate (5 g, 13 mmol) in dichloromethane (10 ml) and the mixture was heated to 40 °C for 18h. All volatiles were removed under vacuum and the resultant solid was washed with ether and crystallized from CHCl_3 / ether to give light yellow crystals (5.3 g, 78%).
m.p. : 187.9-188.6 °C; $^{31}\text{P}\{\text{H}\}$ NMR (CDCl_3 , 25 °C, 80 MHz) : δ 75.2; ^1H NMR (CDCl_3 , 25 °C, 300 MHz) δ 1.30 (d, $J = 6.9$ Hz, 2H, CH_3), 1.40 – 1.64 (m, 8H, CH_2), 2.70 (s, 2H, $\text{CH}_{\text{bridgehead}}$), 2.27 (d, $J_{\text{HP}} = 10.3$, 4H, PCH_2), 3.73 (m, 4H,

NCH); ^{13}C NMR (CDCl_3 , 25 °C, 75 MHz) δ 22.8 (CH_3), 25.8 (CH_2), 32.3 (d, $J_{\text{CP}} = 14.9$ Hz, $\text{CH}_{\text{bridgehead}}$), 33.9 (d, $J_{\text{CP}} = 76.1$ Hz, PCH_2), 47.9 (d, $J_{\text{CP}} = 4.0$ Hz, NCH), 137.0 (d, $J_{\text{CP}} = 13.8$ Hz, C=C)

Phosphorus ylide 3: Liquid ammonia (3 ml) was condensed into the schlenk tube containing **2** (0.281 g, 0.55 mmol) and sodium amide (0.043 g, 1.10 mmol) at -78 °C. After 2 hours at -30 °C, the reaction was allowed to warm to room temperature and the ammonia was allowed to evaporate. The resultant yellow solid was put under vacuum to remove all volatiles. The ylide **3** was then extracted in hexanes and the hexane was removed under vacuum to give analytically pure ylide **3** in an 84% yield (0.168 g). $^{31}\text{P}\{\text{H}\}$ NMR (C_6D_6 , 25 °C, 80 MHz): δ 44.9; ^1H NMR (C_6D_6 , 25 °C, 300 MHz) δ 1.19 (d, $J = 6.6$ Hz, 12H, CH_3), 1.24 (d, $J = 6.7$ Hz, 12H, CH_3), 1.53 (d, $J = 9.1$ Hz, 4H, CH_2), 1.60 (d, $J = 13.4$ Hz, 4H, CH_2), 2.25 [s (broad), 2H, $\text{CH}_{\text{bridgehead}}$], 3.44 (m, 4H, NCH), 5.25 (s, 1H, PCH_2) 5.86 (d, $J = 5.3$ Hz, 1H, PCH_2), 6.21 (s, 1H, PCH); ^{13}C NMR (C_6D_6 , 25 °C, 75 MHz) δ 24.1 (d, $J_{\text{CP}} = 5.4$ Hz, CH_3), 22.5 (d, $J_{\text{CP}} = 7.2$ Hz, CH_3), 26.5 (s, CH_2), 38.2 (s, $\text{CH}_{\text{bridgehead}}$), 41.7 (d, $J_{\text{CP}} = 5.44$ Hz, $\text{CH}_{\text{bridgehead}}$), 47.2 (d, $J_{\text{CP}} = 10.4$ Hz, NCH), 113.2 (d, $J_{\text{CP}} = 24.9$ Hz, PCH_2), 124.7 (d, $J_{\text{CP}} = 10.4$ Hz, PCH) 147.0 (d, $J_{\text{CP}} = 25.0$ Hz, C) 148.6 (s, C).

Phosphonium salt 4: The ylide **3** was dissolved in THF (7 ml) and added dropwise to a solution of carbon tetrachloride (0.07 g, 0.49 mmol) in THF (5 ml). The reaction was stirred for 12 h. All volatiles were removed under vacuum and the

resultant solid was washed with hexanes and ether and crystallized from warm THF to give 0.119 g of **4** as yellowish crystals (65%). m.p. : 213.2-215.1 °C; $^{31}\text{P}\{\text{H}\}$ NMR (CDCl_3 , 25 °C, 80 MHz) : δ 57.2; ^1H NMR (CDCl_3 , 25 °C, 300 MHz) δ 1.22 (d, $J = 6.8$ Hz, 24H, CH_3), 1.72 (dd, $J = 7.6$ and 79.9 Hz, 8H, CH_2), 2.88 (s, 2H, $\text{CH}_{\text{bridgehead}}$), 3.67 (m, 4H, NCH), 6.31 (d, $J_{\text{HP}} = 33.7$ Hz, 2H, PCH); ^{13}C NMR (CDCl_3 , 25 °C, 75 MHz) δ 22.4 (CH_3), 24.1 (CH_2), 31.9 (d, $J_{\text{CP}} = 19.7$ Hz, $\text{CH}_{\text{bridgehead}}$), 48.1 (d, $J_{\text{CP}} = 4.7$ Hz, NCH), 108.7 (d, $J_{\text{CP}} = 111.2$ Hz, PCH), 163.6 (d, $J_{\text{CP}} = 25.9$ Hz, C)

Synthesis of 5: To a mixture of **4** (173 mg, 0.34 mmol) and KHMDS (74 mg, 0.37 mmol) was added THF (5 ml) at -78°C. The solution was stirred at -78 °C for 10 min and then allowed to warm to room temperature. After 1 h, all volatiles were removed under vacuum and **5** was extracted in ether. The ether solution was concentrated and red-brown crystals formed at -30 °C; 32 % yield (22 mg); m.p. 81-82 °C; $^{31}\text{P}\{\text{H}\}$ NMR (C_6D_6 , 25 °C, 243 MHz): δ 86.4; ^1H NMR (C_6D_6 , 25 °C, 300 MHz) δ 1.19 (d, $J = 6.6$ Hz, 12H, CH_3), 1.24 (d, $J = 6.7$ Hz, 12H, CH_3), 1.53 (d, $J = 9.1$ Hz, 4H, CH_2), 1.60 (d, $J = 13.4$ Hz, 4H, CH_2), 2.25 [s (broad), 2H, $\text{CH}_{\text{bridgehead}}$], 3.44 (m, 4H, NCH), 5.25 (s, 1H, PCH_2) 5.86 (d, $J = 5.3$ Hz, 1H, PCH_2), 6.21 (s, 1H, PCH); ^{13}C NMR (C_6D_6 , 25 °C, 151 MHz): δ 22.9 (s, CH_3), 26.2 (s, CH_2), 27.1 (s, CH_2), 34.5 (broad, CH), 37.7 (broad, CH), 46.9 (s, iPr), 113.7 (d, $^1J_{\text{CP}} = 121$ Hz, PCH), 163.1 (broad, C), 164.8 (broad, C), 184.5 (broad, PC).

Palladium complex **6** was synthesized by addition of freshly generated **5** [prepared from salt **4** (271 mg, 0.529 mmol) and KHMDS (116 mg, 0.58 mmol) in thf (5 ml)] to a thf (3 ml) solution of $[\text{Pd}(\text{allyl})\text{Cl}]_2$ (97mg, 0.26 mmol) at -78 °C. The mixture was allowed to warm to room temperature and stir for 4 hours and then all volatiles were removed under vacuum. The resultant solid was extracted in ether and then concentrated to give yellow needles (193 mg, 67%). m.p. : 199-200 °C; $^{31}\text{P}\{\text{H}\}$ NMR (CD_3CN , 25 °C, 243 MHz) : δ 74.9; ^1H NMR (CD_3CN , 25 °C, 600 MHz) : δ 1.28 (d, $J = 3.0$ Hz, 12H, iPr), 1.29 (d, $J = 2.8$ Hz, 12H, iPr), 1.59-1.79 (m, 8H, bicyclic), 2.15 (s, 1H, allyl), 2.65 (s, 1H, bridgehead), 2.79 (s, 1H, bridgehead), 3.05 (d, $J = 13.3$ Hz, 1H, allyl), 3.64 [s(broad), 1H, allyl], 3.85 [s(broad), 1H, allyl], 4.03 [s(broad), 4H, CH iPr], 5.20 (m, 1H, allyl), 5.97 (d, $^2J_{\text{HP}} = 30.2$ Hz, 1H, phosphole) ^{13}C NMR (CDCl_3 , 25 °C, 151 MHz) : δ 24.3 (s, CH_3), 25.7 (s, CH_2), 26.9 (s, CH_2), 34.1 (d, $^3J_{\text{CP}} = 22.5$ Hz, CH), 37.6 (d, $^3J_{\text{CP}} = 35.6$ Hz, CH), 46.5 (s, CH_2 allyl), 49.0 (s, Hz, NCH), 72.1 (s, CH_2 allyl), 110.2 (d, $^1J_{\text{CP}} = 91.9$ Hz, PCH), 113.0 (s, CH allyl), 140.6 (broad, PC), 162.4 (d, $^2J_{\text{CP}} = 23.0$ Hz, C), 164.0 (d, $^2J_{\text{CP}} = 43.7$ Hz, C).

Synthesis of 7: Freshly generated **5** [prepared from **4** (308 mg, 0.601 mmol) and KHMDS (132 mg, 0.662 mmol) in THF (5 ml)] was added to a THF (3 ml) solution of $[\text{RhCl}(\text{COD})]_2$ (148 mg, 0.3 mmol) at -78 °C. The mixture was allowed to warm to room temperature and stirred for 4 h. All volatiles were removed under vacuum, and the resultant solid was washed with ether, and then extracted with

chloroform. Orange single crystals were grown from a concentrated chloroform / ether solution; 42 % yield (154 mg); m.p. 197-198 °C; $^{31}\text{P}\{\text{H}\}$ NMR (CDCl_3 , 25 °C, 243 MHz): δ 73.9 (d, $^2J_{\text{PRh}} = 11.6$ Hz); ^1H NMR (CDCl_3 , 25 °C, 600 MHz) : δ 1.26 (d, $J = 6.9$, 12H, i-Pr), 1.42 [s(broad), 12H, iPr], 1.56 (m, 2H, bicyclic), 1.62-2.03 (m, 10H, COD/bicyclic), 2.10-2.40 (m, 4H, COD), 2.50 (s, 1H, bridgehead), 3.43 (s, 1H, bridgehead), 3.65 (s, 2H, COD), 3.82 [s(broad), 4H, CH iPr], 4.70 (s, 2H, COD), 5.57 (d, $^1J_{\text{PC}} = 30.9$ Hz, 1H, phosphole); ^{13}C NMR (CDCl_3 , 25 °C, 151 MHz): δ 24.1 (broad, CH_3), 24.5 (broad, CH_3), 25.0 (CH_2), 26.6 (CH_2), 29.1 (CH_2), 33.2 (d, $^3J_{\text{CP}} = 22.3$ Hz, CH_2), 33.6 (CH_2), 36.9 (d, $^3J_{\text{CP}} = 35.5$ Hz, CH), 48.0 (d, $^2J_{\text{CP}} = 5.1$ Hz, NCH), 64.3 (CH), 92.9 (CH), 108.6 (d, $^1J_{\text{CP}} = 89.5$ Hz, PCH), 148.0 (dd, $^1J_{\text{CP}} = 41.5$ Hz, $^1J_{\text{CRh}} = 13.7$ Hz, PC), 163.6 (d, $^2J_{\text{CP}} = 22.8$ Hz, C), 163.9 ppm (d, $^2J_{\text{CP}} = 42.6$ Hz, C).

Synthesis of 8: CO was bubbled into a CH_2Cl_2 (3 ml) solution of complex **7** (154 g, 0.252 mmol). The volatiles were removed under vacuum to give **8** as a yellow orange solid; 99 % yield (139 mg); m.p. 138-140 °C; $^{31}\text{P}\{\text{H}\}$ NMR (CDCl_3 , 25 °C, 243 MHz): δ 73.9 (d, $^2J_{\text{PRh}} = 8.5$ Hz); ^1H NMR (CDCl_3 , 25 °C, 600 MHz) : δ 1.28 (d, $J = 6.9$ Hz, 12H, iPr), 1.33 (d, $J = 6.9$ Hz, 12H, iPr), 1.60 (m, 2H, bicyclic), 1.77 (t, $J = 10.9$ Hz, 6H, bicyclic), 2.62 (s, 1H, bridgehead), 3.05 (s, 1H, bridgehead), 4.02 (sept, $J = 6.9$, 4H, CH iPr), 5.73 (d, $^1J_{\text{PC}} = 30.8$ Hz, 1H, phosphole); ^{13}C NMR (CDCl_3 , 25 °C, 151 MHz): δ 23.9 (d, $^3J_{\text{CP}} = 1.7$ Hz, CH_3), 24.0 (d, $^3J_{\text{CP}} = 3.0$ Hz, CH_3), 24.9 (CH_2), 25.5 (CH_2), 33.1 (d, $^3J_{\text{CP}} = 21.6$ Hz, CH), 37.1 (d, $^3J_{\text{CP}} = 32.9$

Hz, CH), 48.3 (d, $^2J_{CP} = 5.1$ Hz, NCH), 110.0 (d, $^1J_{CP} = 94.8$ Hz, PCH), 140.6 (dd, $^1J_{CP} = 35.9$ Hz, $^1J_{CRh} = 30.7$ Hz, PC), 163.8 (dd, $^2J_{CP} = 39.7$ Hz, $^2J_{CRh} = 2.0$ Hz, C), 165.4 (d, $^2J_{CP} = 22.3$ Hz, C), 185.6 (d, $^1J_{CRh} = 78.6$ Hz, CO), 185.6 (dd, $^1J_{CRh} = 53.4$ Hz, $^3J_{CP} = 11.8$ Hz, CO); IR (CH_2Cl_2): $\nu_{\text{CO}} = 2058$ and 1976 cm^{-1} .

References

1. For recent reviews on stable carbenes, see for examples: a) F. E. Hahn, M. C. Jahnke, *Angew. Chem.* **2008**, *120*, 3166; *Angew. Chem. Int. Ed.* **2008**, *47*, 3122; b) E. A. B. Kantchev, C. J. O'Brien, M. G. Organ, *Angew. Chem.* **2007**, *119*, 2824; *Angew. Chem. Int. Ed.* **2007**, *46*, 2768; c) F. Glorius, *N-Heterocyclic Carbenes in Transition Metal Catalysis (Topics in Organometallic Chemistry)* Springer Verlag, **2006**; d) S. P. Nolan, *N-Heterocyclic Carbenes in Synthesis*; Wiley-VCH, **2006**; e) D. Bourissou, O. Guerret, F. P. Gabbaï, G. Bertrand, *Chem. Rev.* **2000**, *100*, 39.
2. For recent reviews on ylides and carbodiphosphoranes, see: a) O. I. Kolodiaznyi, *Tetrahedron*, **1996**, *52*, 1855; b) O. I. Kolodiaznyi, *Phosphorus Ylides: Chemistry and Application in Organic Synthesis*, Wiley-VCH, Weinheim, **1999**; c) H. M. Cristau, *Chem. Rev.* **1994**, *94*, 1299.
3. S. Marrot, T. Kato, H. Gornitzka, A. Baceiredo, *Angew. Chem.* **2006**, *118*, 2660-2663; *Angew. Chem. Int. Ed.* **2006**, *45*, 2598.
4. a) Y. Canac, M. Soleilhavoup, S. Conejero, G. Bertrand, *J. Organomet. Chem.* **2004**, *689*, 3857-3865; b) V. Lavallo, Y. Canac, C. Präsang, B. Donnadieu, G. Bertrand, *Angew. Chem.* **2005**, *117*, 5851; *Angew. Chem. Int. Ed.* **2005**, *44*, 5705; c) V. Lavallo, Y. Canac, A. DeHope, B. Donnadieu, G. Bertrand, *Angew. Chem.* **2005**, *117*, 7402; *Angew. Chem. Int. Ed.* **2005**, *44*, 7236; d) V. Lavallo, J. Mafhouz, Y. Canac, B. Donnadieu, W. W. Schoeller, G. Bertrand, *G. J. Am. Chem. Soc.* **2004**, *126*, 8670.
5. a) R. Tonner, F. Öxler, B. Neumüller, W. Petz, G. Frenking, *Angew. Chem.* **2006**, *118*, 8206; *Angew. Chem. Int. Ed.* **2006**, *45*, 8038 -8042; b) H. Schmidbaur, *Angew. Chem.* **2007**, *119*, 3042; *Angew. Chem. Int. Ed.* **2007**, *46*, 2984; c) G. Frenking, B. Neumüller, W. Petz, R. Tonner, F. Öxler, *Angew. Chem.* **2007**, *119*, 3044; *Angew. Chem. Int. Ed.* **2007**, *46*, 2986.
6. a) C. A. Dyker, V. Lavallo, B. Donnadieu, G. Bertrand, *Angew. Chem.* **2008**, *120*, 3250-3253; *Angew. Chem. Int. Ed.* **2008**, *47*, 3206; b) V. Lavallo, C. A. Dyker, B. Donnadieu, G. Bertrand, *Angew. Chem. Int. Ed.* **2008**, *47*, 5411.

-
7. For calculations on carbo(dicarbenes), see: a) R. Tonner, G. Frenking, *Angew. Chem.* **2007**, 119, 8850-8853; *Angew. Chem. Int. Ed.* **2007**, 46, 8695; b) R. Tonner, G. Frenking, *Chem. Eur. J.* **2008**, 14, 3260; c) R. Tonner, G. Frenking, *Chem. Eur. J.* **2008**, 14, 3273.
 8. For other papers related to bent-allenes, see: a) O. Kaufhold, F. E. Hahn, *Angew. Chem.* **2008**, 120, 4122; *Angew. Chem. Int. Ed.* **2008**, 47, 4057; b) A. Fürstner, M. Alcarazo, R. Goddard, C. W. Lehmann, *Angew. Chem. Int. Ed.* **2008**, 47, 3210.
 9. a) R. W. Saalfrank, H. Maid, *Chem. Commun.* **2005**, 5953; b) R. W. Saalfrank, W. Paul, H. Libenow, *Angew. Chem.* **1980**, 92, 740; *Angew. Chem. Int. Ed.* **1980**, 19, 713; c) R. W. Saalfrank, *Isr. J. Chem.* **1985**, 26, 181.
 10. M. Soleilhavoup, A. Baceiredo, O. Treutler, R. Ahlrichs, M. Nieger, G. Bertrand, *J. Am. Chem. Soc.* **1992**, 114, 10959.
 11. H. J. Bestmann, K. Roth, R. W. Saalfrank, *Angew. Chem.* **1977**, 89, 915-916; *Angew. Chem. Int. Ed.* **1977**, 16, 877.
 12. a) D. Birney, T. K. Lim, J. H. P. Koh, B. R. Pool, J. M. White, *J. Am. Chem. Soc.* **2002**, 124, 5091; b) M. Avenati, O. Pilet, P. A. Carrupt, P. Vogel, *Helv. Chim. Acta* **1982**, 65, 178.
 13. a) A. H. Cowley, R. A. Kemp, J. G. Lasch, N. C. Norman, C. A. Stewart, *J. Am. Chem. Soc.* **1983**, 105, 7444; b) A. H. Cowley, R. A. Kemp, J. G. Lasch, N. C. Norman, C. A. Stewart, B. R. Whittlesey, T. C. Wright, *Inorg. Chem.* **1986**, 25, 740.
 14. H.-J. Cristau, J. Grenier, P. Lexouret, E. Torreilles, *Heteroatom Chem.* **1996**, 7, 471.
 15. Phosphines are known to react with carbon tetrachloride: a) R. Appel, H. F. Schoeler, *Chem. Ber.* **1979**, 112, 1068; b) H. Grützmacher, H. Pritzkow, *Angew. Chem.* **1991**, 103, 976; *Angew. Chem., Int. Ed.* **1991**, 30, 709-710; c) U. Heim, H. Pritzkow, H. Schoenberg, H. Grützmacher, *Chem. Comm.* **1993**, 8, 673.
 16. CCDC 690713 (**4**), 690714 (**5**) and 690715 (**7**) contain the supplementary crystallographic data. These data can be obtained free of charge from The Cambridge Crystallographic Data Centre via www.ccdc.cam.ac.uk/data_request/cif. Additionally crystallographic data all compounds including **6** can be found in the Appendix.

-
17. a) J. C. J. Bart, *J. Chem. Soc. B* **1969**, 350; b) H. Burzlaff, U. Voll, H. J. Bestmann, *Chem. Ber.* **1974**, 107, 1949.
 18. a) W. Kohn, A. D. Becke, R. G. Parr, *J. Phys. Chem.* **1996**, 100, 12974-12980; b) A. D. Becke, *J. Phys. Chem.* **1993**, 98, 5648; c) A. D. Becke, *Phys. Rev. A* **1988**, 38, 3098.
 19. For details concerning the calculations see the Appendix.
 20. D. G. Gilheany, *Chem. Rev.* **1994**, 94, 1339.
 21. Wiberg, K. B. *Tetrahedron* **1968**, 24, 1083.
 22. G. D. Frey, V. Lavallo, B. Donnadieu, W. W. Schoeller, G. Bertrand, *Science* **2007**, 316, 439-441.
 23. a) A. Fürstner, M. Alcarazo, H. Krause, C.W. Lehmann, *J. Am. Chem. Soc.* **2007**, 129, 12676; b) A. R. Chianese, X. W. Li, M. C. Janzen, J.W. Faller, R. H. Crabtree, *Organometallics* **2003**, 22, 1663.

Chapter 4

Catalytic Properties of a Vinylideneephosphorane in Ruthenium Metathesis Chemistry and Gold(I) Hydroamination Chemistry

It has become trite to point out the importance of homogeneous catalysis in synthetic chemistry. Many catalytic systems are based on late transition metal complexes where fine tuning of the ligands can drastically effect the selectivity and activity of the catalyst. This has led to many catalysts that perform reaction that are impossible stoichiometrically and often do so with astounding selectivity at ambient temperature and pressure. The homogeneous catalyst revolution was led by the phosphine ligand, which has electronic and steric properties that can easily be tuned. Perhaps the culmination of this era was the advent and widespread use of chiral phosphine ligands such as BiNAP¹ and DiPAMP^{1c, 2} that allowed for not only near complete regioselectivity but also unheard of stereoselectivity. The synthesis and isolation of the first N-Heterocyclic Carbene (NHC) **A** (Figure 4.1)³ represented the opening of a new epoch in catalysis.⁴ It was not long before carbenes were being used as ligands in transition metal catalysts to great effect.

The carbenic lone pair and nearly filled p π orbital makes NHCs excellent σ -donor and poor π -acceptor ligand, which is ideal for many catalytic processes. Recently, we have synthesized a new type of ligand with σ -donor/ π -acceptor very similar to those of NHCs and other carbenes; the vinylideneephosphorane **B**,

which has a carbenic resonance structure.⁵ In this chapter the vinylidenephosphorane is used as a ligand in both ruthenium metathesis chemistry and gold amination chemistry.

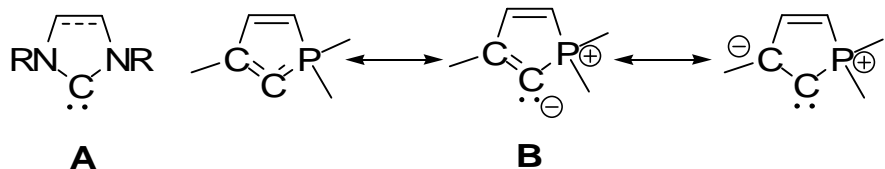


Figure 4.1. General structure of NHCs **A** and vinylidenephosphoranes **B** (with resonance structures).

The importance and usefulness of olefin metathesis chemistry⁶ was dramatically highlighted in 2005 when the Nobel prize for chemistry was given to Yves Chauvin, Robert H. Grubbs and Richard R. Schrock “for the development of the metathesis method in organic synthesis”.⁷ The ruthenium based “Grubbs catalyst” has evolved considerably since the “first generation” catalyst **1** was reported (Figure 4.2).⁸ Two of the most important advances are, first, the replacement of one phosphine ligand by an NHC to form the “second generation” catalyst **2**⁹ and second, the replacement of one phosphine with an alkyl ether that is attached to the benzylidene (creating a bidentate ligand), which is available in both a “first generation” **3** and “second generation” **4** analog and are commonly called Hoveyda-Grubbs catalysts.¹⁰ Additionally, fine tuning can be done by altering the NHC substituents and backbone and by adding/changing substituents of the benzylidene or benzylidene ether.^{10, 11, 12}

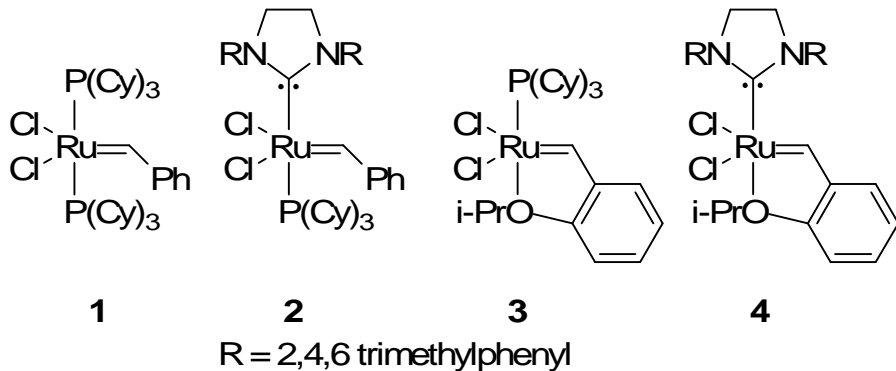


Figure 4.2. Grubbs first generation ruthenium metathesis catalyst **1**, second generation **2**, and Hoveyda-Grubbs first **3** and second **4** generation catalysts.

It is important to point out the two important ways in which the exchange of phosphine for NHC change the activity of the catalyst. First, the catalyst becomes more thermally stable thus allowing the system to be heated, which consequently allows metathesis reactions of difficult substrates to be achieved. Second, the strong σ -donation of the carbene creates a metal center that is very electron rich thus increasing the affinity of the metal center towards π -acidic olefins, which leads to a more active catalyst.¹³

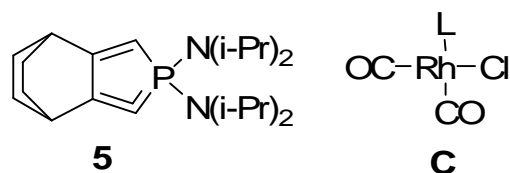


Figure 4.3. Vinylidenephosphorane ligand **5** and rhodium CO complex **C**.

We recently synthesized and reported a stable cyclic vinylidenephosphorane **5** (Figure 4.3) and demonstrated that it acts as a ligand for transition metals.⁵ In

fact, **5** is a much stronger σ -donor ligand than the NHC ($H_2IMes = 1,3$ -dimesityl-4,5-dihydroimidazol-2-ylidene) used in the second generation Grubbs catalyst **2**, which is demonstrated by the ν_{CO} absorbtion of their respective cis-[$Rh(Cl(CO)_2L)$] complexes **C** ($L = \mathbf{5}$; $\nu_{CO} = 2058, 1976\text{ cm}^{-1}$ vs. $L = H_2IMes$; $\nu_{CO} = 2081, 1996\text{ cm}^{-1}$).^{5, 14} Therefore, the question was whether Grubbs type ruthenium based catalysts could be synthesized using ligand **5**. If so would increased donor properties improve the catalytic results?

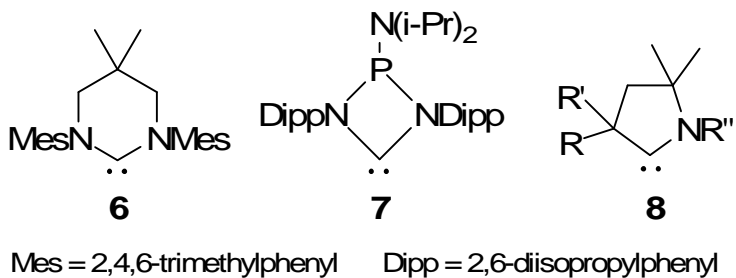


Figure 4.4. Six-membered NHC ligand **6**, four-membered NHC ligand **7** and CAAC ligand **8**.

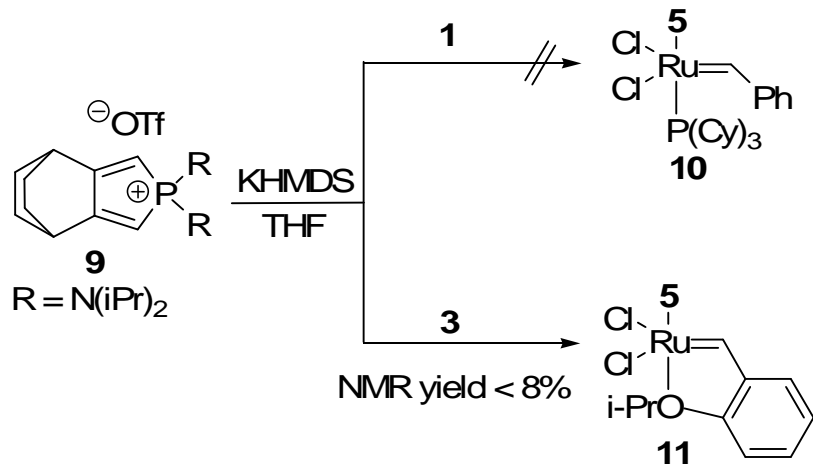
Previous attempts to drastically modify the carbene have met with mixed results. The use of six-membered NHC **6** (Figure 4.4) led to a Hoveyda-Grubbs catalyst that was markedly less active than catalyst **2** most likely due to increased steric interactions of the mesityl groups.¹⁵ The four-membered carbene **7** was also used in a Hoveyda-Grubbs catalyst but once again with decreased activity (again compared to **2**) possibly due to the slightly inferior σ -donating properties of **7** (although the lack of activity is not well understood).¹⁶ Finally Cyclic Alkyl Amino Carbenes (CAACs) of type **8** have been used as

ligands. In this case it was found that by carefully tuning the steric bulk of the aryl group results could be obtained that were comparable to those of **2** and **4**. This result is slightly unexpected because CAACs are substantially better σ -donor ligands than NHCs.¹⁴ These example serve to highlight the complex play of steric and electronic factors that lead to efficient metathesis catalysts. However, we surmised that an effective ruthenium metathesis catalyst may be viable using **5** as the ancillary ligand because of its strong ligand properties and moderate steric bulk.

The simplest method for generating L substituted Grubbs catalysts is by ligand displacement starting from the commercially available **1**. Because **1** is base stable the ligand may be generated in situ. However mixing salt **9** (the protonated precursor of **5**) KHMDS and ruthenium complex **1** led to a complex mixture which included the expected free phosphine but not the desired complex **10** (Scheme 4.1).

In a similar procedure Hoveyda-Grubbs complex **3** (which is also commercially available) was used in hopes that the increased stability of the complex (both the starting material and desired product) would lead to an isolable species.^{10b} The ^{31}P NMR of the crude reaction mixture did show a new signal at 71.4 ppm, which correlates well with the previously reported transition metal complexes of **5**. Additionally, free phosphine was also apparent, which also indicates that ligand substitution may have taken place. However, the yield (by NMR) was less than eight percent and there were several other products in

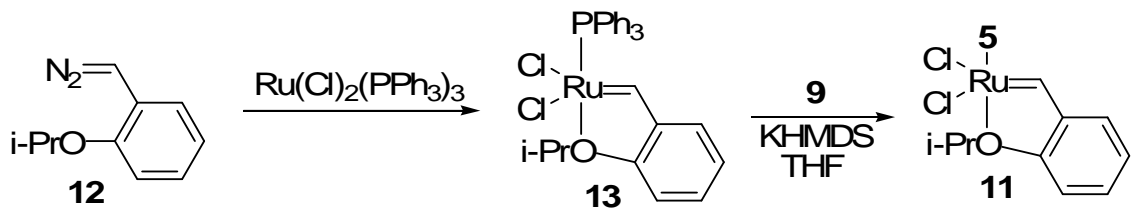
the reaction including the starting complex, which was the major product. Increasing the reaction time had no effect on the product ratio and efforts to isolate the product at 71.4 ppm failed.



Scheme 4.1. Attempted synthesis of ruthenium complex **10** and synthesis of complex **11**.

The precursor of Hoveyda-Grubbs catalyst **3** is the triphenylphosphine analog **13**, which is available in one step by reaction of the commercially available $\text{Ru}(\text{Cl})_2(\text{PPh}_3)_3$ and the benzyl diazo **12** (Scheme 4.2).^{10a} Triphenylphosphine is significantly smaller than the tricyclohexylphosphine and more importantly a poorer ligand making it more likely to undergo ligand substitution reactions. In fact, mixing salt **9** with ruthenium complex **13** and a slight excess of KHMDS in THF at room temperature once again led to the product at 71.4 ppm, free phosphine and more importantly almost no remaining starting material. After evaporation of the THF and washing with copious quantities of hexanes to

remove the phosphine a ^1H NMR spectrum was recorded, which showed the presence of a new benzylidene peak at 18.6 ppm. The ruthenium bonded carbon can be seen in the ^{13}C NMR spectrum as a broad signal at 134.5 ppm. This chemical shift corresponds well with other complexes of **5**. A concentrated solution of toluene yielded X-ray quality crystals, which were analyzed and confirmed the product to be the ruthenium complex **11** (Figure 4.5).



Scheme 4.2. Efficient synthesis of complex **11**.

The X-ray structure¹⁷ shows that the ruthenium carbon bond is 1.996 Å, which is, surprisingly, slightly longer than the corresponding Hoyeveda-Grubbs complex **4** (1.981 Å). One might expect this bond to be shorter with a stronger donating ligand as is the case for the Hoyeveda-Grubbs complex of **8** (1.930 Å, ~0.051 Å shorter).¹⁴ However, the Hoyeveda-Grubbs complex of **7**, which is a slightly weaker ligand than H₂IMes, has an even shorter bond (1.921 Å, ~0.01 Å shorter than the complex with **8** and ~0.06 Å shorter than **4**).¹⁶ This either indicates that the ν_{CO} of complexes **C** are not as good an indicator of ligand donor properties as commonly believed or, more likely, that there are numerous effects that dictate the ruthenium carbon bond length and that sterics may play an important roll in this case.

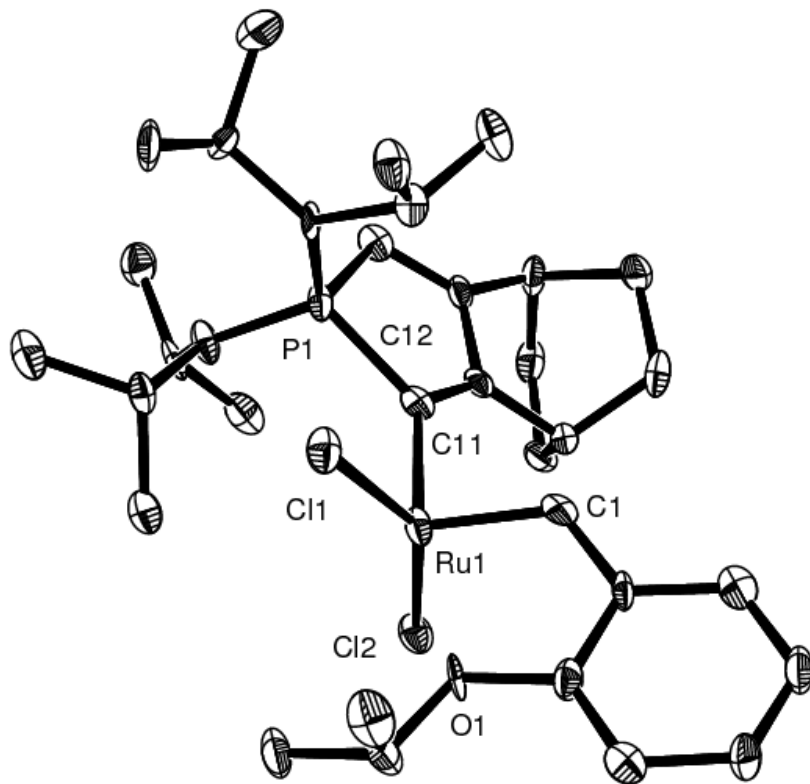
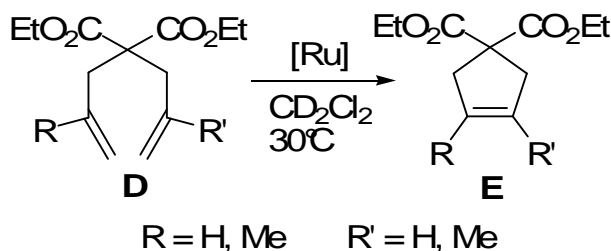


Figure 4.5. X-ray crystal structure of Hoveyda-Grubbs vinylidene phosphorane catalyst **11**. Hydrogen atoms are omitted for clarity. Thermal ellipsoids are drawn at 50% probability. Selected bond lengths (\AA) and angles ($^\circ$): P1–C11 1.836(9), C11–C12 1.370(11), C11–Ru1 1.996(8), C1–Ru1 1.803(8), O1–Ru1 2.333(6), Cl1–Ru1 2.338(2), Cl2–Ru1 2.319(3); P1–C11–C12 102.3(6), C1–Ru1–C11 90.8(4), O1–Ru1–C11 168.9(3) Cl1–Ru1–Cl2 148.12(8).

Clearly, the next step was to test the new catalyst **11** in several metathesis reactions. To do this we looked to the paper published in 2006 by Grubbs and co-workers wherein a standard system of characterization for olefin metathesis catalysts is reported.¹⁸ They define parameters for concentration, catalyst loading and temperature on a set of standard metathesis substrates.

The first tests involve ring closing metathesis (RCM), which was the first widely used metathesis reaction in organic chemistry.^{6e} The standard substrates for this reaction are diethyldiallyl malonates **D** to create di-, tri-, and tetra-substituted cyclopentenes **E** (Scheme 4.3).



Scheme 4.3. RCM test reaction of diallyl malonates **D** to cyclopentenes **E**.

Diethyldiallyl malonate (**D** where $\text{R} = \text{R}' = \text{H}$) was added to a solution of 1 mole percent of catalyst **11**. The reaction was followed by ^1H NMR spectroscopy by taking a spectrum every minute for 45 minutes. The results are plotted in Figure 4.6 along with the results of catalysts **1-4**.¹⁸ From the graph it is clear that the reaction is somewhat slow to initiate. Slower than all the catalysts except **3**, which is even slower to initiate. Unfortunately the nature of this initiation is not understood. However, despite the slow start, catalyst **11** surpasses or matches all of the catalysts by the end of the 45 minutes.

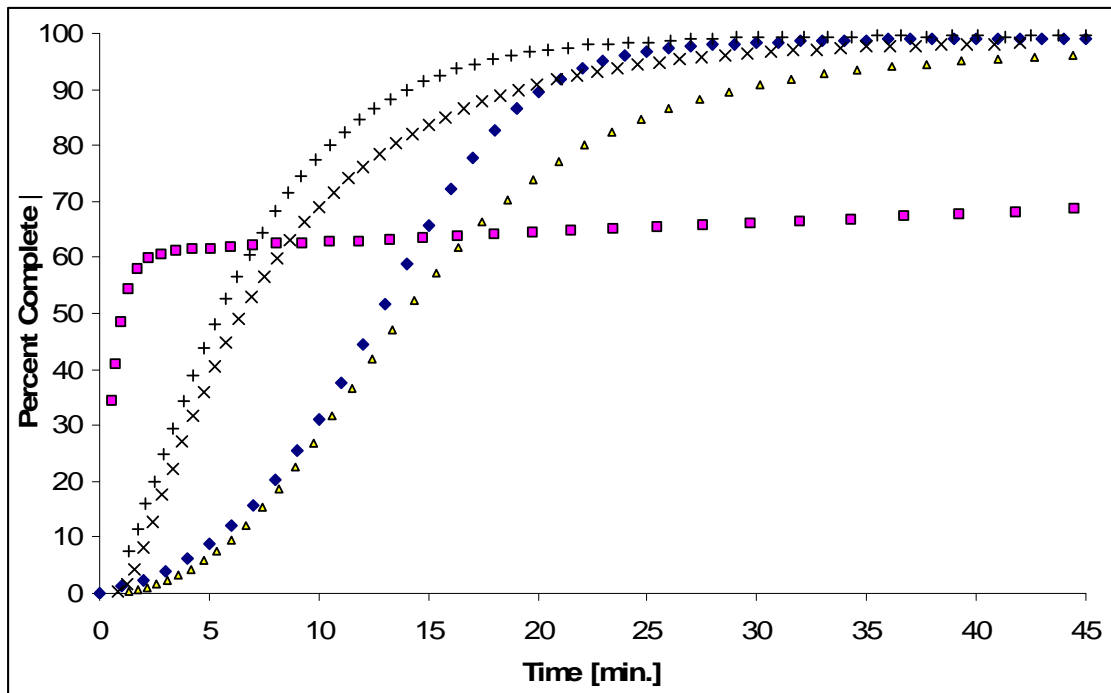


Figure 4.6. Conversion to disubstituted metathesis product **E** ($R = R' = H$) with catalyst **1** (■), **2** (x), **3** (Δ), **4** (+) and **11** (◆).

While **11** is clearly a very active catalyst there is also a question of catalyst stability. The complex is quite robust as a solid (melting point of 141 °C) and stable in air and water as well as typical organic solvents. In order to verify that the catalyst does not decompose during the RCM reaction the plot of the natural log of the starting material versus time was done (Figure 4.7), which is very nearly linear showing that pseudo first order rate kinetics occur over the course of the reaction (the slight non-linear portion at the beginning is due to the initiation effect).

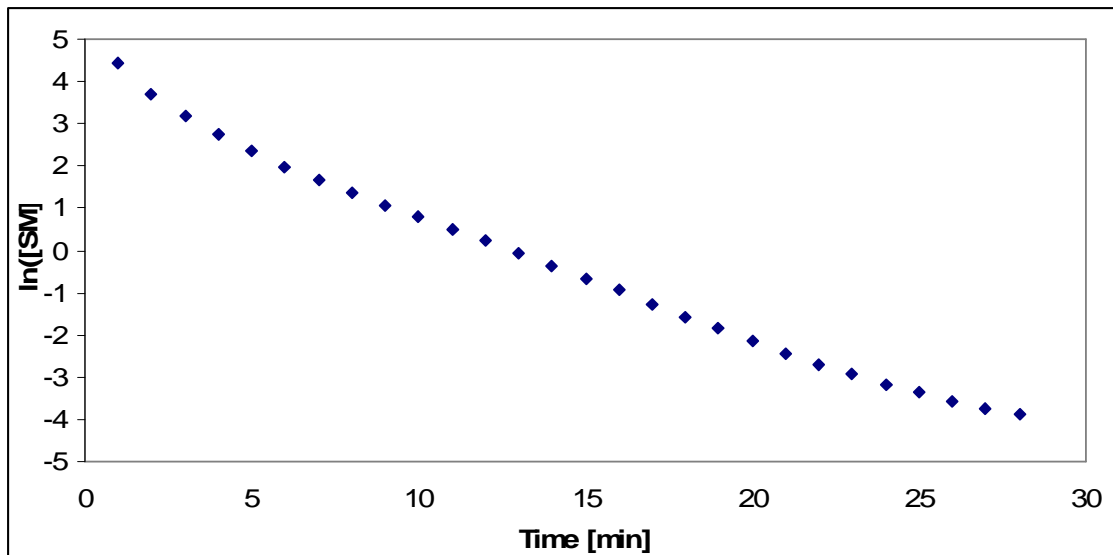


Figure 4.7. Natural log plot of the starting material versus time showing linear, pseudo first order reaction kinetics and thus no catalyst decomposition.

One further test was done in order to verify that the catalyst remains active at the end of the reaction; an additional equivalent of substrate was added. The reaction was once again followed for 30 minutes and while conversion percentage and kinetic information are not quantitatively useful the plot is nonetheless informative qualitatively. As can be seen in Figure 4.8, the reaction continues but of course without any initiation delay. Furthermore the reaction was checked again after one hour and had gone to completion. This is a strong indication that the catalyst is not only active but also robust and therefore perhaps able to function at dramatically lower catalyst loads.

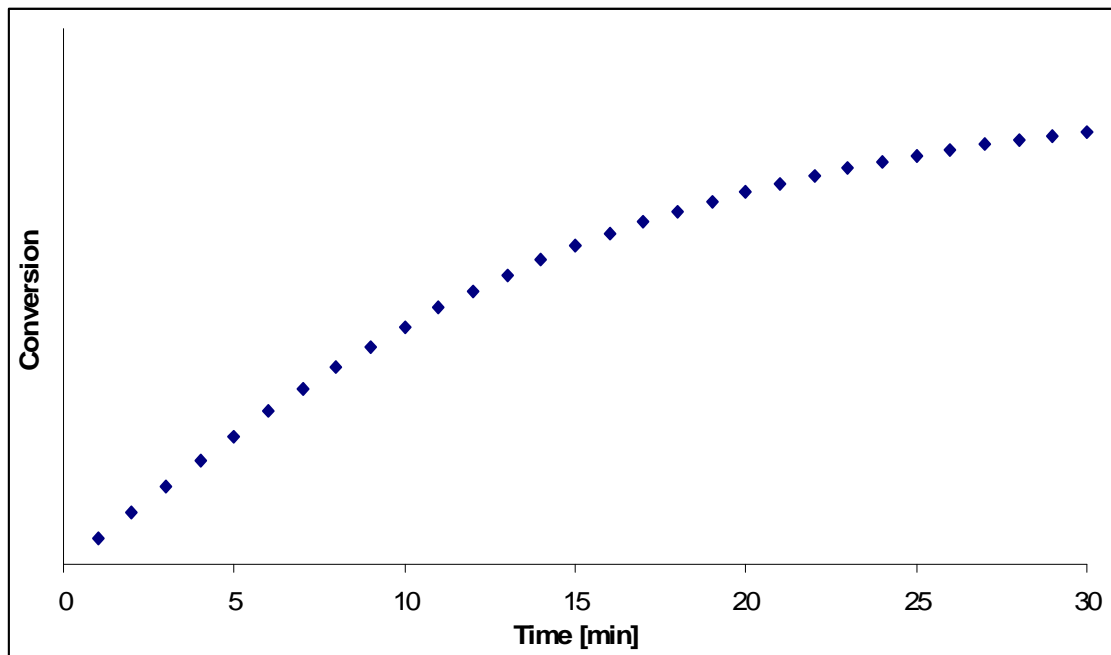


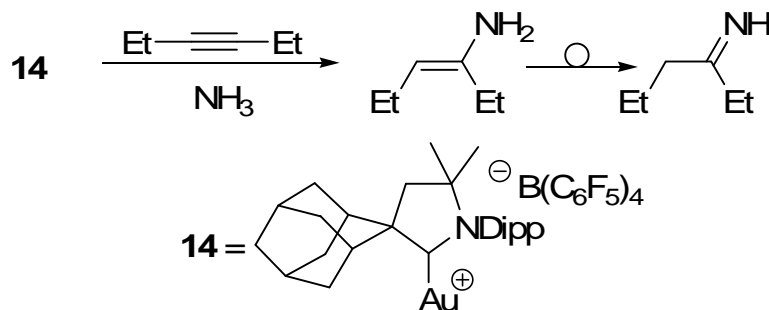
Figure 4.8. A quantitative conversion versus time plot of the RCM reaction of **11** after a second equivalent of diethyldiallyl malonate.

The next two RCM reactions involve the formation of tri-, and tetra-substituted olefins using **D** ($R = H$, $R' = Me$ and $R = R' = Me$, respectively). The results of these reaction are less encouraging. Using 1 mole percent of **11**, under the standard conditions, no tri-substituted olefin was detectable after 18 hours. The desired product could be obtained in 44% yield after one day at $40\text{ }^{\circ}\text{C}$. By changing the solvent to benzene and heating to $60\text{ }^{\circ}\text{C}$ the reaction sped up considerably yielding 14% after one hour and 94% after one day. The tetra-substituted product, on the other hand, was not obtained either under the standard conditions or with heating to $40\text{ }^{\circ}\text{C}$. This reaction was also carried out in benzene at $60\text{ }^{\circ}\text{C}$ for two days with no conversion. These two results point to a

steric problem that is often found with these challenging substrates. In fact catalyst **2** achieves only a 17% yield after 4 days and is the best of the four catalysts mentioned herein. The best way to overcome this limitation has been to create ligands with smaller steric bulk, which would indicate that analogs of **5** with smaller groups are desirable synthetic target ligands.

These preliminary results are very encouraging and warrant further investigation and there are plans to work in concert with the research group of Professor Grubbs to test catalyst **11** with the other standard substrates for cross-metathesis (CM) and ring opening metathesis polymerization (ROMP) reactions. Also these preliminary tests show that new, smaller vinylidenephosphoranes are an excellent target for ruthenium metathesis ligands.

Carbon-nitrogen bond forming reactions are of synthetic importance for academic as well as industrial applications. While use of mono- and di-substituted amines can be catalytically added to carbon-carbon multiple bonds¹⁹ the use of NH₃ in this hydroamination reaction was not known until our group recently remarkable and novel hydroamination of alkynes and allenes with ammonia (Scheme 4.4).²⁰ This reaction presents an incredibly atom efficient process for synthesizing simple amines from inexpensive chemical precursors.

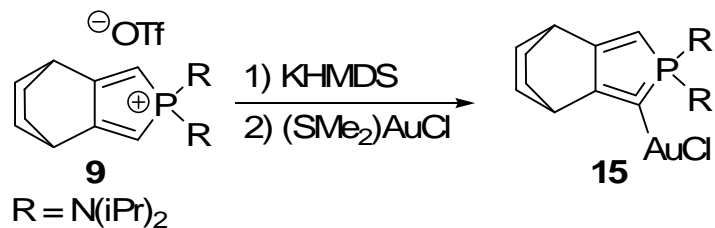


Scheme 4.4. Gold catalyzed hydroamination of 3-hexyne.

The reaction is catalyzed by a cationic CAAC gold (I) complex (**14**) but obviously analogous cationic gold (I) complexes should demonstrate similar reactivity. Therefore, in order to investigate if vinylidenephosphorane **5** can be used as a ligand in this reaction we set out to synthesize the appropriate gold complex. In this case the desired cationic gold complex can be generated *in situ* from the corresponding gold (I) chloride species by addition of $\text{K B}(\text{C}_6\text{F}_5)_4$. Thus the target pre-catalyst is a vinylidenephosphorane gold (I) chloride complex.

The free vinylidenephosphorane **5** was first generated as previously reported (in THF with KHMDS) and then added to a -78°C THF solution of gold (I) chloride dimethylsulfide complex (Scheme 4.5). After stirring the reaction for 12 hours the yellow solution was analyzed by ^{31}P NMR spectroscopy, which showed one major signal at 70.3 ppm. After subsequent work-up ^1H and ^{13}C NMR of the slightly yellow solid showed only signals for the ligated vinylidenephosphorane in complex **15**. Particularly telling is the quaternary carbon bound to the gold which appears as a doublet ($^1J_{CP} = 54 \text{ Hz}$) at 134 ppm

in the ^{13}C spectra, which is in the same area as other complexes of **5**. Importantly, the complex was very thermally stable (m. p. = 186°C with no decomposition), which is necessary for the harsh reaction conditions of the hydroamination reaction (130-200°C).



Scheme 4.5. Synthesis of gold chloride complex **15**.

With this new catalyst in hand a reaction was set up to evaluate the catalysts' activity; the hydroamination of 3-hexyne. This substrate was chosen in order to compare directly the activity of catalyst **15** with that of CAAC complex **14**.

Initial attempts to perform the hydroamination at 160°C failed to obtain significant quantities of the desired product. Increasing the reaction time did not increase the yield, which indicates that the catalyst may not be stable under the harsh reaction conditions. Furthermore, because the unisolated gold cation is the catalytically active species rather than **15** the stability of the active catalyst can not be commented on. While isolating the cationic gold complex remains a goal, initially it was deemed more useful discover if the catalyst was in fact active. Because the high temperature was deemed to be a likely cause of the problem the reaction temperature was decreased to 130°C. At this lower temperature the

results improved markedly and a 39% yield was obtained with a catalyst loading of only 1 mole % after heating for 16 hours.

While there remains much work to be done on this hydroamination chemistry the initial results are promising. With continued effort into isolating the cationic species and modifying the reaction conditions as well as the ligand substituents improved results should be possible. Importantly the reaction proceeds at only 130°C, which is a significant improvement from the previously reported reaction conditions.

In this chapter the first stable free vinylidenephosphorane has been used as a ligand for homogeneous transition metal catalysis. The transition metal complexes presented herein are easy to synthesized and robust in nature making them ideal catalysts. Remarkably, in the ruthenium catalyzed metathesis of olefins the vinylidenephosphorane catalysts compares well with the known catalysts. This is even more remarkable when considering that these results are only the preliminary investigations and that much work is left to do, particularly in modifying the vinylidenephosphorane structure. By carefully tuning the ligand and the conditions even better results may be forthcoming. The design and synthesis of new vinylidenephosphoranes and their corresponding catalysts is ongoing as well as its use in other catalytic systems.

Experimental

All manipulations were performed under an atmosphere of argon using standard schlenk techniques. All solvents were dried and distilled prior to use (THF, hexane, and toluene were dried and distilled over potassium, ether over sodium wire and dichloromethane and chloroform were dried and distilled over calcium hydride). ^1H , ^{13}C and ^{31}P NMR spectra were recorded on Bruker Advace 300 and 600 spectrometers. ^1H and ^{13}C NMR chemical shifts are reported in ppm relative to TMS as an external standard. ^{31}P NMR chemical shifts are reported in ppm relative to 85% H_3PO_4 as an external standard. Melting points are uncorrected.

Ruthenium complex **13** was synthesized according to the previously published procedure.^{10a, 21} Metathesis substrates were purchased or synthesized similar to literature procedures.

Synthesis of ruthenium complex **11**: Ruthenium complex **13** (115 mg, 0.19 mmol), KHMDS (40 mg, 0.20 mmol) and phosphonium salt **9** (98 mg, 0.19 mmol) were mixed and THF was added directly to the solids at room temperature. The reaction was allowed to stir for 10 hours and then all volatiles were removed under vacuum. The resultant red-brown solid was extracted with a large quantity of hexanes. After subsequent evaporation and re-extracted in dichloromethane crystals suitable for X-ray diffraction were grown in toluene to give 53 mg (41 % yield) of complex **11**; m.p. 141.4-142.3 °C; $^{31}\text{P}\{\text{H}\}$ NMR (CDCl_3 , 25 °C, 243 MHz): δ 71.4 ; ^1H NMR (CDCl_3 , 25 °C, 600 Hz) : δ 1.23-1.28 [s(broad), 12H,

N-iPr], 1.33 [s(broad), 12H, N-iPr], 1.50-1.79 (m, 10H, bicyclic), 1.76 [s(broad), 6H, CH₃ O-iPr], 2.40 (s, 1H, bridgehead), 2.54 (s, 1H, bridgehead), 3.96 (broad, 4H, CH N-iPr), 5.07 (sept, J = 6.1 Hz, 1H, CH O-iPr), 5.55 (d, ²J_{PH} = 28.9 Hz, 1H, CH phosphole), 6.99 (dd, J = 8.1 Hz, J = 6.8, 2H, CH aromatic), 7.54 (t, J = 8.1 Hz, 1H, CH aromatic) 7.69 (d, J = 6.8 Hz, 1H, CH aromatic) 18.59 (s, 1H, CH benzylic); ¹³C NMR (CDCl₃, 25 °C, 151 MHz): δ 22.3 (s, CH₃ O-iPr), 23.4 (s, CH₃ N-iPr), 23.8 (s, CH₃ N-iPr), 24.7 (CH₂), 24.8 (CH₂), 32.4 (d, ³J_{CP} = 27.5 Hz, CH), 33.3 (d, ³J_{CP} = 20.3 Hz, CH), 47.9 (d, ²J_{CP} = 4.7 Hz, NCH), 73.9 (s, OCH), 107.4 (d, ¹J_{CP} = 94.0 Hz, PCH phosphole), 113.6 (s, CH arom), 121.2 (s, CH arom), 122.4 (s, CH arom), 127.4 (s, CH arom), 134.5 (broad, PC), 144.5 (s, C arom), 153.6 (s, C arom), 162.1 (d, ²J_{CP} = 36.2 Hz, C), 168.7 (d, ²J_{CP} = 36.0 Hz, C), 275.1 (CH benzylidene),.

Metathesis Reactions

A stock 0.016 M solution of catalyst **11** was prepared in a glove box by weighing (0.008 mmol, 6 mg) of **11** and adding 0.5 ml of CD₂Cl₂. This solution was used for all three RCM reactions.

RCM of Diethyldiallyl malonate: In a glove box, an NMR tube (with a screw cap and septum) was charged with stock solution of **11** (0.016 M, 50 µL, 0.80 µmol, 1.0 mol %) and CD₂Cl₂ (0.75 mL). The sample was equilibrated in the NMR at 30 °C and then the malonate (19.3 µL, 19.2 mg, 0.08 mmol, 0.1 M) was added. The conversion was followed by comparing the methylene protons of the starting

material (δ 2.61) and product (δ 2.98) on a Bruker 600 Advance spectrometer by taking 4 scans at the beginning of each minute.

RCM of Diethylallylmethallyl malonate: In a glove box, an NMR tube (with a screw cap and septum) was charged with stock solution of **11** (0.016 M, 50 μ L, 0.80 μ mol, 1.0 mol %) and CD_2Cl_2 (0.75 mL). The malonate (20.5 μ L, 20.4 mg, 0.08 mmol, 0.1 M) was added and the tube heated at 30 °C for 2 days at which point no reaction had taken place. The NMR tube was then heated to 40 °C for one day at which point the yield was 44%. The same quantities were used exchanging C_6D_6 for CD_2Cl_2 and the NMR was heated to 60°C. After one day the yield was 94%. The conversion was followed by comparing the methylene protons of the starting material (δ 2.67, 2.64) and product (δ 2.93, 2.88).

RCM of Diethyldimethallyl malonate: In a glove box, an NMR tube (with a screw cap and septum) was charged with stock solution of **11** (0.016 M, 250 μ L, 0.80 μ mol, 4.0 mol %) and CD_2Cl_2 (0.55 mL). The malonate (21.6 μ L, 21.5 mg, 0.08 mmol, 0.1 M) was added to the tube and heated to 30 °C for 2 days at which point no reaction had taken place. The NMR tube was then heated to 40 °C for one day at which point there was still no product observed. The conversion was followed by comparing the methylene protons of the starting material (δ 2.71) and product (δ 2.89).

Synthesis of Gold Chloride complex **15** Freshly generated **5** [prepared from **9** (225 mg, 0.57 mmol) and KHMDS (113 mg, 0.57 mmol) in THF (5 ml) at -78 °C] at

room temperature was added to a THF (3 ml) solution of AuCl(SMe₂) (167 mg, 0.57 mmol). The mixture was stirred for 12 h. All volatiles were removed under vacuum, and the resultant solid was washed with hexanes and ether. The desired product was extracted in dichloromethane. After evaporation of the dichloromethane the resultant slightly yellow solid was analytically pure **15**; 63 % yield (212 mg); m.p. 186.5-187.8 °C; ³¹P{¹H} NMR (CDCl₃, 25 °C, 243 MHz): δ 70.3 : ¹H NMR (CDCl₃, 25 °C, 300 MHz) : δ 1.23 (d, J = 6.8 Hz, 12H, i-Pr), 1.38 (d, J = 6.8 Hz, 12H, i-Pr), 1.40-1.78 (m, 8H, bicyclic), 2.68 (s, 1H, bridgehead), 2.92 (s, 1H, bridgehead), 3.83 (m, 4H, CH iPr), 5.72 (d, ¹J_{PC} = 30.4 Hz, 1H, phosphole); ¹³C NMR (CDCl₃, 25 °C, 151 MHz): δ 22.6 (s, CH₃), 23.5 (s, CH₃), 24.7 (CH₂), 24.9 (CH₂), 33.4 (d, ³J_{CP} = 21.5 Hz, CH bridgehead), 36.2 (d, ³J_{CP} = 31.9 Hz, CH bridgehead), 47.6 (d, ²J_{CP} = 4.0 Hz, NCH), 107.2 (d, ¹J_{CP} = 98.7 Hz, PCH), 134.6 (d, ¹J_{CP} = 54.4 Hz, PC), 161.6 (d, ²J_{CP} = 25.2 Hz, C), 166.3 ppm (d, ²J_{CP} = 37.6 Hz, C).

Hydroamination Catalysis

Pre-catalyst **15** (10 mg, 0.017 mmol, 1 mole %) was weighed into a Wilmad QPV thick walled (1.4 mm) NMR tube. The potassium B(C₆F₅)₄ (12 mg, 0.017 mmol, 1 mole %) and 3-hexyne (138 mg, 0.191 ml, 1.70 mmol) are added directly to the NMR tube. C₆D₆ (0.2 ml) and the internal standard benzyl methyl ether (5 mg) are added to the mixture. The NMR tube was connected to a high-vacuum manifold and excess NH₃ (approximately 3 equivalents) was condensed in liquid nitrogen.

The tube was sealed and placed in a oil bath behind a blast shield and heated at

130°C for 16 hours. The ^1H NMR spectrum was used to quantify the yield.

References

1. a) A. Miyashita, A. Yasuda, H. Takaya, K. Toriumi, T. Ito, T. Souchi, R. Noyori, *J. Am. Chem. Soc.* **1980**, *102*, 7932; b) R. Noyori, H. Takaya, *Accts. Chem. Res.* **1990**, *23*, 345; c) W. S. Knowles, R. Noyori, *Accts. Chem. Res.* **2007**, *40*, 1238.
2. W. S. Knowles, *Accts. Chem. Res.* **1983**, *16*, 106.
3. A. J. Arduengo III, R. L. Harlow, M. Kline, *J. Am. Chem. Soc.* **1991**, *113*, 361.
4. For recent reviews on carbenes as ligands, see: a) E. Kantchev, C. O'Brien, M. Organ, *Angew. Chem. Int. Ed.* **2007**, *46*, 2768; b) H. M. Lee, C. C. Lee, P. Y. Cheng, *Curr. Org. Chem.* **2007**, *11*, 1491; c) S. T. Liddle, I. S. Edworthy, P. L. Arnold, *Chem. Soc. Rev.* **2007**, *36*, 1732; d) S. Diez-Gonzalez, S. P. Nolan, *Synlett* **2007**, 2158; e) D. Pugh, A. A. Danopoulos, *Coord. Chem. Rev.* **2007**, *251*, 610; f) I. J. B. Lin, C. S. Vasam, *Coord. Chem. Rev.* **2007**, *251*, 642; g) R. E. Douthwaite, *Coord. Chem. Rev.* **2007**, *251*, 702; h) L. H. Gade, S. Bellemin-Laponnaz, S. *Coord. Chem. Rev.* **2007**, *251*, 718; i) E. Colacino, J. Martinez, F. Lamaty, *Coord. Chem. Rev.* **2007**, *251*, 726; j) V. Dragutan, I. Dragutan, L. Delaude, *Coord. Chem. Rev.* **2007**, *251*, 765; k) W. J. Sommer, M. Weck, *Coord. Chem. Rev.* **2007**, *251*, 860; l) S. Diez-Gonzalez, S. P. Nolan, *Coord. Chem. Rev.* **2007**, *251*, 874; m) F. E. Hahn, *Angew. Chem. Int. Ed.* **2006**, *45*, 1348; n) S. P. Nolan, S. P. *N-Heterocyclic Carbenes in Synthesis*; Wiley-VCH, **2006**; o) F. Glorius, *N-Heterocyclic Carbenes in Transition Metal Catalysis (Topics in Organometallic Chemistry)*; Springer Verlag, **2006**.
5. M. Asay, T. Kato, N. Saffon-Merceron, F. P. Cossío, A. Baceiredo, G. Bertrand, *Angew. Chimie Int. Ed.* **2008**, *47*, 7530
6. For reviews on metathesis catalysis see: a) Y. Chauvin, *Angew. Chem., Int. Ed.* **2006**, *45*, 3740; b) R. R. Schrock, *Angew. Chem., Int. Ed.* **2006**, *45*, 3748; c) R. H. Grubbs, *Angew. Chem., Int. Ed.* **2006**, *45*, 3760; d) K. C. Nicolaou, P. G. Bulger, D. Sarlah, *Angew. Chem., Int. Ed.* **2005**, *44*, 4490, e) R. H. Grubbs, *Tetrahedron* **2004**, *60*, 7117; f) *Handbook of Metathesis* (ed. R. H. Grubbs) Wiley, Weinheim, Germany, **2003**; g) R. R. Schrock, A. H. Hoveyda, *Angew. Chem., Int. Ed.* **2003**, *42*, 4592; h) U. Frenzel, O. Nuyken, *J. Polym. Sci. Part A: Polym. Chem.* **2002**, *40*, 2895; i) T. M. Trnka, R. H. Grubbs, *Acc. Chem. Res.* **2001**, *34*, 18; j) A.

-
- Fürstner, *Angew. Chem., Int. Ed.* **2000**, 39, 3012; k) M. R. Buchmeiser, *Chem. Rev.* **2000**, 100, 1565.
7. http://nobelprize.org/nobel_prizes/chemistry/laureates/2005/index.html
 8. a) G. C. Fu, S. T. Nguyen, R. H. Grubbs, *J. Am. Chem. Soc.* **1993**, 115, 9856; b) S. T. Nguyen, R. H. Grubbs, *J. Am. Chem. Soc.* **1993**, 115, 9858; c) P. Schwab, R.H. Grubbs, J. W. Ziller, *J. Am. Chem. Soc.* **1996**, 118, 100.
 9. a) M. Scholl, S. Ding, C.W. Lee, R.H. Grubbs, *Org. Lett.* **1999**, 1, 953; b) T. Weskamp, F. J. Kohl, W. Hieringer, D. Gleich,W. A. Herrmann, *Angew. Chem. Int. Ed. Engl.* **1999**, 38, 2416.
 10. a) J. S. Kingsbury, J. P. A. Harrity, P. J. Bonitatebus, A. H. Hoveyda, *J. Am. Chem. Soc.* **1999**, 121, 791; b) S. B. Garber, J. S. Kingsbury, A. H. Gray, A. H. Hoveyda, *J. Am. Chem.Soc.* **2000**, 122, 8168.
 11. a) T. Weskamp, W. C. Schattenmann, M. Spiegler, W. A. Hermann, *Angew. Chem. Int. Ed. Engl.* **1998**, 37, 2490; b) J. Huang, E. D. Stevens, S. P. Nolan, J. F. Petersen, *J. Am. Chem. Soc.* **1999**, 121, 2674; c) M. Scholl, J. P. Trnka, J. P. Morgan, R. H. Grubbs, *Tetrahedron Lett.* **1999**, 40, 2247.
 12. a) J. M. Berlin, K. Campbell, T. Ritter, T. W. Funk, A. Chlenov, R. H. Grubbs, *Org. Lett.* **2007**, 9, 1339; b) J. J. Van Veldhuizen, D. G. Gillingham, S. B. Garber, O. Kataoka, A. H. Hoveyda, *J. Am. Chem. Soc.* **2003**, 125, 12502.
 13. M. S. Sanford, J. A. Love, R. H. Grubbs, *J. Am. Chem. Soc.* **2001**, 123, 6543.
 14. D. R. Anderson, V. Lavallo, D. J. O'Leary, G. Bertrand, R. H. Grubbs, *Angew. Ghem. Int. Ed.* **2007**, 46, 7262.
 15. J. Yun, E. R. Martinez, R. H. Grubbs, *Organometallics* **2004**, 23, 4172.
 16. E. Despagnet-Ayoub, R. H. Grubbs, *Organometallics* **2005**, 24, 338.
 17. Full details of the X-ray structure can be found in the appendix.
 18. T. Ritter, A. Hejl, A. G. Wenzel, T. W. Funk, R. H. Grubbs, *Organometallics* **2006**, 25, 5740.

-
19. a) P. Horrillo-Martinez, K. C. Hultsch, A. Gil, V. Branchadell, *Eur. J. Org. Chem.* **2007**, 3311; b) S. Datta, M. T. Gamer, P.W. Roesky, *Organometallics* **2008**, 27, 1207; c) E. Smolensky, M. Kapon, M. S. Eisen, *Organometallics* **2007**, 26, 4510; d) M. Dochnahl, K. Lohnwitz, J.-W. Pisarek, M. Biyikal, S. R. Schulz, S. SchLn, N. Meyer, P. W. Roesky, S. Blechert, *Chem. Eur. J.* **2007**, 13, 6654; e) A. R. Chianese, S. J. Lee, M. R. Gagne, *Angew. Chem. Int. Ed.* **2007**, 46, 4042; f) G. Kovacs, G. Ujaque, A. Lledos, *J. Am. Chem. Soc.* **2008**, 130, 853; g) N. Meyer, K. Lohnwitz, A. Zulys, P.W. Roesky, M. Dochnahl, S. Blechert, *Organometallics* **2006**, 25, 3730; h) X. Y. Liu, C. H. Li, C. M. Che, *Org. Lett.* **2006**, 8, 2707; i) T. Andrea, M. S. Eisen, *Chem. Soc. Rev.* **2008**, 37, 550; j) I. Aillaud, J. Collin, J. Hannedouche, E. Schulz, *Dalton Trans.* **2007**, 5105; k) M. Rastatter, A. Zulys, P.W. Roesky, *Chem. Eur. J.* **2007**, 13, 3606.
 20. V. Lavallo, G. D. Frey, B. Donnadieu, M. Soleilhavoup, G. Bertrand, *Angew. Chem. Int. Ed.* **2008**, 47, 5224.
 21. B. K. R. Shankar, H. Shechter, *Tetrahedron Lett.* **1982**, 23, 2277.

Chapter 5

Towards a Free Stable Allenylidene

Several years ago the first stable derivative of cyclopropenylidene **A**, which is abundant in interstellar space, was reported by our group (Figure 5.1).¹ This species was stabilized by addition of two amino groups to the three member ring (**1**), which act as electron donors. The use of the inherent electron donating ability of nitrogen to stabilize carbenes has been on display since the first N-Heterocyclic Carbene (NHC) **B** was isolated in 1991,² however carbene **1** is the first time the amino groups were used at a location remote from the carbene centre (β). This led us to consider one of the valence isomers of cyclopropenylidene **A**; the propadienylidene **C**. Would amino groups even further from the carbene centre (γ) in diamino propadienylidene **2** sufficiently stabilize the electron deficient carbon to allow for its isolation? Additionally, which resonance structure best describes the molecule; the carbenic structure **2** or the zwitterionic structure **2'**.

The structure of **2** was investigated computationally at the RI-BP86/TZVP level of theory, which shows it to be a minima on the energy hypersurface (Figure 5.2). The singlet-triplet gap (Δ_{s-t}) was calculated to be 60.5 kcal mol⁻¹, which is as large as that of the parent diamino cyclopropenylidene (59.5 kcal mol⁻¹).¹ While this value is lower than that of NHCs **B** (83.8 kcal mol⁻¹)² it is indicative of a species that may be stable.³

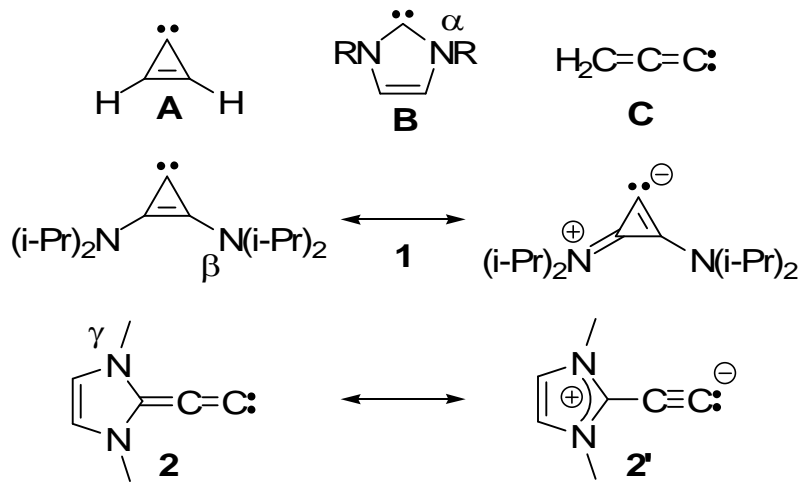


Figure 5.1. Parent cyclopropenylidene **A**, NHC **B**, parent propadienylidene **C** as well as the stabilized cyclopropenylidene **1** and propadienylidene **2**.

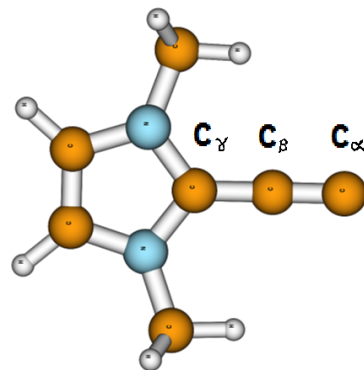


Figure 5.2. Computationally optimized structure of **2**.

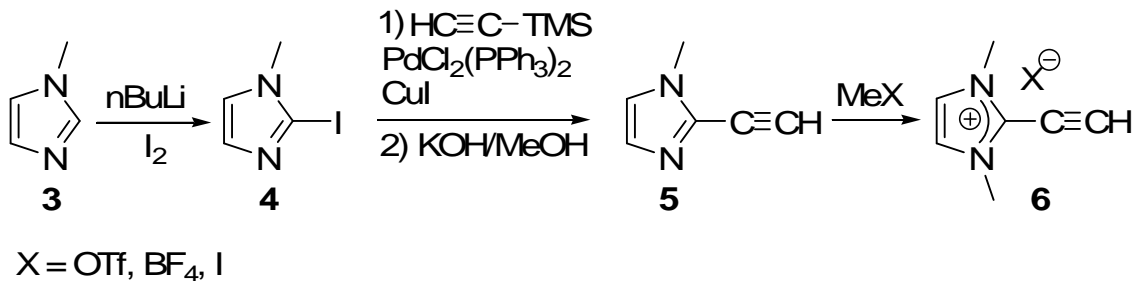
Table 5.1: Computational data for compound **2**.

	C _α	=	C _β	=	C _γ
Charge	-0.056		-0.577		0.391
NMR Shift ^[a]	284.8		99.8		123.5
Bond Length ^[b]			1.263		1.379
NPA ^[c]			2.482		1.263

[a] in ppm [b] in Å [c] in arbitrary units

Table 5.1 contains additional computational data including the bond length and Natural Population Analysis (NPA) of the terminal carbon-carbon bond (1.263 Å and 2.482, respectively). Both of these values show there to be considerable triple bond therefore indicating that the charge separated resonance form **2'** plays a major role in the structure of the molecule.

With this computational data demonstrating the viability of such a species, synthesis began in earnest. Considering the remote nature of the low-valent carbene centre, it seemed likely that sterics would not be useful in stabilizing the species. Additionally there were difficulties synthesizing a desirable precursor with large groups on the nitrogen. However, the commercially available N-methylimidazole **3** can be readily transformed into the 2-iodoimidazole **4** by metalation/halogenation. A classical sonogishira coupling and base catalyzed desilylation then leads to 2-ethynyl-1-methyl imidazole (**5**).^{4, 5} Subsequent reaction with a variety of methylating reagents (MeOTf, Me₃OB₄, and Mel) led to the desired imidazolium precursor (**6**) (Scheme 5.1)⁶. Compound **6** was fully characterized by NMR and X-ray diffraction (Figure 5.3). Importantly the X-ray structure clearly shows the short terminal triple bond (1.18 Å) and a typical single bond between the imidazolium salt and the triple bond (1.420 Å).



Scheme 5.1. Synthesis of 2-ethynyl-imidazolium salt **6**.

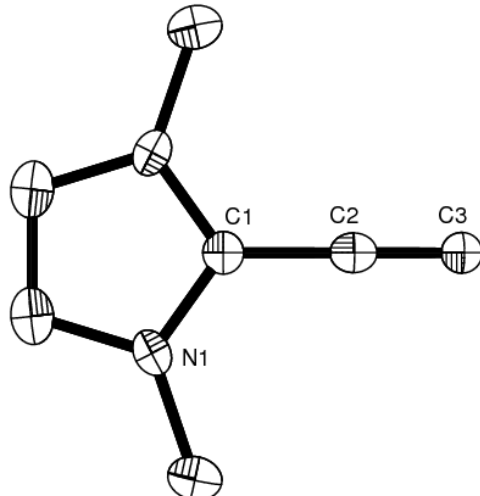
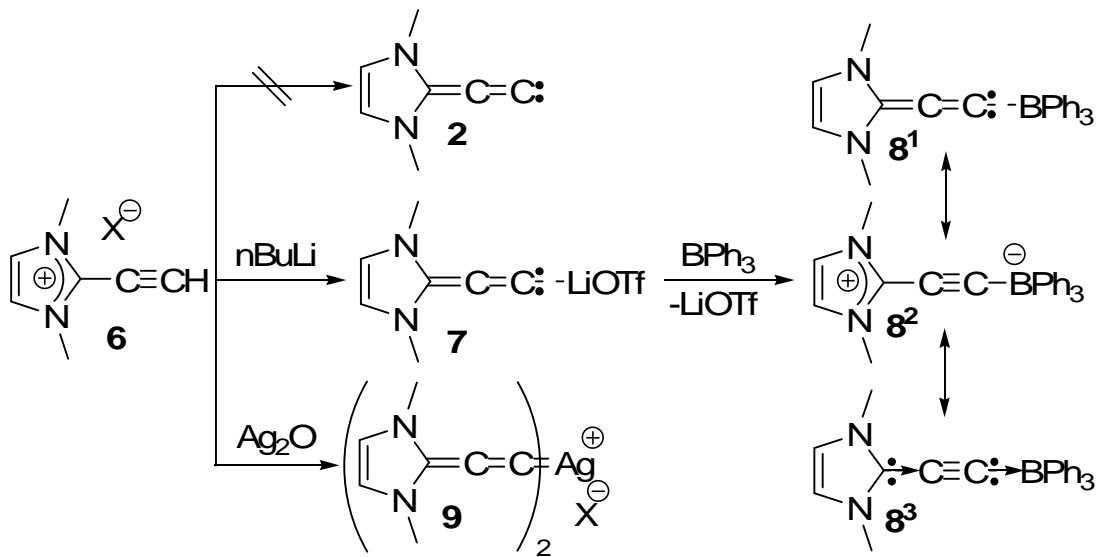


Figure 5.3. X-ray crystal structure of 2-ethynyl-imidazolium salt **6**. Hydrogen atoms and iodide anions are omitted for clarity. Thermal ellipsoids are at 50 % probability. Selected bond lengths (\AA) and angles ($^\circ$): C1–C2 1.420(19), C2–C3 1.18(2), N1–C1 1.339(11), C1–C2–C3 180.000(9), N1–C1–N1a 109.1(11).

Deprotonation of triflate salt **6** with n-BuLi in THF led to a darkly coloured solution. The ^1H NMR spectrum revealed the loss of the alkynyl proton (4.74 ppm in salt **6**) and only two signals attributable to a symmetrical methylimidazole moiety. Subsequent ^{13}C NMR spectroscopy also clearly showed the loss of the

alkynyl CH (96.8 ppm in salt **6**). There is, however, a new quaternary carbon signal that appears at 190.2 ppm.

Calculations were performed in order to ascertain if this value correlates well with the desired product **2** (Table 5.1). The value of the terminal carbon are nearly 100 ppm downfield from the observed shift (285 versus 190 ppm). However, the carbon α to the carbene center has shifted from 63.9 to 90.6, which correlates well with the calculations (100 ppm). A quartet centered at 121 ppm ($^1J_{CF} = 320$ Hz) is apparent, which is typical for a triflate counterion. Subsequent ^7Li NMR spectroscopy also demonstrates the presence of lithium, however attempts at correlation spectroscopy to indicate the interaction of lithium with the quaternary carbon failed. Attempts to remove the lithium triflate by extraction into less polar solvents were unsuccessful due to the insolubility of the product. These facts led us to believe that the species present is, in fact, the lithium triflate salt **7** (Scheme 5.2). Single crystals of salt **7** were not forthcoming therefore we set out to investigate its reactivity.



Scheme 5.2. Reactivity of salt **6** to form lithium **7** and borane **8** adducts as well as silver complex **9**.

In 1989 Bestmann and co-workers reported a borane adduct of an allenylidene **D** with a phosphine moiety in lieu of an NHC (Figure 5.4).⁷ Therein he notes that **D** is, in a “purely hypothetical formulation”, a donor-acceptor complex of C_2 (**D**³). This concept has also been discussed in the case of carbodiphosphoranes **E** where the limit structure **E**³ is a C^0 stabilized by two phosphine donors.⁸ Recently this formulation has been hotly debated with calculations⁹ and the first reported examples of a carbene analog of **E**: The “carbodicarbene” or “bent-allene” **F**.¹⁰ Therefore we targeted a borane adduct of the allenylidene **8**, which continues the current trend of replacing phosphines with NHCs and continues the debate on the “hypothetical formulation” of donor-acceptor complexes of carbon.

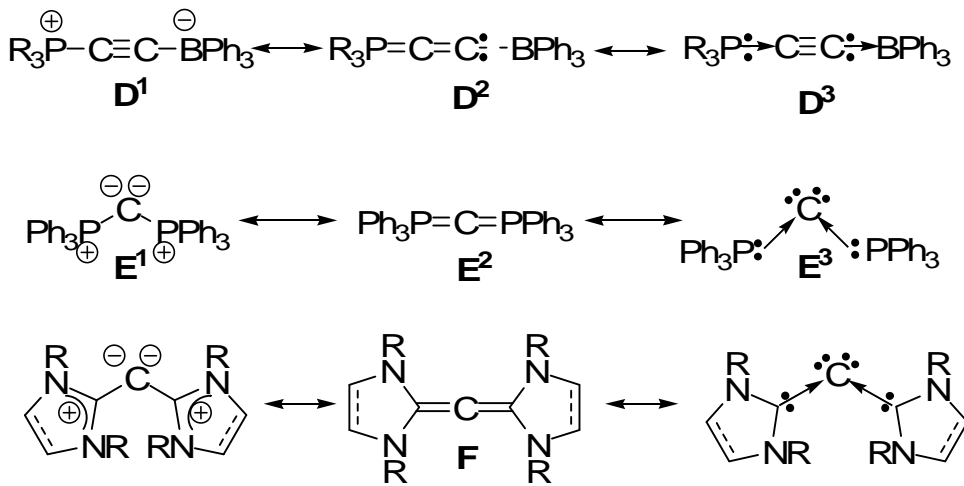


Figure 5.4. Structures and resonance forms for phosphonium allenylidene borane complex **D**, carbodiphosphorane **E** and carbodicarbene (bent-allene) **F**.

To synthesize **8**, triphenylborane was added to a solution of freshly generated **7** at -78 °C. The ¹¹B NMR spectrum of the resultant red solution clearly shows the disappearance of the free triphenylborane at 60.2 ppm¹¹ and a new signal at -11.7 ppm, which is typical for tetracoordinate boron atoms found in structures **D**. The quaternary carbon signal at 190 ppm in **7** is also gone and replaced by a broad signal at 75 ppm (the broad signal is due to coupling with ¹¹B). This reactivity of **7** points to the structural assignment as a deprotonated **6**.

While efforts to synthesize the free species **2** were not fruitful we turned our attention to alternate approaches to make a protected stable version of **2**. This led us to investigate the possibility of direct metallation with silver.

There have been many reports where imidazolium and triazolium salts were deprotonated with silver bases, such as silver acetate,¹² silver carbonate¹³ and

silver oxide,¹⁴ to form directly the corresponding NHC silver complex. This protocol has several advantages. The silver bases used are very stable and relatively inert compared to bases typically used for carbene deprotonations (such as the alkyl lithium used in the case of **7**). This allows them to be used in a much larger array of solvents, which is advantageous in the case of salt **6**, which displays very limited solubility. Also the silver NHC complexes are generally very stable. And finally, despite their stability they are quite reactive and readily undergo transmetallation reactions and thus can open the way to the synthesis of a wide array of metal complexes.¹⁵ A particularly striking example from the literature are the so called “abnormal carbenes” which have not been generated as a free species but, thanks in part to silver complexes and transmetallation, their ligand properties have come to light.¹⁶

To this end salt **6** was mixed with silver oxide in acetonitrile for 10 hours at which point insoluble silver salts and excess silver oxide were filtered off through celite. The ¹H NMR spectroscopy of resultant dark brown product shows the loss of the proton on the alkyne, furthermore there are only two signals, which can be attributed to a symmetrical imidazole ring. Using ¹⁰⁹Ag NMR spectroscopy we were able to ascertain that there was silver in the molecule and the chemical shift (856.2 ppm) is near the region reported for other carbene silver complexes¹⁷ and does not correlate with non-ligated silver salts. The ¹³C NMR spectra confirmed the details of the ¹H spectra and showed that a triflate counterion was present, however, the terminal quaternary carbon could not be

located. This is not uncommon in silver NHC species because of the two silver isotopes and fluxional behavior that is believed to be common in the solution state. Furthermore, in the case of **9**, there are no nearby protons to aid in the detection of the quaternary carbon by through space magnetization transfer.

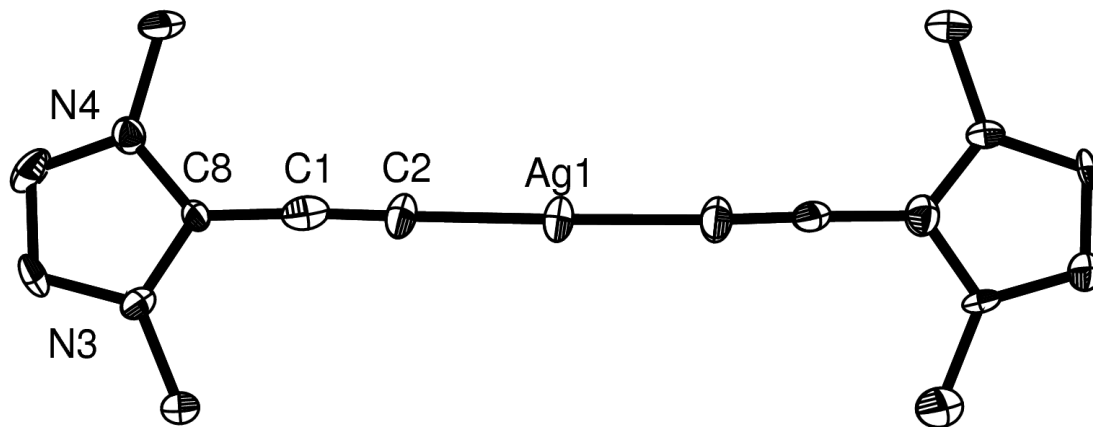
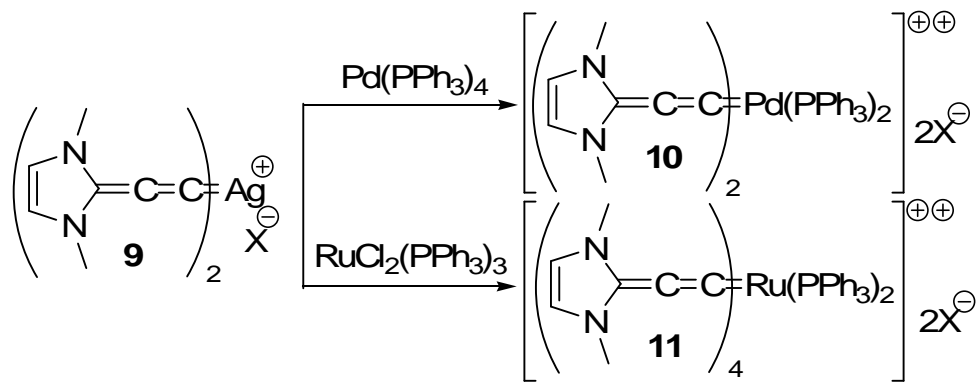


Figure 5.5. X-ray crystal structure of silver salt **9**. Hydrogen atoms, the anion and the solvents of crystallization are omitted for clarity. Thermal ellipsoids are at 50 % probability. Selected bond lengths (\AA) and angles ($^\circ$): Ag1–C2 2.026(10), C1–C2 1.235(15), C1–C8 1.408(15), C8–N3 1.351(12); N3–C8–N4 106.7(8), Ag1–C2–C1 178.8(10), C2–C1–C8 176.8(10), C2–Ag1–C2a 179.0(4).

While it seems clear that the product is in fact a silver complex of salt **6**, it is well known that NHCs can form mono- and bis-silver complexes as well as a wide variety of cluster species. As a general rule, silver NHC complexes with non coordinating counterions ($X = \text{OTf}, \text{BF}_4$) form bis-carbene complexes while small hard halides tend toward mono-carbene complexes as well as clusters. High resolution mass spectroscopy of **9** [$M/Z = 347.0411$ (expected 347.0420)] indicated the bis complex was formed but unfortunately this is not conclusive

because it has been reported that ligand transfer in the gas state can occur. Unfortunately single crystals suitable for X-ray analysis of silver triflate salt **9** eluded our efforts due largely to the minimal solubility of **9**. However, by changing the counterion to iodide, single crystals were obtained by slow evaporation of a dichloromethane solution. Subsequent X-ray diffraction studies prove that **9** is, in fact, a bis-silver complex of **2** (Figure 5.5).⁶ The carbon-silver bond length is shorter (2.026 Å) than all other linear bis-NHC silver complexes reported such as the dimesityl NHC silver triflate complex (2.067 Å)^{17a} and shorter than all other reported carbene-silver complexes, an effect that is most likely caused by the increased s character of the lone pair donating to the silver center (sp hybridized as opposed to sp² hybridized). Additionally the terminal carbon-carbon bond has elongated compared to the starting salt **6** but remains quite short (1.18 to 1.235 Å). The alkyne moiety remains nearly linear as expected (179° at the terminal carbon and 177° at the other sp carbon). The two ligands are also almost linearly ligated to the metal center (179°). Interestingly the NCN bond angle decreases from the salt **6** (109°) to the silver complex (107°). In the case of NHCs and their imidazolium precursors, a similar trend is observed (the NCN bond angle of the carbene is smaller). Upon ligation to metals this bond angle increases but remains smaller than the salt. Thus this decrease in bond angle is in line with this precedence.



Scheme 5.3. Synthesis of palladium complex **10** and ruthenium complex **11**.

With silver complex **9** in hand the next goal was to test if it would undergo transmetallation reactions. Palladium is ubiquitous in late transition metal chemistry therefore it was the initial target for transmetallation of **9**. Additionally, there are many examples of NHC silver complexes undergoing transmetallation reactions with a variety of palladium reagents.¹⁵ We selected tetrakis(triphenylphosphine)palladium (0) and mixed it with one equivalent of silver tetrafluoroborate salt **9** in acetonitrile. After stirring for 12 hours at room temperature the solution was filtered through celite. After evaporation and extraction into dichloromethane crystals formed, which were subjected to analysis. The results of the X-ray diffraction study are given in Figure 5.6⁶ and show that two phosphine groups have been substituted by allenylidene **2** to give square planar complex **10**. Interestingly the palladium has been formally oxidized from 0 to +2 by the silver(tetrafluoroborate) generated as a by product of the transmetallation. The allenylidene ligand remains very similar

geometrically to the silver precursor with a terminal carbon-carbon bond of 1.20 Å and bond angles of 178° and 171° (terminal and internal bonds respectively). The palladium-carbon bond (1.987 Å) is once again slightly shorter than typical carbene palladium bonds (2.01-2.10 Å).

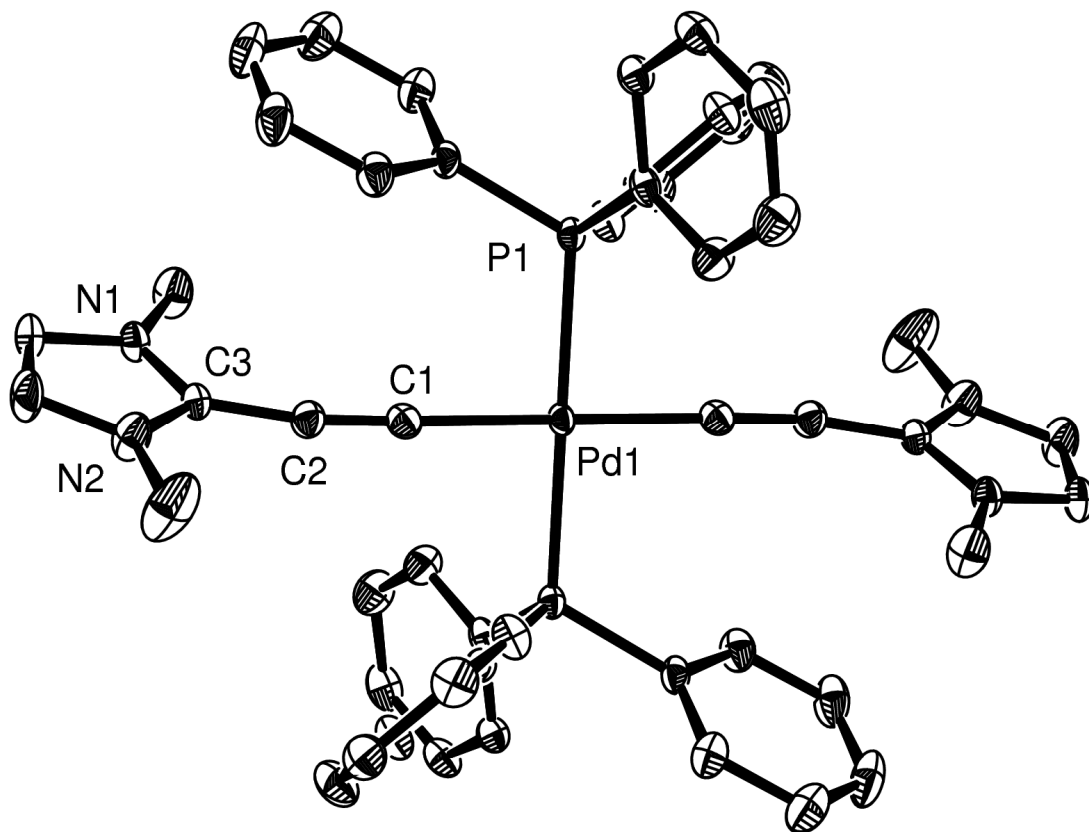


Figure 5.6. X-ray crystal structure of palladium complex **10**. Hydrogen atoms, counterions and solvent molecules are omitted for clarity. Thermal ellipsoids are at 50 % probability. Selected bond lengths (Å) and angles (°): Pd1–C1 1.986(2), C1–C2 1.199(3), C2–C3 1.408(3), Pd1–P1 2.3206(5); Pd1–C1–C2 178.39(19), C1–C2–C3 171.6(2), N1–C3–N2 126.05(17), C1–Pd1–P1 92.61(6), C1–Pd1–C1a 180.00(12).

The ^{31}P , ^1H , and ^{13}C NMR spectrum of the crystals were consistent with the X-ray structure although the carbon coordinated to palladium was not detectable. Additionally, high resolution mass spectrometry also confirmed the presence of **10** [$\text{M} + \text{BF}_4^-$ m/z = 957.2252 (expected 957.2256)]. However, the yield is quite low (51%) and while ^{31}P NMR of the crude reaction mixture shows **10** to be the major product there are several other significant minor products. Performing the same reaction with 2 equivalents of complex **9** did not result in any significant change in product distribution or yield.

Next, we selected a metal that is less common in transmetallation reactions, Ruthenium. In this case tris(triphenylphosphine)ruthenium dichloride was mixed with triflate salt **9** in dichloromethane. Sodium iodide was also added to the solution in an effort to sequester the silver and prevent reduction of the metal. After 8 hours at room temperature the product was extracted into acetonitrile and crystals formed at room temperature. X-ray diffraction studies show that the tetrakis(allenylidene)bis(triphenylphosphine) complex **11** is formed in the reaction (Figure 5.7).⁶ While the metal was not reduced the silver did act as a halogen scavenger to give the octahedral structure with two axial phosphines and four of the small allenylidenes symmetrically placed equatorially. The crystal structure once again shows nearly linear allenylidene ligands with the terminal and internal angles to be 177° and 172° , respectively.

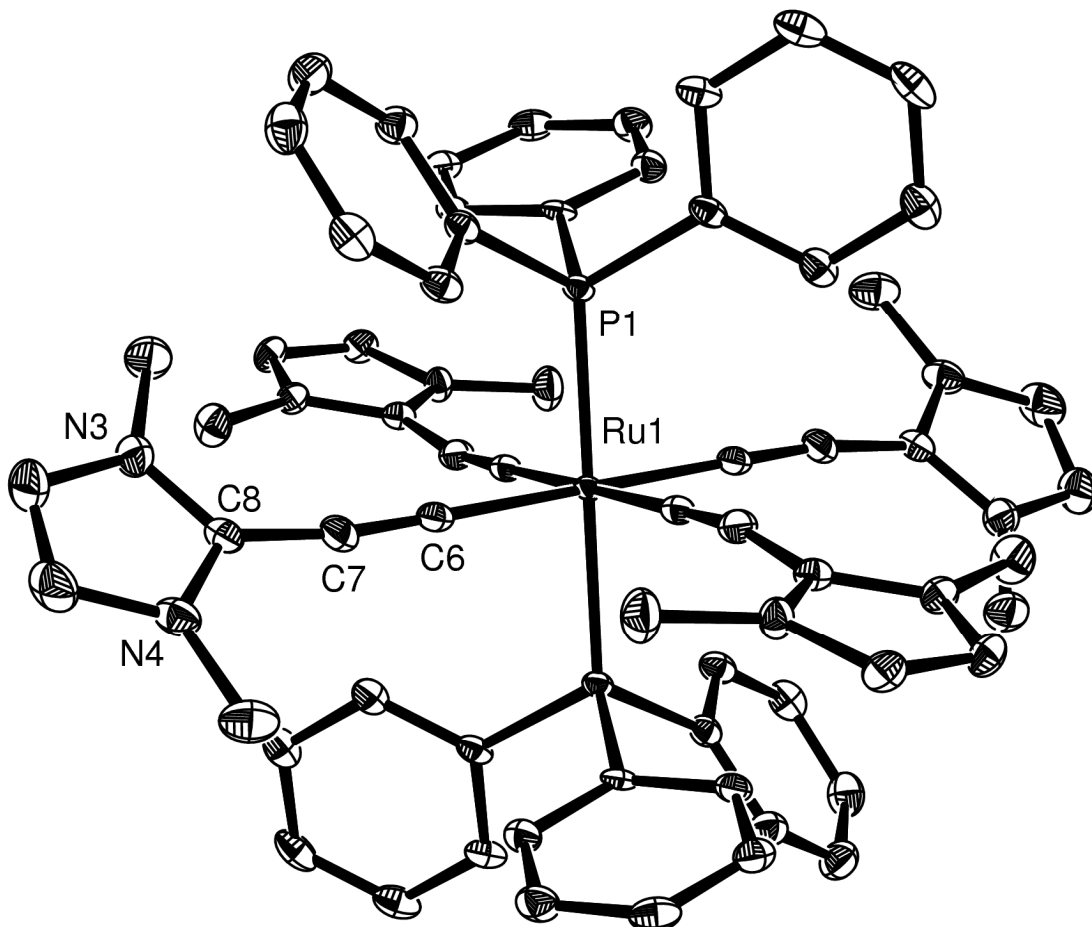


Figure 5.7. X-ray crystal structure of ruthenium complex **11**. Hydrogen atoms, counterions and solvent molecules are omitted for clarity. Thermal ellipsoids are at 50 % probability. Selected bond lengths (\AA) and angles ($^\circ$): Ru1–C6 2.027(4), C6–C7 1.226(7), C7–C8 1.395(6), Ru1–P1 2.3488(11); Ru1–C6–C7 177.1(4), C6–C7–C8 172.0(5), N3–C8–N4 107.5(4), C6–Ru1–P1 91.60(12), C6–Ru1–C6a 180.0(2).

The incredible lack of solubility of **11** made typical solution state NMR extremely difficult as impurities in the solvent and traces of phosphines on the crystals routinely were the only signals visible. Therefore, to further characterize compound **11**, MAS NMR was used. While ^1H MAS NMR is not informative both

^{31}P and ^{13}C MAS NMR did show signals corresponding to **11**. Most interestingly, thanks to the cross polarization used in solid state NMR the quaternary carbon bonded to the ruthenium is visible at 189.2 ppm, which is quite near the chemical shift of the lithium complex **7**. Another interesting aspect is the appearance of two signals for all the carbons except the methyl groups on nitrogen. This indicates that there are two magnetically inequivalent conformations of **11** in the solid state with each conformation crystallizing separately.

To better understand the mode and nature of the coordination of the allenylidene calculations of the silver and palladium complexes were done once again using the RI-BP86/TZVP level of theory.³ The optimized structures can be seen in Figure 5.8. The bond lengths of the allenylidene ligand match closely those found in both crystal structures (Table 5.2) indicating that the calculations accurately describe the molecules in question. The Wiberg bond orders¹⁸ were calculated to understand the nature of the coordination. Interestingly in both cases the carbon-metal bond order is one half, which is indicative of donor/acceptor bonds. This can best be demonstrated by comparing the carbon-metal bond order of palladium complex **10** (0.509) with the phosphorus-metal bond in the same complex (0.398). The slightly higher bond order is expected since the carbene-like ligand should be a stronger donor ligand.

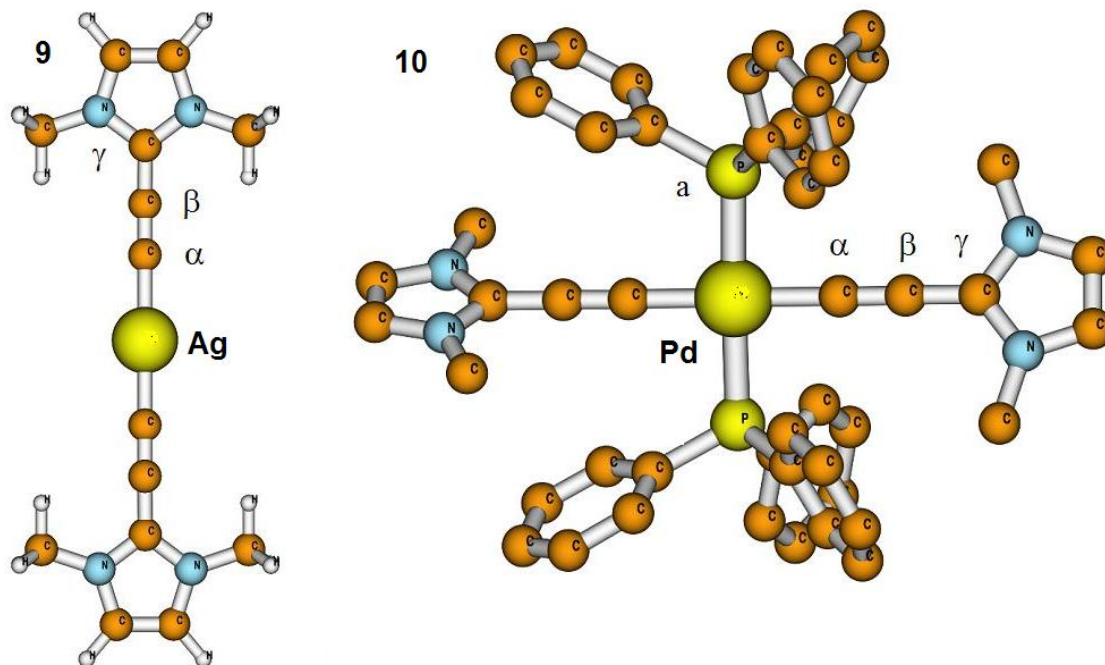


Figure 5.8. Optimized structures of silver complex **9** and palladium complex **10** (hydrogens and counterions omitted for clarity).

Table 5.2: Computational data for Complex **9** and **10**.

	Complex 9		Complex 10	
	Bond Length ^[a]	Bond Order ^[b]	Bond Length ^[a]	Bond Order ^[b]
M–C α	2.030	0.527	1.982	0.509
C α –C β	1.249	2.595	1.247	2.573
C β –C γ	1.397	1.205	1.398	1.200

[a] in Å [b] Wiberg bond orders

Herein we have presented the synthesis of an analog to the linear isomer of C₃H₂, a propadienylidene, stabilized by an NHC donor and several acceptors including lithium, boron and three different transition metals. The silver complex is of particular interest inasmuch as the transmetallation chemistry of this

species remains largely undeveloped. Further efforts to stabilize a free propadienylidene are ongoing.

Experimental

All manipulations were performed under an atmosphere of argon using standard schlenk techniques. All solvents were dried and distilled prior to use (THF, hexane, and toluene were dried and distilled over potassium, ether over sodium wire and acetonitrile, dichloromethane and chloroform were dried and distilled over calcium hydride). ^1H , ^7Li , ^{13}C , ^{31}P and ^{109}Ag NMR spectra were recorded on Bruker Advace 300 and 600 spectrometers. Solid state NMR experiments were performed at 9.4 T on a Bruker DSX spectrometer (^1H frequency 400 MHz). The 9.4 T Bruker DSX spectrometer was equipped with a double-resonance 2.5 mm MAS probe and experiments were performed with an MAS rate of 15 kHz. A $3\mu\text{s}$ ^1H pulse was used before Cross Polarization. During Cross Polarization (CP), the rf power on ^1H was ramped from 75% to 100% at 80 KHz maximum frequency. Accordingly ^{13}C power was adjusted for maximum polarization transfer. A 2 ms contact pulses were used on both channels during CP. An 80 KHz nutation was used for ^1H decoupling (spinal64) during acquisition. ^1H and ^{13}C NMR chemical shifts are reported in ppm relative to TMS as an external standard. ^7Li chemical shifts are reported in ppm relative to a saturated solution of LiCl in water as an external standard. ^{31}P chemical shifts are reported in ppm relative to phosphoric acid as an external standard. ^{109}Ag NMR chemical shifts are reported in ppm relative to a saturated solution of AgNO₃ in D₂O as an external standard. Melting

points are uncorrected. Imidazole **5** was synthesized according to published procedures.^{4, 5}

Compound **6** : To a solution of imidazole **5** (2.7 g, 25.4 mmol in 15 ml of dichloromethane) was added methyltrifluoromethanesulfonate (2.9 ml, 25.4 mmol). The mixture was stirred at room temperature for 12 h. All volatiles were removed under vacuum and the resultant solid was washed with diethyl ether and DCM to give imidizolium salt **6** as a dark brown solid (442 mg, 6%). A similar procedure was used with methyl iodide or trimethyloxonium tetrafluoroborate. m.p. : 168-171 °C; ¹H NMR (CD₃CN, 25 °C, 600 MHz) δ 3.87 (s, 6H, CH₃), 4.74 (s, 1H, C≡CH), 7.42 (s, 2H, CH); ¹³C NMR (CD₃CN, 25 °C, 151 MHz) δ 36.2 (CH₃), 63.9 (C≡CH), 96.8 (C≡CH), 121.1 (q, ¹J_{CF} = 320.7 Hz, CF₃SO₃), 124.2 (CH), 129.2 (C- C≡CH).

Compound **7** : A 1.6 M pentane solution of nBuLi (380 ml, 0.61 mmol) was added to imidazolium salt **6** (150 mg, 0.55 mmol) in THF (5 ml) at -78 °C. The mixture was stirred for 30 min. and then allowed to warm to room temperature. ¹H NMR (thf-d₈, 25 °C, 600 MHz) δ 3.71 (s, 6H, CH₃), 7.22 (s, 2H, CH); ⁷Li (thf-d₈, 25 °C, 233 MHz) δ 0.658; ¹³C NMR (thf-d₈, 25 °C, 151 MHz) δ 35.6 (CH₃), 90.6 (C≡C-Li), 120.7 (CH), 121.8 (q, ¹J_{CF} = 320.0 Hz, CF₃SO₃), 133.6 (C- C≡CH), 190.2 (C≡C-Li).

Compound **8** : To a freshly prepared THF (3 ml) solution of lithium salt **7** [prepared from triflate salt **6** (118 mg, 0.436 mmol) and nBuLi (1.6 M, 0.273 ml)] at -78 °C was added triphenyl borane (106 mg, 0.436 mmol) in THF (3 ml). The solution was stirred for 4 hours and allowed to warm to room temperature. All volatiles were removed under vacuum and the resultant solid was washed with ether (2 times 10 ml). The product **8** was extracted in dichloromethane and crystallized by layering ether on a concentrated dichloromethane solution of **8**. ¹H NMR (CD₂Cl₂, 25 °C, 600 MHz) δ 3.66 (s, 6H, CH₃), 6.63 (s, 2H, CH), 6.90-7.81 (m, 15H, Ph); ¹¹B (CD₂Cl₂, 25 °C, 233 MHz) δ 11.7; ¹³C NMR (CD₂Cl₂, 25 °C, 151 MHz) δ 35.8 (CH₃), 75.5 (broad, C≡C-B), 96.7 (C≡C-B), 120.6 (CH NHC), 123.5 (CH BPh), 126.6 (CH BPh), 134.3 (CH BPh), 158.4 (broad, C-B), 161.7 (NCN).

Compound **9** : Imidazolium iodo salt **6** (296 mg, 1.19 mmol) and Ag₂O (500 mg, 2.16 mmol) were stirred together in acetonitrile (7 ml) for 12 h. The resultant solution was filtered on celite then all volatiles were removed under vacuum. The dark solid was washed with diethyl ether. Crystallization in dichloromethane at -30 °C gave the desired silver salt **9** as red-brown needles (408 mg, 72 %). m.p. : 139.5-140.6 °C; ¹H NMR (CD₃CN, 25 °C, 600 MHz) δ 3.83 (s, 6H, CH₃), 7.32 (s, 2H, CH); ¹³C NMR (CD₃CN, 25 °C, 151 MHz) δ 37.0 (CH₃), 96.7 (C=C=Ag), 122.1 (q, ¹J_{CF} = 321.7 Hz, CF₃SO₃), 123.8 (CH), 130.8 (NCN), (CAg not observed); ¹⁰⁹Ag NMR (CD₃CN, 25 °C, 27.9 MHz) δ 856.2. High resolution mass spectrometry; FAB m/z = 347.0411

Complex 10 : To a mixture of silver tetrafluoroborate salt **9** (159 mg, 0.37 mmol) and tetrakis triphenylphosphine palladium (0) (0.422 g, 0.37 mmol) was added acetonitrile (3 ml). The solution was allowed to react for 12 h and then evaporated to dryness. Palladium complex **10** was then extracted in dichloromethane and concentrated, yellow crystals formed at -30 °C (194 mg, 51 %). m.p. : 208.9-210.0 °C; ^{31}P NMR (CDCl_3 , 25 °C, 242 MHz); δ 26.2; ^1H NMR (CD_3CN , 25 °C, 600 MHz) δ 2.96 (s, 12H, CH_3), 6.90 (s, 4H, CH), 7.1-7.8 (m, 30H, PPh_3); ^{13}C NMR (CD_3CN , 25 °C, 151 MHz) δ 34.5 (CH_3), 93.1 ($\text{C}=\text{C}=\text{Pd}$), 122.3 (s, CH), 128.7 [s (broad), PPh], 131.2 [s (broad), PPh], 134.4 [s (broad), PPh], 140.1 (s, NCN), $\text{C}=\text{Pd}$ not observed. High resolution mass spectrometry; FAB ($\text{M} + \text{BF}_4^-$) m/z = 957.2252 (expected 957.2256).

Complex 11 : Silver triflate salt **9** (0.140 g, 0.28 mmol), dichloro ruthenium (II) tris(triphenylphosphine) (0.135 g, 0.14 mmol), and sodium iodide (0.084 g, 0.56 mmol) were mixed in dichloromethane (5 ml) and stirred for 12 hours at room temperature. The solution was filtered through celite and the solvent was removed under vacuum. Pale yellow crystals were grown in acetonitrile at room temperature (82 mg, 32 %). m.p. : 158.2-160.1 °C; ^{31}P MAS NMR (25 °C, 162 MHz) δ 42.0 ^{13}C MAS NMR (25 °C, 101 MHz) δ 37.9 (CH_3), 96.7 ($\text{C}=\text{C}=\text{Ag}$), 121.9 (CH), 129.7-140.6 (m, PPh_3), 144.1 (NCN), 189.2 ($\text{C}=\text{Ru}$).

References

1. a) V. Lavallo, Y. Canac, B. Donnadieu, W. W. Schoeller, G. Bertrand, *Science*, **2006**, 312, 722, b) V. Lavallo, Y. Ishida, B. Donnadieu, G. Bertrand, *Angew. Chem. Int. Ed.* **2006**, 45, 6652.
2. A. J. Arduengo III, R. L. Harlow, M. Kline, *J. Am. Chem. Soc.* **1991**, 113, 361.
3. Further information on the calculations can be found in the appendix.
4. T. G. Traylor, K. W. Hill, Z.-Q. Tian, A. L. Rheingold, J. Peisach, J. McCracken, *J. Am. Chem. Soc.* **1988**, 110, 5571.
5. J. Schlegel, G. Maas, *Synthesis*, **1999**, 1, 100.
6. Full details for the X-ray crystal structures of compounds **6**, **9**, **10** and **11** can be found in the appendix.
7. a) H. J. Bestmann, H. Behl, M. Bremer, *Angew. Chem. Int. Ed. Engl.* **1989**, 28, 1219, b) H. J. Bestmann, W. Frank, C. Moll, A. Pohlschmidt, T. Clark, A. Göller, *Angew. Chem. Int. Ed.* **1998**, 37, 338.
8. a) F. Tonner, F. Öxler, B. Neumüller, W. Petz, G. Frenking, *Angew. Chem. Int. Ed.* **2006**, 45, 8038, b) H. Schmidbaur, *Angew. Chem. Int. Ed.* **2007**, 46, 2984, c) G. Frenking, B. Neumüller, W. Petz, R. Tonner, F. Öxler, *Angew. Chem. Int. Ed.* **2007**, 46, 2986.
9. R. Tonner, G. Frenking, *Angew. Chem. Int. Ed.* **2007**, 46, 8695.
10. a) C. A. Dyker, V. Lavallo, B. Donnadieu, G. Bertrand, *Angew. Chem. Int. Ed.* **2008**, 47, 3206, b) B. Lavallo, C. A. Dyker, B. Donnadieu, G. Bertrand, *Angew. Chem. Int. Ed.* **2008**, 47, 5411, c) A. Fürstner, M. Alcarazo, R. Goddard, C. W. Lehmann, *Angew. Chem. Int. Ed.* **2008**, 47, 3210, d) O. Kaufhold, F. E. Hahn, *Angew. Chem. Int. Ed.* **2008**, 47, 4057.
11. C. D. Good, D. M. Ritter, *J. Am. Chem. Soc.* **1962**, 84, 1162.
12. O. Guerret, S. Solé, H. Gornitzka, M. Teichert, G. Trinquier, G. Bertrand, *J. Am. Chem. Soc.* **1997**, 119, 6668.
13. A. A. D. Tulloch, A. A. Danopoulos, S. Winston, S. Kleinhenz, G. J. Eastham, *J. Chem. Soc., Dalton Trans.* **2000**, 4499.

-
14. H. M. J. Wang, I. J. B. Lin, *Organometallics* **1998**, *17*, 972.
 15. a) J. C. Garrison, W. J. Youngs, *Chem. Rev.* **2005**, *105*, 3978; b) I. J. B. Lin, C. S. Vasam, *Coord. Chem. Rev.* **2007**, *251*, 642.
 16. a) A. R. Chianese, A. Kovacevic, B. M. Zeglis, J. W. Faller, R. H. Crabtree, *Organometallics*, **2004**, *23*, 2461; b) P. Mathew, A. Neels, M. Albrecht, *J. Am. Chem. Soc.*, **2008**, *130*, 13534, c) P. L. Arnold, S. Pearson, *Coord. Chem. Rev.* **2007**, *251*, 596; d) M. Albrecht, *Chem. Commun.*, **2008**, 3601.
 17. a) A. J. Arduengo III, H. V. R. Dias, J. C. Calabrese, F. Davidson, *Organometallics* **1993**, *12*, 3405; b) B. Bildstein, M. Malaun, H. Kopacka, K. Wurst, M. Mitterböck, K.-H. Ongania, G. Opronolla, P. Zanello, *Organometallics* **1999**, *18*, 4325; c) T. Ramnial, C. D. Abernethy, M. D. Spicer, I. D. McKenzie, I. D. Gay, J. A. C. Clyburne, *Inorg. Chem.* **2003**, *42*, 1391.
 18. Wiberg, K. B. *Tetrahedron* **1968**, *24*, 1083-1096.

Concluding Remarks

Ylide chemistry has been around for nearly 100 years and during that time has yielded an abundance of fundamental and practical results. Remarkably, useful chemistry continues to be gleaned from this fascinating species and it seems clear that this trend will continue. Currently ylides are being used to stabilize species that were once thought of as too ephemeral to isolate and in doing so novel transition metal ligands are created at a remarkable rate. This dissertation describes the synthesis of several new species that take advantage of the stabilizing powers of ylides.

The first phosphorus-sulfur bisylide is one such species. The chemistry of this analog to carbodiphosphoranes is at its very early stages but it is easy to imagine its use as a reagent for synthetic transformations as well as cyclic versions that could be used as ligands in transition metal catalysis.

The chemistry of amino bisylide carbenes has also been introduced. This bidentate ligand forms complexes with a variety of metals. This includes metals such as palladium, which has a variety of uses in catalysis.

A very promising new ligand is the cyclic phosphaallene ylide. Importantly it creates a very active ruthenium metathesis catalyst; a reaction that is of astounding utility is synthesis.

Finally the fundamentally interesting donor/acceptor complex of C₂ has been synthesized. This allenylidene is an isomer of cyclopropanylidene a species that is abundant in interstellar space.

These new carbon based ligands open up numerous possibilities to improve catalytic reactions and even develop new protocols to synthesize small molecules more efficiently. This dissertation contains an important step to obtaining these goals.

Appendix

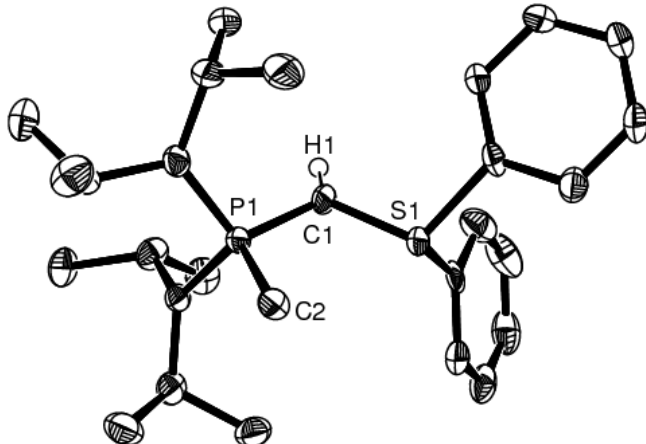


Table 1. Crystal data and structure refinement: Compound 1 Chapter 1

Empirical formula	C ₂₇ H ₄₂ F ₃ N ₂ O ₃ P S ₂					
Formula weight	594.72					
Temperature	133(2) K					
Wavelength	0.71073 Å					
Crystal system	Orthorhombic					
Space group	Pna2(1)					
Unit cell dimensions	a = 20.0766(17) Å	α= 90°	b = 9.8697(9) Å	β= 90°	c = 15.4407(14) Å	γ = 90°
Volume	3059.6(5) Å ³					
Z	4					
Density (calculated)	1.291 Mg/m ³					
Absorption coefficient	0.275 mm ⁻¹					
F(000)	1264					
Crystal size	0.3 x 0.3 x 0.2 mm ³					
Theta range for data collection	5.13 to 23.81°					
Index ranges	-22<=h<=18, -11<=k<=11, -15<=l<=17					
Reflections collected	13707					
Independent reflections	4254 [R(int) = 0.0762]					

Completeness to theta = 23.81°	98.8 %
Absorption correction	Semi-empirical
Max. and min. transmission	1.000000 and 0.519475
Refinement method	Full-matrix least-squares on F ²
Data / restraints / parameters	4254 / 250 / 428
Goodness-of-fit on F ²	0.986
Final R indices [I>2sigma(I)]	R1 = 0.0446, wR2 = 0.0819
R indices (all data)	R1 = 0.0693, wR2 = 0.0893
Absolute structure parameter	0.05(9)
Largest diff. peak and hole	0.312 and -0.240 e.Å ⁻³

Table 2. Atomic coordinates ($\times 10^4$) and equivalent isotropic displacement parameters ($\text{\AA}^2 \times 10^3$). U(eq) is defined as one third of the trace of the orthogonalized U_{ij} tensor.

	x	y	z	U(eq)
C(1)	1895(2)	744(5)	3547(3)	24(1)
P(1)	1413(1)	-255(1)	2881(1)	19(1)
C(2)	1951(2)	-1219(4)	2186(3)	23(1)
N(1)	951(2)	-1250(3)	3492(2)	23(1)
C(3)	1160(2)	-1790(5)	4363(3)	31(1)
C(4)	1033(2)	-785(5)	5077(3)	40(1)
C(5)	1855(2)	-2398(5)	4384(3)	44(1)
C(6)	393(2)	-2042(4)	3076(3)	24(1)
C(7)	-240(2)	-1946(5)	3619(3)	36(1)
C(8)	571(2)	-3515(4)	2924(4)	39(1)
N(2)	867(2)	569(3)	2268(2)	20(1)
C(9)	412(2)	1477(4)	2785(3)	28(1)
C(10)	-315(2)	1340(5)	2484(3)	35(1)
C(11)	632(2)	2958(4)	2770(4)	37(1)
C(12)	910(2)	890(5)	1335(3)	28(1)

	x	y	z	U(eq)
C(13)	801(2)	-354(5)	761(3)	39(1)
C(14)	1540(2)	1673(5)	1066(3)	35(1)
S(1)	2698(1)	993(1)	3271(1)	23(1)
C(15)	2837(2)	2779(4)	3143(3)	25(1)
C(16)	2850(2)	3653(5)	3843(4)	38(1)
C(17)	2960(3)	5029(6)	3708(4)	46(2)
C(18)	3047(2)	5514(5)	2885(4)	40(1)
C(19)	3023(2)	4644(5)	2189(4)	35(1)
C(20)	2922(2)	3258(5)	2317(3)	29(1)
C(21)	3227(2)	702(4)	4204(3)	23(1)
C(22)	2985(2)	632(5)	5020(3)	31(1)
C(23)	3418(2)	456(5)	5713(3)	32(1)
C(24)	4096(2)	333(5)	5554(3)	31(1)
C(25)	4329(2)	376(5)	4723(3)	29(1)
C(26)	3906(2)	574(4)	4025(3)	29(1)
C(27)	3871(9)	8269(16)	699(11)	58(3)
F(1)	3440(8)	7478(15)	1128(13)	82(4)
F(2)	3665(9)	8313(18)	-132(10)	92(4)
F(3)	4473(9)	7670(20)	634(15)	76(3)
S(2)	3812(6)	9769(12)	1314(7)	35(2)
O(1)	3177(10)	10340(40)	1120(30)	47(4)
O(2)	3774(8)	8920(20)	2148(8)	80(4)
O(3)	4380(6)	10515(15)	1176(13)	64(4)
C(27')	3845(6)	8394(12)	627(8)	60(2)
F(1')	3325(5)	7567(11)	700(8)	79(3)
F(2')	3847(6)	8764(15)	-242(6)	103(3)
F(3')	4395(6)	7678(16)	849(11)	91(4)
S(2')	3839(4)	9972(7)	1153(5)	42(1)
O(1')	3159(7)	10400(20)	1075(17)	47(3)
O(2')	4034(6)	9643(13)	2046(6)	75(3)

	x	y	z	U(eq)
O(3')	4316(4)	10708(9)	680(8)	60(3)

Table 3. Bond lengths [\AA] and angles [°] for starting.

C(1)-S(1)	1.685(4)	C(18)-C(19)	1.376(7)
C(1)-P(1)	1.723(5)	C(19)-C(20)	1.397(6)
P(1)-N(1)	1.646(3)	C(21)-C(22)	1.353(6)
P(1)-N(2)	1.661(3)	C(21)-C(26)	1.398(5)
P(1)-C(2)	1.796(4)	C(22)-C(23)	1.389(6)
N(1)-C(3)	1.507(5)	C(23)-C(24)	1.388(6)
N(1)-C(6)	1.509(5)	C(24)-C(25)	1.366(6)
C(3)-C(4)	1.504(6)	C(25)-C(26)	1.386(6)
C(3)-C(5)	1.519(6)	C(27)-F(1)	1.340(14)
C(6)-C(8)	1.516(6)	C(27)-F(3)	1.349(14)
C(6)-C(7)	1.525(6)	C(27)-F(2)	1.349(15)
N(2)-C(12)	1.477(6)	C(27)-S(2)	1.762(12)
N(2)-C(9)	1.508(5)	S(2)-O(3)	1.373(12)
C(9)-C(11)	1.527(6)	S(2)-O(1)	1.428(12)
C(9)-C(10)	1.538(5)	S(2)-O(2)	1.537(12)
C(12)-C(13)	1.530(6)	C(27')-F(1')	1.329(11)
C(12)-C(14)	1.539(6)	C(27')-F(3')	1.356(11)
S(1)-C(15)	1.796(4)	C(27')-F(2')	1.391(12)
S(1)-C(21)	1.811(4)	C(27')-S(2')	1.757(10)
C(15)-C(20)	1.371(6)	S(2')-O(3')	1.406(8)
C(15)-C(16)	1.383(6)	S(2')-O(1')	1.434(9)
C(16)-C(17)	1.392(7)	S(2')-O(2')	1.469(8)
C(17)-C(18)	1.370(8)		
S(1)-C(1)-P(1)	118.1(3)	N(1)-P(1)-C(1)	108.5(2)
N(1)-P(1)-N(2)	104.35(16)	N(2)-P(1)-C(1)	115.47(19)

N(1)-P(1)-C(2)	111.45(19)	C(22)-C(21)-C(26)	122.0(4)
N(2)-P(1)-C(2)	108.4(2)	C(22)-C(21)-S(1)	122.6(3)
C(1)-P(1)-C(2)	108.7(2)	C(26)-C(21)-S(1)	115.4(4)
C(3)-N(1)-C(6)	113.8(3)	C(21)-C(22)-C(23)	120.0(4)
C(3)-N(1)-P(1)	124.4(3)	C(24)-C(23)-C(22)	119.3(4)
C(6)-N(1)-P(1)	118.9(3)	C(25)-C(24)-C(23)	119.9(4)
C(4)-C(3)-N(1)	111.9(4)	C(24)-C(25)-C(26)	121.7(4)
C(4)-C(3)-C(5)	113.6(4)	C(25)-C(26)-C(21)	117.1(5)
N(1)-C(3)-C(5)	114.5(4)	F(1)-C(27)-F(3)	111.3(16)
N(1)-C(6)-C(8)	112.8(3)	F(1)-C(27)-F(2)	106.9(13)
N(1)-C(6)-C(7)	110.6(3)	F(3)-C(27)-F(2)	102.5(15)
C(8)-C(6)-C(7)	110.0(4)	F(1)-C(27)-S(2)	100.4(13)
C(12)-N(2)-C(9)	115.1(3)	F(3)-C(27)-S(2)	117.8(13)
C(12)-N(2)-P(1)	128.5(3)	F(2)-C(27)-S(2)	117.7(13)
C(9)-N(2)-P(1)	112.9(3)	O(3)-S(2)-O(1)	119.7(16)
N(2)-C(9)-C(11)	112.7(3)	O(3)-S(2)-O(2)	117.6(9)
N(2)-C(9)-C(10)	111.3(4)	O(1)-S(2)-O(2)	110.3(16)
C(11)-C(9)-C(10)	110.8(4)	O(3)-S(2)-C(27)	108.2(10)
N(2)-C(12)-C(13)	112.6(4)	O(1)-S(2)-C(27)	106.2(15)
N(2)-C(12)-C(14)	114.8(3)	O(2)-S(2)-C(27)	89.9(10)
C(13)-C(12)-C(14)	111.4(4)	F(1')-C(27')-F(3')	107.3(11)
C(1)-S(1)-C(15)	108.6(2)	F(1')-C(27')-F(2')	104.2(9)
C(1)-S(1)-C(21)	109.7(2)	F(3')-C(27')-F(2')	112.3(12)
C(15)-S(1)-C(21)	98.76(19)	F(1')-C(27')-S(2')	120.0(9)
C(20)-C(15)-C(16)	120.6(4)	F(3')-C(27')-S(2')	110.5(9)
C(20)-C(15)-S(1)	117.4(3)	F(2')-C(27')-S(2')	102.4(9)
C(16)-C(15)-S(1)	121.9(4)	O(3')-S(2')-O(1')	117.0(10)
C(15)-C(16)-C(17)	119.6(5)	O(3')-S(2')-O(2')	114.9(7)
C(18)-C(17)-C(16)	120.1(5)	O(1')-S(2')-O(2')	113.4(11)
C(17)-C(18)-C(19)	120.1(5)	O(3')-S(2')-C(27')	102.3(7)
C(18)-C(19)-C(20)	120.3(5)	O(1')-S(2')-C(27')	103.0(10)
C(15)-C(20)-C(19)	119.2(5)	O(2')-S(2')-C(27')	103.7(7)

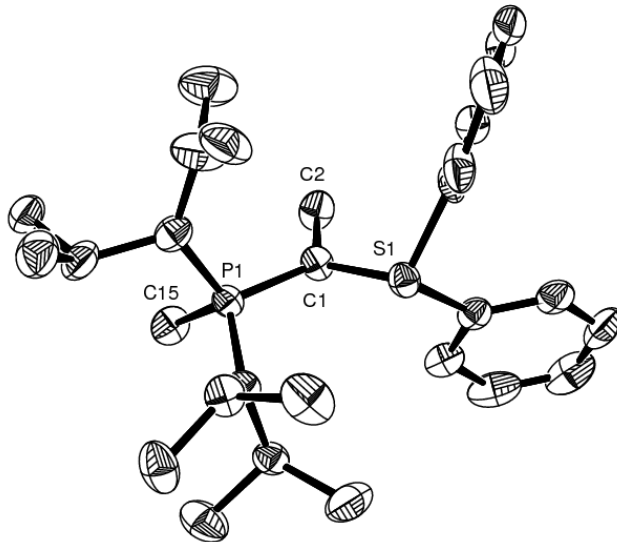


Table 1. Crystal data and structure refinement: Compound **4** Chapter 1.

Empirical formula	C ₂₇ H ₄₄ I N ₂ P S		
Formula weight	586.57		
Temperature	173(2) K		
Wavelength	0.71073 Å		
Crystal system	Monoclinic		
Space group	P2(1)/n		
Unit cell dimensions	a = 11.0585(9) Å	α= 90°	
	b = 16.0898(14) Å	β= 90.564(2)°	
	c = 16.5255(14) Å	γ = 90°	
Volume	2940.2(4) Å ³		
Z	4		
Density (calculated)	1.325 Mg/m ³		
Absorption coefficient	1.231 mm ⁻¹		
F(000)	1216		
Crystal size	0.1 x 0.1 x 0.02 mm ³		
Theta range for data collection	5.13 to 23.25°		
Index ranges	-12<=h<=11, -12<=k<=17, -18<=l<=18		
Reflections collected	12882		

Independent reflections	4178 [R(int) = 0.0812]
Completeness to theta =	23.25° 98.9 %
Absorption correction	Semi-empirical
Max. and min. transmission	1.000000 and 0.166103
Refinement method	Full-matrix least-squares on F^2
Data / restraints / parameters	4178 / 153 / 350
Goodness-of-fit on F^2	0.984
Final R indices [$ I >2\sigma(I)$]	R1 = 0.0486, wR2 = 0.0839
R indices (all data)	R1 = 0.1014, wR2 = 0.0970
Largest diff. peak and hole	0.873 and -0.611 e. \AA^{-3}

Table 2. Atomic coordinates ($\times 10^4$) and equivalent isotropic displacement parameters ($\text{\AA}^2 \times 10^3$). U(eq) is defined as one third of the trace of the orthogonalized U_{ij}^2 tensor.

	x	y	z	U(eq)
I(1)	8012(1)	6432(1)	711(1)	57(1)
P(1)	2764(1)	2528(1)	4552(1)	28(1)
S(1)	3452(1)	3938(1)	3553(1)	31(1)
C(1)	3194(5)	2914(4)	3624(3)	30(1)
C(2)	3190(5)	2374(4)	2873(3)	41(2)
C(3)	4862(5)	4078(4)	3026(3)	32(2)
C(4)	5766(5)	3504(4)	3186(3)	41(2)
C(5)	6899(5)	3632(5)	2848(4)	57(2)
C(6)	7095(6)	4300(6)	2352(4)	61(2)
C(7)	6196(6)	4870(5)	2193(4)	54(2)
C(8)	5061(5)	4759(4)	2538(3)	40(2)
C(9)	2396(5)	4427(4)	2863(3)	33(2)
C(10)	2306(5)	4209(4)	2050(4)	44(2)
C(11)	1385(7)	4546(5)	1585(4)	60(2)
C(12)	561(6)	5097(5)	1930(6)	67(2)
C(13)	672(6)	5311(5)	2730(5)	65(2)

	x	y	z	U(eq)
C(14)	1605(5)	4977(4)	3203(4)	43(2)
C(15)	3398(5)	1496(4)	4618(3)	39(2)
N(1)	3324(4)	3094(3)	5299(2)	30(1)
C(16)	2536(5)	3577(4)	5852(3)	36(1)
C(17)	2675(6)	3354(4)	6727(3)	49(2)
C(18)	2570(6)	4503(4)	5710(3)	55(2)
C(19)	4668(5)	3044(4)	5412(3)	33(2)
C(20)	5072(5)	2508(4)	6131(3)	55(2)
C(21)	5303(5)	3877(4)	5438(4)	57(2)
N(2)	1292(4)	2436(3)	4651(3)	35(1)
C(22)	335(12)	2786(9)	4156(8)	59(3)
C(23)	-209(16)	3550(11)	4410(8)	57(3)
C(24)	83(13)	2409(10)	3390(7)	67(3)
C(25)	979(9)	1838(7)	5344(7)	44(2)
C(26)	23(9)	2186(8)	5919(6)	50(3)
C(27)	588(9)	973(7)	5057(8)	46(2)
C(22')	597(14)	3173(10)	4224(9)	54(3)
C(23')	-359(19)	3508(15)	4760(10)	57(3)
C(24')	104(15)	2977(11)	3404(9)	56(3)
C(25')	444(11)	1744(8)	4831(8)	44(2)
C(26')	543(13)	1599(11)	5744(8)	50(3)
C(27')	609(12)	968(8)	4340(10)	52(3)

Table 3. Bond lengths [Å] and angles [°].

P(1)-N(2)	1.644(4)	S(1)-C(9)	1.804(5)
P(1)-N(1)	1.649(4)	S(1)-C(3)	1.806(5)
P(1)-C(1)	1.727(5)	C(1)-C(2)	1.515(7)
P(1)-C(15)	1.805(6)	C(3)-C(8)	1.380(8)
S(1)-C(1)	1.677(6)	C(3)-C(4)	1.384(8)

C(4)-C(5)	1.391(8)	C(19)-C(21)	1.513(8)
C(5)-C(6)	1.371(10)	C(19)-C(20)	1.532(7)
C(6)-C(7)	1.376(9)	N(2)-C(22)	1.445(10)
C(7)-C(8)	1.395(8)	N(2)-C(25')	1.488(12)
C(9)-C(14)	1.370(7)	N(2)-C(25)	1.540(11)
C(9)-C(10)	1.391(8)	N(2)-C(22')	1.576(13)
C(10)-C(11)	1.380(8)	C(22)-C(24)	1.429(12)
C(11)-C(12)	1.396(10)	C(22)-C(23)	1.434(14)
C(12)-C(13)	1.370(9)	C(25)-C(27)	1.531(14)
C(13)-C(14)	1.396(8)	C(25)-C(26)	1.534(13)
N(1)-C(16)	1.488(7)	C(22')-C(23')	1.487(17)
N(1)-C(19)	1.499(6)	C(22')-C(24')	1.489(15)
C(16)-C(17)	1.496(7)	C(25')-C(27')	1.502(15)
C(16)-C(18)	1.508(8)	C(25')-C(26')	1.529(15)
N(2)-P(1)-N(1)	109.9(2)	C(6)-C(7)-C(8)	119.1(7)
N(2)-P(1)-C(1)	113.7(2)	C(3)-C(8)-C(7)	119.4(6)
N(1)-P(1)-C(1)	111.2(2)	C(14)-C(9)-C(10)	121.3(5)
N(2)-P(1)-C(15)	107.2(3)	C(14)-C(9)-S(1)	115.7(4)
N(1)-P(1)-C(15)	108.7(2)	C(10)-C(9)-S(1)	122.7(5)
C(1)-P(1)-C(15)	105.9(3)	C(11)-C(10)-C(9)	118.9(6)
C(1)-S(1)-C(9)	111.3(3)	C(10)-C(11)-C(12)	120.2(7)
C(1)-S(1)-C(3)	107.7(3)	C(13)-C(12)-C(11)	120.0(6)
C(9)-S(1)-C(3)	101.4(3)	C(12)-C(13)-C(14)	120.2(7)
C(2)-C(1)-S(1)	120.4(4)	C(9)-C(14)-C(13)	119.4(6)
C(2)-C(1)-P(1)	121.5(4)	C(16)-N(1)-C(19)	122.5(4)
S(1)-C(1)-P(1)	117.7(3)	C(16)-N(1)-P(1)	122.1(3)
C(8)-C(3)-C(4)	121.5(5)	C(19)-N(1)-P(1)	115.3(3)
C(8)-C(3)-S(1)	121.6(5)	N(1)-C(16)-C(17)	114.4(5)
C(4)-C(3)-S(1)	116.8(5)	N(1)-C(16)-C(18)	113.9(5)
C(3)-C(4)-C(5)	118.5(7)	C(17)-C(16)-C(18)	112.6(5)
C(6)-C(5)-C(4)	120.3(7)	N(1)-C(19)-C(21)	114.6(5)
C(5)-C(6)-C(7)	121.3(6)	N(1)-C(19)-C(20)	114.1(4)

C(21)-C(19)-C(20)	110.1(5)	C(24)-C(22)-N(2)	118.1(10)
C(22)-N(2)-C(25')	86.8(9)	C(23)-C(22)-N(2)	118.4(10)
C(22)-N(2)-C(25)	119.7(8)	C(27)-C(25)-C(26)	109.3(9)
C(25')-N(2)-C(25)	40.1(6)	C(27)-C(25)-N(2)	113.7(9)
C(22)-N(2)-C(22')	26.1(7)	C(26)-C(25)-N(2)	113.2(9)
C(25')-N(2)-C(22')	110.3(8)	C(23')-C(22')-C(24')	111.3(13)
C(25)-N(2)-C(22')	133.7(8)	C(23')-C(22')-N(2)	110.7(13)
C(22)-N(2)-P(1)	129.0(7)	C(24')-C(22')-N(2)	114.9(12)
C(25')-N(2)-P(1)	135.5(6)	N(2)-C(25')-C(27')	115.7(10)
C(25)-N(2)-P(1)	111.1(5)	N(2)-C(25')-C(26')	105.8(10)
C(22')-N(2)-P(1)	111.6(7)	C(27')-C(25')-C(26')	113.5(12)
C(24)-C(22)-C(23)	123.0(10)		

Symmetry transformations used to generate equivalent atoms:

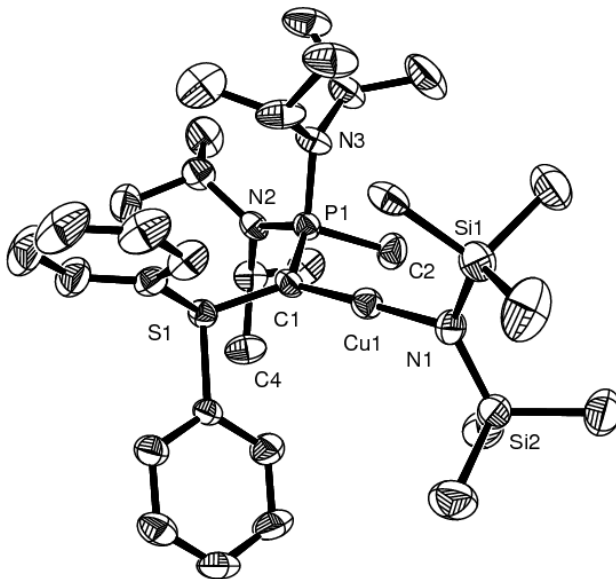


Table 1. Crystal data and structure refinement: Compound **5** Chapter 1.

Empirical formula	C ₃₂ H ₅₉ CuN ₃ PSSi ₂		
Formula weight	668.57		
Temperature	173(2) K		
Wavelength	0.71073 Å		
Crystal system	Monoclinic		
Space group	P2(1)/n		
Unit cell dimensions	a = 10.1942(3) Å	α= 90°.	
	b = 22.4074(7) Å	β= 04.047(2)°.	
	c = 17.1331(6) Å	γ = 90°.	
Volume	3796.6(2) Å ³		
Z	4		
Density (calculated)	1.170 Mg/m ³		
Absorption coefficient	0.759 mm ⁻¹		
F(000)	1440		
Crystal size	0.40 x 0.10 x 0.10 mm ³		
Theta range for data collection	5.15 to 22.72°		
Index ranges	-11<=h<=11, -24<=k<=24, -18<=l<=18		
Reflections collected	40255		

Independent reflections	5033 [R(int) = 0.1238]
Completeness to theta = 22.72°	98.7 %
Absorption correction	Semi-empirical
Max. and min. transmission	1.000000 and 0.796497
Refinement method	Full-matrix least-squares on F^2
Data / restraints / parameters	5033 / 210 / 462
Goodness-of-fit on F^2	1.021
Final R indices [$ I >2\text{sigma}(I)$]	R1 = 0.0423, wR2 = 0.0762
R indices (all data)	R1 = 0.1067, wR2 = 0.1006
Largest diff. peak and hole	0.305 and -0.294 e. \AA^{-3}

Table 2. Atomic coordinates ($\times 10^4$) and equivalent isotropic displacement parameters ($\text{\AA}^2 \times 10^3$). U(eq) is defined as one third of the trace of the orthogonalized U_{ij} tensor.

	x	y	z	U(eq)
Cu(1)	9248(1)	2463(1)	980(1)	32(1)
S(1)	8368(1)	3781(1)	370(1)	28(1)
P(1)	10171(1)	3637(1)	1922(1)	28(1)
Si(2)	10423(1)	1380(1)	381(1)	38(1)
C(1)	9271(5)	3311(2)	1055(3)	29(1)
C(2)	11764(5)	3245(2)	2182(3)	45(1)
N(2)	10542(4)	4364(2)	1928(2)	30(1)
C(3)	11599(7)	4664(4)	1597(4)	37(2)
C(4)	11543(8)	4473(5)	739(4)	46(2)
C(5)	13033(8)	4618(5)	2149(6)	47(2)
C(3')	11670(20)	4374(13)	1483(16)	38(4)
C(4')	11440(30)	4824(14)	800(16)	42(5)
C(5')	13120(20)	4419(17)	2010(20)	43(6)
C(6)	9702(5)	4815(2)	2217(3)	40(1)
C(7)	10533(6)	5219(2)	2880(3)	60(2)
C(8)	8839(6)	5194(2)	1541(3)	55(2)

	x	y	z	U(eq)
C(9)	10294(6)	3646(2)	3514(3)	46(1)
C(10)	10924(7)	3080(3)	3958(3)	78(2)
C(11)	9579(6)	4009(3)	4046(3)	61(2)
N(3)	9450(4)	3533(2)	2683(2)	34(1)
C(12)	7975(12)	3375(9)	2512(15)	47(3)
C(13)	7620(30)	2875(10)	3034(15)	64(4)
C(14)	7008(14)	3906(12)	2453(14)	59(4)
C(12')	8107(17)	3223(12)	2540(20)	49(4)
C(13')	8130(30)	2693(13)	3100(20)	63(5)
C(14')	6972(19)	3657(15)	2546(19)	52(4)
N(1)	9322(4)	1630(2)	905(2)	35(1)
Si(1)	8328(11)	1217(6)	1361(6)	41(1)
C(15)	6748(13)	1628(11)	1446(13)	39(3)
C(16)	7730(30)	496(7)	834(14)	73(4)
C(17)	9201(19)	1012(11)	2423(8)	64(5)
Si(1')	8260(30)	1269(16)	1372(18)	40(3)
C(15')	6560(30)	1650(40)	1220(30)	31(6)
C(16')	7900(80)	480(20)	1010(40)	73(8)
C(17')	8970(50)	1210(20)	2489(19)	54(8)
C(18)	11192(6)	641(2)	746(4)	61(2)
C(19)	11899(5)	1903(2)	469(3)	52(2)
C(20)	9627(6)	1294(3)	-721(3)	64(2)
C(21)	6559(5)	3664(2)	209(3)	33(1)
C(22)	6054(5)	3126(2)	373(3)	43(1)
C(23)	4675(6)	3054(3)	258(4)	59(2)
C(24)	3827(6)	3514(4)	-39(4)	73(2)
C(25)	4321(6)	4060(3)	-206(4)	69(2)
C(26)	5717(5)	4137(3)	-78(3)	48(2)
C(27)	8551(5)	3514(2)	-605(3)	27(1)
C(28)	7564(5)	3589(2)	-1302(3)	38(1)

	x	y	z	U(eq)
C(29)	7803(6)	3400(2)	-2028(3)	45(1)
C(30)	9007(6)	3149(2)	-2053(3)	48(2)
C(31)	9998(6)	3081(3)	-1351(3)	55(2)
C(32)	9772(5)	3265(2)	-627(3)	42(1)

Table 3. Bond lengths [Å] and angles [°].

Cu(1)-N(1)	1.874(4)	C(9)-C(11)	1.533(7)
Cu(1)-C(1)	1.903(4)	C(9)-C(10)	1.537(7)
S(1)-C(1)	1.677(5)	N(3)-C(12')	1.502(14)
S(1)-C(21)	1.815(5)	N(3)-C(12)	1.503(10)
S(1)-C(27)	1.825(4)	C(12)-C(13)	1.530(11)
P(1)-N(3)	1.661(4)	C(12)-C(14)	1.532(11)
P(1)-N(2)	1.671(4)	C(12')-C(14')	1.514(15)
P(1)-C(1)	1.709(5)	C(12')-C(13')	1.527(14)
P(1)-C(2)	1.804(5)	N(1)-Si(1)	1.696(6)
Si(2)-N(1)	1.695(4)	N(1)-Si(1')	1.698(14)
Si(2)-C(18)	1.873(5)	Si(1)-C(17)	1.878(8)
Si(2)-C(20)	1.875(5)	Si(1)-C(16)	1.879(8)
Si(2)-C(19)	1.885(5)	Si(1)-C(15)	1.891(8)
N(2)-C(6)	1.485(6)	Si(1')-C(17')	1.879(16)
N(2)-C(3)	1.494(7)	Si(1')-C(16')	1.880(16)
N(2)-C(3')	1.524(17)	Si(1')-C(15')	1.892(16)
C(3)-C(4)	1.519(9)	C(21)-C(22)	1.367(7)
C(3)-C(5)	1.540(8)	C(21)-C(26)	1.377(7)
C(3')-C(4')	1.520(18)	C(22)-C(23)	1.381(7)
C(3')-C(5')	1.539(17)	C(23)-C(24)	1.363(8)
C(6)-C(8)	1.530(7)	C(24)-C(25)	1.379(9)
C(6)-C(7)	1.535(6)	C(25)-C(26)	1.397(7)
C(9)-N(3)	1.496(6)	C(27)-C(32)	1.373(6)

C(27)-C(28)	1.373(6)	C(30)-C(31)	1.379(7)
C(28)-C(29)	1.390(6)	C(31)-C(32)	1.378(6)
C(29)-C(30)	1.362(7)		
N(1)-Cu(1)-C(1)	176.97(18)	C(4')-C(3')-C(5')	110(2)
C(1)-S(1)-C(21)	112.4(2)	N(2)-C(3')-C(5')	116(2)
C(1)-S(1)-C(27)	105.9(2)	N(2)-C(6)-C(8)	113.4(4)
C(21)-S(1)-C(27)	98.0(2)	N(2)-C(6)-C(7)	112.9(4)
N(3)-P(1)-N(2)	105.88(19)	C(8)-C(6)-C(7)	110.2(4)
N(3)-P(1)-C(1)	112.1(2)	N(3)-C(9)-C(11)	114.2(4)
N(2)-P(1)-C(1)	119.7(2)	N(3)-C(9)-C(10)	114.0(4)
N(3)-P(1)-C(2)	106.3(2)	C(11)-C(9)-C(10)	110.2(4)
N(2)-P(1)-C(2)	106.5(2)	C(9)-N(3)-C(12')	121.6(14)
C(1)-P(1)-C(2)	105.5(2)	C(9)-N(3)-C(12)	122.8(10)
N(1)-Si(2)-C(18)	113.1(2)	C(12')-N(3)-C(12)	13.9(13)
N(1)-Si(2)-C(20)	112.8(2)	C(9)-N(3)-P(1)	117.5(3)
C(18)-Si(2)-C(20)	106.9(3)	C(12')-N(3)-P(1)	119.8(14)
N(1)-Si(2)-C(19)	111.7(2)	C(12)-N(3)-P(1)	119.5(10)
C(18)-Si(2)-C(19)	105.2(3)	N(3)-C(12)-C(13)	115.1(12)
C(20)-Si(2)-C(19)	106.6(3)	N(3)-C(12)-C(14)	115.3(10)
S(1)-C(1)-P(1)	115.3(3)	C(13)-C(12)-C(14)	111.6(9)
S(1)-C(1)-Cu(1)	125.7(3)	N(3)-C(12')-C(14')	111.7(16)
P(1)-C(1)-Cu(1)	118.7(2)	N(3)-C(12')-C(13')	112.5(16)
C(6)-N(2)-C(3)	110.3(5)	C(14')-C(12')-C(13')	112.9(14)
C(6)-N(2)-C(3')	136.2(12)	Si(2)-N(1)-Si(1)	127.6(5)
C(3)-N(2)-C(3')	26.3(10)	Si(2)-N(1)-Si(1')	132.1(14)
C(6)-N(2)-P(1)	121.2(3)	Si(1)-N(1)-Si(1')	4.6(18)
C(3)-N(2)-P(1)	128.2(4)	Si(2)-N(1)-Cu(1)	114.2(2)
C(3')-N(2)-P(1)	102.0(12)	Si(1)-N(1)-Cu(1)	118.3(5)
N(2)-C(3)-C(4)	112.4(6)	Si(1')-N(1)-Cu(1)	113.7(14)
N(2)-C(3)-C(5)	113.7(6)	N(1)-Si(1)-C(17)	112.6(6)
C(4)-C(3)-C(5)	112.4(6)	N(1)-Si(1)-C(16)	114.0(6)
C(4')-C(3')-N(2)	114.0(18)	C(17)-Si(1)-C(16)	106.1(6)

N(1)-Si(1)-C(15)	112.6(6)	C(24)-C(23)-C(22)	119.8(6)
C(17)-Si(1)-C(15)	104.9(5)	C(23)-C(24)-C(25)	121.2(6)
C(16)-Si(1)-C(15)	105.9(6)	C(24)-C(25)-C(26)	119.1(6)
N(1)-Si(1')-C(17')	112.4(16)	C(21)-C(26)-C(25)	119.0(6)
N(1)-Si(1')-C(16')	113.2(17)	C(32)-C(27)-C(28)	120.3(4)
C(17')-Si(1')-C(16')	105.4(15)	C(32)-C(27)-S(1)	117.0(4)
N(1)-Si(1')-C(15')	112.9(16)	C(28)-C(27)-S(1)	122.6(4)
C(17')-Si(1')-C(15')	106.3(13)	C(27)-C(28)-C(29)	119.4(5)
C(16')-Si(1')-C(15')	106.0(16)	C(30)-C(29)-C(28)	120.7(5)
C(22)-C(21)-C(26)	121.2(5)	C(29)-C(30)-C(31)	119.5(5)
C(22)-C(21)-S(1)	121.0(4)	C(32)-C(31)-C(30)	120.4(5)
C(26)-C(21)-S(1)	117.8(4)	C(27)-C(32)-C(31)	119.8(5)
C(21)-C(22)-C(23)	119.7(5)		

Symmetry transformations used to generate equivalent atoms:

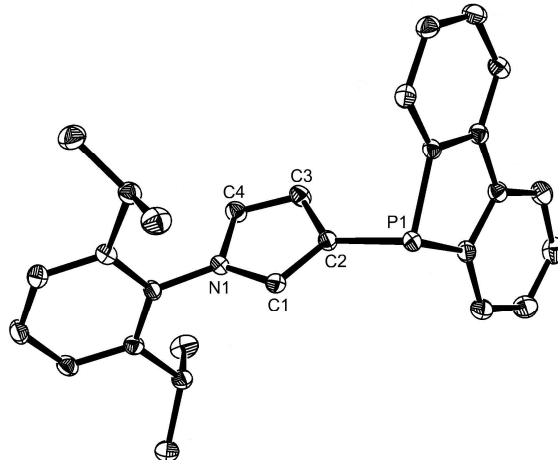


Table S1. Crystal data and structure refinement for: Compound 4 Chapter 2.

Empirical formula	C ₂₈ H ₂₈ NP		
Formula weight	409.48		
Temperature	100(2) K		
Wavelength	0.71073 Å		
Crystal system	Monoclinic		
Space group	C2/c		
Unit cell dimensions	a = 32.419(3) Å	α= 90°	
	b = 8.1259(9) Å	β= 132.117(4)°	
	c = 22.485(2) Å	γ = 90°	
Volume	4393.8(8) Å ³		
Z	8		
Density (calculated)	1.238 Mg/m ³		
Absorption coefficient	0.140 mm ⁻¹		
F(000)	1744		
Crystal size	0.28 x 0.14 x 0.12 mm ³		
Theta range for data collection	1.69 to 30.51°		
Index ranges	-46<=h<=44, -7<=k<=11, -32<=l<=32		
Reflections collected	21738		
Independent reflections	6606 [R(int) = 0.0393]		

Completeness to theta = 30.51°	98.4 %
Absorption correction	Sadabs
Max. and min. transmission	0.9834 and 0.9618
Refinement method	Full-matrix least-squares on F ²
Data / restraints / parameters	6606 / 0 / 275
Goodness-of-fit on F ²	1.042
Final R indices [I>2sigma(I)]	R1 = 0.0437, wR2 = 0.1107
R indices (all data)	R1 = 0.0654, wR2 = 0.1196
Largest diff. peak and hole	0.429 and -0.327 e.Å ⁻³

Table S2. *Atomic coordinates (x 10⁴) and equivalent isotropic displacement parameters (Å²x 10³). U(eq) is defined as one third of the trace of the orthogonalized U^{ij} tensor.*

	x	y	z	U(eq)
P(1)	822(1)	9870(1)	2526(1)	16(1)
N(1)	-713(1)	10918(1)	519(1)	16(1)
C(1)	-281(1)	10954(2)	1333(1)	16(1)
C(2)	150(1)	10023(2)	1526(1)	16(1)
C(3)	-30(1)	9406(2)	789(1)	19(1)
C(4)	-556(1)	9977(2)	187(1)	19(1)
C(5)	-1213(1)	11888(2)	57(1)	15(1)
C(6)	-1679(1)	11274(2)	-89(1)	16(1)
C(7)	-2165(1)	12215(2)	-577(1)	19(1)
C(8)	-2186(1)	13675(2)	-910(1)	21(1)
C(9)	-1717(1)	14257(2)	-748(1)	20(1)
C(10)	-1217(1)	13394(2)	-248(1)	17(1)
C(11)	-1664(1)	9635(2)	250(1)	19(1)
C(12)	-2051(1)	9589(2)	415(1)	25(1)
C(13)	-1804(1)	8218(2)	-305(1)	29(1)
C(14)	-690(1)	14113(2)	-11(1)	20(1)
C(15)	-805(1)	15189(2)	-664(1)	29(1)

	x	y	z	U(eq)
C(16)	-368(1)	15098(2)	770(1)	27(1)
C(17)	1279(1)	9878(2)	2317(1)	16(1)
C(18)	1402(1)	11205(2)	2068(1)	19(1)
C(19)	1770(1)	10987(2)	1952(1)	22(1)
C(20)	2009(1)	9466(2)	2075(1)	22(1)
C(21)	1890(1)	8137(2)	2325(1)	20(1)
C(22)	1525(1)	8335(2)	2449(1)	16(1)
C(23)	1343(1)	7078(2)	2701(1)	17(1)
C(24)	1527(1)	5452(2)	2916(1)	22(1)
C(25)	1321(1)	4439(2)	3162(1)	26(1)
C(26)	944(1)	5032(2)	3210(1)	26(1)
C(27)	760(1)	6654(2)	3006(1)	22(1)
C(28)	953(1)	7672(2)	2741(1)	18(1)

Table S3. Bond lengths [Å] and angles [°].

P(1)-C(2)	1.8020(13)	P(1)-C(28)	1.8250(14)
P(1)-C(17)	1.8287(13)	N(1)-C(1)	1.3686(16)
N(1)-C(4)	1.3825(16)	N(1)-C(5)	1.4397(16)
C(1)-C(2)	1.3791(18)	C(2)-C(3)	1.4277(18)
C(3)-C(4)	1.3633(19)	C(5)-C(10)	1.3984(18)
C(5)-C(6)	1.4044(17)	C(6)-C(7)	1.3966(18)
C(6)-C(11)	1.5180(18)	C(7)-C(8)	1.380(2)
C(8)-C(9)	1.3859(19)	C(9)-C(10)	1.3928(18)
C(10)-C(14)	1.5259(18)	C(11)-C(13)	1.525(2)
C(11)-C(12)	1.5324(19)	C(14)-C(15)	1.5250(19)
C(14)-C(16)	1.535(2)	C(17)-C(18)	1.3913(18)
C(17)-C(22)	1.4074(18)	C(18)-C(19)	1.3931(19)
C(19)-C(20)	1.385(2)	C(20)-C(21)	1.387(2)
C(21)-C(22)	1.3967(18)	C(22)-C(23)	1.4696(18)

C(23)-C(24)	1.3955(19)	C(23)-C(28)	1.4108(18)
C(24)-C(25)	1.387(2)	C(25)-C(26)	1.386(2)
C(26)-C(27)	1.391(2)	C(27)-C(28)	1.3885(18)
C(2)-P(1)-C(28)	105.66(6)	C(2)-P(1)-C(17)	100.87(6)
C(28)-P(1)-C(17)	89.23(6)	C(1)-N(1)-C(4)	108.56(10)
C(1)-N(1)-C(5)	126.88(11)	C(4)-N(1)-C(5)	123.87(10)
N(1)-C(1)-C(2)	108.68(11)	C(1)-C(2)-C(3)	106.74(11)
C(1)-C(2)-P(1)	123.51(10)	C(3)-C(2)-P(1)	129.47(10)
C(4)-C(3)-C(2)	107.44(12)	C(3)-C(4)-N(1)	108.58(11)
C(10)-C(5)-C(6)	122.79(12)	C(10)-C(5)-N(1)	117.91(11)
C(6)-C(5)-N(1)	119.27(11)	C(7)-C(6)-C(5)	117.26(12)
C(7)-C(6)-C(11)	121.03(11)	C(5)-C(6)-C(11)	121.69(11)
C(8)-C(7)-C(6)	121.09(12)	C(7)-C(8)-C(9)	120.25(12)
C(8)-C(9)-C(10)	121.18(13)	C(9)-C(10)-C(5)	117.34(12)
C(9)-C(10)-C(14)	120.95(12)	C(5)-C(10)-C(14)	121.64(12)
C(6)-C(11)-C(13)	111.18(11)	C(6)-C(11)-C(12)	112.74(11)
C(13)-C(11)-C(12)	109.62(12)	C(15)-C(14)-C(10)	112.98(11)
C(15)-C(14)-C(16)	110.04(12)	C(10)-C(14)-C(16)	109.96(11)
C(18)-C(17)-C(22)	119.98(12)	C(18)-C(17)-P(1)	127.37(10)
C(22)-C(17)-P(1)	112.64(9)	C(17)-C(18)-C(19)	119.39(13)
C(20)-C(19)-C(18)	120.77(13)	C(19)-C(20)-C(21)	120.30(12)
C(20)-C(21)-C(22)	119.74(13)	C(21)-C(22)-C(17)	119.82(12)
C(21)-C(22)-C(23)	127.62(12)	C(17)-C(22)-C(23)	112.55(11)
C(24)-C(23)-C(28)	119.71(12)	C(24)-C(23)-C(22)	127.02(12)
C(28)-C(23)-C(22)	113.23(12)	C(25)-C(24)-C(23)	119.41(13)
C(26)-C(25)-C(24)	120.76(14)	C(25)-C(26)-C(27)	120.48(13)
C(28)-C(27)-C(26)	119.43(13)	C(27)-C(28)-C(23)	120.19(13)
C(27)-C(28)-P(1)	127.24(11)	C(23)-C(28)-P(1)	112.20(10)

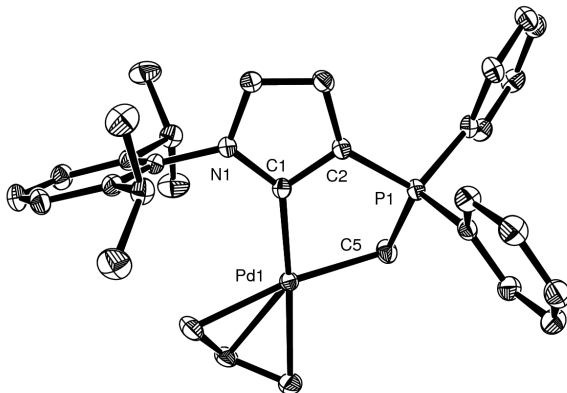


Table S1. Crystal data and structure refinement: Compound **9** Chapter 2.

Empirical formula	$C_{32}H_{36}NPPd$		
Formula weight	571.99		
Temperature	100(2) K		
Wavelength	0.71073 Å		
Crystal system	Monoclinic		
Space group	P2(1)/n		
Unit cell dimensions	$a = 15.8239(9)$ Å	$\alpha = 90^\circ$	
	$b = 10.6847(6)$ Å	$\beta =$	
	$c = 17.6997(9)$ Å	$\gamma = 90^\circ$	
Volume	$2689.6(3)$ Å ³		
Z	4		
Density (calculated)	1.413 Mg/m ³		
Absorption coefficient	0.770 mm ⁻¹		
F(000)	1184		
Crystal size	0.42 x 0.36 x 0.34 mm ³		
Theta range for data collection	1.44 to 30.50°		
Index ranges	-22<=h<=22, -15<=k<=15, -25<=l<=25		
Reflections collected	44442		
Independent reflections	8211 [R(int) = 0.0235]		
Completeness to theta = 30.50°	99.9 %		
Absorption correction	Sadabs		

Max. and min. transmission	0.7797 and 0.7379
Refinement method	Full-matrix least-squares on F^2
Data / restraints / parameters	8211 / 0 / 345
Goodness-of-fit on F^2	1.044
Final R indices [$ I > 2\text{sigma}(I)$]	R1 = 0.0235, wR2 = 0.0656
R indices (all data)	R1 = 0.0269, wR2 = 0.0695
Largest diff. peak and hole	0.674 and -0.847 e. \AA^{-3}

Table S2. Atomic coordinates ($\times 10^4$) and equivalent isotropic displacement parameters ($\text{\AA}^2 \times 10^3$). $U(\text{eq})$ is defined as one third of the trace of the orthogonalized U_{ij} tensor.

	x	y	z	$U(\text{eq})$
Pd(1)	9340(1)	2132(1)	1752(1)	16(1)
P(1)	10867(1)	865(1)	3362(1)	16(1)
N(1)	8861(1)	-751(1)	1526(1)	16(1)
C(1)	9396(1)	259(1)	1958(1)	16(1)
C(2)	10103(1)	-258(1)	2691(1)	17(1)
C(3)	9982(1)	-1584(1)	2697(1)	20(1)
C(4)	9204(1)	-1855(1)	1968(1)	19(1)
C(5)	10263(1)	2289(1)	3054(1)	22(1)
C(6A)	9312(2)	4079(3)	1362(2)	25(1)
C(7A)	8462(2)	3479(2)	870(1)	24(1)
C(6B)	8958(6)	4046(10)	1279(7)	28(2)
C(7B)	8903(5)	3334(6)	643(4)	25(1)
C(8)	8409(1)	2331(2)	435(1)	27(1)
C(9)	8009(1)	-677(1)	760(1)	16(1)
C(10)	7189(1)	-268(1)	799(1)	19(1)
C(11)	6370(1)	-178(2)	44(1)	24(1)
C(12)	6368(1)	-505(2)	-713(1)	26(1)
C(13)	7187(1)	-927(2)	-733(1)	23(1)
C(14)	8028(1)	-1012(1)	2(1)	18(1)

	x	y	z	U(eq)
C(15)	7162(1)	37(1)	1625(1)	22(1)
C(16)	6543(2)	-895(2)	1807(1)	35(1)
C(17)	6827(2)	1367(2)	1638(1)	35(1)
C(18)	8924(1)	-1448(1)	-31(1)	21(1)
C(19)	8960(1)	-2881(2)	-67(1)	32(1)
C(20)	9038(1)	-870(2)	-773(1)	33(1)
C(21)	11181(1)	377(1)	4433(1)	18(1)
C(22)	10934(1)	1097(1)	4962(1)	21(1)
C(23)	11088(1)	642(2)	5750(1)	24(1)
C(24)	11491(1)	-525(2)	6011(1)	24(1)
C(25)	11760(1)	-1238(2)	5496(1)	24(1)
C(26)	11609(1)	-785(1)	4710(1)	22(1)
C(27)	11951(1)	934(1)	3250(1)	18(1)
C(28)	12467(1)	2044(1)	3408(1)	23(1)
C(29)	13306(1)	2076(2)	3331(1)	27(1)
C(30)	13634(1)	1010(2)	3106(1)	27(1)
C(31)	13131(1)	-96(2)	2953(1)	27(1)
C(32)	12286(1)	-133(1)	3019(1)	23(1)

Table S3. Bond lengths [Å] and angles [°].

Pd(1)-C(1)	2.0302(13)	Pd(1)-C(5)	2.1268(15)
Pd(1)-C(7A)	2.1303(19)	Pd(1)-C(8)	2.1529(15)
Pd(1)-C(6A)	2.186(3)	Pd(1)-C(7B)	2.188(6)
Pd(1)-C(6B)	2.191(10)	P(1)-C(2)	1.7472(14)
P(1)-C(5)	1.7523(15)	P(1)-C(27)	1.8111(15)
P(1)-C(21)	1.8132(14)	N(1)-C(1)	1.3778(17)
N(1)-C(4)	1.3881(18)	N(1)-C(9)	1.4349(16)
C(1)-C(2)	1.4013(18)	C(2)-C(3)	1.4307(19)
C(3)-C(4)	1.3681(19)	C(6A)-C(7A)	1.398(3)

C(7A)-C(8)	1.431(3)	C(6B)-C(7B)	1.329(14)
C(7B)-C(8)	1.282(8)	C(9)-C(10)	1.3984(19)
C(9)-C(14)	1.4025(18)	C(10)-C(11)	1.399(2)
C(10)-C(15)	1.517(2)	C(11)-C(12)	1.383(2)
C(12)-C(13)	1.388(2)	C(13)-C(14)	1.3977(19)
C(14)-C(18)	1.518(2)	C(15)-C(17)	1.520(2)
C(15)-C(16)	1.527(2)	C(18)-C(20)	1.531(2)
C(18)-C(19)	1.535(2)	C(21)-C(22)	1.3935(19)
C(21)-C(26)	1.397(2)	C(22)-C(23)	1.394(2)
C(23)-C(24)	1.384(2)	C(24)-C(25)	1.391(2)
C(25)-C(26)	1.390(2)	C(27)-C(32)	1.393(2)
C(27)-C(28)	1.397(2)	C(28)-C(29)	1.394(2)
C(29)-C(30)	1.381(2)	C(30)-C(31)	1.384(2)
C(31)-C(32)	1.393(2)		
C(1)-Pd(1)-C(5)	85.85(5)	C(1)-Pd(1)-C(7A)	139.58(7)
C(5)-Pd(1)-C(7A)	131.22(7)	C(1)-Pd(1)-C(8)	104.31(6)
C(5)-Pd(1)-C(8)	169.83(6)	C(7A)-Pd(1)-C(8)	39.02(8)
C(1)-Pd(1)-C(6A)	171.25(10)	C(5)-Pd(1)-C(6A)	100.17(10)
C(7A)-Pd(1)-C(6A)	37.75(9)	C(8)-Pd(1)-C(6A)	69.81(10)
C(1)-Pd(1)-C(7B)	135.4(2)	C(5)-Pd(1)-C(7B)	136.3(2)
C(8)-Pd(1)-C(7B)	34.3(2)	C(1)-Pd(1)-C(6B)	166.4(3)
C(5)-Pd(1)-C(6B)	106.5(3)	C(8)-Pd(1)-C(6B)	63.3(3)
C(7B)-Pd(1)-C(6B)	35.3(4)	C(2)-P(1)-C(5)	105.32(7)
C(2)-P(1)-C(27)	111.13(6)	C(5)-P(1)-C(27)	110.15(7)
C(2)-P(1)-C(21)	107.70(6)	C(5)-P(1)-C(21)	115.85(7)
C(27)-P(1)-C(21)	106.72(6)	C(1)-N(1)-C(4)	111.05(11)
C(1)-N(1)-C(9)	125.16(11)	C(4)-N(1)-C(9)	123.53(11)
N(1)-C(1)-C(2)	104.61(11)	N(1)-C(1)-Pd(1)	134.78(10)
C(2)-C(1)-Pd(1)	120.60(10)	C(1)-C(2)-C(3)	110.02(12)
C(1)-C(2)-P(1)	113.10(10)	C(3)-C(2)-P(1)	136.85(11)
C(4)-C(3)-C(2)	105.68(12)	C(3)-C(4)-N(1)	108.63(12)
P(1)-C(5)-Pd(1)	106.86(7)	C(7A)-C(6A)-Pd(1)	68.94(15)

C(6A)-C(7A)-C(8)	122.8(2)	C(6A)-C(7A)-Pd(1)	73.30(15)
C(8)-C(7A)-Pd(1)	71.35(10)	C(7B)-C(6B)-Pd(1)	72.2(5)
C(8)-C(7B)-C(6B)	121.8(6)	C(8)-C(7B)-Pd(1)	71.3(3)
C(6B)-C(7B)-Pd(1)	72.4(5)	C(7B)-C(8)-Pd(1)	74.3(3)
C(7A)-C(8)-Pd(1)	69.64(10)	C(10)-C(9)-C(14)	122.46(12)
C(10)-C(9)-N(1)	118.61(12)	C(14)-C(9)-N(1)	118.93(12)
C(9)-C(10)-C(11)	117.72(13)	C(9)-C(10)-C(15)	122.25(12)
C(11)-C(10)-C(15)	120.00(13)	C(12)-C(11)-C(10)	121.09(14)
C(11)-C(12)-C(13)	120.05(14)	C(12)-C(13)-C(14)	121.08(14)
C(13)-C(14)-C(9)	117.58(13)	C(13)-C(14)-C(18)	120.55(13)
C(9)-C(14)-C(18)	121.87(12)	C(10)-C(15)-C(17)	111.85(13)
C(10)-C(15)-C(16)	110.80(13)	C(17)-C(15)-C(16)	110.31(14)
C(14)-C(18)-C(20)	111.90(13)	C(14)-C(18)-C(19)	111.10(12)
C(20)-C(18)-C(19)	110.23(13)	C(22)-C(21)-C(26)	119.35(13)
C(22)-C(21)-P(1)	121.00(11)	C(26)-C(21)-P(1)	119.44(10)
C(21)-C(22)-C(23)	120.15(14)	C(24)-C(23)-C(22)	120.11(14)
C(23)-C(24)-C(25)	120.16(14)	C(26)-C(25)-C(24)	119.84(14)
C(25)-C(26)-C(21)	120.36(13)	C(32)-C(27)-C(28)	119.30(14)
C(32)-C(27)-P(1)	119.97(11)	C(28)-C(27)-P(1)	120.72(11)
C(29)-C(28)-C(27)	119.95(14)	C(30)-C(29)-C(28)	120.23(15)
C(29)-C(30)-C(31)	120.25(15)	C(30)-C(31)-C(32)	119.92(15)
C(31)-C(32)-C(27)	120.34(15)		

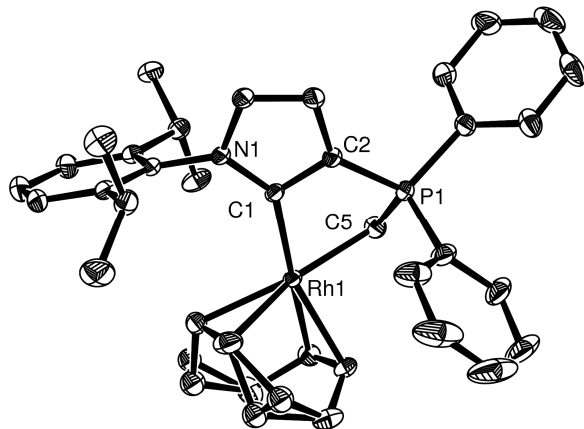


Table 1. Crystal data and structure refinement: Compound **10** chapter 2.

Empirical formula	C ₃₇ H ₄₃ N P Rh		
Formula weight	635.60		
Temperature	100(2) K		
Wavelength	0.71073 Å		
Crystal system	Monoclinic		
Space group	P2(1)/n		
Unit cell dimensions	a = 10.0764(9) Å	α= 90°	b = 19.8136(19) Å
	c = 15.5223(14) Å	β= 93.112(5)°	γ = 90°
Volume	3094.5(5) Å ³		
Z	4		
Density (calculated)	1.364 Mg/m ³		
Absorption coefficient	0.630 mm ⁻¹		
F(000)	1328		
Crystal size	0.20 x 0.15 x 0.11 mm ³		
Theta range for data collection	2.27 to 35.93°		
Index ranges	-16<=h<=16, -31<=k<=31, -25<=l<=25		
Reflections collected	86681		
Independent reflections	13588 [R(int) = 0.0452]		
Completeness to theta = 35.93°	93.1 %		

Absorption correction	None
Max. and min. transmission	0.9351 and 0.8839
Refinement method	Full-matrix least-squares on F^2
Data / restraints / parameters	13588 / 0 / 367
Goodness-of-fit on F^2	1.028
Final R indices [$ I > 2\text{sigma}(I)$]	$R_1 = 0.0317$, $wR_2 = 0.0753$
R indices (all data)	$R_1 = 0.0502$, $wR_2 = 0.0817$
Largest diff. peak and hole	0.880 and -0.567 e. \AA^{-3}

Table 2. Atomic coordinates ($\times 10^4$) and equivalent isotropic displacement parameters ($\text{\AA}^2 \times 10^3$). $U(\text{eq})$ is defined as one third of the trace of the orthogonalized U_{ij}^{ij} tensor.

	x	y	z	$U(\text{eq})$
Rh(1)	8495(1)	1646(1)	7353(1)	15(1)
P(1)	8178(1)	351(1)	8314(1)	18(1)
N(1)	5425(1)	1191(1)	6936(1)	15(1)
C(1)	6699(1)	1137(1)	7309(1)	15(1)
C(2)	6708(1)	502(1)	7710(1)	17(1)
C(3)	5446(1)	178(1)	7575(1)	19(1)
C(4)	4676(1)	624(1)	7104(1)	19(1)
C(5)	8745(1)	1164(1)	8574(1)	21(1)
C(6)	4870(1)	1781(1)	6529(1)	16(1)
C(7)	4616(1)	2342(1)	7044(1)	18(1)
C(8)	4094(2)	2917(1)	6630(1)	24(1)
C(9)	3818(2)	2928(1)	5750(1)	27(1)
C(10)	4051(2)	2361(1)	5257(1)	24(1)
C(11)	4585(1)	1777(1)	5634(1)	18(1)
C(12)	4819(2)	1156(1)	5093(1)	23(1)
C(13)	5499(2)	1326(1)	4263(1)	36(1)
C(14)	3517(2)	782(1)	4864(1)	32(1)
C(15)	4876(1)	2342(1)	8016(1)	20(1)

	x	y	z	U(eq)
C(16)	6094(2)	2770(1)	8286(1)	28(1)
C(17)	3655(2)	2588(1)	8474(1)	25(1)
C(18)	10259(1)	2263(1)	7599(1)	22(1)
C(19)	10231(2)	2905(1)	7073(1)	31(1)
C(20A)	8900(2)	3058(1)	6661(1)	24(1)
C(20B)	9189(7)	2873(4)	6268(5)	28(1)
C(21)	8108(2)	2412(1)	6386(1)	32(1)
C(22)	8550(2)	1840(1)	5990(1)	36(1)
C(23A)	9965(2)	1827(1)	5674(1)	26(1)
C(23B)	9870(7)	1422(4)	5709(4)	28(1)
C(24)	10962(2)	1529(1)	6340(1)	31(1)
C(25)	10612(1)	1646(1)	7261(1)	22(1)
C(26)	9416(2)	-48(1)	7688(1)	28(1)
C(27)	9113(2)	-183(1)	6821(1)	38(1)
C(28)	10099(3)	-416(1)	6300(2)	62(1)
C(29)	11358(3)	-508(1)	6628(3)	78(1)
C(30)	11673(2)	-382(1)	7485(3)	73(1)
C(31)	10704(2)	-152(1)	8038(2)	46(1)
C(32)	7833(1)	-199(1)	9206(1)	24(1)
C(33)	8406(2)	-832(1)	9344(1)	30(1)
C(34)	8069(2)	-1215(1)	10051(1)	39(1)
C(35)	7171(2)	-971(1)	10614(1)	44(1)
C(36)	6596(2)	-346(1)	10482(1)	45(1)
C(37)	6928(2)	43(1)	9779(1)	37(1)

Table 3. Bond lengths [Å] and angles [°] for rhcom plexypyrolle.

Rh(1)-C(1)	2.0698(13)	Rh(1)-C(22)	2.1542(16)
Rh(1)-C(5)	2.1250(14)	Rh(1)-C(21)	2.1553(16)
Rh(1)-C(25)	2.1449(14)	Rh(1)-C(18)	2.1729(14)

P(1)-C(2)	1.7359(13)	C(18)-C(19)	1.512(2)
P(1)-C(5)	1.7482(15)	C(19)-C(20A)	1.486(3)
P(1)-C(26)	1.8050(17)	C(19)-C(20B)	1.589(7)
P(1)-C(32)	1.8107(15)	C(20A)-C(21)	1.556(3)
N(1)-C(1)	1.3842(16)	C(20B)-C(21)	1.441(7)
N(1)-C(4)	1.3862(17)	C(21)-C(22)	1.375(3)
N(1)-C(6)	1.4280(17)	C(22)-C(23A)	1.532(3)
C(1)-C(2)	1.4045(19)	C(22)-C(23B)	1.645(7)
C(2)-C(3)	1.4286(18)	C(23A)-C(24)	1.522(3)
C(3)-C(4)	1.3617(19)	C(23B)-C(24)	1.450(7)
C(6)-C(7)	1.3998(19)	C(24)-C(25)	1.509(2)
C(6)-C(11)	1.4030(18)	C(26)-C(27)	1.389(3)
C(7)-C(8)	1.397(2)	C(26)-C(31)	1.395(2)
C(7)-C(15)	1.5180(19)	C(27)-C(28)	1.394(3)
C(8)-C(9)	1.378(2)	C(28)-C(29)	1.354(5)
C(9)-C(10)	1.386(2)	C(29)-C(30)	1.374(5)
C(10)-C(11)	1.392(2)	C(30)-C(31)	1.411(4)
C(11)-C(12)	1.516(2)	C(32)-C(33)	1.392(2)
C(12)-C(13)	1.530(2)	C(32)-C(37)	1.393(3)
C(12)-C(14)	1.531(2)	C(33)-C(34)	1.391(2)
C(15)-C(16)	1.533(2)	C(34)-C(35)	1.379(3)
C(15)-C(17)	1.533(2)	C(35)-C(36)	1.378(3)
C(18)-C(25)	1.383(2)	C(36)-C(37)	1.392(2)
C(1)-Rh(1)-C(5)	82.61(5)	C(22)-Rh(1)-C(21)	37.22(8)
C(1)-Rh(1)-C(25)	150.30(5)	C(1)-Rh(1)-C(18)	170.06(5)
C(5)-Rh(1)-C(25)	89.40(6)	C(5)-Rh(1)-C(18)	92.31(5)
C(1)-Rh(1)-C(22)	97.07(6)	C(25)-Rh(1)-C(18)	37.37(6)
C(5)-Rh(1)-C(22)	161.40(7)	C(22)-Rh(1)-C(18)	90.47(6)
C(25)-Rh(1)-C(22)	81.70(6)	C(21)-Rh(1)-C(18)	80.91(6)
C(1)-Rh(1)-C(21)	101.24(5)	C(2)-P(1)-C(5)	103.00(7)
C(5)-Rh(1)-C(21)	161.12(7)	C(2)-P(1)-C(26)	112.25(8)
C(25)-Rh(1)-C(21)	95.53(6)	C(5)-P(1)-C(26)	107.56(7)

C(2)-P(1)-C(32)	108.83(6)	C(25)-C(18)-C(19)	122.41(14)
C(5)-P(1)-C(32)	116.87(7)	C(25)-C(18)-Rh(1)	70.22(8)
C(26)-P(1)-C(32)	108.36(8)	C(19)-C(18)-Rh(1)	112.81(10)
C(1)-N(1)-C(4)	111.18(11)	C(20A)-C(19)-C(18)	113.18(15)
C(1)-N(1)-C(6)	125.42(11)	C(20A)-C(19)-C(20B)	29.2(3)
C(4)-N(1)-C(6)	122.90(11)	C(18)-C(19)-C(20B)	112.5(3)
N(1)-C(1)-C(2)	103.73(11)	C(19)-C(20A)-C(21)	112.84(16)
N(1)-C(1)-Rh(1)	140.04(10)	C(21)-C(20B)-C(19)	113.4(4)
C(2)-C(1)-Rh(1)	115.96(9)	C(22)-C(21)-C(20B)	101.5(3)
C(1)-C(2)-C(3)	110.67(11)	C(22)-C(21)-C(20A)	128.86(16)
C(1)-C(2)-P(1)	112.21(10)	C(20B)-C(21)-C(20A)	29.9(3)
C(3)-C(2)-P(1)	136.78(11)	C(22)-C(21)-Rh(1)	71.35(10)
C(4)-C(3)-C(2)	105.37(12)	C(20B)-C(21)-Rh(1)	115.2(3)
C(3)-C(4)-N(1)	109.02(11)	C(20A)-C(21)-Rh(1)	108.50(11)
P(1)-C(5)-Rh(1)	100.79(6)	C(21)-C(22)-C(23A)	119.03(18)
C(7)-C(6)-C(11)	122.33(12)	C(21)-C(22)-C(23B)	145.0(3)
C(7)-C(6)-N(1)	118.48(12)	C(23A)-C(22)-C(23B)	29.3(3)
C(11)-C(6)-N(1)	119.19(12)	C(21)-C(22)-Rh(1)	71.43(9)
C(8)-C(7)-C(6)	117.46(13)	C(23A)-C(22)-Rh(1)	112.66(12)
C(8)-C(7)-C(15)	119.82(13)	C(23B)-C(22)-Rh(1)	103.6(3)
C(6)-C(7)-C(15)	122.72(12)	C(24)-C(23A)-C(22)	112.37(16)
C(9)-C(8)-C(7)	121.25(14)	C(24)-C(23B)-C(22)	110.0(4)
C(8)-C(9)-C(10)	120.21(14)	C(23B)-C(24)-C(25)	117.1(3)
C(9)-C(10)-C(11)	120.95(13)	C(23B)-C(24)-C(23A)	31.5(3)
C(10)-C(11)-C(6)	117.77(13)	C(25)-C(24)-C(23A)	113.80(14)
C(10)-C(11)-C(12)	120.65(13)	C(18)-C(25)-C(24)	125.00(14)
C(6)-C(11)-C(12)	121.56(12)	C(18)-C(25)-Rh(1)	72.42(8)
C(11)-C(12)-C(13)	112.24(14)	C(24)-C(25)-Rh(1)	110.38(10)
C(11)-C(12)-C(14)	111.38(12)	C(27)-C(26)-C(31)	120.01(18)
C(13)-C(12)-C(14)	109.20(14)	C(27)-C(26)-P(1)	118.98(13)
C(7)-C(15)-C(16)	111.38(12)	C(31)-C(26)-P(1)	120.62(17)
C(7)-C(15)-C(17)	111.23(12)	C(26)-C(27)-C(28)	120.0(2)
C(16)-C(15)-C(17)	110.38(12)	C(29)-C(28)-C(27)	120.6(3)

C(28)-C(29)-C(30)	120.2(2)	C(34)-C(33)-C(32)	119.72(18)
C(29)-C(30)-C(31)	121.1(2)	C(35)-C(34)-C(33)	120.34(18)
C(26)-C(31)-C(30)	118.1(3)	C(36)-C(35)-C(34)	120.41(17)
C(33)-C(32)-C(37)	119.53(15)	C(35)-C(36)-C(37)	119.8(2)
C(33)-C(32)-P(1)	124.36(13)	C(36)-C(37)-C(32)	120.17(19)
C(37)-C(32)-P(1)	116.12(12)		

Symmetry transformations used to generate equivalent atoms:

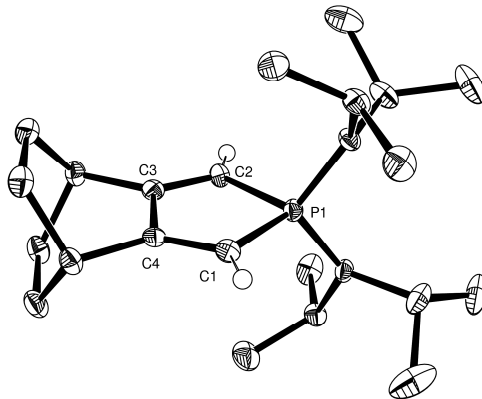


Table S1. Crystal data and structure refinement: Compound 4 Chapter 3.

Empirical formula	$C_{22}H_{40}N_2P$, CF_3SO_3	
Formula weight	512.60	
Temperature	100(2) K	
Wavelength	0.71073 Å	
Crystal system	Triclinic	
Space group	P-1	
Unit cell dimensions	$a = 9.564(2)$ Å	$\alpha = 110.245(5)^\circ$
	$b = 11.923(3)$ Å	$\beta = 93.188(4)^\circ$
	$c = 12.070(3)$ Å	$\gamma = 92.195(4)^\circ$
Volume	$1286.9(5)$ Å ³	
Z	2	
Density (calculated)	1.323 Mg/m ³	
Absorption coefficient	0.237 mm ⁻¹	
F(000)	548	
Crystal size	0.16 x 0.12 x 0.11 mm ³	
Theta range for data collection	1.80 to 26.91°	
Index ranges	-10≤h≤12, -15≤k≤15, -15≤l≤15	
Reflections collected	12739	
Independent reflections	5508 [R(int) = 0.0508]	
Completeness to theta = 26.91°	98.9 %	

Absorption correction	Sadabs
Max. and min. transmission	0.9744 and 0.9631
Refinement method	Full-matrix least-squares on F^2
Data / restraints / parameters	5508 / 0 / 306
Goodness-of-fit on F^2	1.052
Final R indices [$I > 2\sigma(I)$]	$R_1 = 0.0540$, $wR_2 = 0.1100$
R indices (all data)	$R_1 = 0.0899$, $wR_2 = 0.1276$
Largest diff. peak and hole	0.538 and -0.389 e. \AA^{-3}

Table S2. *Atomic coordinates ($x \times 10^4$) and equivalent isotropic displacement parameters ($\text{\AA}^2 \times 10^3$). $U(\text{eq})$ is defined as one third of the trace of the orthogonalized U_{ij} tensor.*

	x	y	z	$U(\text{eq})$
P(1)	2368(1)	7781(1)	2141(1)	14(1)
N(1)	4044(2)	8070(2)	2121(2)	15(1)
N(2)	1568(2)	7816(2)	923(2)	15(1)
C(1)	1987(2)	6478(2)	2513(2)	16(1)
C(2)	1322(2)	6834(2)	3516(2)	15(1)
C(3)	667(3)	6172(2)	4219(2)	18(1)
C(4)	-874(3)	6519(2)	4346(2)	22(1)
C(5)	-938(3)	7891(2)	4966(2)	21(1)
C(6)	555(3)	8504(2)	5219(2)	17(1)
C(7)	1385(3)	7988(2)	6038(2)	22(1)
C(8)	1443(3)	6616(2)	5464(2)	22(1)
C(9)	1206(2)	8158(2)	4060(2)	15(1)
C(10)	1651(2)	8787(2)	3415(2)	14(1)
C(11)	4430(3)	9302(2)	2134(3)	23(1)
C(12)	5416(3)	9285(3)	1187(3)	35(1)
C(13)	5021(3)	10117(3)	3357(3)	34(1)
C(14)	5209(3)	7358(2)	2356(2)	19(1)

	x	y	z	U(eq)
C(15)	5243(3)	6165(3)	1356(3)	27(1)
C(16)	5229(3)	7235(3)	3564(2)	25(1)
C(17)	2181(3)	7174(3)	-221(2)	24(1)
C(18)	2213(3)	7957(3)	-981(3)	36(1)
C(19)	1417(4)	5956(3)	-863(3)	44(1)
C(20)	78(2)	8143(2)	818(2)	19(1)
C(21)	-53(3)	9490(3)	1323(3)	27(1)
C(22)	-952(3)	7464(3)	1304(3)	30(1)
S(1)	2642(1)	2847(1)	1967(1)	24(1)
O(1)	2798(2)	3580(2)	1249(2)	37(1)
O(2)	3059(2)	1651(2)	1458(2)	44(1)
O(3)	1349(2)	2972(2)	2543(2)	39(1)
C(23)	3945(3)	3545(3)	3196(3)	27(1)
F(1)	3679(2)	4670(2)	3807(2)	41(1)
F(2)	5222(2)	3565(2)	2844(2)	62(1)
F(3)	3979(2)	2971(2)	3970(2)	51(1)

Table S3. Bond lengths [Å] and angles [°].

P(1)-N(1)	1.629(2)	P(1)-N(2)	1.633(2)
P(1)-C(10)	1.783(2)	P(1)-C(1)	1.791(3)
N(1)-C(11)	1.496(3)	N(1)-C(14)	1.499(3)
N(2)-C(17)	1.493(3)	N(2)-C(20)	1.502(3)
C(1)-C(2)	1.342(3)	C(2)-C(3)	1.490(3)
C(2)-C(9)	1.496(4)	C(3)-C(8)	1.544(4)
C(3)-C(4)	1.547(3)	C(4)-C(5)	1.551(4)
C(5)-C(6)	1.543(3)	C(6)-C(9)	1.494(3)
C(6)-C(7)	1.535(4)	C(7)-C(8)	1.544(4)
C(9)-C(10)	1.330(3)	C(11)-C(12)	1.517(4)
C(11)-C(13)	1.522(4)	C(14)-C(16)	1.514(4)

C(14)-C(15)	1.517(4)	C(17)-C(18)	1.519(4)
C(17)-C(19)	1.524(4)	C(20)-C(22)	1.517(4)
C(20)-C(21)	1.521(4)	S(1)-O(1)	1.437(2)
S(1)-O(2)	1.427(2)	S(1)-C(23)	1.818(3)
S(1)-O(3)	1.439(2)	C(23)-F(1)	1.331(3)
C(23)-F(2)	1.317(3)	C(23)-F(3)	1.336(3)
N(1)-P(1)-N(2)	108.93(11)	N(1)-P(1)-C(10)	112.22(11)
N(2)-P(1)-C(10)	111.20(11)	N(1)-P(1)-C(1)	112.91(11)
N(2)-P(1)-C(1)	116.37(11)	C(10)-P(1)-C(1)	94.64(12)
C(11)-N(1)-C(14)	117.28(19)	C(11)-N(1)-P(1)	114.53(16)
C(14)-N(1)-P(1)	126.72(17)	C(17)-N(2)-C(20)	115.4(2)
C(17)-N(2)-P(1)	118.05(17)	C(20)-N(2)-P(1)	124.35(16)
C(2)-C(1)-P(1)	107.17(19)	C(1)-C(2)-C(3)	132.8(2)
C(1)-C(2)-C(9)	115.0(2)	C(3)-C(2)-C(9)	112.1(2)
C(2)-C(3)-C(8)	107.7(2)	C(2)-C(3)-C(4)	107.3(2)
C(8)-C(3)-C(4)	108.4(2)	C(3)-C(4)-C(5)	110.6(2)
C(6)-C(5)-C(4)	110.2(2)	C(9)-C(6)-C(7)	108.7(2)
C(9)-C(6)-C(5)	106.7(2)	C(7)-C(6)-C(5)	107.7(2)
C(6)-C(7)-C(8)	111.1(2)	C(3)-C(8)-C(7)	110.1(2)
C(10)-C(9)-C(6)	132.6(2)	C(10)-C(9)-C(2)	114.9(2)
C(6)-C(9)-C(2)	112.4(2)	C(9)-C(10)-P(1)	107.96(19)
N(1)-C(11)-C(12)	112.1(2)	N(1)-C(11)-C(13)	111.3(2)
C(12)-C(11)-C(13)	111.8(2)	N(1)-C(14)-C(16)	113.8(2)
N(1)-C(14)-C(15)	111.2(2)	C(16)-C(14)-C(15)	113.0(2)
N(2)-C(17)-C(18)	110.3(2)	N(2)-C(17)-C(19)	111.5(2)
C(18)-C(17)-C(19)	112.5(3)	N(2)-C(20)-C(22)	113.5(2)
N(2)-C(20)-C(21)	111.9(2)	C(22)-C(20)-C(21)	112.4(2)
O(2)-S(1)-O(1)	115.27(14)	O(2)-S(1)-O(3)	115.57(14)
O(1)-S(1)-O(3)	114.17(13)	O(2)-S(1)-C(23)	103.97(13)
O(1)-S(1)-C(23)	102.63(13)	O(3)-S(1)-C(23)	102.76(13)
F(2)-C(23)-F(1)	107.2(3)	F(2)-C(23)-F(3)	106.9(2)
F(1)-C(23)-F(3)	106.1(2)	F(2)-C(23)-S(1)	112.4(2)

F(1)-C(23)-S(1)

111.99(19)

F(3)-C(23)-S(1)

111.9(2)

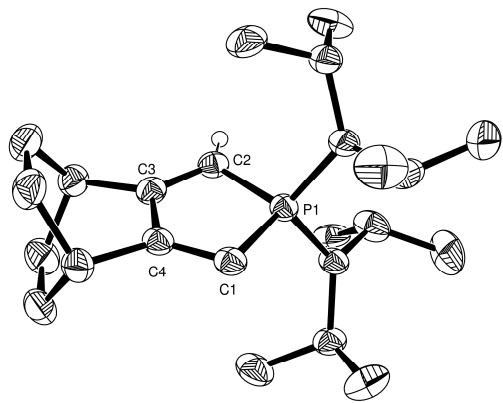


Table 1. Crystal data and structure refinement: Compound 5 Chapter 3.

Empirical formula	C ₂₂ H ₃₉ N ₂ P		
Formula weight	362.52		
Temperature	173(2) K		
Wavelength	0.71073 Å		
Crystal system	Monoclinic		
Space group	P2(1)/n		
Unit cell dimensions	a = 9.9789(2) Å	α= 90°	
	b = 12.7203(3) Å	β=	
100.8640(10)°.			
	c = 17.7730(4) Å	γ = 90°.	
Volume	2215.57(8) Å ³		
Z	4		
Density (calculated)	1.087 Mg/m ³		
Absorption coefficient	0.131 mm ⁻¹		
F(000)	800		
Crystal size	0.60 x 0.60 x 0.10 mm ³		
Theta range for data collection	5.14 to 26.37°		
Index ranges	-12<=h<=12, -15<=k<=14, -21<=l<=22		
Reflections collected	19683		
Independent reflections	4492 [R(int) = 0.0325]		
Completeness to theta = 26.37°	99.2 %		
Absorption correction	Semi-empirical		
Max. and min. transmission	0.9870 and 0.9254		

Refinement method	Full-matrix least-squares on F^2
Data / restraints / parameters	4492 / 234 / 316
Goodness-of-fit on F^2	1.024
Final R indices [$I > 2\text{sigma}(I)$]	$R_1 = 0.0418$, $wR_2 = 0.1059$
R indices (all data)	$R_1 = 0.0569$, $wR_2 = 0.1168$
Largest diff. peak and hole	0.338 and -0.231 e. \AA^{-3}

Table 2. Atomic coordinates ($\times 10^4$) and equivalent isotropic displacement parameters ($\text{\AA}^2 \times 10^3$)

for matt5m. $U(\text{eq})$ is defined as one third of the trace of the orthogonalized U^{ij} tensor.

	x	y	z	$U(\text{eq})$
P(1)	7968(1)	8634(1)	2192(1)	26(1)
C(1)	7396(1)	9747(1)	2654(1)	29(1)
C(2)	7269(2)	7566(1)	2649(1)	29(1)
C(3)	6665(1)	8070(1)	3159(1)	29(1)
C(4)	6696(1)	9256(1)	3137(1)	29(1)
C(5)	5901(2)	9715(1)	3702(1)	36(1)
C(6)	4439(2)	9273(2)	3512(1)	43(1)
C(7)	4456(2)	8062(2)	3585(1)	45(1)
C(8)	5936(2)	7654(1)	3765(1)	36(1)
C(9)	6649(2)	8125(2)	4536(1)	47(1)
C(10)	6577(2)	9337(2)	4508(1)	45(1)
N(1)	7430(1)	8593(1)	1246(1)	30(1)
C(11)	6179(7)	8039(8)	851(7)	35(1)
C(12)	6461(15)	6868(7)	785(8)	50(2)
C(13)	4915(8)	8235(12)	1204(6)	45(2)
C(11')	6080(18)	8120(20)	910(20)	37(3)
C(12')	6140(30)	6950(20)	790(20)	47(3)
C(13')	4880(20)	8520(30)	1236(17)	42(3)
C(14)	7770(30)	9580(20)	829(18)	40(3)

	x	y	z	U(eq)
C(15)	8250(30)	9270(20)	123(17)	56(4)
C(16)	6650(30)	10400(20)	742(18)	55(4)
C(14')	7974(11)	9405(9)	786(6)	40(1)
C(15')	8343(11)	8943(14)	55(6)	65(2)
C(16')	6991(13)	10337(8)	599(6)	54(2)
C(17)	10614(2)	9236(1)	2874(1)	35(1)
C(18)	10392(2)	9193(2)	3699(1)	49(1)
C(19)	10652(2)	10362(2)	2585(1)	52(1)
N(2)	9658(1)	8573(1)	2332(1)	30(1)
C(20)	10280(30)	7644(16)	2008(15)	43(3)
C(21)	11380(30)	8010(30)	1577(14)	59(4)
C(22)	10765(19)	6847(15)	2638(15)	39(3)
C(20')	10203(10)	7540(6)	2135(7)	41(1)
C(21')	11305(10)	7683(12)	1644(5)	56(2)
C(22')	10708(10)	6838(7)	2830(8)	50(2)

Table 3. Bond lengths [Å] and angles [°] for matt5m .

P(1)-N(2)	1.6595(12)	C(7)-C(8)	1.542(2)
P(1)-N(1)	1.6667(12)	C(8)-C(9)	1.541(2)
P(1)-C(1)	1.7831(15)	C(9)-C(10)	1.544(3)
P(1)-C(2)	1.7893(16)	N(1)-C(14')	1.483(10)
C(1)-C(4)	1.358(2)	N(1)-C(11)	1.490(6)
C(2)-C(3)	1.342(2)	N(1)-C(11')	1.495(14)
C(3)-C(8)	1.505(2)	N(1)-C(14)	1.53(3)
C(3)-C(4)	1.510(2)	C(11)-C(12)	1.524(6)
C(4)-C(5)	1.510(2)	C(11)-C(13)	1.531(6)
C(5)-C(6)	1.541(2)	C(11')-C(12')	1.509(14)
C(5)-C(10)	1.541(2)	C(11')-C(13')	1.522(14)
C(6)-C(7)	1.547(3)	C(14)-C(15)	1.48(2)

C(14)-C(16)	1.52(2)	N(2)-C(20')	1.489(6)
C(14')-C(15')	1.533(7)	N(2)-C(20)	1.498(14)
C(14')-C(16')	1.534(6)	C(20)-C(22)	1.520(13)
C(17)-N(2)	1.4851(19)	C(20)-C(21)	1.533(14)
C(17)-C(19)	1.524(2)	C(20')-C(22')	1.530(5)
C(17)-C(18)	1.525(2)	C(20')-C(21')	1.538(6)
N(2)-P(1)-N(1)	105.90(6)	C(11)-N(1)-C(11')	7.0(13)
N(2)-P(1)-C(1)	111.89(6)	C(14')-N(1)-C(14)	12.1(12)
N(1)-P(1)-C(1)	114.75(7)	C(11)-N(1)-C(14)	113.8(13)
N(2)-P(1)-C(2)	111.64(7)	C(11')-N(1)-C(14)	113.5(19)
N(1)-P(1)-C(2)	110.77(7)	C(14')-N(1)-P(1)	116.9(5)
C(1)-P(1)-C(2)	102.04(8)	C(11)-N(1)-P(1)	124.9(5)
C(4)-C(1)-P(1)	99.94(11)	C(11')-N(1)-P(1)	121.0(14)
C(3)-C(2)-P(1)	101.97(12)	C(14)-N(1)-P(1)	113.9(12)
C(2)-C(3)-C(8)	130.93(15)	N(1)-C(11)-C(12)	110.3(7)
C(2)-C(3)-C(4)	116.44(13)	N(1)-C(11)-C(13)	114.3(6)
C(8)-C(3)-C(4)	112.63(13)	C(12)-C(11)-C(13)	111.7(5)
C(1)-C(4)-C(3)	119.46(13)	N(1)-C(11')-C(12')	113.4(17)
C(1)-C(4)-C(5)	129.80(14)	N(1)-C(11')-C(13')	115.1(16)
C(3)-C(4)-C(5)	110.73(13)	C(12')-C(11')-C(13')	116.0(15)
C(4)-C(5)-C(6)	107.86(13)	C(15)-C(14)-C(16)	116.6(19)
C(4)-C(5)-C(10)	107.75(13)	C(15)-C(14)-N(1)	109.1(19)
C(6)-C(5)-C(10)	108.72(14)	C(16)-C(14)-N(1)	112.7(19)
C(5)-C(6)-C(7)	110.51(14)	N(1)-C(14')-C(15')	111.8(7)
C(8)-C(7)-C(6)	110.35(14)	N(1)-C(14')-C(16')	111.8(6)
C(3)-C(8)-C(9)	107.15(13)	C(15')-C(14')-C(16')	111.1(5)
C(3)-C(8)-C(7)	107.89(13)	N(2)-C(17)-C(19)	111.64(13)
C(9)-C(8)-C(7)	108.47(15)	N(2)-C(17)-C(18)	114.32(14)
C(8)-C(9)-C(10)	110.46(14)	C(19)-C(17)-C(18)	112.01(16)
C(5)-C(10)-C(9)	110.55(14)	C(17)-N(2)-C(20')	115.8(4)
C(14')-N(1)-C(11)	115.5(7)	C(17)-N(2)-C(20)	115.9(11)
C(14')-N(1)-C(11')	116.9(15)	C(20')-N(2)-C(20)	10.9(10)

C(17)-N(2)-P(1)	125.52(10)	C(22)-C(20)-C(21)	114.3(14)
C(20')-N(2)-P(1)	114.4(4)	N(2)-C(20')-C(22')	113.9(6)
C(20)-N(2)-P(1)	117.4(11)	N(2)-C(20')-C(21')	111.2(6)
N(2)-C(20)-C(22)	110.0(15)	C(22')-C(20')-C(21')	111.4(5)
N(2)-C(20)-C(21)	109.8(14)		

Symmetry transformations used to generate equivalent atoms:

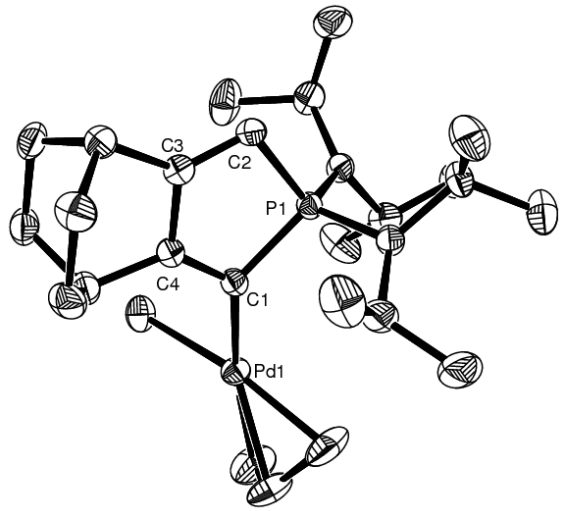


Table S1. Crystal data and structure refinement: Compound **6** Chapter 3.

Empirical formula	$C_{25}H_{39}ClN_2PPd$		
Formula weight	540.40		
Temperature	180(2) K		
Wavelength	0.71073 Å		
Crystal system	Monoclinic		
Space group	P2(1)/c		
Unit cell dimensions	$a = 11.480(3)$ Å	$\alpha = 90^\circ$	
	$b = 11.827(4)$ Å	$\beta = 91.796(4)^\circ$	
	$c = 19.574(6)$ Å	$\gamma = 90^\circ$	
Volume	2656.5(14) Å ³		
Z	4		
Density (calculated)	1.351 Mg/m ³		
Absorption coefficient	0.873 mm ⁻¹		
F(000)	1124		
Crystal size	0.38 x 0.17 x 0.13 mm ³		
Theta range for data collection	1.77 to 26.37°		
Index ranges	-14<=h<=14, -14<=k<=14, -22<=l<=24		
Reflections collected	19127		
Independent reflections	5410 [R(int) = 0.0455]		
Completeness to theta = 26.37°	99.4 %		

Absorption correction	Sadabs
Max. and min. transmission	0.8949 and 0.7326
Refinement method	Full-matrix least-squares on F2
Data / restraints / parameters	5410 / 0 / 288
Goodness-of-fit on F2	1.078
Final R indices [$I > 2\sigma(I)$]	$R_1 = 0.0369$, $wR_2 = 0.0981$
R indices (all data)	$R_1 = 0.0451$, $wR_2 = 0.1050$
Largest diff. peak and hole	0.630 and -0.744 e. \AA^{-3}

Table S2. *Atomic coordinates (x 104) and equivalent isotropic displacement parameters ($\text{\AA}^2 \times 103$). U(eq) is defined as one third of the trace of the orthogonalized U_{ij} tensor.*

	x	y	z	U(eq)
Pd(1)	7750(1)	5077(1)	1381(1)	25(1)
Cl(1)	7949(1)	4976(1)	2590(1)	34(1)
P(1)	7444(1)	2239(1)	998(1)	21(1)
N(1)	7394(2)	2238(2)	153(1)	25(1)
N(2)	8767(2)	1873(2)	1256(1)	25(1)
C(1)	6896(2)	3555(2)	1318(1)	22(1)
C(2)	6369(2)	1317(2)	1342(1)	24(1)
C(3)	5603(2)	2005(2)	1629(1)	23(1)
C(4)	5924(2)	3231(2)	1634(1)	22(1)
C(5)	5047(2)	3923(2)	2010(2)	28(1)
C(6)	4956(3)	3451(2)	2733(2)	35(1)
C(7)	4633(3)	2174(2)	2710(2)	34(1)
C(8)	4480(2)	1768(2)	1969(2)	27(1)
C(9)	3518(2)	2485(2)	1616(2)	36(1)
C(10)	3847(2)	3753(2)	1635(2)	37(1)
C(11)	9045(3)	1123(3)	1853(2)	33(1)
C(12)	8543(3)	1541(3)	2510(2)	49(1)

	x	y	z	U(eq)
C(13)	8748(3)	-113(2)	1715(2)	43(1)
C(14)	9758(2)	2561(2)	1002(2)	31(1)
C(15)	10292(3)	3345(3)	1554(2)	48(1)
C(16)	10685(3)	1814(3)	710(2)	39(1)
C(17)	6585(3)	3048(2)	-199(2)	35(1)
C(18)	5311(3)	2684(3)	-247(2)	53(1)
C(19)	7014(4)	3414(3)	-889(2)	54(1)
C(20)	7789(3)	1173(2)	-182(2)	30(1)
C(21)	6807(3)	405(3)	-450(2)	46(1)
C(22)	8687(3)	1372(3)	-727(2)	45(1)
C(23)	8725(4)	6693(3)	1287(2)	57(1)
C(24A)	7932(5)	6595(4)	789(3)	49(1)
C(24B)	8906(9)	6070(8)	748(6)	45(3)
C(25)	7889(4)	5568(3)	345(2)	53(1)

Table S3. Bond lengths [Å] and angles [°].

Pd(1)-C(1)	2.053(3)	Pd(1)-C(25)	2.120(4)
Pd(1)-C(24A)	2.150(5)	Pd(1)-C(24B)	2.186(9)
Pd(1)-C(23)	2.225(3)	Pd(1)-Cl(1)	2.3748(11)
P(1)-N(2)	1.643(2)	P(1)-N(1)	1.652(2)
P(1)-C(2)	1.794(3)	P(1)-C(1)	1.799(3)
N(1)-C(17)	1.488(3)	N(1)-C(20)	1.497(3)
N(2)-C(11)	1.494(3)	N(2)-C(14)	1.496(4)
C(1)-C(4)	1.349(4)	C(2)-C(3)	1.336(4)
C(3)-C(4)	1.495(3)	C(3)-C(8)	1.495(4)
C(4)-C(5)	1.508(4)	C(5)-C(6)	1.527(4)
C(5)-C(10)	1.554(4)	C(6)-C(7)	1.556(4)
C(7)-C(8)	1.533(4)	C(8)-C(9)	1.539(4)
C(9)-C(10)	1.546(4)	C(11)-C(12)	1.509(5)
C(11)-C(13)	1.524(4)	C(14)-C(16)	1.509(4)

C(14)-C(15)	1.536(4)	C(17)-C(19)	1.515(5)
C(17)-C(18)	1.524(5)	C(20)-C(22)	1.526(4)
C(20)-C(21)	1.527(4)	C(23)-C(24B)	1.310(12)
C(23)-C(24A)	1.318(6)	C(24A)-C(25)	1.494(7)
C(24B)-C(25)	1.510(11)		
C(1)-Pd(1)-C(25)	103.46(12)	C(1)-Pd(1)-C(24A)	139.00(16)
C(25)-Pd(1)-C(24A)	40.96(19)	C(1)-Pd(1)-C(24B)	137.3(3)
C(25)-Pd(1)-C(24B)	41.0(3)	C(24A)-Pd(1)-C(24B)	34.4(3)
C(1)-Pd(1)-C(23)	171.59(14)	C(25)-Pd(1)-C(23)	68.47(14)
C(24A)-Pd(1)-C(23)	35.01(17)	C(24B)-Pd(1)-C(23)	34.5(3)
C(1)-Pd(1)-Cl(1)	92.66(8)	C(25)-Pd(1)-Cl(1)	163.70(10)
C(24A)-Pd(1)-Cl(1)	124.84(16)	C(24B)-Pd(1)-Cl(1)	123.5(3)
C(23)-Pd(1)-Cl(1)	95.31(11)	N(2)-P(1)-N(1)	108.11(12)
N(2)-P(1)-C(2)	111.36(12)	N(1)-P(1)-C(2)	111.85(12)
N(2)-P(1)-C(1)	116.79(11)	N(1)-P(1)-C(1)	110.33(11)
C(2)-P(1)-C(1)	98.20(13)	C(17)-N(1)-C(20)	122.2(2)
C(17)-N(1)-P(1)	117.64(19)	C(20)-N(1)-P(1)	115.95(17)
C(11)-N(2)-C(14)	115.9(2)	C(11)-N(2)-P(1)	124.75(19)
C(14)-N(2)-P(1)	117.35(17)	C(4)-C(1)-P(1)	102.58(18)
C(4)-C(1)-Pd(1)	128.5(2)	P(1)-C(1)-Pd(1)	127.46(15)
C(3)-C(2)-P(1)	104.93(19)	C(2)-C(3)-C(4)	115.3(2)
C(2)-C(3)-C(8)	131.4(2)	C(4)-C(3)-C(8)	113.3(2)
C(1)-C(4)-C(3)	118.7(2)	C(1)-C(4)-C(5)	130.1(2)
C(3)-C(4)-C(5)	111.2(2)	C(4)-C(5)-C(6)	108.6(2)
C(4)-C(5)-C(10)	107.1(2)	C(6)-C(5)-C(10)	107.8(2)
C(5)-C(6)-C(7)	110.6(2)	C(8)-C(7)-C(6)	110.6(2)
C(3)-C(8)-C(7)	106.7(2)	C(3)-C(8)-C(9)	108.2(2)
C(7)-C(8)-C(9)	108.2(2)	C(8)-C(9)-C(10)	110.6(2)
C(9)-C(10)-C(5)	110.4(2)	N(2)-C(11)-C(12)	113.2(2)
N(2)-C(11)-C(13)	113.0(3)	C(12)-C(11)-C(13)	112.1(3)
N(2)-C(14)-C(16)	111.1(2)	N(2)-C(14)-C(15)	112.6(3)
C(16)-C(14)-C(15)	110.4(2)	N(1)-C(17)-C(19)	112.3(3)

N(1)-C(17)-C(18)	115.5(3)	C(19)-C(17)-C(18)	111.3(3)
N(1)-C(20)-C(22)	113.4(2)	N(1)-C(20)-C(21)	114.9(2)
C(22)-C(20)-C(21)	111.1(3)	C(24B)-C(23)-C(24A)	58.5(5)
C(24B)-C(23)-Pd(1)	71.1(4)	C(24A)-C(23)-Pd(1)	69.4(2)
C(23)-C(24A)-C(25)	120.7(5)	C(23)-C(24A)-Pd(1)	75.6(3)
C(25)-C(24A)-Pd(1)	68.5(2)	C(23)-C(24B)-C(25)	120.2(8)
C(23)-C(24B)-Pd(1)	74.4(5)	C(25)-C(24B)-Pd(1)	67.2(3)
C(24A)-C(25)-C(24B)	50.6(5)	C(24A)-C(25)-Pd(1)	70.6(2)
C(24B)-C(25)-Pd(1)	71.8(4)		

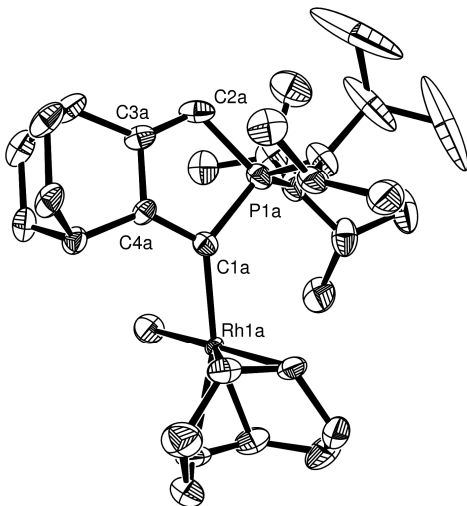


Table S1. Crystal data and structure refinement: Compound **6** Chapter 3.

Empirical formula	$C_{64}H_{106}Cl_{14}N_4P_2Rh_2$		
Formula weight	1695.59		
Temperature	100(2) K		
Wavelength	0.71073 Å		
Crystal system	Monoclinic		
Space group	P2(1)/c		
Unit cell dimensions	$a = 20.381(2)$ Å	$\alpha = 90^\circ$	
	$b = 18.0937(19)$ Å	$\beta = 113.5540(10)^\circ$	
	$c = 22.967(2)$ Å	$\gamma = 90^\circ$	
Volume	7763.7(14) Å ³		
Z	4		
Density (calculated)	1.451 Mg/m ³		
Absorption coefficient	0.988 mm ⁻¹		
F(000)	3504		
Crystal size	0.47 x 0.32 x 0.12 mm ³		
Theta range for data collection	7.60 to 21.03°		
Index ranges	-20<=h<=20, -18<=k<=18, -23<=l<=23		
Reflections collected	29337		
Independent reflections	7835 [R(int) = 0.0312]		
Completeness to theta =	21.03°		

Absorption correction	Sadabs
Max. and min. transmission	0.8907 and 0.6539
Refinement method	Full-matrix least-squares on F2
Data / restraints / parameters	7835 / 0 / 917
Goodness-of-fit on F2	1.068
Final R indices [$I > 2\sigma(I)$]	$R_1 = 0.0454$, $wR_2 = 0.1064$
R indices (all data)	$R_1 = 0.0474$, $wR_2 = 0.1079$
Largest diff. peak and hole	1.361 and -0.434 e. \AA^{-3}

Table S2. *Atomic coordinates (x 104) and equivalent isotropic displacement parameters ($\text{\AA}^2 \times 103$). U(eq) is defined as one third of the trace of the orthogonalized U_{ij} tensor.*

	x	y	z	U(eq)
Rh(1A)	4166(2)	7268(2)	1521(1)	14(1)
Rh(1C)	4223(7)	7397(7)	1468(7)	57(4)
Cl(1A)	3750(1)	6024(1)	1328(1)	38(1)
P(1A)	5306(1)	6744(1)	3057(1)	28(1)
N(1A)	5681(2)	7508(3)	3449(2)	39(1)
N(2A)	4658(2)	6498(2)	3274(2)	34(1)
C(1A)	5079(2)	6867(3)	2220(2)	23(1)
C(2A)	5948(3)	6018(3)	3194(3)	33(1)
C(3A)	6037(2)	5947(3)	2649(2)	26(1)
C(4A)	5538(2)	6404(3)	2107(2)	22(1)
C(5A)	5629(3)	6242(3)	1503(2)	29(1)
C(6A)	6412(3)	6430(3)	1617(3)	36(1)
C(7A)	6934(3)	5979(3)	2182(3)	40(1)
C(8A)	6520(3)	5474(3)	2455(3)	37(1)
C(9A)	6047(3)	4960(3)	1927(3)	42(2)
C(10A)	5508(3)	5411(3)	1369(3)	37(1)
C(11A)	6014(3)	8036(3)	3149(3)	35(1)
C(12A)	5987(3)	8825(3)	3348(3)	53(2)

	x	y	z	U(eq)
C(13A)	6768(3)	7834(3)	3217(3)	45(2)
C(14A)	5893(5)	7472(6)	4147(3)	95(3)
C(15A)	5618(8)	8096(8)	4407(6)	169(7)
C(16A)	6685(6)	7342(11)	4512(4)	173(8)
C(17A)	4532(3)	5734(3)	3465(3)	42(1)
C(18A)	4487(3)	5150(3)	2988(3)	44(2)
C(19A)	5045(4)	5543(4)	4133(3)	64(2)
C(20A)	4079(3)	7046(3)	3183(3)	43(2)
C(21A)	3371(3)	6838(4)	2627(3)	51(2)
C(22A)	3951(4)	7152(4)	3786(3)	66(2)
C(23A)	4713(3)	8170(3)	1348(3)	35(1)
C(24A)	4435(3)	8305(4)	637(3)	52(2)
C(25A)	3636(3)	8187(4)	299(3)	49(2)
C(26A)	3356(3)	7602(3)	588(3)	40(2)
C(27A)	3084(3)	7705(4)	1038(3)	46(2)
C(28A)	3051(4)	8429(4)	1348(4)	63(2)
C(29A)	3718(3)	8889(4)	1526(3)	55(2)
C(30A)	4388(3)	8413(3)	1740(3)	37(1)
Rh(1B)	766(1)	2508(1)	3580(1)	16(1)
Rh(1D)	788(7)	2617(6)	3508(6)	65(4)
P(1B)	-258(1)	3021(1)	1984(1)	24(1)
Cl(1B)	1296(1)	3736(1)	3790(1)	44(1)
N(1B)	-630(2)	2245(2)	1607(2)	29(1)
N(2B)	427(2)	3210(2)	1805(2)	32(1)
C(1B)	-79(2)	2968(3)	2815(2)	23(1)
C(2B)	-893(3)	3769(3)	1784(2)	27(1)
C(3B)	-1002(2)	3899(3)	2309(2)	25(1)
C(4B)	-522(2)	3480(2)	2888(2)	21(1)
C(5B)	-622(3)	3725(3)	3470(2)	31(1)
C(6B)	-1403(3)	3566(3)	3365(3)	43(2)

	x	y	z	U(eq)
C(7B)	-1921(3)	3951(3)	2753(3)	38(1)
C(8B)	-1499(3)	4407(3)	2453(3)	32(1)
C(9B)	-1025(3)	4973(3)	2954(3)	40(1)
C(10B)	-491(3)	4562(3)	3538(3)	41(1)
C(11B)	-1053(3)	1794(3)	1882(2)	32(1)
C(12B)	-1072(3)	973(3)	1725(3)	44(2)
C(13B)	-1802(3)	2075(3)	1747(3)	41(1)
C(14B)	-760(3)	2194(3)	926(3)	45(2)
C(15B)	-1528(4)	2293(4)	469(3)	56(2)
C(16B)	-429(4)	1502(4)	763(3)	63(2)
C(17B)	607(3)	3953(3)	1641(3)	42(1)
C(18B)	642(3)	4557(3)	2106(3)	45(2)
C(19B)	150(4)	4159(4)	960(3)	51(2)
C(20B)	1008(3)	2633(3)	1951(3)	41(1)
C(21B)	1186(3)	2489(4)	1378(3)	55(2)
C(22B)	1682(3)	2819(4)	2530(3)	51(2)
C(23B)	528(4)	1416(3)	3301(3)	58(2)
C(24B)	1187(6)	923(6)	3551(5)	151(6)
C(25B)	1830(4)	1242(4)	3936(5)	80(2)
C(26B)	1783(3)	2006(4)	4182(3)	57(2)
C(27B)	1426(3)	2185(4)	4553(3)	54(2)
C(28B)	1024(5)	1648(4)	4788(3)	69(2)
C(29B)	354(6)	1442(8)	4344(4)	136(5)
C(30B)	160(4)	1644(4)	3656(3)	53(2)
C(29)	3530(3)	5737(3)	9818(3)	47(2)
Cl(1E)	4314(3)	6108(2)	9766(2)	36(1)
Cl(2E)	2765(4)	6013(6)	9139(4)	102(3)
Cl(3E)	3621(3)	4759(3)	9872(2)	42(1)
Cl(1F)	4309(9)	6009(10)	9791(7)	147(7)
Cl(2F)	2836(8)	6133(9)	9222(7)	142(7)

	x	y	z	U(eq)
Cl(3F)	3411(11)	4837(9)	9735(9)	173(8)
C(30)	1619(3)	4372(3)	5236(3)	44(2)
Cl(1C)	1462(3)	5610(3)	281(2)	96(1)
Cl(2C)	1683(2)	6074(2)	1524(2)	61(1)
Cl(3C)	2170(2)	4648(2)	1321(2)	45(1)
Cl(1D)	1853(5)	5516(6)	203(4)	118(3)
Cl(2D)	1522(4)	6272(5)	1143(5)	106(3)
Cl(3D)	2269(6)	4968(11)	1677(13)	276(13)
C(31)	2900(3)	4352(4)	3805(3)	52(2)
Cl(7A)	2683(2)	4736(2)	3023(2)	36(1)
Cl(8A)	3305(3)	5065(3)	4362(2)	67(1)
Cl(9A)	3517(4)	3630(4)	3927(3)	61(2)
Cl(7B)	2709(7)	4867(12)	3230(13)	279(14)
Cl(9B)	3499(10)	3675(10)	3870(10)	137(8)
Cl(8B)	3110(7)	4862(12)	4476(12)	287(15)
C(32)	2075(3)	5591(3)	1077(3)	51(2)
Cl(4C)	2052(3)	5191(2)	5116(2)	92(2)
Cl(5C)	2154(2)	4207(3)	6068(2)	70(1)
Cl(6C)	761(2)	4524(3)	5097(2)	73(1)
Cl(4D)	1611(8)	5270(4)	5190(5)	149(5)
Cl(5D)	2175(4)	3810(5)	5834(3)	95(2)
Cl(6D)	722(3)	4085(4)	5204(3)	55(2)

Table S3. Bond lengths [Å] and angles [°].

Rh(1A)-C(1A)	2.045(5)	Rh(1A)-C(23A)	2.101(6)
Rh(1A)-C(30A)	2.137(6)	Rh(1A)-C(27A)	2.182(6)
Rh(1A)-C(26A)	2.203(6)	Rh(1A)-Cl(1A)	2.383(3)
Rh(1C)-C(23A)	1.802(14)	Rh(1C)-C(30A)	1.928(15)
Rh(1C)-C(26A)	2.119(15)	Rh(1C)-C(1A)	2.130(15)

Rh(1C)-C(27A)	2.201(15)	Rh(1C)-Cl(1A)	2.637(13)
P(1A)-N(2A)	1.647(4)	P(1A)-N(1A)	1.661(5)
P(1A)-C(2A)	1.791(5)	P(1A)-C(1A)	1.801(5)
N(1A)-C(14A)	1.486(9)	N(1A)-C(11A)	1.491(7)
N(2A)-C(20A)	1.491(7)	N(2A)-C(17A)	1.503(7)
C(1A)-C(4A)	1.358(7)	C(2A)-C(3A)	1.341(8)
C(3A)-C(8A)	1.499(7)	C(3A)-C(4A)	1.501(7)
C(4A)-C(5A)	1.498(7)	C(5A)-C(10A)	1.535(8)
C(5A)-C(6A)	1.549(7)	C(6A)-C(7A)	1.542(8)
C(7A)-C(8A)	1.536(8)	C(8A)-C(9A)	1.525(9)
C(9A)-C(10A)	1.546(8)	C(11A)-C(12A)	1.507(8)
C(11A)-C(13A)	1.525(8)	C(14A)-C(15A)	1.486(18)
C(14A)-C(16A)	1.511(16)	C(17A)-C(18A)	1.498(9)
C(17A)-C(19A)	1.510(9)	C(20A)-C(22A)	1.521(9)
C(20A)-C(21A)	1.543(9)	C(23A)-C(30A)	1.386(8)
C(23A)-C(24A)	1.520(8)	C(24A)-C(25A)	1.514(9)
C(25A)-C(26A)	1.479(9)	C(26A)-C(27A)	1.366(9)
C(27A)-C(28A)	1.505(10)	C(28A)-C(29A)	1.505(10)
C(29A)-C(30A)	1.520(8)		
Rh(1B)-C(30B)	2.043(6)	Rh(1B)-C(23B)	2.073(6)
Rh(1B)-C(1B)	2.080(5)	Rh(1B)-C(27B)	2.177(6)
Rh(1B)-C(26B)	2.179(6)	Rh(1B)-Cl(1B)	2.433(3)
Rh(1D)-C(1B)	1.952(14)	Rh(1D)-C(23B)	2.242(13)
Rh(1D)-Cl(1B)	2.248(12)	Rh(1D)-C(30B)	2.280(14)
Rh(1D)-C(26B)	2.286(14)	Rh(1D)-C(27B)	2.359(14)
P(1B)-N(2B)	1.642(4)	P(1B)-N(1B)	1.665(4)
P(1B)-C(1B)	1.796(5)	P(1B)-C(2B)	1.801(5)
N(1B)-C(14B)	1.480(7)	N(1B)-C(11B)	1.499(7)
N(2B)-C(17B)	1.481(7)	N(2B)-C(20B)	1.511(7)
C(1B)-C(4B)	1.351(7)	C(2B)-C(3B)	1.332(7)
C(3B)-C(8B)	1.499(7)	C(3B)-C(4B)	1.503(7)
C(4B)-C(5B)	1.498(7)	C(5B)-C(10B)	1.535(8)
C(5B)-C(6B)	1.538(8)	C(6B)-C(7B)	1.546(8)

C(7B)-C(8B)	1.538(8)	C(8B)-C(9B)	1.555(8)
C(9B)-C(10B)	1.540(8)	C(11B)-C(13B)	1.518(8)
C(11B)-C(12B)	1.525(8)	C(14B)-C(15B)	1.507(9)
C(14B)-C(16B)	1.538(9)	C(17B)-C(18B)	1.509(8)
C(17B)-C(19B)	1.513(9)	C(20B)-C(22B)	1.521(8)
C(20B)-C(21B)	1.522(9)	C(23B)-C(30B)	1.373(10)
C(23B)-C(24B)	1.520(10)	C(24B)-C(25B)	1.382(13)
C(25B)-C(26B)	1.511(11)	C(26B)-C(27B)	1.363(10)
C(27B)-C(28B)	1.505(11)	C(28B)-C(29B)	1.389(11)
C(29B)-C(30B)	1.512(11)		
C(29)-Cl(3F)	1.645(18)	C(29)-Cl(2F)	1.685(14)
C(29)-Cl(1F)	1.687(18)	C(29)-Cl(3E)	1.777(8)
C(29)-Cl(2E)	1.780(10)	C(29)-Cl(1E)	1.780(8)
C(30)-Cl(4D)	1.627(10)	C(30)-Cl(6C)	1.670(7)
C(30)-Cl(5D)	1.721(8)	C(30)-Cl(4C)	1.800(7)
C(30)-Cl(5C)	1.806(7)	C(30)-Cl(6D)	1.875(9)
Cl(1C)-C(32)	1.754(8)	Cl(2C)-C(32)	1.764(8)
Cl(3C)-C(32)	1.782(7)	Cl(1D)-C(32)	1.879(12)
Cl(2D)-C(32)	1.718(11)	Cl(3D)-C(32)	1.700(16)
C(31)-Cl(7B)	1.533(18)	C(31)-Cl(9B)	1.69(2)
C(31)-Cl(8B)	1.697(18)	C(31)-Cl(9A)	1.757(9)
C(31)-Cl(8A)	1.771(8)	C(31)-Cl(7A)	1.807(8)

C(1A)-Rh(1A)-C(23A)	92.2(2)	C(1A)-Rh(1A)-C(30A)	96.8(2)
C(23A)-Rh(1A)-C(30A)	38.2(2)	C(1A)-Rh(1A)-C(27A)	161.0(3)
C(23A)-Rh(1A)-C(27A)	97.3(3)	C(30A)-Rh(1A)-C(27A)	81.0(2)
C(1A)-Rh(1A)-C(26A)	162.6(3)	C(23A)-Rh(1A)-C(26A)	81.5(2)
C(30A)-Rh(1A)-C(26A)	88.2(2)	C(27A)-Rh(1A)-C(26A)	36.3(2)
C(1A)-Rh(1A)-Cl(1A)	87.43(16)	C(23A)-Rh(1A)-Cl(1A)	151.0(2)
C(30A)-Rh(1A)-Cl(1A)	170.1(2)	C(27A)-Rh(1A)-Cl(1A)	92.1(2)
C(26A)-Rh(1A)-Cl(1A)	90.33(18)	C(23A)-Rh(1C)-C(30A)	43.5(4)
C(23A)-Rh(1C)-C(26A)	91.2(6)	C(30A)-Rh(1C)-C(26A)	96.5(6)
C(23A)-Rh(1C)-C(1A)	98.6(7)	C(30A)-Rh(1C)-C(1A)	100.7(7)

C(26A)-Rh(1C)-C(1A)	162.3(7)	C(23A)-Rh(1C)-C(27A)	106.5(6)
C(30A)-Rh(1C)-C(27A)	85.4(5)	C(26A)-Rh(1C)-C(27A)	36.8(3)
C(1A)-Rh(1C)-C(27A)	148.5(7)	C(23A)-Rh(1C)-Cl(1A)	155.6(7)
C(30A)-Rh(1C)-Cl(1A)	161.0(7)	C(26A)-Rh(1C)-Cl(1A)	85.6(5)
C(1A)-Rh(1C)-Cl(1A)	79.4(4)	C(27A)-Rh(1C)-Cl(1A)	85.1(5)
N(2A)-P(1A)-N(1A)	108.1(2)	N(2A)-P(1A)-C(2A)	111.5(2)
N(1A)-P(1A)-C(2A)	111.7(2)	N(2A)-P(1A)-C(1A)	117.4(2)
N(1A)-P(1A)-C(1A)	110.0(2)	C(2A)-P(1A)-C(1A)	97.9(2)
C(14A)-N(1A)-C(11A)	122.6(5)	C(14A)-N(1A)-P(1A)	114.9(5)
C(11A)-N(1A)-P(1A)	118.6(3)	C(20A)-N(2A)-C(17A)	115.7(4)
C(20A)-N(2A)-P(1A)	117.6(4)	C(17A)-N(2A)-P(1A)	126.0(4)
C(4A)-C(1A)-P(1A)	103.0(3)	C(4A)-C(1A)-Rh(1A)	123.3(4)
P(1A)-C(1A)-Rh(1A)	130.4(3)	C(4A)-C(1A)-Rh(1C)	121.7(5)
P(1A)-C(1A)-Rh(1C)	134.4(4)	C(3A)-C(2A)-P(1A)	105.5(4)
C(2A)-C(3A)-C(8A)	133.0(5)	C(2A)-C(3A)-C(4A)	115.0(4)
C(8A)-C(3A)-C(4A)	112.0(4)	C(1A)-C(4A)-C(5A)	130.4(4)
C(1A)-C(4A)-C(3A)	118.1(4)	C(5A)-C(4A)-C(3A)	111.5(4)
C(4A)-C(5A)-C(10A)	108.0(4)	C(4A)-C(5A)-C(6A)	107.4(4)
C(10A)-C(5A)-C(6A)	108.7(4)	C(7A)-C(6A)-C(5A)	110.1(4)
C(8A)-C(7A)-C(6A)	110.5(4)	C(3A)-C(8A)-C(9A)	107.6(4)
C(3A)-C(8A)-C(7A)	108.3(4)	C(9A)-C(8A)-C(7A)	108.4(5)
C(8A)-C(9A)-C(10A)	110.6(4)	C(5A)-C(10A)-C(9A)	110.2(4)
N(1A)-C(11A)-C(12A)	112.9(5)	N(1A)-C(11A)-C(13A)	115.1(4)
C(12A)-C(11A)-C(13A)	110.7(5)	N(1A)-C(14A)-C(15A)	113.9(10)
N(1A)-C(14A)-C(16A)	112.9(7)	C(15A)-C(14A)-C(16A)	112.7(10)
C(18A)-C(17A)-N(2A)	113.7(4)	C(18A)-C(17A)-C(19A)	113.4(6)
N(2A)-C(17A)-C(19A)	112.1(5)	N(2A)-C(20A)-C(22A)	111.8(5)
N(2A)-C(20A)-C(21A)	112.3(5)	C(22A)-C(20A)-C(21A)	109.9(5)
C(30A)-C(23A)-C(24A)	125.3(5)	C(30A)-C(23A)-Rh(1C)	73.1(6)
C(24A)-C(23A)-Rh(1C)	107.3(6)	C(30A)-C(23A)-Rh(1A)	72.3(3)
C(24A)-C(23A)-Rh(1A)	109.2(4)	C(25A)-C(24A)-C(23A)	113.0(5)
C(26A)-C(25A)-C(24A)	113.5(5)	C(27A)-C(26A)-C(25A)	125.9(6)
C(27A)-C(26A)-Rh(1C)	74.8(5)	C(25A)-C(26A)-Rh(1C)	103.3(5)

C(27A)-C(26A)-Rh(1A)	71.0(3)	C(25A)-C(26A)-Rh(1A)	111.1(4)
C(26A)-C(27A)-C(28A)	125.9(6)	C(26A)-C(27A)-Rh(1A)	72.7(3)
C(28A)-C(27A)-Rh(1A)	107.6(4)	C(26A)-C(27A)-Rh(1C)	68.3(5)
C(28A)-C(27A)-Rh(1C)	104.3(5)	C(29A)-C(28A)-C(27A)	113.8(5)
C(28A)-C(29A)-C(30A)	111.8(5)	C(23A)-C(30A)-C(29A)	124.8(5)
C(23A)-C(30A)-Rh(1C)	63.4(5)	C(29A)-C(30A)-Rh(1C)	114.7(6)
C(23A)-C(30A)-Rh(1A)	69.5(3)	C(29A)-C(30A)-Rh(1A)	113.3(4)
C(30B)-Rh(1B)-C(23B)	39.0(3)	C(30B)-Rh(1B)-C(1B)	93.1(2)
C(23B)-Rh(1B)-C(1B)	96.2(2)	C(30B)-Rh(1B)-C(27B)	81.6(3)
C(23B)-Rh(1B)-C(27B)	91.9(3)	C(1B)-Rh(1B)-C(27B)	159.6(3)
C(30B)-Rh(1B)-C(26B)	94.6(3)	C(23B)-Rh(1B)-C(26B)	81.0(3)
C(1B)-Rh(1B)-C(26B)	163.7(3)	C(27B)-Rh(1B)-C(26B)	36.5(3)
C(30B)-Rh(1B)-Cl(1B)	156.6(3)	C(23B)-Rh(1B)-Cl(1B)	164.1(3)
C(1B)-Rh(1B)-Cl(1B)	87.40(15)	C(27B)-Rh(1B)-Cl(1B)	89.9(2)
C(26B)-Rh(1B)-Cl(1B)	91.2(2)	C(1B)-Rh(1D)-C(23B)	94.7(5)
C(1B)-Rh(1D)-Cl(1B)	96.0(5)	C(23B)-Rh(1D)-Cl(1B)	167.5(6)
C(1B)-Rh(1D)-C(30B)	89.7(5)	C(23B)-Rh(1D)-C(30B)	35.4(3)
Cl(1B)-Rh(1D)-C(30B)	150.9(6)	C(1B)-Rh(1D)-C(26B)	168.1(7)
C(23B)-Rh(1D)-C(26B)	75.2(4)	Cl(1B)-Rh(1D)-C(26B)	93.3(5)
C(30B)-Rh(1D)-C(26B)	85.7(5)	C(1B)-Rh(1D)-C(27B)	152.7(7)
C(23B)-Rh(1D)-C(27B)	83.2(5)	Cl(1B)-Rh(1D)-C(27B)	90.1(5)
C(30B)-Rh(1D)-C(27B)	73.0(4)	C(26B)-Rh(1D)-C(27B)	34.1(3)
N(2B)-P(1B)-N(1B)	107.5(2)	N(2B)-P(1B)-C(1B)	116.4(2)
N(1B)-P(1B)-C(1B)	111.4(2)	N(2B)-P(1B)-C(2B)	112.1(2)
N(1B)-P(1B)-C(2B)	111.7(2)	C(1B)-P(1B)-C(2B)	97.6(2)
C(14B)-N(1B)-C(11B)	121.4(4)	C(14B)-N(1B)-P(1B)	117.1(3)
C(11B)-N(1B)-P(1B)	117.3(3)	C(17B)-N(2B)-C(20B)	115.6(4)
C(17B)-N(2B)-P(1B)	125.0(4)	C(20B)-N(2B)-P(1B)	118.0(4)
C(4B)-C(1B)-P(1B)	103.5(3)	C(4B)-C(1B)-Rh(1D)	123.6(5)
P(1B)-C(1B)-Rh(1D)	128.1(4)	C(4B)-C(1B)-Rh(1B)	122.6(4)
P(1B)-C(1B)-Rh(1B)	131.8(3)	C(3B)-C(2B)-P(1B)	105.4(4)
C(2B)-C(3B)-C(8B)	132.9(5)	C(2B)-C(3B)-C(4B)	115.2(4)
C(8B)-C(3B)-C(4B)	111.9(4)	C(1B)-C(4B)-C(5B)	130.5(4)

C(1B)-C(4B)-C(3B)	117.9(4)	C(5B)-C(4B)-C(3B)	111.6(4)
C(4B)-C(5B)-C(10B)	107.6(4)	C(4B)-C(5B)-C(6B)	107.7(4)
C(10B)-C(5B)-C(6B)	109.2(4)	C(5B)-C(6B)-C(7B)	110.3(4)
C(8B)-C(7B)-C(6B)	110.4(4)	C(3B)-C(8B)-C(7B)	108.6(4)
C(3B)-C(8B)-C(9B)	106.9(4)	C(7B)-C(8B)-C(9B)	108.4(5)
C(10B)-C(9B)-C(8B)	109.9(4)	C(5B)-C(10B)-C(9B)	110.8(5)
N(1B)-C(11B)-C(13B)	115.6(4)	N(1B)-C(11B)-C(12B)	113.3(4)
C(13B)-C(11B)-C(12B)	110.5(4)	N(1B)-C(14B)-C(15B)	115.3(5)
N(1B)-C(14B)-C(16B)	113.4(5)	C(15B)-C(14B)-C(16B)	111.2(5)
N(2B)-C(17B)-C(18B)	115.1(4)	N(2B)-C(17B)-C(19B)	112.0(5)
C(18B)-C(17B)-C(19B)	112.8(5)	N(2B)-C(20B)-C(22B)	113.3(5)
N(2B)-C(20B)-C(21B)	111.3(5)	C(22B)-C(20B)-C(21B)	110.5(5)
C(30B)-C(23B)-C(24B)	124.2(8)	C(30B)-C(23B)-Rh(1B)	69.3(3)
C(24B)-C(23B)-Rh(1B)	112.4(5)	C(30B)-C(23B)-Rh(1D)	73.9(5)
C(24B)-C(23B)-Rh(1D)	113.0(6)	C(25B)-C(24B)-C(23B)	117.8(7)
C(24B)-C(25B)-C(26B)	115.8(6)	C(27B)-C(26B)-C(25B)	125.5(7)
C(27B)-C(26B)-Rh(1B)	71.7(4)	C(25B)-C(26B)-Rh(1B)	109.3(5)
C(27B)-C(26B)-Rh(1D)	75.9(5)	C(25B)-C(26B)-Rh(1D)	111.2(5)
C(26B)-C(27B)-C(28B)	125.1(6)	C(26B)-C(27B)-Rh(1B)	71.8(4)
C(28B)-C(27B)-Rh(1B)	109.9(4)	C(26B)-C(27B)-Rh(1D)	70.0(5)
C(28B)-C(27B)-Rh(1D)	114.9(5)	C(29B)-C(28B)-C(27B)	115.2(6)
C(28B)-C(29B)-C(30B)	118.2(7)	C(23B)-C(30B)-C(29B)	124.8(8)
C(23B)-C(30B)-Rh(1B)	71.7(4)	C(29B)-C(30B)-Rh(1B)	111.1(5)
C(23B)-C(30B)-Rh(1D)	70.8(5)	C(29B)-C(30B)-Rh(1D)	114.5(6)
Cl(3F)-C(29)-Cl(2F)	106.8(10)	Cl(3F)-C(29)-Cl(1F)	112.5(9)
Cl(2F)-C(29)-Cl(1F)	110.0(9)	Cl(3F)-C(29)-Cl(2E)	98.0(8)
Cl(3E)-C(29)-Cl(2E)	111.8(5)	Cl(3E)-C(29)-Cl(1E)	108.0(4)
Cl(2E)-C(29)-Cl(1E)	109.3(4)	Cl(4D)-C(30)-Cl(5D)	128.9(7)
Cl(6C)-C(30)-Cl(4C)	112.0(4)	Cl(6C)-C(30)-Cl(5C)	111.9(4)
Cl(4C)-C(30)-Cl(5C)	99.9(3)	Cl(4D)-C(30)-Cl(6D)	106.8(6)
Cl(5D)-C(30)-Cl(6D)	100.8(5)	Cl(7B)-C(31)-Cl(9B)	116.2(12)
Cl(7B)-C(31)-Cl(8B)	109.7(16)	Cl(9B)-C(31)-Cl(8B)	113.7(10)
Cl(9A)-C(31)-Cl(8A)	109.3(5)	Cl(9A)-C(31)-Cl(7A)	108.7(4)

Cl(8A)-C(31)-Cl(7A)	107.3(4)	Cl(3D)-C(32)-Cl(2D)	110.6(10)
Cl(1C)-C(32)-Cl(2C)	107.3(4)	Cl(1C)-C(32)-Cl(3C)	106.8(4)
Cl(2C)-C(32)-Cl(3C)	108.0(4)	Cl(3D)-C(32)-Cl(1D)	134.2(11)
Cl(2D)-C(32)-Cl(1D)	105.0(6)		

Computational Methods. Calculations on compound **5** at the singlet and triplet states were carried out using the Gaussian 03 suite of programs.¹ The hybrid functional B3LYP² (using the RHF and UHF for the singlet and triplet states, respectively) and the split-valence 6-31G* basis set were used in both cases.³ Zero-point vibrational energies (ZPVE) were included in the energy calculations. Both Hessian matrices for **5** at singlet and triplet states were found to be positive definite (NIMAG=0).

5 (Singlet state)

Sum of electronic and zero-point Energies=	-1312.009864 a.u.
Sum of electronic and thermal Energies=	-1311.981584 a.u.
Sum of electronic and thermal Enthalpies=	-1311.980640 a.u.
Sum of electronic and thermal Free Energies=	-1312.066144 a.u.

Center Number	Atomic Number	Atomic Type	Coordinates (Angstroms)		
			X	Y	Z
1	6	0	1.906981	0.011100	0.760081
2	6	0	3.305924	-0.012513	1.311377
3	6	0	4.006527	-1.285737	0.767075
4	6	0	4.013843	-1.275843	-0.793864
5	6	0	3.259024	-0.029517	-1.322685
6	6	0	1.857080	-0.034722	-0.745137
7	6	0	3.998703	1.232082	-0.811576
8	6	0	4.050611	1.228804	0.748590
9	6	0	0.665944	-0.095578	-1.409104
10	15	0	-0.459754	-0.010360	-0.020825
11	6	0	0.705212	0.075276	1.375044
12	7	0	-1.486296	-1.353512	0.072665
13	7	0	-1.484407	1.347744	-0.027342
14	6	0	-1.346556	-2.573954	-0.778414

Center Number	Atomic Number	Atomic Type	Coordinates (Angstroms)		
			X	Y	Z
15	6	0	-2.334503	-1.464781	1.287598
16	6	0	0.002999	-3.293255	-0.630033
17	6	0	-1.674767	-2.295926	-2.251721
18	6	0	-1.790635	-2.471948	2.314039
19	6	0	-3.804839	-1.752744	0.942809
20	6	0	-2.342881	1.454397	-1.246611
21	6	0	-1.247341	2.611894	0.723132
22	6	0	0.127823	3.265837	0.505747
23	6	0	-1.582496	2.472891	2.214945
24	6	0	-1.722070	2.322006	-2.350871
25	6	0	-3.774213	1.892955	-0.899697
26	1	0	3.319987	-0.004101	2.407516
27	1	0	3.492932	-2.175556	1.148502
28	1	0	5.028995	-1.317562	1.163430
29	1	0	3.542609	-2.184186	-1.184640
30	1	0	5.044296	-1.265352	-1.171988
31	1	0	3.216430	-0.038077	-2.416069
32	1	0	3.482886	2.127513	-1.175272
33	1	0	5.013660	1.258114	-1.228293
34	1	0	5.087531	1.199893	1.106061
35	1	0	3.603910	2.143014	1.155851
36	1	0	0.522554	0.083221	2.442350
37	1	0	-2.115129	-3.253434	-0.396167
38	1	0	-2.314326	-0.472422	1.750707
39	1	0	-0.030529	-4.255487	-1.155802
40	1	0	0.238598	-3.488187	0.421174
41	1	0	0.805994	-2.692988	-1.065835
42	1	0	-1.632228	-3.230762	-2.823948
43	1	0	-0.951933	-1.591206	-2.674647
44	1	0	-2.684410	-1.882125	-2.354083

Center Number	Atomic Number	Atomic Type	Coordinates (Angstroms)		
			X	Y	Z
45	1	0	-2.395102	-2.445145	3.228619
46	1	0	-0.754352	-2.238335	2.578147
47	1	0	-1.822118	-3.497395	1.928989
48	1	0	-4.418195	-1.693772	1.849528
49	1	0	-3.943095	-2.755280	0.522885
50	1	0	-4.186055	-1.025620	0.220042
51	1	0	-2.414887	0.434943	-1.636192
52	1	0	-1.984354	3.305205	0.307819
53	1	0	0.125863	4.275174	0.935447
54	1	0	0.363566	3.346766	-0.558842
55	1	0	0.922745	2.693857	0.990364
56	1	0	-1.530695	3.453014	2.704266
57	1	0	-0.878384	1.812601	2.729060
58	1	0	-2.594055	2.076437	2.351223
59	1	0	-2.358216	2.302805	-3.244276
60	1	0	-0.735738	1.928522	-2.615828
61	1	0	-1.624412	3.369284	-2.040242
62	1	0	-4.410464	1.801309	-1.787457
63	1	0	-3.827041	2.938405	-0.574695
64	1	0	-4.197816	1.268348	-0.106946

5 (Triplet state)

S2=2.008283 a.u.

S2A=2.000032 a.u.

Sum of electronic and zero-point Energies= -1311.958307 a.u.

Sum of electronic and thermal Energies= -1311.929654 a.u.

Sum of electronic and thermal Enthalpies= -1311.928709 a.u.

Sum of electronic and thermal Free Energies= -1312.016458 a.u.

Center Number	Atomic Number	Atomic Type	Coordinates (Angstroms)		
			X	Y	Z
1	6	0	-1.991412	-0.000864	-0.705461
2	6	0	-3.379149	-0.013106	-1.292832
3	6	0	-4.114372	-1.280551	-0.776189
4	6	0	-4.138860	-1.281353	0.784164
5	6	0	-3.384705	-0.035262	1.325082
6	6	0	-1.997818	-0.039150	0.732528
7	6	0	-4.125809	1.226670	0.806528
8	6	0	-4.144344	1.227574	-0.753939
9	6	0	-0.720983	-0.106922	1.247110
10	15	0	0.481977	-0.007310	-0.036013
11	6	0	-0.729013	0.038947	-1.315919
12	7	0	1.600651	-1.305570	-0.002237
13	7	0	1.558095	1.328591	-0.006235
14	6	0	1.260820	-2.604300	0.649871
15	6	0	2.610786	-1.363020	-1.095948
16	6	0	-0.058661	-3.248402	0.188691
17	6	0	1.340200	-2.506823	2.180069
18	6	0	2.184762	-2.245442	-2.282722
19	6	0	3.999654	-1.768756	-0.575289
20	6	0	2.538688	1.384439	1.117537
21	6	0	1.179897	2.645631	-0.600586

Center Number	Atomic Number	Atomic Type	Coordinates (Angstroms)		
			X	Y	Z
22	6	0	-0.183197	3.207214	-0.159607
23	6	0	1.324879	2.644963	-2.128843
24	6	0	2.028883	2.170730	2.338108
25	6	0	3.913143	1.895197	0.656515
26	1	0	-3.357585	-0.002989	-2.388857
27	1	0	-3.608011	-2.174608	-1.155715
28	1	0	-5.135488	-1.296238	-1.178855
29	1	0	-3.673266	-2.190916	1.178691
30	1	0	-5.172429	-1.265836	1.154289
31	1	0	-3.361866	-0.045470	2.419727
32	1	0	-3.627051	2.124061	1.187955
33	1	0	-5.148747	1.235379	1.204737
34	1	0	-5.176209	1.204527	-1.128306
35	1	0	-3.684736	2.141226	-1.146395
36	1	0	-0.538758	0.001723	-2.380973
37	1	0	2.064008	-3.279655	0.338393
38	1	0	2.698457	-0.335894	-1.461744
39	1	0	-0.137754	-4.258924	0.609076
40	1	0	-0.103788	-3.328447	-0.900999
41	1	0	-0.921802	-2.670071	0.526579
42	1	0	1.203162	-3.498546	2.628363
43	1	0	0.560267	-1.846968	2.573119
44	1	0	2.316045	-2.120773	2.494040
45	1	0	2.916348	-2.161687	-3.095454
46	1	0	1.206740	-1.940600	-2.667570
47	1	0	2.125752	-3.303202	-2.002052
48	1	0	4.738120	-1.680600	-1.381066
49	1	0	4.025343	-2.807529	-0.226895
50	1	0	4.316199	-1.125677	0.251123
51	1	0	2.674763	0.345720	1.429062

Center Number	Atomic Number	Atomic Type	Coordinates (Angstroms)		
			X	Y	Z
52	1	0	1.937798	3.337165	-0.220316
53	1	0	-0.289942	4.234268	-0.531055
54	1	0	-0.271967	3.229081	0.930112
55	1	0	-1.007622	2.612150	-0.559095
56	1	0	1.194406	3.662005	-2.518561
57	1	0	0.570804	2.007163	-2.597291
58	1	0	2.317960	2.289865	-2.424317
59	1	0	2.744622	2.085368	3.164795
60	1	0	1.064193	1.781204	2.678628
61	1	0	1.910025	3.237494	2.116028
62	1	0	4.639753	1.787136	1.470614
63	1	0	3.894217	2.955912	0.381556
64	1	0	4.276834	1.327194	-0.205079

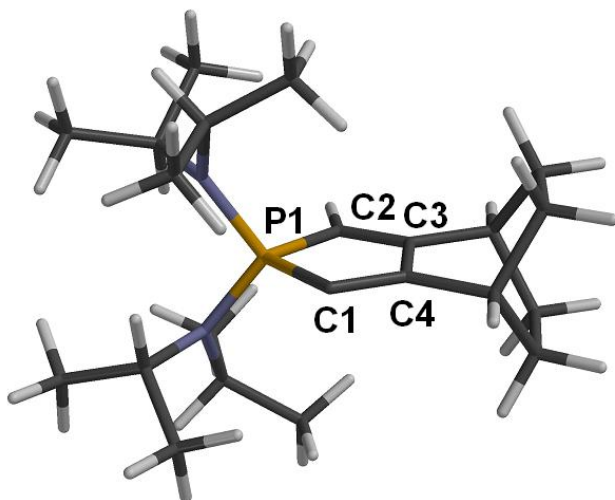


Figure S1. (A) Chief geometric features of **5** computed at the B3LYP/6-31G* level of theory. Relevant bond distances (\AA) and angles ($^\circ$): P1-C1=1.789; P1-C2=1.820; C2-C3=1.351; C3-C4=1.507; C1-C4=1.365; P1-C1-C4 = 99.8, P1-C2-C3 = 102.6, C1-P1-C2 = 101.2.

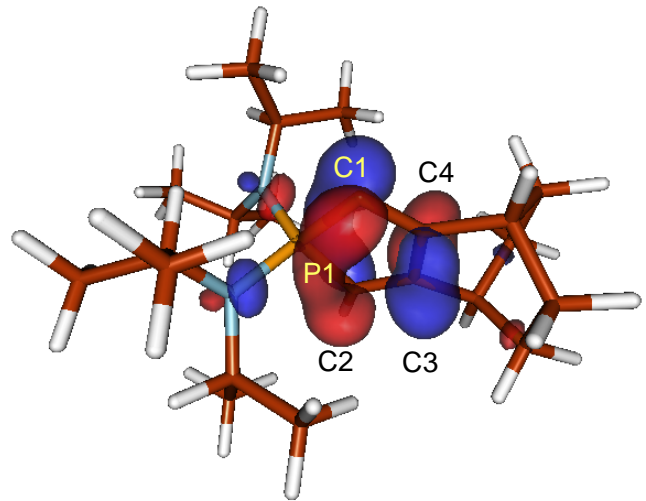


Figure S2. LUMO of compound 5. Calculated main p_z MO coefficients:
 $C1=0.576$; $C2=-0.400$; $P1=-0.453$; $C3=-0.467$; $C4=0.289$.

References

-
- ¹ Gaussian 03, Revision C.02, M. J. Frisch, G. W. Trucks, H. B. Schlegel, G. E. Scuseria, M. A. Robb, J. R. Cheeseman, J. A. Montgomery, Jr., T. Vreven, K. N. Kudin, J. C. Burant, J. M. Millam, S. S. Iyengar, J. Tomasi, V. Barone, B. Mennucci, M. Cossi, G. Scalmani, N. Rega, G. A. Petersson, H. Nakatsuji, M. Hada, M. Ehara, K. Toyota, R. Fukuda, J. Hasegawa, M. Ishida, T. Nakajima, Y. Honda, O. Kitao, H. Nakai, M. Klene, X. Li, J. E. Knox, H. P. Hratchian, J. B. Cross, V. Bakken, C. Adamo, J. Jaramillo, R. Gomperts, R. E. Stratmann, O. Yazyev, A. J. Austin, R. Cammi, C. Pomelli, J. W. Ochterski, P. Y. Ayala, K. Morokuma, G. A. Voth, P. Salvador, J. J. Dannenberg, V. G. Zakrzewski, S. Dapprich, A. D. Daniels, M. C. Strain, O. Farkas, D. K. Malick, A. D. Rabuck, K. Raghavachari, J. B. Foresman, J. V. Ortiz, Q. Cui, A. G. Baboul, S. Clifford, J. Cioslowski, B. B. Stefanov, G. Liu, A. Liashenko, P. Piskorz, I. Komaromi, R. L. Martin, D. J. Fox, T. Keith, M. A. Al-Laham, C. Y. Peng, A. Nanayakkara, M. Challacombe, P. M. W. Gill, B. Johnson, W. Chen, M. W. Wong, C. Gonzalez, and J. A. Pople, Gaussian, Inc., Wallingford CT, 2004.
- ² a) W. Kohn, A. D. Becke, R. G. Parr, *J. Phys. Chem.* **1996**, *100*, 12974; b) A. D. Becke, *J. Chem. Soc.* **1993**, *98*, 5648; c) A. D. Becke, *Phys. Rev. A* **1988**, *38*, 3098.
- ³ W. J. Hehre, L. Radom, P. V. R. Schleyer, A. J. Pople, *Ab Initio Molecular Orbital Theory*, Wiley, New York, **1986**, pp. 76-87 and references therein.

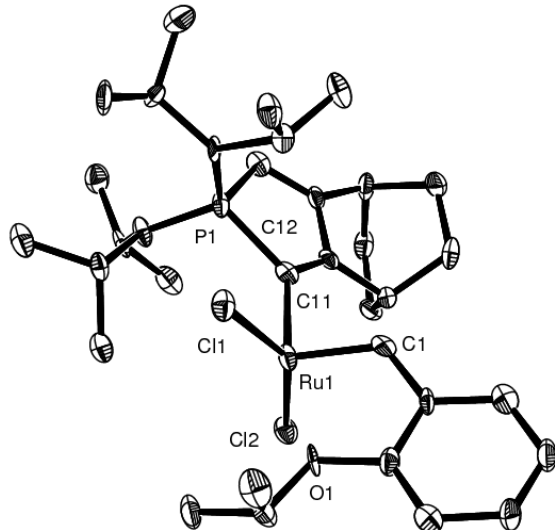


Table S1. Crystal data and structure refinement: Compound 11 Chapter 4.

Empirical formula	$C_{32}H_{50.74}Cl_{2.26}N_2OPRu$		
Formula weight	691.64		
Temperature	100(2) K		
Wavelength	0.71073 Å		
Crystal system	Monoclinic		
Space group	P2(1)/n		
Unit cell dimensions	$a = 14.366(4)$ Å	$\alpha = 90^\circ$	
	$b = 10.270(3)$ Å	$\beta = 102.884(4)^\circ$	
	$c = 23.048(6)$ Å	$\gamma = 90^\circ$	
Volume	$3314.7(15)$ Å ³		
Z	4		
Density (calculated)	1.386 Mg/m ³		
Absorption coefficient	0.731 mm ⁻¹		
F(000)	1449		
Crystal size	0.24 x 0.17 x 0.10 mm ³		
Theta range for data collection	1.81 to 21.26°		
Index ranges	-14 <= h <= 14, -10 <= k <= 10, -23 <= l <= 21		
Reflections collected	14560		
Independent reflections	3684 [R(int) = 0.1254]		

Completeness to theta = 21.26°	99.8 %
Absorption correction	None
Max. and min. transmission	0.9305 and 0.8442
Refinement method	Full-matrix least-squares on F^2
Data / restraints / parameters	3684 / 6 / 375
Goodness-of-fit on F^2	1.015
Final R indices [$ I >2\text{sigma}(I)$]	R1 = 0.0525, wR2 = 0.1103
R indices (all data)	R1 = 0.1096, wR2 = 0.1392
Extinction coefficient	0.0034(4)
Largest diff. peak and hole	1.021 and -0.823 e. \AA^{-3}

Table S2. *Atomic coordinates ($x \times 10^4$) and equivalent isotropic displacement parameters ($\text{\AA}^2 \times 10^3$). U(eq) is defined as one third of the trace of the orthogonalized U^{ij} tensor.*

	x	y	z	U(eq)
Ru(1)	7098(1)	3254(1)	9176(1)	19(1)
P(1)	4899(2)	2379(2)	8326(1)	20(1)
Cl(1)	6279(2)	2515(2)	9883(1)	24(1)
Cl(2)	8122(2)	2787(2)	8556(1)	24(1)
Cl(3)	3167(7)	2989(8)	7266(4)	29(2)
O(1)	8425(4)	3539(5)	9959(3)	21(2)
N(1)	5073(5)	798(6)	8269(3)	21(2)
N(2)	4212(5)	2605(6)	8805(3)	19(2)
C(1)	7164(6)	5004(8)	9235(4)	18(2)
C(2)	7948(6)	5630(8)	9646(4)	18(2)
C(3)	8086(6)	6981(8)	9671(4)	24(2)
C(4)	8838(7)	7532(8)	10088(4)	28(3)
C(5)	9439(7)	6753(8)	10484(4)	28(2)
C(6)	9326(6)	5385(8)	10475(4)	26(2)
C(7)	8594(6)	4850(8)	10046(4)	21(2)
C(8)	8917(7)	2638(8)	10418(4)	26(3)

	x	y	z	U(eq)
C(9)	8519(7)	2748(9)	10963(4)	32(3)
C(10)	8798(7)	1298(8)	10139(4)	34(3)
C(11)	5984(6)	3381(8)	8484(4)	16(2)
C(12)	5888(6)	4102(8)	7975(4)	17(2)
C(13)	6559(6)	5026(7)	7775(4)	21(2)
C(14)	6097(6)	6385(8)	7707(4)	25(2)
C(15)	5083(6)	6319(8)	7281(4)	27(3)
C(16)	4917(6)	4928(7)	7014(4)	24(2)
C(17)	5732(6)	4621(8)	6707(4)	29(3)
C(18)	6698(6)	4583(8)	7162(4)	23(2)
C(19)	4984(6)	4002(8)	7515(4)	18(2)
C(20)	4379(7)	3048(9)	7608(4)	20(3)
C(21)	5142(6)	135(8)	7712(4)	23(2)
C(22)	5765(7)	768(9)	7341(4)	34(3)
C(23)	4140(6)	-217(8)	7337(4)	31(3)
C(24)	5470(6)	92(7)	8833(4)	20(2)
C(25)	6547(6)	-164(8)	8909(4)	27(3)
C(26)	4945(7)	-1187(8)	8871(4)	31(3)
C(27)	4268(7)	3922(8)	9092(4)	28(3)
C(28)	3745(7)	5009(8)	8697(4)	33(3)
C(29)	3984(7)	3915(8)	9685(4)	27(2)
C(30)	3383(6)	1727(8)	8765(4)	29(3)
C(31)	2422(7)	2376(9)	8509(5)	45(3)
C(32)	3392(7)	1047(8)	9367(5)	39(3)

Table S3. Bond lengths [Å] and angles [°].

Ru(1)-C(1)	1.803(8)	Ru(1)-C(11)	1.996(8)
Ru(1)-Cl(2)	2.319(3)	Ru(1)-O(1)	2.333(6)
Ru(1)-Cl(1)	2.338(2)	P(1)-N(1)	1.652(7)

P(1)-N(2)	1.654(7)	P(1)-C(20)	1.793(10)
P(1)-C(11)	1.836(9)	Cl(3)-C(20)	1.745(14)
O(1)-C(7)	1.375(9)	O(1)-C(8)	1.463(10)
N(1)-C(21)	1.477(11)	N(1)-C(24)	1.486(10)
N(2)-C(30)	1.480(10)	N(2)-C(27)	1.500(10)
C(1)-C(2)	1.450(12)	C(2)-C(3)	1.401(11)
C(2)-C(7)	1.406(11)	C(3)-C(4)	1.396(12)
C(4)-C(5)	1.367(12)	C(5)-C(6)	1.413(12)
C(6)-C(7)	1.386(12)	C(8)-C(9)	1.496(13)
C(8)-C(10)	1.513(12)	C(11)-C(12)	1.370(11)
C(12)-C(19)	1.486(11)	C(12)-C(13)	1.496(12)
C(13)-C(14)	1.538(11)	C(13)-C(18)	1.541(12)
C(14)-C(15)	1.566(11)	C(15)-C(16)	1.552(11)
C(16)-C(19)	1.483(12)	C(16)-C(17)	1.529(12)
C(17)-C(18)	1.542(11)	C(19)-C(20)	1.357(13)
C(21)-C(22)	1.516(12)	C(21)-C(23)	1.547(12)
C(24)-C(26)	1.526(11)	C(24)-C(25)	1.540(12)
C(27)-C(29)	1.512(12)	C(27)-C(28)	1.528(11)
C(30)-C(31)	1.528(12)	C(30)-C(32)	1.550(13)
C(1)-Ru(1)-C(11)	90.8(4)	C(1)-Ru(1)-Cl(2)	102.9(3)
C(11)-Ru(1)-Cl(2)	91.5(3)	C(1)-Ru(1)-O(1)	78.3(3)
C(11)-Ru(1)-O(1)	168.9(3)	Cl(2)-Ru(1)-O(1)	88.98(16)
C(1)-Ru(1)-Cl(1)	107.3(3)	C(11)-Ru(1)-Cl(1)	98.0(3)
Cl(2)-Ru(1)-Cl(1)	148.12(8)	O(1)-Ru(1)-Cl(1)	87.31(16)
N(1)-P(1)-N(2)	108.3(4)	N(1)-P(1)-C(20)	110.1(4)
N(2)-P(1)-C(20)	112.0(4)	N(1)-P(1)-C(11)	115.4(4)
N(2)-P(1)-C(11)	113.3(4)	C(20)-P(1)-C(11)	97.4(4)
C(7)-O(1)-C(8)	118.2(7)	C(7)-O(1)-Ru(1)	108.9(5)
C(8)-O(1)-Ru(1)	131.3(5)	C(21)-N(1)-C(24)	116.6(6)
C(21)-N(1)-P(1)	124.2(6)	C(24)-N(1)-P(1)	116.5(6)
C(30)-N(2)-C(27)	122.7(7)	C(30)-N(2)-P(1)	117.6(6)
C(27)-N(2)-P(1)	116.1(6)	C(2)-C(1)-Ru(1)	120.7(6)

C(3)-C(2)-C(7)	118.1(8)	C(3)-C(2)-C(1)	123.3(8)
C(7)-C(2)-C(1)	118.6(7)	C(4)-C(3)-C(2)	120.7(9)
C(5)-C(4)-C(3)	120.0(8)	C(4)-C(5)-C(6)	121.2(9)
C(7)-C(6)-C(5)	118.1(8)	O(1)-C(7)-C(6)	125.0(8)
O(1)-C(7)-C(2)	113.1(7)	C(6)-C(7)-C(2)	121.8(7)
O(1)-C(8)-C(9)	110.3(7)	O(1)-C(8)-C(10)	106.1(7)
C(9)-C(8)-C(10)	113.4(8)	C(12)-C(11)-P(1)	102.3(6)
C(12)-C(11)-Ru(1)	129.1(6)	P(1)-C(11)-Ru(1)	128.1(5)
C(11)-C(12)-C(19)	118.6(8)	C(11)-C(12)-C(13)	131.2(8)
C(19)-C(12)-C(13)	110.2(8)	C(12)-C(13)-C(14)	108.3(7)
C(12)-C(13)-C(18)	108.6(7)	C(14)-C(13)-C(18)	108.4(7)
C(13)-C(14)-C(15)	110.2(7)	C(16)-C(15)-C(14)	109.1(7)
C(19)-C(16)-C(17)	107.7(7)	C(19)-C(16)-C(15)	107.7(7)
C(17)-C(16)-C(15)	107.9(7)	C(16)-C(17)-C(18)	111.0(8)
C(13)-C(18)-C(17)	109.5(7)	C(20)-C(19)-C(16)	130.8(8)
C(20)-C(19)-C(12)	115.2(8)	C(16)-C(19)-C(12)	113.9(7)
C(19)-C(20)-Cl(3)	124.3(8)	C(19)-C(20)-P(1)	105.9(6)
Cl(3)-C(20)-P(1)	124.8(7)	N(1)-C(21)-C(22)	117.1(7)
N(1)-C(21)-C(23)	111.0(7)	C(22)-C(21)-C(23)	112.2(7)
N(1)-C(24)-C(26)	111.8(7)	N(1)-C(24)-C(25)	111.3(7)
C(26)-C(24)-C(25)	110.1(7)	N(2)-C(27)-C(29)	113.3(7)
N(2)-C(27)-C(28)	115.2(7)	C(29)-C(27)-C(28)	110.3(8)
N(2)-C(30)-C(31)	113.8(7)	N(2)-C(30)-C(32)	111.8(7)
C(31)-C(30)-C(32)	111.6(8)		

All calculations were performed with the Turbomole 5.7 program package.¹ As basis set the SVP basis set developed by Ahlrichs et al. was used.² Throughout the BP86 density functional^{3, 4} in combination with the “Resolution of the Identity” routine was employed.

Cartesian coordinate matrix for optimized structure of compound **2** chapter 5.

C	1.7857031	-0.7220376	0.0000400
N	0.4536760	-1.1075420	0.0000764
C	-0.3579445	0.0082144	-0.0000108
N	0.5028732	1.0864256	-0.0000956
C	1.8162817	0.6415557	-0.0000420
C	-1.7315080	0.0387344	-0.0000188
C	-2.9944171	0.0659010	0.0000064
C	0.0525764	2.4724176	0.0000596
H	2.6555061	1.3261881	-0.0000594
H	2.5933997	-1.4436254	0.0000568
C	-0.0584077	-2.4719336	-0.0000234
H	0.2799497	-3.0061575	0.8979297
H	-1.1537338	-2.4077272	0.0011584
H	0.2779750	-3.0053626	-0.8992010
H	0.4148658	2.9910349	-0.8977128
H	-1.0445363	2.4575063	-0.0014460
H	0.4123065	2.9901074	0.8994089

Cartesian coordinate matrix for optimized structure of compound **9** chapter 5.

C	-2.030299	0.000595	0.000881
C	2.030306	0.000573	-0.001265
C	3.278943	0.000298	-0.001441
C	4.675456	-0.000184	-0.000731
N	5.496282	-1.101507	0.001715
C	6.817970	-0.688127	0.002047
C	6.818470	0.686214	-0.000707
N	5.497081	1.100547	-0.002628
C	5.031486	-2.487000	0.006488
C	5.033284	2.486377	-0.004293
H	5.376668	-3.000262	0.928249
H	3.923899	-2.479945	-0.019522
H	5.419956	-3.019463	-0.886473
H	7.649840	-1.401029	0.003677
H	7.650856	1.398516	-0.001987

H	5.416020	3.012602	-0.903445
H	5.385088	3.005507	0.911626
H	3.925541	2.479942	-0.022869
C	-3.278930	0.000296	0.001258
C	-4.675450	-0.000184	0.000803
N	-5.497074	1.100552	0.002823
C	-6.818458	0.686217	0.001238
C	-6.817962	-0.688126	-0.001497
N	-5.496280	-1.101512	-0.001490
C	-5.033283	2.486388	0.004739
C	-5.031514	-2.487008	-0.006058
H	-5.387967	3.006584	-0.909445
H	-3.925493	2.479928	0.019851
H	-5.413157	3.011607	0.905703
H	-7.650850	1.398509	0.002664
H	-7.649835	-1.401029	-0.002991
H	-5.417092	-3.018492	0.888755
H	-5.379651	-3.001298	-0.926119
H	-3.923853	-2.479918	0.016428
Ag	-0.000003	0.000735	-0.000256

Cartesian coordinate matrix for optimized structure of compound **10** chapter 5.

C	-2.018768	-0.000180	0.000248
C	1.964984	-0.000175	-0.000336
C	3.212806	-0.000054	-0.000457
C	4.613881	0.000051	-0.000496
N	5.435497	0.286594	1.062257
C	6.755328	0.179331	0.663305
C	6.755322	-0.179042	-0.664352
N	5.435493	-0.286426	-1.063270
C	4.982410	0.648620	2.404355
C	4.982394	-0.648352	-2.405391
H	5.361109	1.656988	2.670054
H	3.874985	0.658158	2.413550
H	5.353864	-0.094981	3.139572
H	7.588216	0.365257	1.350810
H	7.588202	-0.364936	-1.351874
H	5.362225	-1.656132	-2.671678
H	5.352697	0.096042	-3.140392
H	3.874979	-0.659231	-2.414242
C	-3.265294	-0.000082	0.000484
C	-4.663328	0.000009	0.000728

N	-5.482206	-0.972206	-0.515752
C	-6.802631	-0.606964	-0.322424
C	-6.802382	0.607498	0.324504
N	-5.481816	0.972394	0.517497
C	-5.003765	-2.173532	-1.198283
C	-5.002758	2.173747	1.199562
H	-4.192115	-2.637914	-0.603033
H	-4.613099	-1.911859	-2.205110
H	-5.846128	-2.885327	-1.295303
H	-7.636483	-1.233796	-0.657643
H	-7.635995	1.234487	0.660032
H	-5.846285	2.883429	1.301715
H	-4.606837	1.911383	2.204135
H	-4.195011	2.641020	0.601229
Pd	-0.036590	-0.000225	-0.000060
P	-0.001623	0.093077	-2.394120
P	-0.000863	-0.093249	2.394024
C	0.657325	1.679841	-3.063944
C	1.032283	-1.275222	-3.077309
C	-1.617910	-0.096619	-3.268811
C	0.658902	-1.679630	3.064008
C	1.032717	1.275607	3.076596
C	-1.616929	0.095937	3.269199
C	0.386298	2.055793	-4.402233
C	0.908673	3.252396	-4.919389
C	1.693735	4.090849	-4.108593
C	1.954971	3.729393	-2.776017
C	1.440682	2.530743	-2.253274
H	-0.246560	1.422012	-5.043948
H	0.692345	3.534519	-5.962582
H	2.094204	5.033754	-4.515124
H	2.558616	4.390835	-2.133269
H	1.647177	2.253809	-1.207277
C	1.720037	-1.151994	-4.304691
C	2.419856	-2.251034	-4.833409
C	2.437450	-3.477769	-4.145877
C	1.759298	-3.603537	-2.920242
C	1.062935	-2.506729	-2.384940
H	1.711642	-0.198150	-4.856110
H	2.946946	-2.148595	-5.796157
H	2.978217	-4.340142	-4.568886
H	1.769761	-4.563237	-2.378264
H	0.534746	-2.607392	-1.421032

C	-1.949093	-1.276358	-3.967813
C	-3.179598	-1.375432	-4.643636
C	-4.084231	-0.300107	-4.628388
C	-3.760875	0.875497	-3.924277
C	-2.538664	0.976399	-3.242093
H	-1.241459	-2.119404	-4.007044
H	-3.418904	-2.293725	-5.204597
H	-5.036450	-0.370291	-5.179462
H	-4.460249	1.727672	-3.920859
H	-2.291415	1.906843	-2.704977
C	0.388317	-2.055431	4.402431
C	0.911280	-3.251724	4.919703
C	1.696461	-4.090048	4.108888
C	1.957239	-3.728762	2.776176
C	1.442380	-2.530405	2.253318
H	-0.244692	-1.421801	5.044145
H	0.695280	-3.533727	5.962995
H	2.097401	-5.032715	4.515500
H	2.560943	-4.390121	2.133399
H	1.648465	-2.253640	1.207196
C	-1.948083	1.275352	3.968751
C	-3.178463	1.374014	4.644872
C	-4.082933	0.298555	4.629456
C	-3.759570	-0.876744	3.924842
C	-2.537523	-0.977210	3.242297
H	-1.240580	2.118503	4.008081
H	-3.417784	2.292072	5.206214
H	-5.035046	0.368400	5.180758
H	-4.458824	-1.729021	3.921282
H	-2.290272	-1.907408	2.704760
C	1.720370	1.153090	4.304114
C	2.419929	2.252506	4.832393
C	2.437437	3.478897	4.144239
C	1.759405	3.603947	2.918465
C	1.063243	2.506781	2.383636
H	1.712087	0.199507	4.855995
H	2.946942	2.150626	5.795244
H	2.978056	4.341547	4.566887
H	1.769784	4.563382	2.376005
H	0.535107	2.606918	1.419644

References

-
- 1 R. Ahlrichs, M. Bär, M. Häser, H. Horn, C. Kölmel, “*Electronic structure calculations on workstation computers: The program system Turbomole*”, *Chem. Phys. Lett.* **1989**, 162, 165.
 - 2 A. Schäfer, H. Horn, R. Ahlrichs, *J. Chem. Phys.* **1992**, 97, 2571.
 - 3 A.D. Becke, *Phys. Rev. A*, **1988**, 38, 3098.
 - 4 J.P. Perdew, *Phys. Rev. B*, **1986**, 33, 8822.

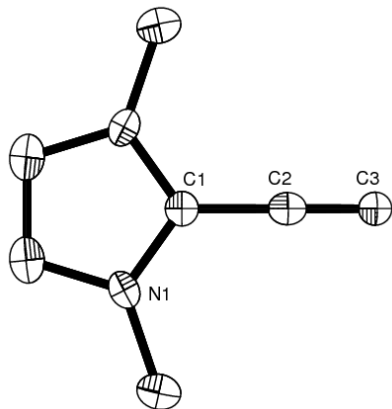


Table S1. Crystal data and structure refinement : Compound **6** Chapter 5.

Empirical formula	$C_{1.75}H_{2.25}I_{0.75}N_{0.5}$		
Formula weight	125.47		
Temperature	100(2) K		
Wavelength	0.71073 Å		
Crystal system	Orthorhombic		
Space group	Cmma		
Unit cell dimensions	$a = 6.7289(9)$ Å	$\alpha = 90^\circ$	
	$b = 17.926(2)$ Å	$\beta = 90^\circ$	
	$c = 10.2161(14)$ Å	$\gamma = 90^\circ$	
Volume	1232.3(3) Å ³		
Z	16		
Density (calculated)	2.705 Mg/m ³		
Absorption coefficient	7.568 mm ⁻¹		
F(000)	896		
Crystal size	0.33 x 0.17 x 0.10 mm ³		
Theta range for data collection	3.80 to 23.53°		
Index ranges	-7 <= h <= 7, -20 <= k <= 18, -11 <= l <= 11		
Reflections collected	3287		
Independent reflections	512 [R(int) = 0.0150]		
Completeness to theta = 23.53°	97.0 %		

Absorption correction	Sadabs
Max. and min. transmission	0.5182 and 0.1891
Refinement method	Full-matrix least-squares on F^2
Data / restraints / parameters	512 / 0 / 44
Goodness-of-fit on F^2	1.144
Final R indices [$\ >2\sigma(I)$]	$R_1 = 0.0267, wR_2 = 0.0662$
R indices (all data)	$R_1 = 0.0268, wR_2 = 0.0662$
Extinction coefficient	0.0007(2)
Largest diff. peak and hole	0.873 and -1.322 e. \AA^{-3}

Table S2. *Atomic coordinates ($x \times 10^4$) and equivalent isotropic displacement parameters ($\text{\AA}^2 \times 10^3$). $U(\text{eq})$ is defined as one third of the trace of the orthogonalized U_{ij} tensor.*

	x	y	z	$U(\text{eq})$
I(1)	5000	5900(1)	1593(1)	22(1)
I(2)	7500	5000	0	36(1)
N(1)	5000	8109(5)	6978(7)	21(2)
C(1)	5000	7500	6218(13)	18(3)
C(2)	5000	7500	4828(14)	20(3)
C(3)	5000	7500	3672(15)	25(3)
C(4)	5000	8873(6)	6521(10)	30(2)
C(5)	5000	7885(6)	8257(10)	28(2)

Table S3. *Bond lengths [\AA] and angles [°].*

I(1)-I(2)#1	2.8423(5)	I(1)-I(2)	2.8423(5)
I(2)-I(1)#1	2.8423(5)	I(2)-I(1)#2	2.8423(5)
I(2)-I(1)#3	2.8423(5)	N(1)-C(1)	1.339(11)
N(1)-C(5)	1.367(13)	N(1)-C(4)	1.449(13)
C(1)-N(1)#4	1.339(11)	C(1)-C(2)	1.420(19)
C(2)-C(3)	1.18(2)	C(5)-C(5)#4	1.38(2)

I(2)#1-I(1)-I(2)	72.576(16)	I(1)#1-I(2)-I(1)#2	110.15(2)
I(1)#1-I(2)-I(1)	107.424(16)	I(1)#2-I(2)-I(1)	110.86(2)
I(1)#1-I(2)-I(1)#3	110.86(2)	I(1)#2-I(2)-I(1)#3	107.424(16)
I(1)-I(2)-I(1)#3	110.15(2)	C(1)-N(1)-C(5)	108.4(8)
C(1)-N(1)-C(4)	125.7(8)	C(5)-N(1)-C(4)	125.9(8)
N(1)-C(1)-N(1)#4	109.1(11)	N(1)-C(1)-C(2)	125.4(6)
N(1)#4-C(1)-C(2)	125.4(6)	C(3)-C(2)-C(1)	180.000(9)
N(1)-C(5)-C(5)#4	107.0(6)		

Symmetry transformations used to generate equivalent atoms: #1 -x+1,-y+1,-z
#2 x+1/2,y,-z #3 -x+3/2,-y+1,z
#4 -x+1,-y+3/2,z

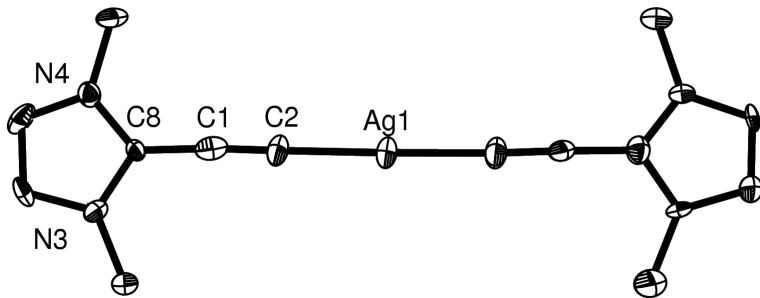


Table S1. Crystal data and structure refinement : Compound **9** Chapter 5.

Empirical formula	$C_{16}H_{20}AgCl_4IN_4$	
Formula weight	644.93	
Temperature	100(2) K	
Wavelength	0.71073 Å	
Crystal system	Triclinic	
Space group	P-1	
Unit cell dimensions	$a = 6.675(2)$ Å	$\alpha = 94.262(4)^\circ$
	$b = 8.292(2)$ Å	$\beta = 91.284(4)^\circ$
	$c = 20.702(6)$ Å	$\gamma = 90.782(4)^\circ$
Volume	$1142.3(6)$ Å ³	
Z	2	
Density (calculated)	1.875 Mg/m ³	
Absorption coefficient	2.710 mm ⁻¹	
F(000)	624	
Crystal size	0.23 x 0.16 x 0.11 mm ³	
Theta range for data collection	1.97 to 23.26°	
Index ranges	-7<=h<=6, -9<=k<=9, -22<=l<=22	
Reflections collected	5895	
Independent reflections	3234 [R(int) = 0.0294]	
Completeness to theta = 23.26°	98.4 %	
Absorption correction	Sadabs	
Max. and min. transmission	0.7548 and 0.5745	

Refinement method	Full-matrix least-squares on F ²
Data / restraints / parameters	3234 / 36 / 266
Goodness-of-fit on F ²	1.090
Final R indices [$I > 2\sigma(I)$]	R1 = 0.0540, wR2 = 0.1296
R indices (all data)	R1 = 0.0754, wR2 = 0.1400
Largest diff. peak and hole	2.415 and -1.116 e. \AA^{-3}

Table S2. *Atomic coordinates ($x \times 10^4$) and equivalent isotropic displacement parameters ($\text{\AA}^2 \times 10^3$). U(eq) is defined as one third of the trace of the orthogonalized U^{ij} tensor.*

	x	y	z	U(eq)
Ag(1)	7423(1)	9335(1)	4392(1)	33(1)
I(1A)	1947(1)	3962(1)	1328(1)	28(1)
N(1)	7749(14)	9316(9)	7070(4)	31(2)
N(2)	7766(13)	11882(9)	6975(4)	25(2)
N(3)	6999(12)	6817(10)	1849(4)	24(2)
N(4)	7028(11)	9357(9)	1672(4)	21(2)
C(1)	7218(15)	8687(12)	2819(5)	28(2)
C(2)	7315(16)	8922(13)	3415(5)	31(3)
C(3)	7544(16)	9791(13)	5370(5)	31(3)
C(4)	7622(16)	10119(11)	5957(5)	26(2)
C(5)	7735(14)	10458(12)	6642(5)	24(2)
C(6)	7855(16)	10076(12)	7689(5)	28(2)
C(7)	7849(15)	11650(12)	7630(4)	23(2)
C(8)	7111(14)	8325(11)	2143(4)	19(2)
C(9)	6850(15)	8531(13)	1093(5)	29(3)
C(10)	6862(16)	6937(12)	1186(5)	30(3)
C(11)	7660(30)	7576(15)	6885(7)	79(6)
C(12)	7760(20)	13425(13)	6668(6)	56(4)
C(13)	7034(16)	5338(11)	2184(5)	26(2)
C(14)	7101(17)	11139(11)	1795(6)	32(3)

	x	y	z	U(eq)
C(1S)	8334(17)	2395(11)	-198(5)	30(3)
Cl(1S)	8107(4)	395(3)	-589(1)	32(1)
Cl(2S)	6235(4)	2863(3)	273(1)	35(1)
C(2A)	3280(50)	6510(40)	5281(16)	74(9)
Cl(3A)	1811(19)	4552(12)	4887(5)	93(3)
Cl(4A)	3030(16)	6209(14)	6138(5)	74(3)
C(2B)	1920(50)	6500(40)	5315(16)	62(8)
Cl(3B)	3150(19)	4542(13)	4881(6)	90(3)
Cl(4B)	2097(19)	6340(16)	6141(7)	83(4)

Table S3. Bond lengths [Å] and angles [°].

Ag(1)-C(2)	2.026(10)	Ag(1)-C(3)	2.031(10)
N(1)-C(5)	1.345(12)	N(1)-C(6)	1.385(14)
N(1)-C(11)	1.465(15)	N(2)-C(5)	1.323(13)
N(2)-C(7)	1.383(12)	N(2)-C(12)	1.470(13)
N(3)-C(8)	1.351(12)	N(3)-C(10)	1.384(13)
N(3)-C(13)	1.454(12)	N(4)-C(9)	1.337(14)
N(4)-C(8)	1.346(11)	N(4)-C(14)	1.481(13)
C(1)-C(2)	1.235(15)	C(1)-C(8)	1.408(15)
C(3)-C(4)	1.225(15)	C(4)-C(5)	1.425(15)
C(6)-C(7)	1.320(14)	C(9)-C(10)	1.350(14)
C(1S)-Cl(2S)	1.757(11)	C(1S)-Cl(1S)	1.793(10)
C(2A)-Cl(4A)	1.82(3)	C(2A)-Cl(3A)	1.99(3)
C(2B)-Cl(4B)	1.73(3)	C(2B)-Cl(3B)	1.99(3)
C(2)-Ag(1)-C(3)	179.0(4)	C(5)-N(1)-C(6)	108.4(8)
C(5)-N(1)-C(11)	123.8(9)	C(6)-N(1)-C(11)	127.8(9)
C(5)-N(2)-C(7)	109.0(8)	C(5)-N(2)-C(12)	123.1(9)
C(7)-N(2)-C(12)	127.8(9)	C(8)-N(3)-C(10)	108.5(8)

C(8)-N(3)-C(13)	124.7(8)	C(10)-N(3)-C(13)	126.8(8)
C(9)-N(4)-C(8)	110.0(8)	C(9)-N(4)-C(14)	126.4(8)
C(8)-N(4)-C(14)	123.6(8)	C(2)-C(1)-C(8)	176.8(10)
C(1)-C(2)-Ag(1)	178.8(10)	C(4)-C(3)-Ag(1)	177.9(9)
C(3)-C(4)-C(5)	178.4(11)	N(2)-C(5)-N(1)	107.6(8)
N(2)-C(5)-C(4)	128.4(9)	N(1)-C(5)-C(4)	124.0(9)
C(7)-C(6)-N(1)	107.4(9)	C(6)-C(7)-N(2)	107.6(9)
N(4)-C(8)-N(3)	106.7(8)	N(4)-C(8)-C(1)	128.4(8)
N(3)-C(8)-C(1)	124.8(8)	N(4)-C(9)-C(10)	108.2(9)
C(9)-C(10)-N(3)	106.6(9)	Cl(2S)-C(1S)-Cl(1S)	111.0(6)
Cl(4A)-C(2A)-Cl(3A)	100.5(16)	Cl(4B)-C(2B)-Cl(3B)	107.9(17)

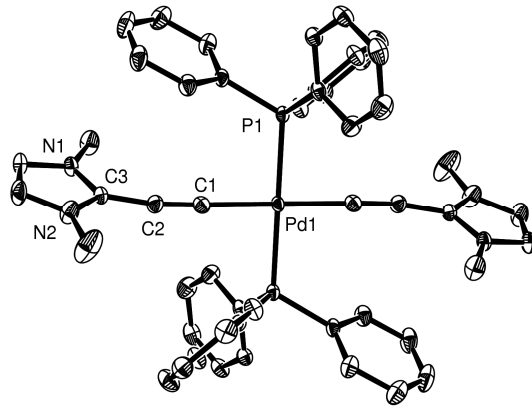


Table S1. *Crystal data and structure refinement.*

Empirical formula	$C_{50}H_{46}B_2F_8N_4P_2Pd$		
Formula weight	1044.86		
Temperature	100(2) K		
Wavelength	0.71073 Å		
Crystal system	Monoclinic		
Space group	P2(1)/c		
Unit cell dimensions	$a = 12.3163(14)$ Å	$\alpha = 90^\circ$	
	$b = 19.539(2)$ Å	$\beta = 90.814(2)^\circ$	
	$c = 10.6859(12)$ Å	$\gamma = 90^\circ$	
Volume	$2571.3(5)$ Å ³		
Z	4		
Density (calculated)	1.350 Mg/m ³		
Absorption coefficient	0.489 mm ⁻¹		
F(000)	1064		
Crystal size	0.26 x 0.13 x 0.10 mm ³		
Theta range for data collection	1.95 to 29.03°		
Index ranges	-16<=h<=16, -25<=k<=26, -12<=l<=13		
Reflections collected	20579		
Independent reflections	6410 [R(int) = 0.0329]		
Completeness to theta = 29.03°	93.4 %		

Absorption correction	Sadabs
Max. and min. transmission	0.9527 and 0.8834
Refinement method	Full-matrix least-squares on F^2
Data / restraints / parameters	6410 / 0 / 306
Goodness-of-fit on F^2	1.049
Final R indices [$I > 2\sigma(I)$]	$R_1 = 0.0330$, $wR_2 = 0.0779$
R indices (all data)	$R_1 = 0.0487$, $wR_2 = 0.0824$
Largest diff. peak and hole	0.570 and -0.612 e. \AA^{-3}

Table S2. *Atomic coordinates ($\times 10^4$) and equivalent isotropic displacement parameters ($\text{\AA}^2 \times 10^3$). $U(\text{eq})$ is defined as one third of the trace of the orthogonalized U^{ij} tensor.*

	x	y	z	$U(\text{eq})$
Pd(1)	0	0	0	15(1)
P(1)	-817(1)	1011(1)	629(1)	15(1)
N(1)	3684(1)	1491(1)	631(2)	20(1)
N(2)	3970(2)	726(1)	2059(2)	29(1)
C(1)	1476(2)	341(1)	439(2)	20(1)
C(2)	2356(2)	561(1)	714(2)	21(1)
C(3)	3307(2)	905(1)	1104(2)	19(1)
C(4)	4596(2)	1690(1)	1305(2)	25(1)
C(5)	4762(2)	1216(1)	2190(2)	31(1)
C(6)	3194(2)	1852(1)	-438(2)	31(1)
C(7)	3821(3)	118(1)	2836(3)	55(1)
C(8)	-1712(2)	1320(1)	-616(2)	17(1)
C(9)	-1300(2)	1340(1)	-1823(2)	24(1)
C(10)	-1948(2)	1548(1)	-2817(2)	27(1)
C(11)	-3016(2)	1735(1)	-2624(2)	27(1)
C(12)	-3430(2)	1718(1)	-1431(2)	31(1)
C(13)	-2783(2)	1511(1)	-427(2)	25(1)
C(14)	-1627(2)	916(1)	2027(2)	18(1)

	x	y	z	U(eq)
C(15)	-1933(2)	270(1)	2440(2)	25(1)
C(16)	-2567(2)	203(1)	3504(2)	32(1)
C(17)	-2881(2)	775(1)	4159(2)	28(1)
C(18)	-2573(2)	1418(1)	3763(2)	24(1)
C(19)	-1944(2)	1491(1)	2704(2)	20(1)
C(20)	58(2)	1733(1)	1014(2)	19(1)
C(21)	770(2)	1666(1)	2034(2)	26(1)
C(22)	1474(2)	2198(1)	2350(2)	33(1)
C(23)	1463(2)	2800(1)	1667(2)	37(1)
C(24)	750(2)	2877(1)	671(2)	35(1)
C(25)	48(2)	2343(1)	329(2)	27(1)
B(1)	4284(2)	1423(1)	5498(3)	29(1)
F(1)	4708(1)	771(1)	5434(2)	42(1)
F(2)	4095(1)	1603(1)	6727(1)	53(1)
F(3)	5026(1)	1887(1)	4989(1)	32(1)
F(4)	3311(1)	1446(1)	4814(2)	42(1)

Table S3. Bond lengths [Å] and angles [°]

Pd(1)-C(1)#1	1.986(2)	Pd(1)-C(1)	1.986(2)
Pd(1)-P(1)	2.3206(5)	Pd(1)-P(1)#1	2.3206(5)
P(1)-C(14)	1.817(2)	P(1)-C(8)	1.8184(19)
P(1)-C(20)	1.8195(19)	N(1)-C(3)	1.338(2)
N(1)-C(4)	1.381(2)	N(1)-C(6)	1.464(2)
N(2)-C(3)	1.344(2)	N(2)-C(5)	1.371(3)
N(2)-C(7)	1.463(3)	C(1)-C(2)	1.199(3)
C(2)-C(3)	1.408(3)	C(4)-C(5)	1.337(3)
C(8)-C(13)	1.388(3)	C(8)-C(9)	1.393(3)
C(9)-C(10)	1.381(3)	C(10)-C(11)	1.384(3)
C(11)-C(12)	1.380(3)	C(12)-C(13)	1.388(3)

C(14)-C(15)	1.391(3)	C(14)-C(19)	1.395(3)
C(15)-C(16)	1.394(3)	C(16)-C(17)	1.378(3)
C(17)-C(18)	1.379(3)	C(18)-C(19)	1.388(3)
C(20)-C(21)	1.396(3)	C(20)-C(25)	1.399(3)
C(21)-C(22)	1.393(3)	C(22)-C(23)	1.384(3)
C(23)-C(24)	1.378(3)	C(24)-C(25)	1.401(3)
B(1)-F(1)	1.380(3)	B(1)-F(2)	1.383(3)
B(1)-F(4)	1.396(3)	B(1)-F(3)	1.402(3)
C(1)#1-Pd(1)-C(1)	180.00(12)	C(1)#1-Pd(1)-P(1)	87.39(6)
C(1)-Pd(1)-P(1)	92.61(6)	C(1)#1-Pd(1)-P(1)#1	92.61(6)
C(1)-Pd(1)-P(1)#1	87.39(6)	P(1)-Pd(1)-P(1)#1	180.00(2)
C(14)-P(1)-C(8)	107.55(9)	C(14)-P(1)-C(20)	102.90(9)
C(8)-P(1)-C(20)	105.04(9)	C(14)-P(1)-Pd(1)	113.34(7)
C(8)-P(1)-Pd(1)	109.38(6)	C(20)-P(1)-Pd(1)	117.86(7)
C(3)-N(1)-C(4)	109.14(16)	C(3)-N(1)-C(6)	124.37(16)
C(4)-N(1)-C(6)	126.49(17)	C(3)-N(2)-C(5)	108.70(17)
C(3)-N(2)-C(7)	124.19(19)	C(5)-N(2)-C(7)	127.08(19)
C(2)-C(1)-Pd(1)	178.39(19)	C(1)-C(2)-C(3)	171.6(2)
N(1)-C(3)-N(2)	107.33(16)	N(1)-C(3)-C(2)	126.05(17)
N(2)-C(3)-C(2)	126.53(19)	C(5)-C(4)-N(1)	106.81(18)
C(4)-C(5)-N(2)	108.02(18)	C(13)-C(8)-C(9)	119.14(18)
C(13)-C(8)-P(1)	123.35(16)	C(9)-C(8)-P(1)	117.48(14)
C(10)-C(9)-C(8)	120.43(19)	C(9)-C(10)-C(11)	120.2(2)
C(12)-C(11)-C(10)	119.79(19)	C(11)-C(12)-C(13)	120.3(2)
C(12)-C(13)-C(8)	120.1(2)	C(15)-C(14)-C(19)	119.14(19)
C(15)-C(14)-P(1)	120.55(15)	C(19)-C(14)-P(1)	120.31(15)
C(14)-C(15)-C(16)	120.1(2)	C(17)-C(16)-C(15)	120.2(2)
C(16)-C(17)-C(18)	120.1(2)	C(17)-C(18)-C(19)	120.2(2)
C(18)-C(19)-C(14)	120.20(19)	C(21)-C(20)-C(25)	119.36(18)
C(21)-C(20)-P(1)	117.89(16)	C(25)-C(20)-P(1)	122.75(15)
C(22)-C(21)-C(20)	120.0(2)	C(23)-C(22)-C(21)	120.4(2)
C(24)-C(23)-C(22)	120.1(2)	C(23)-C(24)-C(25)	120.3(2)

C(20)-C(25)-C(24)	119.8(2)	F(4)-B(1)-F(3)	109.62(19)
F(1)-B(1)-F(2)	110.6(2)	F(1)-B(1)-F(4)	109.1(2)
F(2)-B(1)-F(4)	109.5(2)	F(1)-B(1)-F(3)	109.15(19)
F(2)-B(1)-F(3)	108.9(2)		

Symmetry transformations used to generate equivalent atoms: #1 -x,-y,-z

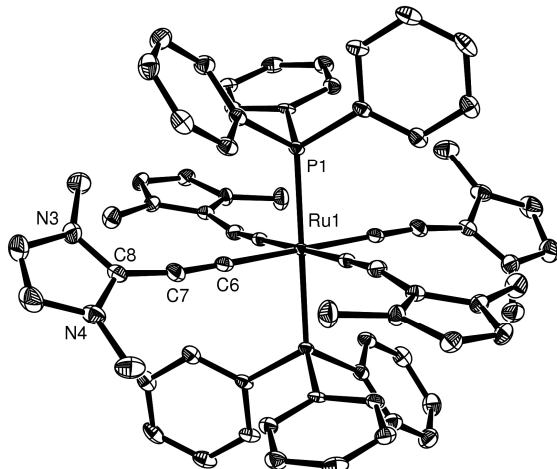


Table S1. Crystal data and structure refinement: Compound X Chapter 5.

Empirical formula	$C_{68}H_{62}Ag_2I_4N_{10}P_2Ru$		
Formula weight	1905.63		
Temperature	100(2) K		
Wavelength	0.71073 Å		
Crystal system	Triclinic		
Space group	P-1		
Unit cell dimensions	$a = 14.7744(14)$ Å	$\alpha = 75.412(3)^\circ$	
	$b = 15.0528(11)$ Å	$\beta = 84.275(3)^\circ$	
	$c = 17.6086(13)$ Å	$\gamma = 89.048(3)^\circ$	
Volume	$3770.8(5)$ Å ³		
Z	2		
Density (calculated)	1.678 Mg/m ³		
Absorption coefficient	2.435 mm ⁻¹		
F(000)	1840		
Crystal size	0.17 x 0.16 x 0.10 mm ³		
Theta range for data collection	6.55 to 26.37°		
Index ranges	-18<=h<=10, -18<=k<=18, -21<=l<=22		
Reflections collected	28181		
Independent reflections	14571 [R(int) = 0.0142]		
Completeness to theta = 26.37°	94.5 %		

Absorption correction	Sadabs
Max. and min. transmission	0.7928 and 0.6823
Refinement method	Full-matrix least-squares on F^2
Data / restraints / parameters	14571 / 0 / 765
Goodness-of-fit on F^2	1.127
Final R indices [$I > 2\sigma(I)$]	$R_1 = 0.0404$, $wR_2 = 0.1118$
R indices (all data)	$R_1 = 0.0421$, $wR_2 = 0.1132$
Largest diff. peak and hole	3.925 and -2.809 e. \AA^{-3}

Table S2. *Atomic coordinates ($x \times 10^4$) and equivalent isotropic displacement parameters ($\text{\AA}^2 \times 10^3$). $U(\text{eq})$ is defined as one third of the trace of the orthogonalized U^{ij} tensor.*

	x	y	z	$U(\text{eq})$
Ru(1A)	5000	5000	0	10(1)
P(1A)	3680(1)	4250(1)	710(1)	12(1)
N(1A)	3326(3)	7015(2)	-2493(2)	16(1)
N(2A)	3604(3)	5790(3)	-2909(2)	17(1)
N(3A)	4322(3)	8491(3)	243(2)	21(1)
N(4A)	3920(3)	7829(3)	1463(2)	22(1)
C(1A)	4302(3)	5416(3)	-956(2)	14(1)
C(2A)	3888(3)	5689(3)	-1545(3)	17(1)
C(3A)	3609(3)	6135(3)	-2269(3)	15(1)
C(4A)	3167(3)	7227(3)	-3278(3)	19(1)
C(5A)	3342(3)	6466(3)	-3538(3)	19(1)
C(6A)	4610(3)	6128(3)	375(2)	15(1)
C(7A)	4385(3)	6816(3)	597(3)	19(1)
C(8A)	4215(3)	7665(3)	765(3)	17(1)
C(9A)	4092(4)	9172(4)	624(4)	31(1)
C(10A)	3845(4)	8765(4)	1377(3)	31(1)
C(11A)	3879(4)	4856(3)	-2922(3)	27(1)
C(12A)	3201(4)	7636(3)	-1973(3)	24(1)

	x	y	z	U(eq)
C(13A)	4633(4)	8619(4)	-595(3)	27(1)
C(14A)	3736(4)	7110(4)	2198(3)	30(1)
C(15A)	3682(3)	4062(3)	1773(2)	13(1)
C(16A)	3251(3)	4672(3)	2174(3)	18(1)
C(17A)	3355(3)	4579(3)	2970(3)	20(1)
C(18A)	3878(3)	3881(3)	3372(3)	21(1)
C(19A)	4304(3)	3265(3)	2984(3)	18(1)
C(20A)	4214(3)	3361(3)	2189(3)	16(1)
C(21A)	3390(3)	3114(3)	580(3)	15(1)
C(22A)	3066(3)	2377(3)	1199(3)	20(1)
C(23A)	2797(4)	1553(3)	1055(3)	25(1)
C(24A)	2862(4)	1461(3)	287(3)	25(1)
C(25A)	3199(3)	2183(3)	-334(3)	22(1)
C(26A)	3456(3)	3006(3)	-192(3)	18(1)
C(27A)	2575(3)	4815(3)	533(2)	15(1)
C(28A)	1762(3)	4316(3)	808(3)	18(1)
C(29A)	931(3)	4739(4)	701(3)	23(1)
C(30A)	880(3)	5657(4)	312(3)	24(1)
C(31A)	1680(3)	6160(3)	28(3)	21(1)
C(32A)	2522(3)	5741(3)	137(3)	18(1)
Ru(1B)	0	5000	5000	9(1)
P(1B)	996(1)	6237(1)	4434(1)	10(1)
N(1B)	-1367(3)	6464(3)	2245(3)	32(1)
N(2B)	-1362(3)	5069(3)	2100(2)	27(1)
N(3B)	1851(3)	2560(2)	3501(2)	17(1)
N(4B)	2456(3)	2375(3)	4600(2)	17(1)
C(1B)	-597(3)	5178(3)	3984(2)	14(1)
C(2B)	-906(3)	5272(3)	3353(3)	22(1)
C(3B)	-1196(3)	5578(4)	2604(3)	23(1)
C(4B)	-1642(4)	6501(5)	1509(3)	42(2)

	x	y	z	U(eq)
C(5B)	-1648(4)	5641(5)	1416(3)	41(2)
C(6B)	863(3)	4139(3)	4580(2)	13(1)
C(7B)	1349(3)	3604(3)	4319(3)	16(1)
C(8B)	1868(3)	2886(3)	4143(3)	16(1)
C(9B)	2445(3)	1830(3)	3553(3)	19(1)
C(10B)	2818(3)	1716(3)	4242(3)	20(1)
C(11B)	-1230(4)	7237(4)	2578(4)	39(1)
C(12B)	-1209(4)	4088(4)	2242(3)	34(1)
C(13B)	1280(4)	2923(4)	2868(3)	25(1)
C(14B)	2670(4)	2516(3)	5350(3)	24(1)
C(15B)	2213(3)	6061(3)	4562(2)	14(1)
C(16B)	2538(3)	5218(3)	4973(3)	15(1)
C(17B)	3468(3)	5074(3)	4999(3)	20(1)
C(18B)	4083(3)	5770(3)	4618(3)	21(1)
C(19B)	3764(3)	6618(3)	4220(3)	22(1)
C(20B)	2845(3)	6761(3)	4194(3)	17(1)
C(21B)	737(3)	7246(3)	4815(2)	14(1)
C(22B)	1132(3)	7356(3)	5470(3)	19(1)
C(23B)	863(4)	8065(3)	5817(3)	25(1)
C(24B)	191(4)	8672(3)	5513(3)	28(1)
C(25B)	-215(4)	8563(3)	4873(3)	25(1)
C(26B)	43(3)	7845(3)	4523(3)	19(1)
C(27B)	1100(3)	6684(3)	3353(2)	14(1)
C(28B)	1194(3)	7614(3)	2966(3)	18(1)
C(29B)	1324(4)	7895(3)	2145(3)	24(1)
C(30B)	1369(4)	7254(4)	1704(3)	25(1)
C(31B)	1291(3)	6323(3)	2084(3)	21(1)
C(32B)	1155(3)	6037(3)	2904(3)	16(1)
Ag(1)	4551(1)	9655(1)	5824(1)	28(1)
Ag(2)	4294(1)	10934(1)	6728(1)	35(1)

	x	y	z	U(eq)
I(1)	3843(1)	12384(1)	7304(1)	24(1)
I(2)	2670(1)	9905(1)	6315(1)	22(1)
I(3)	4840(1)	8394(1)	4950(1)	19(1)
I(4)	5414(1)	9414(1)	7264(1)	21(1)
C(102)	2451(4)	9337(4)	4194(4)	37(1)
C(101)	2091(4)	9649(4)	3432(4)	38(1)
N(100)	1837(5)	9895(5)	2822(4)	58(2)
C(201)	2346(4)	9342(4)	9144(4)	37(1)
C(202)	2711(5)	10096(5)	8560(4)	48(2)
N(200)	2135(5)	8629(5)	9616(4)	62(2)

Table S3. *Bond lengths [Å] and angles [°]*

Ru(1A)-C(1A)#1	2.021(4)	Ru(1A)-C(1A)	2.021(4)
Ru(1A)-C(6A)#1	2.027(4)	Ru(1A)-C(6A)	2.027(4)
Ru(1A)-P(1A)#1	2.3488(11)	Ru(1A)-P(1A)	2.3488(11)
P(1A)-C(15A)	1.822(4)	P(1A)-C(21A)	1.844(4)
P(1A)-C(27A)	1.847(4)	N(1A)-C(3A)	1.355(6)
N(1A)-C(4A)	1.382(6)	N(1A)-C(12A)	1.462(6)
N(2A)-C(3A)	1.356(6)	N(2A)-C(5A)	1.385(6)
N(2A)-C(11A)	1.461(6)	N(3A)-C(8A)	1.349(6)
N(3A)-C(9A)	1.380(6)	N(3A)-C(13A)	1.465(6)
N(4A)-C(8A)	1.344(6)	N(4A)-C(10A)	1.382(7)
N(4A)-C(14A)	1.468(7)	C(1A)-C(2A)	1.234(6)
C(2A)-C(3A)	1.382(6)	C(4A)-C(5A)	1.349(7)
C(6A)-C(7A)	1.226(7)	C(7A)-C(8A)	1.395(6)
C(9A)-C(10A)	1.330(8)	C(15A)-C(16A)	1.401(6)
C(15A)-C(20A)	1.402(6)	C(16A)-C(17A)	1.396(6)
C(17A)-C(18A)	1.383(7)	C(18A)-C(19A)	1.391(7)
C(19A)-C(20A)	1.390(6)	C(21A)-C(22A)	1.397(6)

C(21A)-C(26A)	1.404(6)	C(22A)-C(23A)	1.398(7)
C(23A)-C(24A)	1.387(7)	C(24A)-C(25A)	1.391(7)
C(25A)-C(26A)	1.389(7)	C(27A)-C(32A)	1.397(6)
C(27A)-C(28A)	1.404(6)	C(28A)-C(29A)	1.383(7)
C(29A)-C(30A)	1.383(8)	C(30A)-C(31A)	1.394(7)
C(31A)-C(32A)	1.393(6)		
Ru(1B)-C(6B)	2.023(4)	Ru(1B)-C(6B)#2	2.023(4)
Ru(1B)-C(1B)#2	2.028(4)	Ru(1B)-C(1B)	2.028(4)
Ru(1B)-P(1B)#2	2.3431(10)	Ru(1B)-P(1B)	2.3431(10)
P(1B)-C(21B)	1.830(4)	P(1B)-C(15B)	1.840(4)
P(1B)-C(27B)	1.844(4)	N(1B)-C(3B)	1.356(7)
N(1B)-C(4B)	1.384(7)	N(1B)-C(11B)	1.453(8)
N(2B)-C(3B)	1.353(7)	N(2B)-C(5B)	1.392(7)
N(2B)-C(12B)	1.451(8)	N(3B)-C(8B)	1.342(6)
N(3B)-C(9B)	1.385(6)	N(3B)-C(13B)	1.455(6)
N(4B)-C(8B)	1.343(6)	N(4B)-C(10B)	1.378(6)
N(4B)-C(14B)	1.454(6)	C(1B)-C(2B)	1.218(7)
C(2B)-C(3B)	1.392(6)	C(4B)-C(5B)	1.344(11)
C(6B)-C(7B)	1.216(6)	C(7B)-C(8B)	1.394(6)
C(9B)-C(10B)	1.352(7)	C(15B)-C(16B)	1.398(6)
C(15B)-C(20B)	1.404(6)	C(16B)-C(17B)	1.391(6)
C(17B)-C(18B)	1.390(7)	C(18B)-C(19B)	1.392(7)
C(19B)-C(20B)	1.375(7)	C(21B)-C(22B)	1.390(6)
C(21B)-C(26B)	1.402(6)	C(22B)-C(23B)	1.392(7)
C(23B)-C(24B)	1.391(8)	C(24B)-C(25B)	1.375(8)
C(25B)-C(26B)	1.402(7)	C(27B)-C(28B)	1.397(6)
C(27B)-C(32B)	1.398(6)	C(28B)-C(29B)	1.395(7)
C(29B)-C(30B)	1.380(7)	C(30B)-C(31B)	1.393(7)
C(31B)-C(32B)	1.394(6)	Ag(1)-I(3)	2.7324(5)
Ag(1)-Ag(2)	2.7891(5)	Ag(1)-I(2)	2.8742(6)
Ag(1)-I(4)	2.8908(5)	Ag(1)-Ag(1)#3	3.0035(8)
Ag(1)-I(3)#3	3.0195(5)	Ag(2)-I(1)	2.6782(5)
Ag(2)-I(4)	2.8216(5)	Ag(2)-I(3)#3	3.0281(6)

Ag(2)-I(2)	3.1173(6)	I(3)-Ag(1)#3	3.0195(5)
I(3)-Ag(2)#3	3.0281(6)	C(102)-C(101)	1.456(9)
C(101)-N(100)	1.143(9)	C(201)-N(200)	1.204(10)
C(201)-C(202)	1.399(10)		
C(1A)#1-Ru(1A)-C(1A)	180.000(1)	C(1A)#1-Ru(1A)-C(6A)#1	191.06(17)
C(1A)-Ru(1A)-C(6A)#1	88.94(17)	C(1A)#1-Ru(1A)-C(6A)	88.94(17)
C(1A)-Ru(1A)-C(6A)	91.06(17)	C(6A)#1-Ru(1A)-C(6A)	180.0(2)
C(1A)#1-Ru(1A)-P(1A)#1	189.13(12)	C(1A)-Ru(1A)-P(1A)#1	90.87(12)
C(6A)#1-Ru(1A)-P(1A)#1	188.40(12)	C(6A)-Ru(1A)-P(1A)#1	91.60(12)
C(1A)#1-Ru(1A)-P(1A)	90.87(12)	C(1A)-Ru(1A)-P(1A)	89.13(12)
C(6A)#1-Ru(1A)-P(1A)	91.60(12)	C(6A)-Ru(1A)-P(1A)	88.40(12)
P(1A)#1-Ru(1A)-P(1A)	180.000(1)	C(15A)-P(1A)-C(21A)	104.01(19)
C(15A)-P(1A)-C(27A)	102.06(19)	C(21A)-P(1A)-C(27A)	98.6(2)
C(15A)-P(1A)-Ru(1A)	113.09(14)	C(21A)-P(1A)-Ru(1A)	118.42(15)
C(27A)-P(1A)-Ru(1A)	118.20(15)	C(3A)-N(1A)-C(4A)	109.8(4)
C(3A)-N(1A)-C(12A)	124.7(4)	C(4A)-N(1A)-C(12A)	125.5(4)
C(3A)-N(2A)-C(5A)	109.5(4)	C(3A)-N(2A)-C(11A)	123.9(4)
C(5A)-N(2A)-C(11A)	126.5(4)	C(8A)-N(3A)-C(9A)	109.2(4)
C(8A)-N(3A)-C(13A)	124.0(4)	C(9A)-N(3A)-C(13A)	126.7(4)
C(8A)-N(4A)-C(10A)	109.5(4)	C(8A)-N(4A)-C(14A)	124.0(4)
C(10A)-N(4A)-C(14A)	126.5(4)	C(2A)-C(1A)-Ru(1A)	178.5(4)
C(1A)-C(2A)-C(3A)	165.8(5)	N(1A)-C(3A)-N(2A)	106.2(4)
N(1A)-C(3A)-C(2A)	127.0(4)	N(2A)-C(3A)-C(2A)	126.7(4)
C(5A)-C(4A)-N(1A)	107.1(4)	C(4A)-C(5A)-N(2A)	107.3(4)
C(7A)-C(6A)-Ru(1A)	179.2(4)	C(6A)-C(7A)-C(8A)	172.0(5)
N(4A)-C(8A)-N(3A)	106.5(4)	N(4A)-C(8A)-C(7A)	127.8(4)
N(3A)-C(8A)-C(7A)	125.8(4)	C(10A)-C(9A)-N(3A)	107.6(5)
C(9A)-C(10A)-N(4A)	107.3(4)	C(16A)-C(15A)-C(20A)	118.6(4)
C(16A)-C(15A)-P(1A)	121.3(3)	C(20A)-C(15A)-P(1A)	119.7(3)
C(17A)-C(16A)-C(15A)	120.3(4)	C(18A)-C(17A)-C(16A)	120.4(4)
C(17A)-C(18A)-C(19A)	119.9(4)	C(18A)-C(19A)-C(20A)	120.0(4)
C(19A)-C(20A)-C(15A)	120.7(4)	C(22A)-C(21A)-C(26A)	118.5(4)

C(22A)-C(21A)-P(1A)	123.8(3)	C(26A)-C(21A)-P(1A)	117.5(3)
C(21A)-C(22A)-C(23A)	121.0(4)	C(24A)-C(23A)-C(22A)	119.6(5)
C(23A)-C(24A)-C(25A)	120.0(4)	C(24A)-C(25A)-C(26A)	120.4(4)
C(25A)-C(26A)-C(21A)	120.4(4)	C(32A)-C(27A)-C(28A)	118.5(4)
C(32A)-C(27A)-P(1A)	121.5(3)	C(28A)-C(27A)-P(1A)	119.9(3)
C(29A)-C(28A)-C(27A)	120.5(4)	C(28A)-C(29A)-C(30A)	120.9(4)
C(29A)-C(30A)-C(31A)	119.4(4)	C(30A)-C(31A)-C(32A)	120.1(5)
C(31A)-C(32A)-C(27A)	120.6(4)		
C(6B)-Ru(1B)-C(6B)#2	180.000(1)	C(6B)-Ru(1B)-C(1B)#2	93.43(17)
C(6B)#2-Ru(1B)-C(1B)#2	286.57(17)	C(6B)-Ru(1B)-C(1B)	86.57(17)
C(6B)#2-Ru(1B)-C(1B)	93.43(17)	C(1B)#2-Ru(1B)-C(1B)	180.000(1)
C(6B)-Ru(1B)-P(1B)#2	89.41(12)	C(6B)#2-Ru(1B)-P(1B)#2	290.59(12)
C(1B)#2-Ru(1B)-P(1B)#2	291.40(12)	C(1B)-Ru(1B)-P(1B)#2	88.60(12)
C(6B)-Ru(1B)-P(1B)	90.59(12)	C(6B)#2-Ru(1B)-P(1B)	89.41(12)
C(1B)#2-Ru(1B)-P(1B)	88.60(12)	C(1B)-Ru(1B)-P(1B)	91.40(12)
P(1B)#2-Ru(1B)-P(1B)	180.000(1)	C(21B)-P(1B)-C(15B)	102.7(2)
C(21B)-P(1B)-C(27B)	104.50(19)	C(15B)-P(1B)-C(27B)	98.21(19)
C(21B)-P(1B)-Ru(1B)	113.23(14)	C(15B)-P(1B)-Ru(1B)	117.69(14)
C(27B)-P(1B)-Ru(1B)	118.20(14)	C(3B)-N(1B)-C(4B)	108.6(5)
C(3B)-N(1B)-C(11B)	124.4(5)	C(4B)-N(1B)-C(11B)	126.9(5)
C(3B)-N(2B)-C(5B)	109.2(5)	C(3B)-N(2B)-C(12B)	124.5(4)
C(5B)-N(2B)-C(12B)	126.2(5)	C(8B)-N(3B)-C(9B)	109.2(4)
C(8B)-N(3B)-C(13B)	124.2(4)	C(9B)-N(3B)-C(13B)	126.6(4)
C(8B)-N(4B)-C(10B)	109.2(4)	C(8B)-N(4B)-C(14B)	124.3(4)
C(10B)-N(4B)-C(14B)	126.5(4)	C(2B)-C(1B)-Ru(1B)	176.1(4)
C(1B)-C(2B)-C(3B)	167.4(5)	N(2B)-C(3B)-N(1B)	107.1(4)
N(2B)-C(3B)-C(2B)	127.6(5)	N(1B)-C(3B)-C(2B)	125.2(5)
C(5B)-C(4B)-N(1B)	108.2(5)	C(4B)-C(5B)-N(2B)	106.8(5)
C(7B)-C(6B)-Ru(1B)	177.1(4)	C(6B)-C(7B)-C(8B)	170.2(5)
N(3B)-C(8B)-N(4B)	107.5(4)	N(3B)-C(8B)-C(7B)	126.6(4)
N(4B)-C(8B)-C(7B)	125.9(4)	C(10B)-C(9B)-N(3B)	106.8(4)
C(9B)-C(10B)-N(4B)	107.4(4)	C(16B)-C(15B)-C(20B)	118.4(4)
C(16B)-C(15B)-P(1B)	121.5(3)	C(20B)-C(15B)-P(1B)	120.0(3)

C(17B)-C(16B)-C(15B)	120.5(4)	C(18B)-C(17B)-C(16B)	120.2(4)
C(17B)-C(18B)-C(19B)	119.7(4)	C(20B)-C(19B)-C(18B)	120.1(4)
C(19B)-C(20B)-C(15B)	121.1(4)	C(22B)-C(21B)-C(26B)	118.9(4)
C(22B)-C(21B)-P(1B)	120.2(3)	C(26B)-C(21B)-P(1B)	120.3(3)
C(21B)-C(22B)-C(23B)	120.6(5)	C(22B)-C(23B)-C(24B)	120.2(5)
C(25B)-C(24B)-C(23B)	119.7(4)	C(24B)-C(25B)-C(26B)	120.5(5)
C(21B)-C(26B)-C(25B)	120.0(5)	C(28B)-C(27B)-C(32B)	118.9(4)
C(28B)-C(27B)-P(1B)	124.0(3)	C(32B)-C(27B)-P(1B)	116.9(3)
C(29B)-C(28B)-C(27B)	120.7(4)	C(30B)-C(29B)-C(28B)	120.2(4)
C(29B)-C(30B)-C(31B)	119.7(4)	C(32B)-C(31B)-C(30B)	120.5(4)
C(31B)-C(32B)-C(27B)	120.1(4)	I(3)-Ag(1)-Ag(2)	178.70(2)
I(3)-Ag(1)-I(2)	114.383(16)	Ag(2)-Ag(1)-I(2)	66.775(15)
I(3)-Ag(1)-I(4)	119.338(17)	Ag(2)-Ag(1)-I(4)	59.540(14)
I(2)-Ag(1)-I(4)	103.177(15)	I(3)-Ag(1)-Ag(1)#3	63.321(14)
Ag(2)-Ag(1)-Ag(1)#3	116.63(2)	I(2)-Ag(1)-Ag(1)#3	125.23(2)
I(4)-Ag(1)-Ag(1)#3	126.22(2)	I(3)-Ag(1)-I(3)#3	117.278(15)
Ag(2)-Ag(1)-I(3)#3	62.692(14)	I(2)-Ag(1)-I(3)#3	101.552(15)
I(4)-Ag(1)-I(3)#3	98.299(14)	Ag(1)#3-Ag(1)-I(3)#3	53.957(13)
I(1)-Ag(2)-Ag(1)	166.33(2)	I(1)-Ag(2)-I(4)	131.54(2)
Ag(1)-Ag(2)-I(4)	62.023(14)	I(1)-Ag(2)-I(3)#3	109.075(17)
Ag(1)-Ag(2)-I(3)#3	62.379(14)	I(4)-Ag(2)-I(3)#3	99.647(16)
I(1)-Ag(2)-I(2)	115.364(19)	Ag(1)-Ag(2)-I(2)	57.919(14)
I(4)-Ag(2)-I(2)	98.918(16)	I(3)#3-Ag(2)-I(2)	95.982(15)
Ag(1)-I(2)-Ag(2)	55.306(13)	Ag(1)-I(3)-Ag(1)#3	62.722(15)
Ag(1)-I(3)-Ag(2)#3	117.635(15)	Ag(1)#3-I(3)-Ag(2)#3	54.929(12)
Ag(2)-I(4)-Ag(1)	58.437(13)	N(100)-C(101)-C(102)	177.8(7)
N(200)-C(201)-C(202)	170.9(8)		

Symmetry transformations used to generate equivalent atoms:

#1 -x+1,-y+1,-z

#2 -x,-y+1,-z+1

#3 -x+1,-y+2,-z+1